LATE QUATERNARY SEDIMENTOLOGY AND SEDIMENT INSTABILITY OF A SMALL AREA ON THE SCOTIAN SLOPE

DAVID COLE MOSHER

CANADIAN THESES

THÈSES CANADIENNES

NOTICE

The quality of this microfiche is heavily dependent upon the quality of the original thesis submitted for microfilming. Every effort has been made to ensure the highest quality of reproduction possible.

If pages are missing, contact the university which granted the degree.

Some pages may have indistinct print especially if the original pages were typed with a poor typewriter ribbon or if the university sent us an inferior photocopy.

Previously copyrighted materials (journal articles, published tests, etc.) are not filmed.

Reproduction in full or in part of this film is governed by the Canadian Copyright Act, R.S.C. 1970, c. C-30.

AVIS

La qualité de cette microfiche dépend grandement de la qualité de la thèse soumise au microfilmage. Nous avons tout fait pour assurer une qualité supérieure de reproduction.

S'il manque des pages, veuillez communiquer avec l'université qui a conféré le grade.

La qualité d'impression de certaines pages peut laisser à désirer, surtout si les pages originales ont été dactylographiées à l'aide d'un ruban usé ou si l'université nous a fait parvenir une photocopie de qualité inférieure.

Les documents qui font déjà l'objet d'un droit d'auteur (articles de revue, examens publiés, etc.) ne sont pas microfilmés.

La reproduction, même partielle, de ce microfilm est soumise à la Loi canadienne sur le droit d'auteur, SRC 1970, c. C-30.

THIS DISSERTATION HAS BEEN MICROFILMED EXACTLY AS RECEIVED

LA THÈSE A ÉTÉ MICROFILMÉE TELLE QUE NOUS L'AVONS REÇUE

Canada

NL-339 (r.86/06)

Late Quaternary Sedimentology and Sediment Instability of a Small
Area on the Scotian Slope

by

© David Cole Mosher, B.Sc.

A thesis submitted to the School of Graduate
Studies in partial fulfillment of the
requirements for the degree of
Master of Science

Department of Earth Sciences
Memorial University of Newfoundland
May 1987

St. John's

Newfoundland

ABSTRACT

The Late Quaternary stratigraphy and sedimentation of a small, morphologically smooth region on the Scotian Slope, known as the Verrill Canyon area, has been investigated using high-resolution seismic profiles and piston cores.

The acoustic stratigraphy in the area has been established with the use of high resolution seismic profiles. Most of the study area is underlain by evenly stratified, coherent reflectors which thin downslope. These reflectors are rooted in outer shelf/ upper slope tills and till-like tongues which extend over the shelf break and interfinger with upper slope sediments. Gullies cut the upper slope and a few extend downslope as erosional valleys. Widespread sediment failure has resulted in detachment scarps, slumps, and acoustically-defined disturbed zones.

Piston cores from undisturbed and erosional zones within the study area provide a composite stratigraphic section over 20 m thick which extends into the Mid-Wisconsinan (approx. 32,000 yBP). Five lithofacies are identified: (1) bioturbated, mottled mud; (2) homogeneous mud; (3) laminated mud; (4) thin-bedded sand; and (5) poorly sorted mud. Hemipelagic, or "no-event" lithofacies comprise about 50% of total sediment cored. Mass-transported sediment, or "event" lithofacies, including fine-grained turbidites and debris flows, comprise the remaining cored material. Synsedimentary deformation features were observed in cores taken from the acoustically identified disturbed zones.

Wisconsinan sedimentation on the Scotian Slope has been largely affected by glacial events. Processes related to ice margins and lower sea levels served to transport material to the slope. High sedimentation rates and vigorous environmental conditions resulted in abundant sediment failures, producing the event lithofacies. During non-active sedimentation periods, background depositional processes resulted in hemipelagic deposition with abundant bioturbation. The entire study area is

covered by a one to two metre drape of fine-grained, bioturbated, Holocene sediment.

The acoustically-defined disturbed zones record the occurrence of a large scale sediment failure. Sediment deformation in cores from these failed zones indicates they are composed of a complex arrangement of slide blocks, which transform at the distal margins of the disturbed zones into debrites. Erosional scours downslope of the disturbed zones suggest that this sediment failure developed into a large turbidity current. This failure event was likely seismically triggered.

ACKNOWLEDGEMENTS

TABLE OF CONTENTS

LIST OF TABLES

LIST OF FIGURES

CHAPTER 1
INTRODUCTION

1.1 General

During the last decade continental slopes have received
increasing geological attention (see bibliographies of publications
edited by Shepard, 1973; Burke and Drake, 1974; Bouma, Moore, and
Coleman, 1976; Doyle and Pilkey, 1979; and Stow and Piper, 1984).
This trend is in part due to the recent development of deep-towed
instrumentation, permitting detailed surveys of continental slopes,
and in part to the need to explore for natural resources. Research
by both academic and industrial communities is beginning to provide
an understanding of the geological processes that take place along
passive margin continental slopes.

This thesis examines the Late Quaternary sedimentology of an
area on the Scotian Slope. The locality is a target of recent
hydrocarbon exploration, and an area of demonstrable seabed
instability. A thorough investigation of the site will lead to a
greater understanding of geological processes on the slope, and
define possible hazards that may be met while exploring in this
environment.

Heezen et al. (1959) define the slope as "that relatively
steep (3-6°) portion of the sea floor which lies at the seaward
border of the continental shelf." Morphologically the slope
begins at the shelf break and ends at the continental rise, though
this latter boundary is less well defined (Bouma, 1979). It is
thus a transitional environment between the continental shelf and
the continental rise - ocean basin floor.

Morphologically the continental slope is a diverse
environment, in places monotonously smooth (Swift, 1985), and in
others rugged, unstable, and prone to slumps and other mass
movements (Jacobi, 1976; Embley and Jacobi, 1977). These mass

1

movements (slumps, slides, debris flows, turbidity currents) are now acknowledged as common and important slope processes (Doyle and Pilkey, 1979; Embley, 1980; Stow and Piper, 1984).

With increasing interest in exploiting offshore deep water, (>200 m) resources, a greater knowledge of slope morphology and processes will be required (Palmer, 1979; Pereira, 1984). Such an interest has developed within the petroleum industry for offshore Atlantic Canada with the discovery of the hydrocarbon potential in the area (Pereira, 1984).

1.2 Purpose

It is the purpose of this thesis to study and interpret the Late Quaternary geological history of a small area on the Scotian Slope. A priority in this study is to analyze sediment stability based predominantly on geological information. Data were collected by studying:

1) Acoustic characteristics of the bottom sediments using side-scan sonar images, high-resolution seismic reflection profiles, and bathymetric profiles.
2) Sediment lithologies and structures from piston cores.
3) Physical properties of the sediments in these cores.
4) Radiocarbon dates, micropaleontological, and oxygen isotope data from the cores.

Acoustic information helped to establish a geological framework within which to site core positions. It also facilitated correlation of the stratigraphy from one core site to another. Piston cores provided the sediment from which to study the detailed geology. Such a study helped refine interpretation of the acoustic data. Physical property measurements provided quantitative data on the stability of the sediments. Down core physical property measurements were used as a tool for stratigraphic correlation and aided in the interpretation of the geology. Radiocarbon, oxygen isotope, and micropaleontologic (foraminifera) data provided a time framework for the geology and useful information concerning

paleoenvironmental conditions.

1.3 Location and Bathymetry

The study area, informally referred to as the Verrill Canyon area, is a site of approximately 60 km^2 in size lying between 42° 30'N and 43° 00'N latitudes, and 61° 15'W and 62° 00'W longitudes (Fig. 1.1). The area lies on the Scotian Slope from about 200 to 2500 m water depth (Figs. 1.1 and 1.2). Two petroleum exploration wells, the Acadia K-62 and Shubenacadie H-100, are located in the area.

The large scale bathymetry of the Scotian Slope (Fig. 1.1) shows two distinct morphologies: a highly dissected, or canyoned area to the east of the 61° 30' W longitude line, and a smooth, relatively featureless area to the west. Verrill Canyon, which is located in the eastern part of the survey area (Fig. 1.2) marks the beginning of the canyoned slope. This study, however, concentrates on the western part of the study area which is characterised by a broad scale sinuosity of the isobaths. Sharp indentations of the isobaths in the westernmost part of the area define the East and West Acadia Valleys. In the upper slope region small inflexions can be seen in the contour lines. These features represent small slope gullies which in some cases indent the shelf break. The upper slope, defined by the steepest part of the slope (approximately 5°), extends from the shelf break to the 700 m isobath. The gradient of the remainder of the slope averages 2.5°.

1.4 Geological Setting

Heezen (1974) described the continental slope of eastern North America as part of a tectonically stable trailing edge) (i.e. Atlantic type) margin. The stratigraphic framework of the outer Scotian Shelf and Slope is discussed by McIver (1972), Jansa and Wade (1975), King and Young (1977), and Piper et al. (1987). The overall sedimentary sequence of the slope comprises a thick progradational Tertiary succession, overlain both conformably and unconformably by Pleistocene sediments. The Tertiary strata are

3

Figure 1.1   Location of Study Area (black box) and bathymetry of
             Nova Scotia continental margin.

GRAND BANKS

LAURENTIAN CHANNEL

ST. PIERRE BANK

HALIBUT CHANNEL

GREEN BANK

HADDOCK CHANNEL

WHALE BANK

NOVA SCOTIA

SCOTIAN SHELF

BANQUEREAU

SABLE ISLAND BANK

THE GULLY

LAURENTIAN FAN

EMERALD BASIN

WESTERN BANK

SCOTIAN SLOPE

LA HAVE BASIN

EMERALD BANK

LA HAVE BANK

BROWN'S BANK

NORTHEAST CHANNEL

GEORGES BANK

100m
200m
1000m
2000m
3000m
4000m
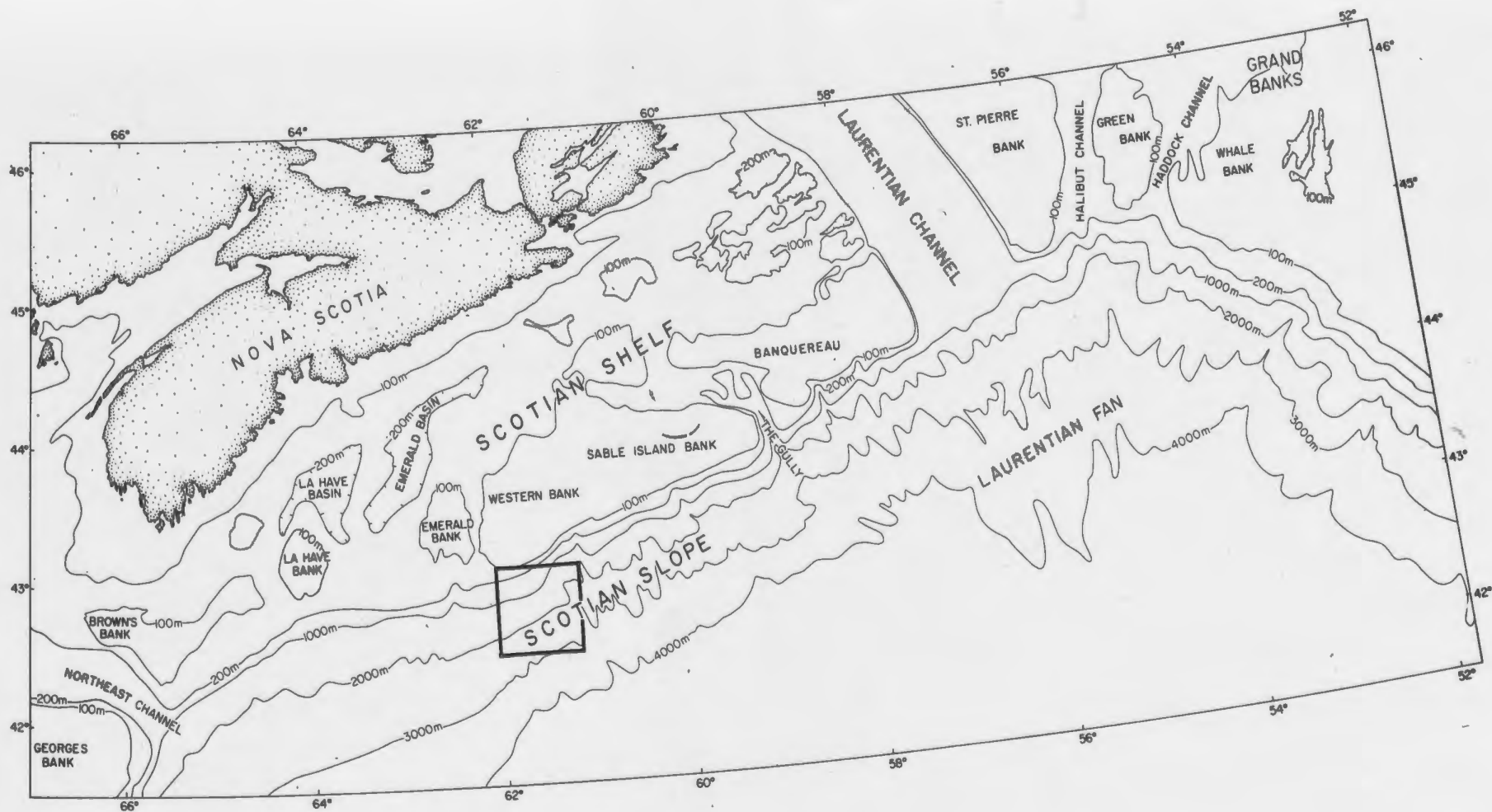
Figure 1.2   Bathymetry of study area showing core locations
             (modified from Piper et al., 1985). Isobaths are in
             metres, solid lines representing areas of good control
             and dashed lines of less control. Open circles
             represent piston core locations and the two closed
             circles are petroleum exploration wells.
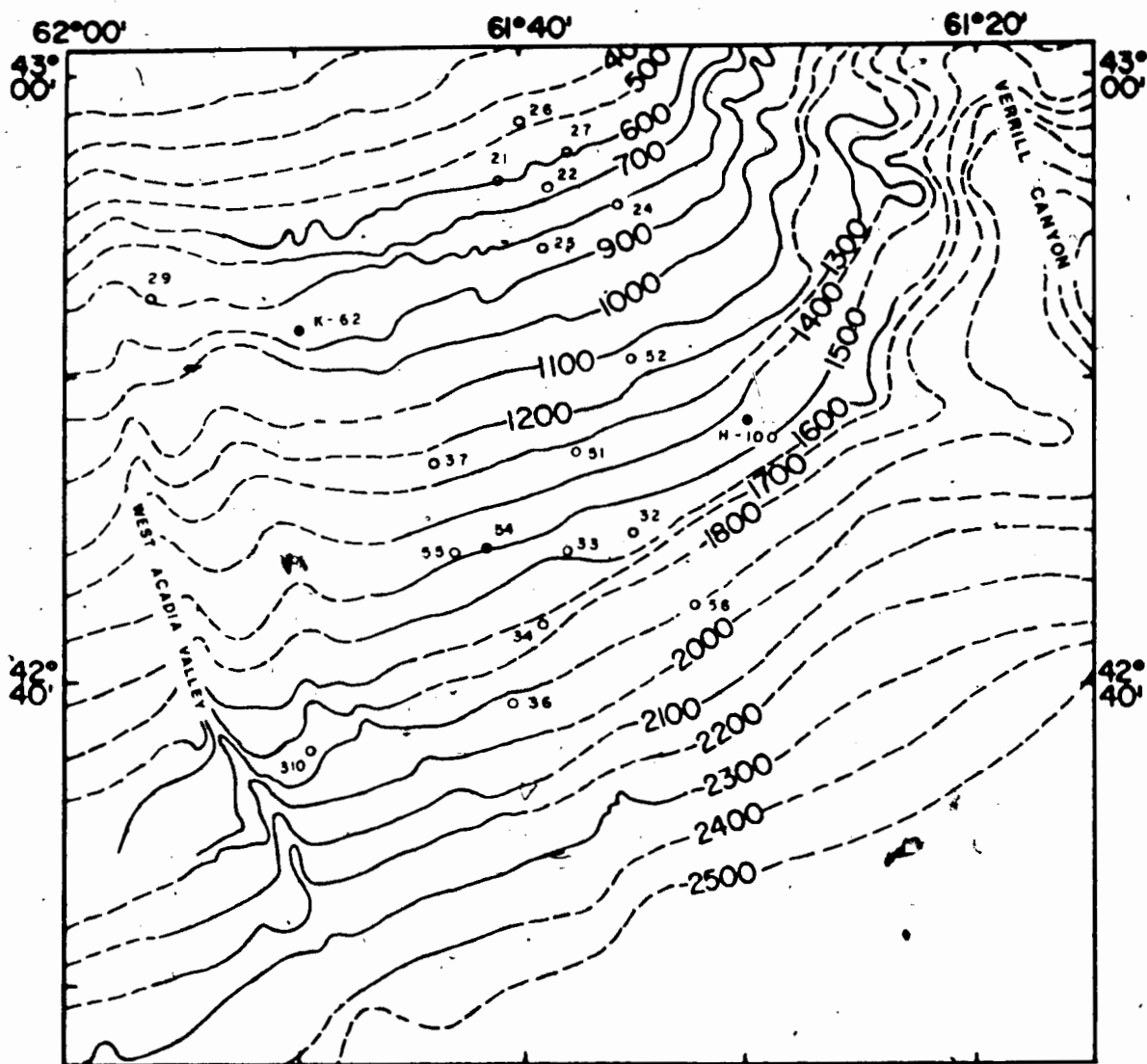
assigned to the Banquereau Formation (Jansa and Wade, 1975) which consists predominantly of shales that thicken seawards. The Quaternary sediments have accumulated on the slope as a well stratified progradational sequence (Piper et al., 1987).

Piper et al. (1987) suggest that much of the Pleistocene sedimentary sequence on the Scotian Slope was deposited rapidly in a proglacial environment. Rapid deposition creates high pore pressures in the sediment (low consolidation and low shear strengths) (Morgenstern, 1967; Keller et al., 1979; Prior and Coleman, 1984). Combined with the effects of rapid and extreme loading, or steep slopes, these properties can result in mass wasting.

Mass movements are, and have been, important processes on most continental slopes. Mass-wasting processes were involved in the creation of both the dissected and smooth morphologic regions on the Scotian Slope (Hill, 1983, 1984a; Swift, 1985), thus attesting to the complexity of the sedimentary processes that have occurred there.

On a local scale even the apparently smooth region of the Scotian Slope is actually rugged, being marked by slide scars, scarps, slump blocks, debris flows, and small incised channels and valleys (Hill, 1981, 1983). These small-scale irregularities were produced by mass movements, folding and faulting, diapirism, and slope erosion during Pleistocene and especially Late Wisconsinan events. Evidence for diverse sedimentary processes during the Wisconsinan were seen by Hill (1981, 1983) from his study area on the Scotian Slope (Lat. 42° 40' to 43° 00'N, and Long. 63° 20' to 63° 30'W). He found it very difficult to correlate Wisconsinan sediments from core to core because of the small scale facies changes and sequence discontinuities.

In contrast to Wisconsinan deposition, the Holocene record is one of uniform, hemipelagic deposition (Hill, 1981, 1983; Stow, 1977; Swift, 1985). Hill (1981, 1983) records only one apparently slumped bed in the Holocene section of his studied cores. The

8

Holocene section drapes the underlying sediments and is everywhere less than 2 m thick (Hill, 1983). The contact between this section and the underlying unit is recognizable throughout the Scotian Slope. This contact has been dated at 17,000 to 20,000 yBP (Hill, 1981, 1983).

1.5 Regional Geology and Environmental Setting

There is a close oceanographic and sedimentological relationship between the Scotian Slope and its adjacent shelf (Bouma, 1979; Hill, 1981, 1983, 1984a, 1984b; Hill and Bowen, 1983; Hill et al., 1983; Swift, 1985). The shelf geology affects the slope as it is the source area for slope sediments. The sea level over the shelf affects the slope by determining the amount and style of off-shelf transport of sediment. Glaciation acts on the slope because it affects the geology of the shelf and determines the sea-level history over the shelf and slope. To better understand Quaternary sedimentation on the Scotian Slope it is first necessary to review the shelf geology and its sea-level and glacial histories.

Scotian Shelf:

The Scotian Shelf is 125 km wide in the west and 250 km wide in the east. It has been divided into three physiographic provinces by King (1970): 1) an inner shelf of rough topography which borders mainland Nova Scotia; 2) a central zone of isolated banks and intervening basins; and 3) an outer zone of wide, flat, shallow banks. The Pleistocene sediments of the central and outer shelf are underlain by well stratified Tertiary and Cretaceous sequences that dip gently to the southeast (King and Fader, 1986).

The central shelf ranges from 145 to 225 m in water depth. The isolated banks within the central shelf are erosional features resembling mesas, and are composed of Tertiary strata. The outer shelf is shallower, ranging from 85 m water depth on the banks to 100-125 m in the saddles, or depressions. This outer region is

9

approximately 50-65 km wide. The outer banks form a chain which is interrupted by the saddles. These banks are composed of Tertiary strata underlain by Cretaceous and Jurassic sediments. Erosion has transformed them into cuestas. King (1970) suggested that the shelf morphology was largely determined by fluvial processes during a mid-Tertiary low sea level. Subsequent sedimentation has, for the most part, draped the underlying topography.

The lithology and sedimentology of the surficial sediments on the shelf have been studied by King (1970), King and McLean (1976), King and Fader (1986), and Amos and Knoll (in press). King (1970) has identified five "map units" (i.e. formations): 1) Scotian Shelf Drift, 2) Emerald Silt, 3) Sambro Sand, 4) LaHave Clay, and 5) Sable Island Sand and Gravel. These sediments are flat lying and rest unconformably on the pre-Pleistocene strata. They are interpreted as variably reworked glacial debris from various stages of Wisconsinan glaciation.

King (1970) grouped the upper slope sands with the relatively poorly sorted Sable Island Sand and Gravel unit. Hill et al. (1983), during a submersible dive, observed large erratic boulders on the upper slope and outer shelf. They also noticed that the surficial sediment grades from gravelly sand at the shelf break, through sand to silty sand at about 400 m depth, and finally to silty mud at depths greater than 400 m. Hill and Bowen (1983) and Stanley et al. (1972b) have recognized recent transport of sediment over the shelf edge. Doyle et al. (1979) suggest that spillover of material occurs along the entire eastern North American shelf-slope boundary.

Glaciation:

Enormous amounts of sediment can be transported long distances as a result of glacial action (Flint, 1971). It is believed by King and co-workers (King, 1970; King and MacLean, 1976; Grant and King, 1984; King and Fader, 1986) that the majority of Quaternary sediment on the Scotian Shelf is glacial in origin and that most of this sediment was deposited during the Middle to Late Wisconsinan.

Older deposits were essentially removed by erosion during the last
major glacial advance (King and Fader, 1986).

The extent and timing of the last (Wisconsinan) ice sheet in
eastern Canada and northeastern USA is a controversial topic
(e.g. Ives, 1978; Prest, 1984), that consists of two "end-member"
theories advocating maximum and minimum extent. As far as Atlantic
Canada is concerned, the maximum theory proposes that the
Laurentide ice sheet extended seaward as far as the edge of the
continental shelf during the Late Wisconsinan. The minimum theory
argues that only local ice caps developed in the Atlantic region
during the Late Wisconsinan, leaving some coastal regions ice-free
(Mayewski, et al., 1978; Ives, 1978; Prest, 1984).

The Wisconsinan Stage refers to the last major period of
glaciation. For reasons discussed by Prest (1984) this stage
begins at the end of oxygen isotope stage 5, approximately 75,000
yBP. The Wisconsinan is divided into Early, Middle, and Late
substages (Fulton, 1984). Early Wisconsinan has been referred to
as a time of major glacial advance, with many workers proposing
that Wisconsinan ice-sheets reached their maximum extent in Eastern
Canada during this time. The Middle Wisconsinan substage is a time
when ice retreated from much of western and southern Canada, and
there was probable thinning of ice in the Atlantic region. The age
of the base of this substage is defined as the boundary between
oxygen isotope stages 3 and 4 (approximately 64,000 yBP). The Late
Wisconsinan ranges from the base of the Holocene to approximately
32,000 yBP. It corresponds to the last time Canada was covered by
major ice sheets.

Glacial advances in the Early and Late Wisconsinan are
incorporated by King and Fader (1986) in their five-phase model for
the Wisconsinan glacial history and sedimentation on the Scotian
Shelf (Fig. 1.3). This model is based on abundant geological
evidence, and numerous radiocarbon dates.

In phase 1 of the model (70,000 to 50,000 yBP) the Laurentide
ice sheet had extended to the shelf edge as a grounded, dry-base

11

Figure 1.3   5-phase model of Wisconsinan glacial advance and
retreat across the outer Scotian Shelf (after King and
Fader, 1986).   The attributes of these phases are
discussed in the text.

INNER SHELF EMERALD BASIN OUTER SHELF SHELF EDGE

1. ICE SHEET — RELATIVE SEA LEVEL — 70,000 - 50,000 yBP

2. ICE SHEET — ICE SHELF — 50,000 - 45,000 yBP

3. ICE SHEET — ICE SHELF — WATER — 45,000 - 32,000 yBP

4. ICE SHEET — WATER — 32,000 - 16,000 yBP

5. TRANSGRESSING SEA LEVEL — WATER — LOWEST RELATIVE SEA LEVEL — 16,000 - 10,000 yBP

13
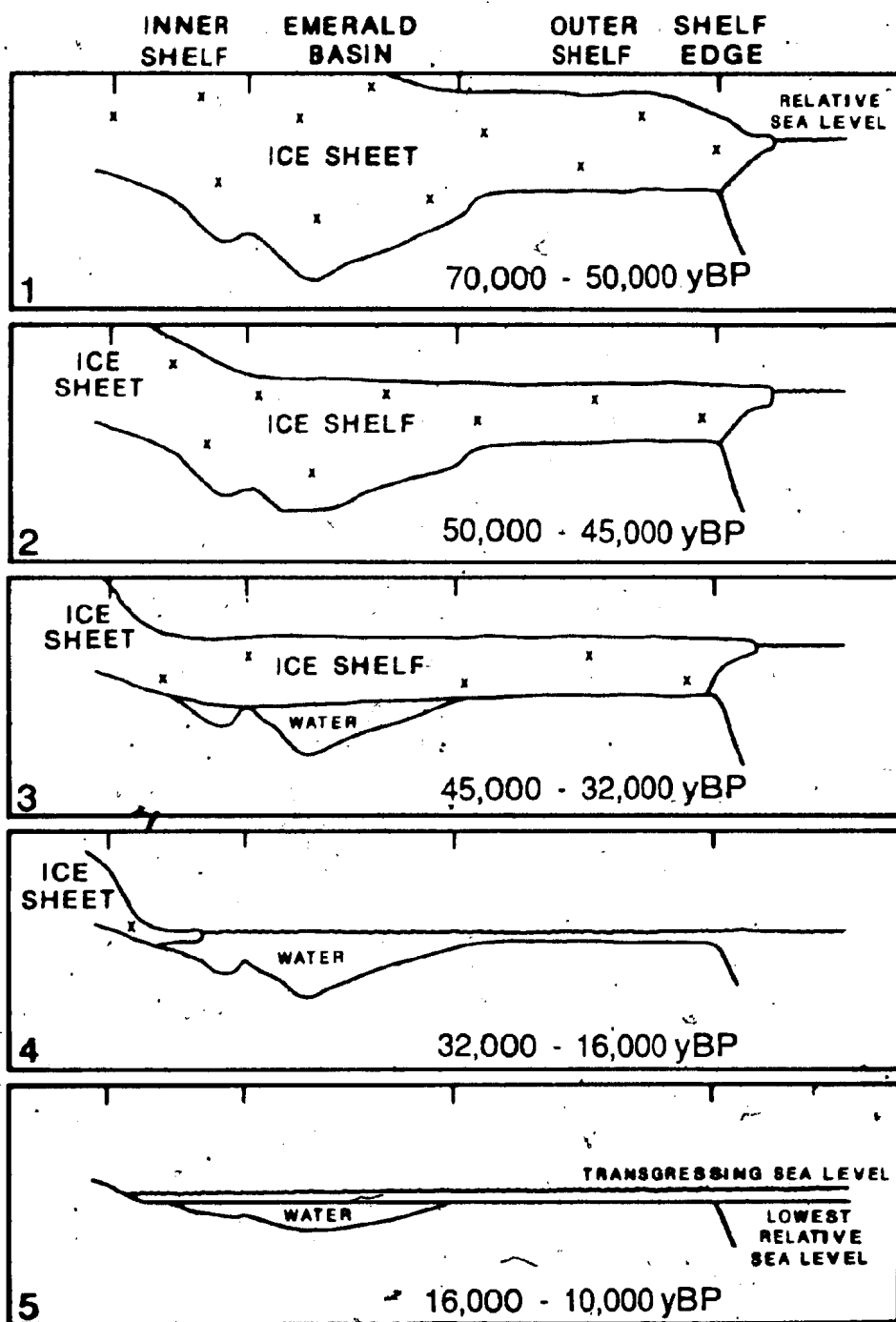
ice sheet. This advance is known as the Scotian Shelf - Grand Banks advance. The ice sheet had presumably entrained abundant basal and englacial debris as it advanced across terrestrial and shallow marine areas.

Rafting from icebergs, as proposed by Piper and Slatt (1977), and Stow (1977), commencing during this phase and ending at the end of phase 5, could have provided a significant amount of sediment to the Scotian Slope and Shelf.

Phase 2 (50,000-45,000 yBP) represents an early recessional phase (beginning of the Scotian Shelf - Grand Banks recession). As the ice melted and receded, lift-off moraines and early glaciomarine sediments were deposited. Deposition beyond the shelf edge was probably most active at this phase. The ice sheet became an ice shelf, estimated at 200-500 m thick (King and Fader, 1986).

Phase 3 extends from 45,000 to 32,000 yBP. Recession rates of the ice margin reached a maximum during the early part of this phase. The greater part of phase 3 involved minor surges and retreats of the buoyancy line (line of seabed - ice shelf contact). This oscillation of the buoyancy line is believed to be responsible for the development of mapped till tongues (King and Fader, 1986). Moraine development and deposition of glaciomarine sediments continued with increased melting of the ice shelf. The larger banks may have sustained local ice domes with dry-base ice for periods during this phase, accompanied by local erosion on the banks (King and Fader, 1986). This situation would result in further contribution of sediment beyond the continental shelf edge.

In phase 4 (32,000-16,000 yBP) the ice shelf retreated to present land areas. A surge of grounded ice to parts of the inner and outer shelf may have occurred for a short interval (King and Fader, 1986). Biological activity on the shelf increased during this phase and sedimentation rates decreased.

The lowest sea-level stand (115-120 m below present sea level) occurred during phase 5 (16,000-10,000 yBP). This low sea-level

stand left some shelf sediments subaerially exposed. As the
Holocene transgression progressed, these shelf sediments were
reworked, leaving large areas of clean, well sorted sands and
gravels that now underlie the Scotian Shelf.

Sea Level:

Fluctuations in sea level can be associated with episodes of
glaciation. Sea level, in turn, can control significantly the
amount and coarseness of sediment supplied to the slope (Emery,
1968; Bouma, 1979; Piper et al., 1987). Changes in the physical
oceanographic setting at the shelf break brought about by sea-level
changes cause the style of sedimentation at the margin to change.

Evidence for the Late Wisconsinan low stand of sea level is
well expressed along the entire Scotian Shelf (King and Fader,
1986). Based on the presence of terraces and associated textural
changes, such as sorted and rounded sand and gravels, on the outer
Scotian Shelf, King (1970) and King and Fader (1986) suggest that
the lowest stand of sea level in the Pleistocene occurred about
15,000 yBP at 110 to 120 m below present sea level (Fig. 1.4b).
These data correspond well to the sea-level curve produced by
Milliman and Emery (1968) for the Atlantic Continental Shelf
(Fig. 1.4a).

Using a migrating peripheral bulge mathematical model, Quinlan
and Beaumont (1981) calculated the maximum lowering of sea level
following the last glaciation to be 50-70 m. The difference
between this estimate and the previous one of King (1970) and King
and Fader (1986) is quite significant in terms of sedimentological
conditions. If the sea level were 120 m lower than at present,
much of the outer-shelf banks would be exposed. If the level were
only 70 m lower then only Sable Island bank and Banquereau would be
exposed. No independent geological evidence exists for the -70 m
lowstand of sea level.

The last sea-level rise (Holocene transgression) began between
15,000 and 13,000 yBP (Milliman and Emery, 1968; King and Fader,

15

Figure 1.4   a) Sea level curve for the Atlantic continental shelf
(Milliman and Emery, 1968).   b) Cross-section of the
Scotian Shelf, showing sea levels at 15,000 yBP, 10,000
yBP and present (from King and Fader, 1986).   Note the
exposed outer banks during lower sea levels.

a

THOUSANDS OF YEARS AGO

b

17
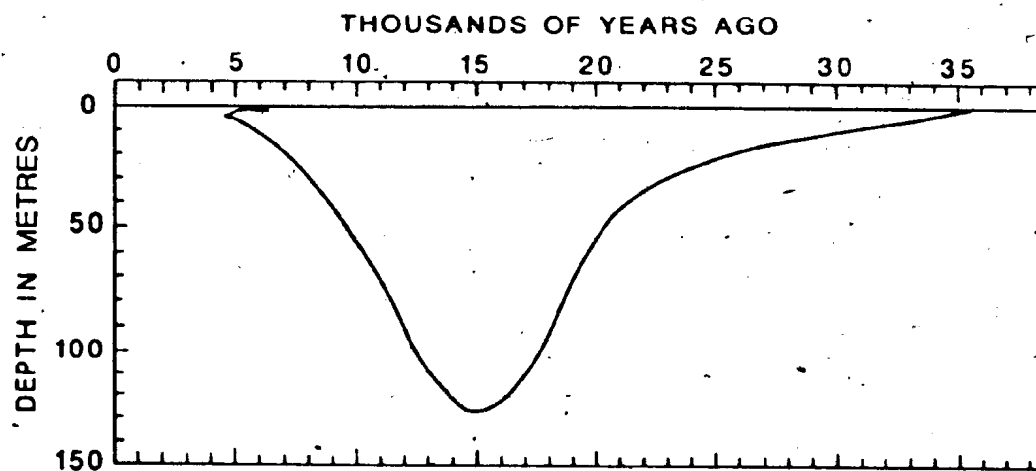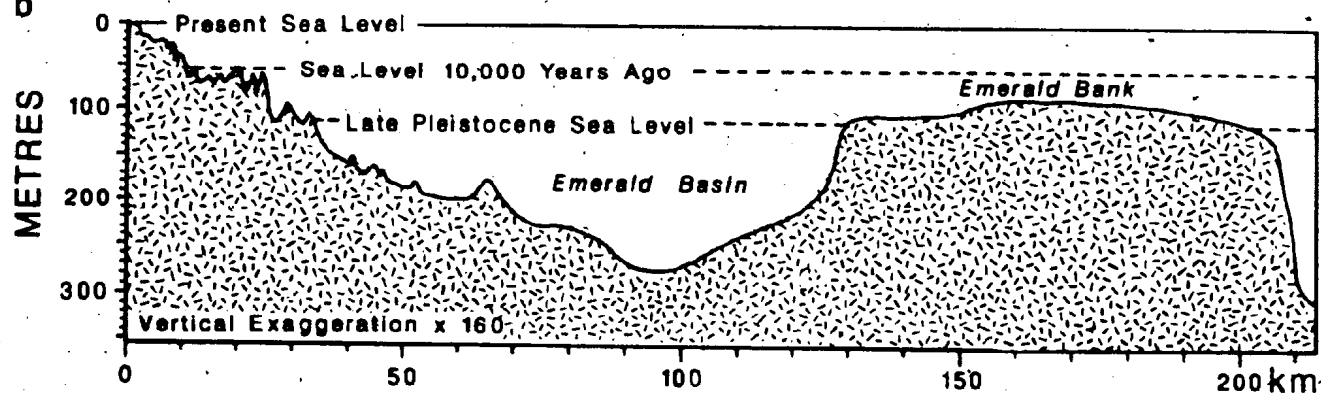
1986). Transgression over the Scotian Shelf is indicated by large areas of well washed, well sorted sands and gravels (King, 1970). The shelf break now rests in 100-200 m of water so that shelf influences on slope sedimentation are significantly reduced.

1.6 Terminology

The term <u>disturbed zone</u> is a descriptive term used by Piper <u>et al.</u> (1985) to define areas of characteristically rough seabed lacking internal reflectors on acoustic profiles and interpreted as consisting of either slump, slide or debris flow deposits.

A <u>slide</u> as defined by Saxov (1982), and Cook <u>et al.</u> (1981) is sediment displaced by any slope failure. They define a <u>slump</u> as a slide in which the mass of material moves as a unit or as several subsidiary units along one or several curved slip surfaces, usually with backward rotation of the mass. Embley and Jacobi (1977), and Jacobi (1984) further distinguish sediment that is deformed and liquified during transport downslope in a slide, resulting ultimately in a slurry or debris flow. In a slump, sediment is downdropped and rotated, but contortion of internal layering is minimal.

The term <u>debrite</u> is used for sediment interpreted to have been deposited by a debris flow. A debrite consists of mixed lithologies, ranging from muds containing only a few sand- to boulder-sized clasts to a bouldery mass containing little mud (Stow, 1986, p. 414). The use of the term in this study is in reference to beds showing characteristics such as clasts supported in a matrix (i.e. pebbly mudstone), erosional bases to beds, and inverse and normal grading (cf. Walker, 1984, p. 177).

<u>Turbidites</u> are sediments deposited by a turbidity current. The use of the term in this thesis is generally restricted to the fine-grained turbidite variety as described in Stow (1986, p. 415), Stow and Shanmugam (1980), Piper (1978), and Hesse (1975). A <u>disorganized turbidite</u> is a sediment package deposited by a current that has not fully developed into a classic turbidity current.

The term _facies_ is used as defined by Middleton (1978): A unit
distinguished by lithological, structural, and organic aspects
detectable in the field. It is understood that facies will
·ultimately be given an environmental interpretation. _Facies
associations_ are groups of facies that occur together and are.
considered to be genetically or environmentally related (Reading,
1986, p. 5). For this study facies associations were created by
observation only, not by any mathematical or statistical
calculations. The association makes environmental interpretation
easier than treating each facies in isolation.

Other sedimentary geology terms can be found in sedimentology
texts by Pettijohn (1975), Blatt, Middleton, and Murray (1980),
Leeder (1982), Walker (1984), and Reading (1986). Other terms
referring to gravity flows are defined by Lowe (1979, 1982) and
Nardin et al. (1979) ·

1.7 Methods

Acoustic data and piston cores were collected during the
following Atlantic Geoscience Centre cruises: C.S.S. Dawson 82004
and 83012, and C.S.S. Hudson 82014, 84029, and 85001. Ship
navigation data were acquired with an integrated system of
hyperbolic LORAN-C and satellite navigation (BIONAV). It is
accurate to within ±100 m in the survey area. Figure 1.5 shows the
ship tracks for the various cruises. Most laboratory analyses were
conducted at the Atlantic Geoscience Centre, Bedford Institute of
Oceanography.

Acoustics:

Various acoustic systems were used to collect data in the
Verrill Canyon area, the results of which have been reported in
several reports (Piper et al., 1983, 1985; Piper and Wilson, 1983)
and in this thesis. All calculations·of depth (in metres), both to
seabed and subbottom, were calculated assuming an acoustic velocity
of 1500 m/s. Over 2000 line-km of bathymetric data have been

Figure 1.5 Ships tracks over study area and piston core positions.
Open circles represent piston core positions.

62°00'   61°50'   61°40'   61°30'   61°20'
43°00'
42°50'
42°40'
42°30'

26
27
22
21
24
25
29
K-62
52
H-100
37   51
32
55   54   33
34   56
36
3J0

SHIP TRACK	CRUISE
··············	HU 85001
————	HU 84029
– – – –	DW 83012
—— — ——	HU 82014
—·—·—	DW 82004

21
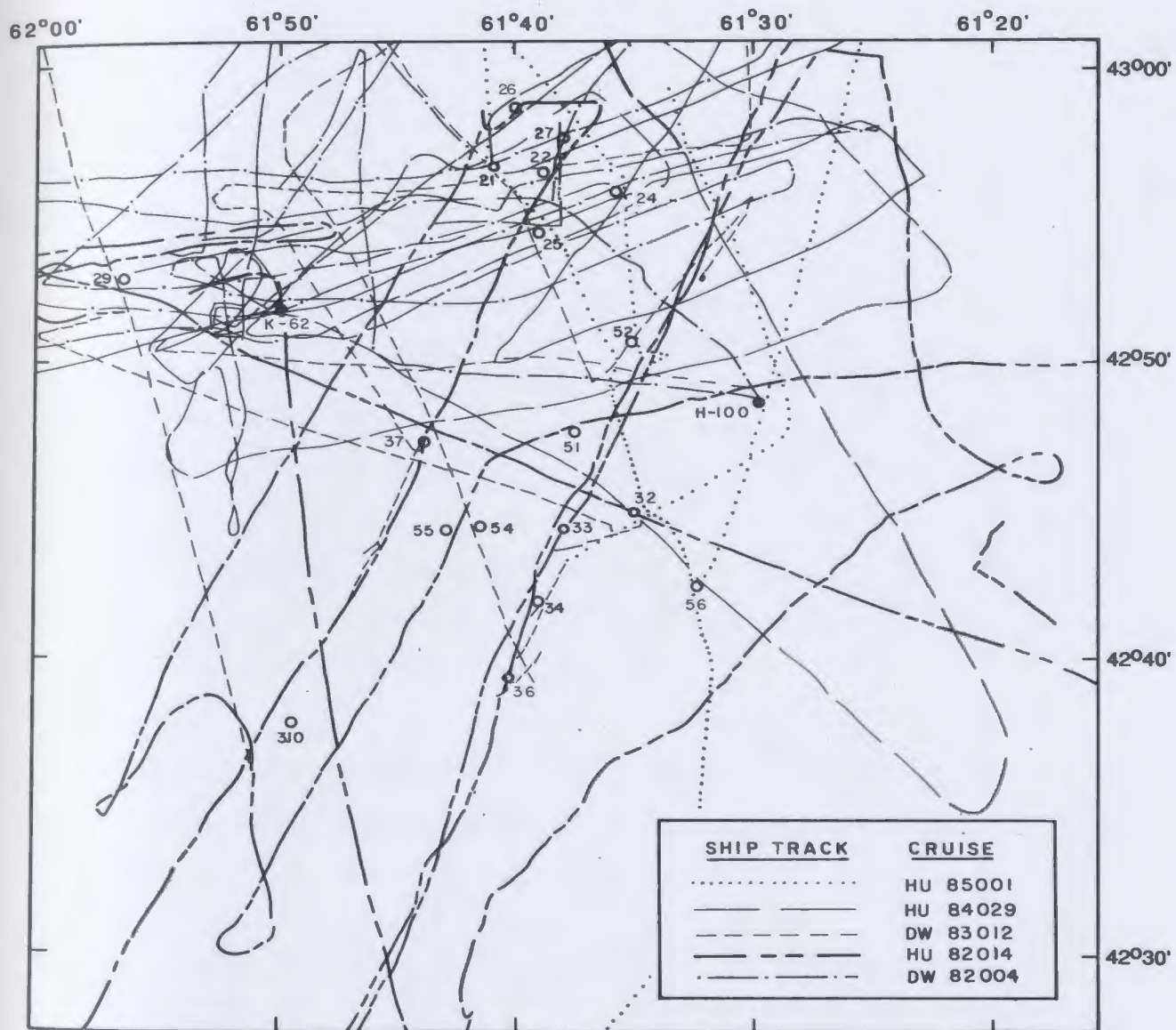
collected in the study area with hull-mounted 12 kHz transducers.
Approximately 790 line-km of 3.5 kHz high-resolution seismic
profiles were collected using hull-mounted transducers on the
C.S.S. Dawson, and towing an ORE polywog from the C.S.S. Hudson.
Using a V-fin sparker system (see Bidgood, 1974), 380 line-km of
high-resolution seismic profiles were collected. This system uses
a 300-7000 Hz sparker sound source with a 250 joule output, firing
at 250 or 500 ms. The towfish, containing sparker, hydrophone and
depth transducer is depth compensated. It was towed at a depth of
approximately 100 m. A short (47 km) Huntec DTS profile (broadband
deep-towed boomer source and receiver; see Hutchins et al., 1976)
and a 110 km 40 in^3 air gun line were run through the area during
the Hudson 85001 cruise.

The Study Area (Fig. 1.2) was surveyed with two different
combined-deep-tow sidescan sonar and high-resolution seismic
profiling systems. During Hudson cruise 82014, 315 line-km of Sea
MARC I data were collected, providing coverage of over 1500 km^2.
Sea MARC I is a neutrally buoyant vehicle towed about 300 m off the
sea floor (Kosalos and Chayes, 1983). The system is equipped with
27 and 30 kHz side looking sonars, producing a maximum swath width
of 5 km, and a high-resolution subbottom profiling system operating
with a 4.5 kHz pulse length.

The SEABED II 2000 m system utilizes sidescan sonar
transducers similar to those on Sea MARC I, but with a swath width
of 1.5 km, and a prototype-pressure compensated deep-ocean boomer
(seismic source - similar to the Huntec DTS) (Hutchins et al.,
1985). About 190 line-km of SEABED II high-resolution seismic
reflection, and 236 line-km of SEABED II sidescan data were
collected during Hudson cruise 84029. This survey was conducted
during development of the SEABED II system. Inherent heave is
present on the seismic records due to the motion of the tow
vehicle, thus severely limiting the use of these profiles.

Coring:

Piston cores were collected during Dawson cruises 82004 and

83012, and Hudson cruise 85001. A gravity trigger-weight core was used with each piston coring attempt. Comparison of the trigger-weight core with the piston core suggests that the uppermost metre or so of sediment was lost in piston coring. The core positions are illustrated on Figures 1.2 and 1.5, and are given in Table 1.1.

For the most part coring was carried out with a split-piston, 3.5 in. (8.9 cm) internal diameter corer. Core barrel lengths of 20, 30, or 40 ft. were used. Cores 85001-01 and 85001-02 were collected using a system known informally as the giant piston corer. It is similar to the above described system except the barrels have an 8 in. (20 cm) internal diameter. Once on board ship the cores were cut into 1.5 m lengths and sealed with end caps. Cores taken for geotechnical analysis were carefully handled and the ends were sealed with beeswax to prevent desiccation.

Core descriptions:

To split the cores, the plastic liners were first cut lengthwise on each side of the core. The sediment was then cut lengthwise with a thin wire. One half was saved as an archive section, the other as a working section. The core halves were sealed, then stored at 4° C. Detailed descriptions, using techniques of Piper (1980), were conducted on each core. The cores were examined under white fluorescent light and described in conjunction with X-radiographs of the half core, or of core slabs (Mosher and Asprey 1986), and with smear slides of the sediment. Descriptions included the noting of structures, lithologies and colours (using the Munsell colour scale for soils). Many of the cores were photographed to keep a visual log of the material.

Geotechnical Analysis:

Geotechnical tests were carried out as soon as possible after coring to avoid any subsequent disturbance to the cores. Vane shear tests determined the shear strength of the sediment. A computer-integrated Wykeham-Farrance miniature vane shear apparatus with a vane 0.5 x 0.5 inches was employed. Sampling intervals of

Table 1.1: Piston core locations and lengths

Cruise Core number	Thesis Core no.	Latitude	Longitude	Length cm	TWC Length cm
Dw82004-01	21	42° 56.73'	61° 40.76'	641	48
" -02	22	42° 56.75'	61° 38.86'	850	53
" -04	24	42° 55.98'	61° 35.54'	340	126
" -05	25	42° 54.65'	61° 38.72'	740	150
" -06	26	42° 58.83'	61° 39.95'	353	
" -07	27	42° 57.83'	61° 37.90'	267	
" -09	29	42° 52.89'	61° 56.19'	1020	125.
Dw83012-02	32	42° 44.63'	61° 34.89'	877	26
" -03	33	42° 44.28'	61° 37.74'	539	
" -04	34	42° 41.84'	61° 38.93'	700	75
" -06	36	42° 39.10'	61° 40.02'	471	75
" -07	37	42° 47.22'	61° 43.85'	287	60
" -10	31	42° 38.61'	61° 49.06'	614	25
Hu85001-01	51	42° 47.85'	61° 37.20'	610	
" -02	52	42° 50.95'	61° 35.02'	725	
" -04	54	42° 44.71'	61° 41.30'	840	141
" -05	55	42° 44.60'	61° 42.54'	1099	
" -06	56	42° 42.83'	61° 32.12'	122	142

15 to 25 cm were generally attempted. The result is the undrained shear strength of the sediment in kiloPascals (kPa). In some cases the vane was twisted several times in the sediment and the test was run again to give the remolded shear strength of the sediment.

Samples for bulk density and water content measurements were taken from the cores at 15 to 25 cm intervals. They were extracted with a thin walled, stainless steel piston sampler. This sampler, if used correctly, provided "plugs" of sediment of a known volume. These plugs were weighed in pretared bottles, oven dried at 40° C for 24 hours, then weighed again. The bulk density (BD) was calculated as the wet weight of the sediment plug divided by its volume, which is the internal volume of the piston sampler. The natural water content (WC) is defined as the ratio, given as a percent, of the weight of water to the weight of sediment grains based on the oven-dried weight of the sediment (Holtz and Kovacs, 1981). All water content values were corrected for salt content according to ASTM procedure D2216-71 (Bowles, 1970; ASTM, 1981).

Sediment analysis:

Grain size analyses were conducted on 139 samples from chosen intervals in the cores. The phi scale is used for grain size measures (Krumbein, 1934). Ninety-three complete grain size analyses (down to 11 phi at 0.2 phi intervals) were run at the Atlantic Geoscience Centre on the computer-driven settling tower and sedigraph 5000D. Sample preparation included dispersing the original sediment by 45 minutes of rigorous shaking in a 4 % sodium hexametaphosphate (calgon) solution, separating the sand and gravel fraction from the muds using a 4.25 phi (53 micron) mesh sieve, separating the gravel from the sand using a -1 phi (2 mm) sieve, and splitting the sand to a sample size of about 1.5 g for analysis in the settling tower. Size data were calculated from the settling velocity using Gibbs' equation (Gibbs et al., 1971). The fine fraction was subsampled using a pipette to obtain about 1.5 g of sample. This fraction was then insonified in an electrolyte solution for about 10 seconds before analyzing in the sedigraph.

25

Gravel, sand, silt, and clay percentages only were determined
for 46 samples. The gravel and sand fractions were separated from
the mud by sieve according to the methods explained above. The
remaining fine fraction was analysed in the sedigraph 5000D
system.

Grain size percentages are given and discussed throughout this
thesis as weight percentages. Data were output as computer
calculations of cumulative and frequency curves, moment measures on
mean and median grain size, standard deviation, skewness, and
kurtosis values (see Hackett et al., 1986). Statistical measures
were computed using the method of moments (Krumbein, 1936; Krumbein
and Pettijohn, 1938; Inman, 1952). The terminology used for
referring to grain size classifications is that proposed by
Wentworth (1922), as presented in Folk (1980).

Other Analysis:

Organic carbon content was determined using the loss-on-
ignition technique on a Leco Carbon Analyser, model WR12.
Approximately 1 g of sediment was oven dried and crushed for each
analysis. The difference in weight before and after incineration
yields the weight of carbon in the sample. It is expressed as a
weight percent.

Over 300 foraminifera per sample were hand picked from the
sand fraction of selected samples for foraminiferal abundance
studies. Foraminifera were identified by Gus Vilks at the Atlantic
Geoscience Centre.

Radiocarbon dating was conducted by Beta Analytic
Laboratories. These dates were obtained by analyzing material from
mollusc shells found within the cores. Due to the small sample
size analysis required the recently developed Accelerator Mass
Spectometry (AMS) technique for dating.

Oxygen isotope analyses were conducted on the planktonic
foraminifera Neogloboquadrina pachyderma by A.E. Aksu at Dalhousie
University according to the methods discussed by Aksu (1985). All

samples analysed contained more than 0.5 mg carbonate (200 specimens). The isotopic ratios are expressed as per mil ($^O/_{OO}$) difference between the $^{18}O/^{16}O$ in the samples and that in the laboratory standard "Pee Dee Belemnite" (PDB) (Aksu, 1985).

1.8 Statement of Work

Piper and co-workers have conducted extensive surveys in the Verrill Canyon area, and have published on the results and interpretations of this work. Their interpretations are based primarily on acoustic data and lack sedimentologic groundtruthing. They also had no chronologic or climatic framework on which to base interpretations. These insufficiencies are especially evident in their interpretation of the disturbed zones, in spite of little sedimentologic evidence. This thesis is aimed at examining sediments of the area in order to integrate acoustic and sedimentologic information. The results may serve to support, refine, or challenge the theories of Piper and others on the Wisconsinan geologic history of the Verrill Canyon area.

The author commenced work on this project in January, 1984. Abundant data had been collected prior to this date. Cruises 82004, 82014, and 83012 had taken place and thus the majority of acoustic information and cores had been collected. The cores from these cruises were described preliminarily (Piper and Wilson, 1983) and the acoustic information was interpreted (Piper et al., 1983). The author did not take part in cruise 84029 but the data had not been used beyond interpretation of small sections of the seismic and sidescan records (Hutchins et al., 1985). The author did, however, take part in cruise 85001 to the Verrill Canyon area, and cruise 84003 on the St. Pierre Slope - Laurentian Fan, as this area was initially to be part of the project.

As part of the research for this thesis the author conducted the following work: 1) detailed descriptions of all cores including taking and processing X-radiographs of the cores (including all cores collected from 84003); 2) the development of the slabbing technique (Mosher and Asprey, 1986) for viewing the

fine structures of sediments in X-radiographic prints. 3) the
design and construction of light boxes to facilitate simultaneous
X-radiograph viewing and core description; 4) grain size analysis
on all sediment samples from the studied cores; 5) Taking of vane-
shear, water content, and bulk density measurements on the 85001
cores (and 84003 cores), and subsampling of all cores for other
geotechnical tests; 6) review of previously collected and new
(84029 and 85001) acoustic information, and revision of
interpretations based on this review; and 7) the extension of the
previously established acoustic stratigraphy to accommodate new
data and the establishment of this acoustic stratigraphy at the
core sites.

CHAPTER 2
ACOUSTIC DATA

2.1 Introduction

Side-scan sonographs and high-resolution seismic reflection profiles have proven useful for the interpretation of sedimentation processes active both at the present and during the Late Quaternary (Knott and Hersey, 1956; Egloff and Johnson, 1975; Damuth, 1978, 1980; Flood, 1980; Ryan, 1982; Simm and Kidd, 1983; Hutchins et al., 1985). As discussed in the preceding chapter, the thesis area has been surveyed with various acoustic systems. Data collected during surveys prior to 1984 have been presented in two open file reports and one publication: Piper and Wilson (1983), Piper et al. (1983), and Piper et al. (1985). Figure 2.1 is a morphologic map resulting from these studies. This chapter shall integrate the findings of these reports with data collected during two subsequent cruises (Hu84029 and Hu85001).

2.2 Acoustic Characteristics

Verrill Canyon:

The steep slopes of the canyon walls' yield poor acoustic return signals, and the irregular morphology of the walls and floor causes hyperbolic reflections, thus few useful seismic data can be collected from Verrill Canyon. Parts of the canyon walls and the floor appear to be overlain by 5 to 10 ms (7-15 m) of acoustically transparent sediments which Piper and Wilson (1983) interpret as debris flow deposits.

Scotian Shelf:

V-fin sparker profiles on the continental shelf north of the study area reveal up to 40 ms (ca. 30 m) of sediment overlying a strong reflector inferred by Piper and Wilson (1983) to be Tertiary bedrock. The lower 20-25 ms (15-19 m) has the acoustic

Figure 2.1 Morphologic features map of Verrill Canyon area with
          core locations. Main features of the map are two
          disturbed zones and two valleys. Verrill Canyon is in
          the northeast of the map area (after Piper et al.,
          1983, 1985).

62°00'　　　　61°50'　　　　61°40'　　　　61°30'　　　　61°20'

RELICT ICEBERG SCOURS

POCKMARKS

43°00'

26
○

27
500m

VERRILL CANYON

21
○

22
○

24

25
○

29
○

EASTERN
DISTURBED
ZONE

K-62

WESTERN
DISTURBED
ZONE

52
○

42°50'

51
○

H-100

37

33
○

32
○

56
○

55　54

34
○

SCOURS

42°40'

SCOURS

36

SCOURS

EAST

310

ACADIA

WEST

ACADIA

VALLEY

| | SANDY VALLEY FLOOR |
| | DISTURBED MATERIAL |

SCARPS

	>30m
	10-30m
	<10m
	ROUGH SEABED
	FLAT VALLEY FLOOR
●	WELL
○	CORE
	TILL TONGUES

B　A

VALLEY

2500m

0　　　5　　　10

km

42°30'

31

characteristics of till (cf. King and Fader, 1986). Overlying this
unit is 10 ms (ca. 7 m) of evenly stratified sediment interpreted
as either sand and gravel or till (Piper and Wilson, 1983). The
uppermost 2-7 ms (1-5 m) of sediment rests unconformably on the
underlying sequence. It shows discontinuous stratification,
including prograding channel fill. This configuration may have
developed during progradation of a barrier beach system (Piper and
Wilson, 1983). Figures 2.5 and 2.6 (p. 40 and 42) show the
massive, incoherent character to acoustic records, interpreted to
represent till, on the outer shelf and uppermost slope.

Upper Slope:

The shelf break and slope, to about 400 m water depth, are
characterised by a sharp initial bottom return with no or little
subbottom penetration on the 3.5 kHz and V-fin sparker systems (the
SEABED II system achieved some penetration). This type of record
is created by acoustic reflections from a hard bottom. It
originates from a coarse sand and gravel lag, relict from the
Wisconsinan low sea-level stand (King, 1970; Swift, 1985). A
rough, erosional seafloor and downslope trending gullies have been
observed in this area (<700 m) (Fig. 2.2).

Sidescan images from the SEABED II system reveal relict
iceberg furrows and pockmarks (gas escape features, see Josenhans
et al., 1978) on the seabed in this area down to about 600 m water
depth (Figs. 2.3 and 2.4). Relict scours and pockmarks have been
noted on the Scotian Shelf (King and MacLean, 1970; Josenhans et
al., 1978; King, 1980) but not this deep on the Scotian Slope prior
to cruise Hu84029 with the SEABED II system.

Acoustic penetration increases beyond about 400 m water depth
to reveal a thick sequence of parallel reflectors representing well
stratified sediments (Figs. 2.5, 2.6, 2.7). Throughout much of the
study area Quaternary sediments are relatively evenly stratified.
Individual reflectors can be correlated over tens of kilometers
(Piper et al., 1985), though sediment thicknesses tend to decrease
downslope and locally vary along strike. Most reflectors

Figure 2.2 V-fin sparker profile of the uppermost slope. Note
poor acoustic penetration and erosional characteristic
of the seabed (gullies and depressions).

34

Figure 2.3 Nova Scotia Research Foundation sidescan image of
upperslope - shelf break area showing relict iceberg
furrows.

RELICT ICEBERG SCOURS

NORTH

SOUTH

RANGE IN METRES

150   75   0   75   150

DISTANCE (KM)

0   1   2   3

36
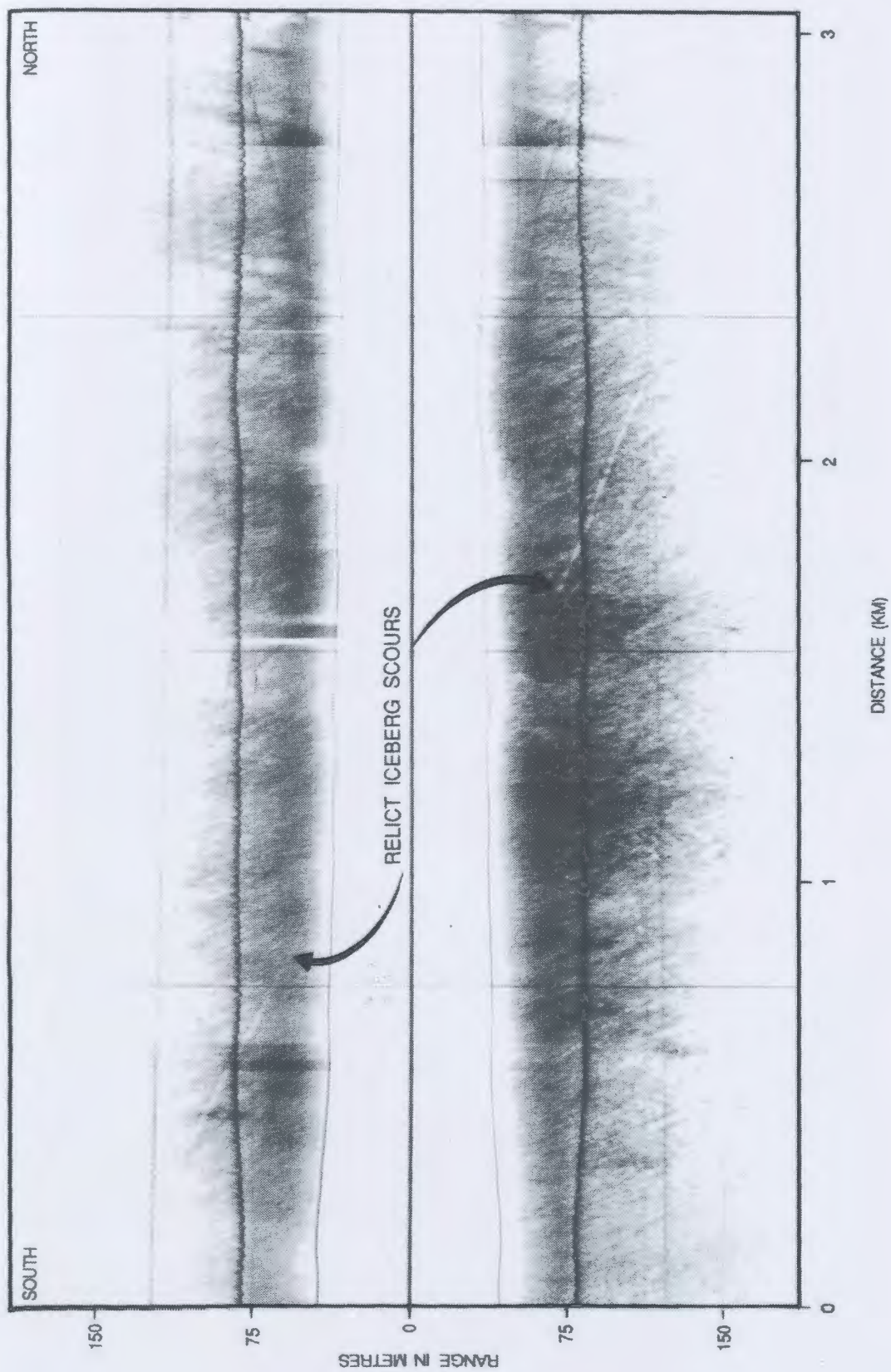
Figure 2.4 SEABED II sidescan image of upperslope showing
            pockmarks, marginal escarpment, and hummocky surface
            characteristic of disturbed zone (note that the
            pockmarks continue into the upper portion of the
            disturbed zone).
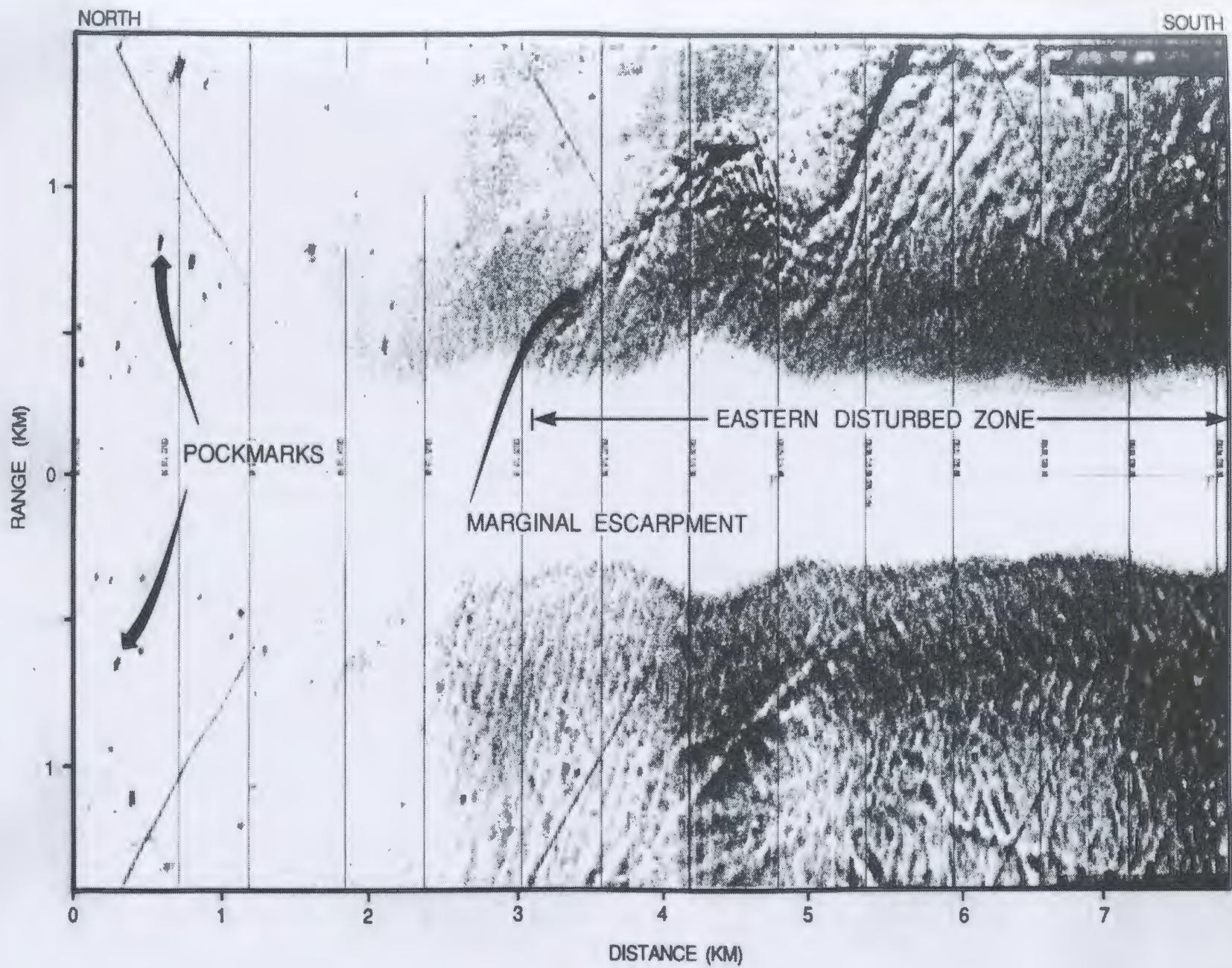
Figure 2.5 Forty cubic inch airgun profile from the upper slope
showing coherent, parallel reflectors which thin in the
downslope direction. Note the two sediment tongues
which show a till-like echocharacter and extend into
the upperslope stratigraphy from till deposits on the
outer shelf.

WATER DEPTH IN MILLISECONDS
(2-WAY TRAVELTIME)

WATER DEPTH IN MILLISECONDS
(2-WAY TRAVELTIME)

TILL-LIKE
TONGUES

TILL-LIKE
TONGUES

RED

NORTH

SOUTH

KILOMETRES

WATER DEPTH IN METRES

WATER DEPTH IN METRES
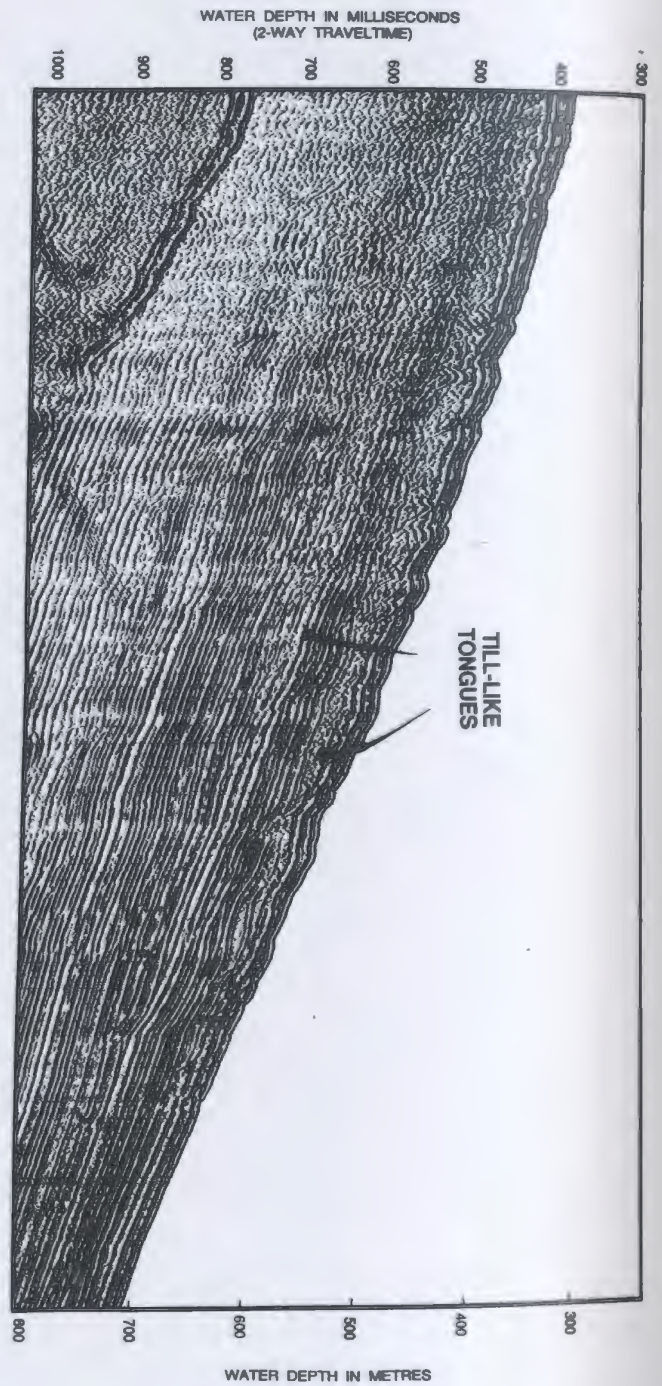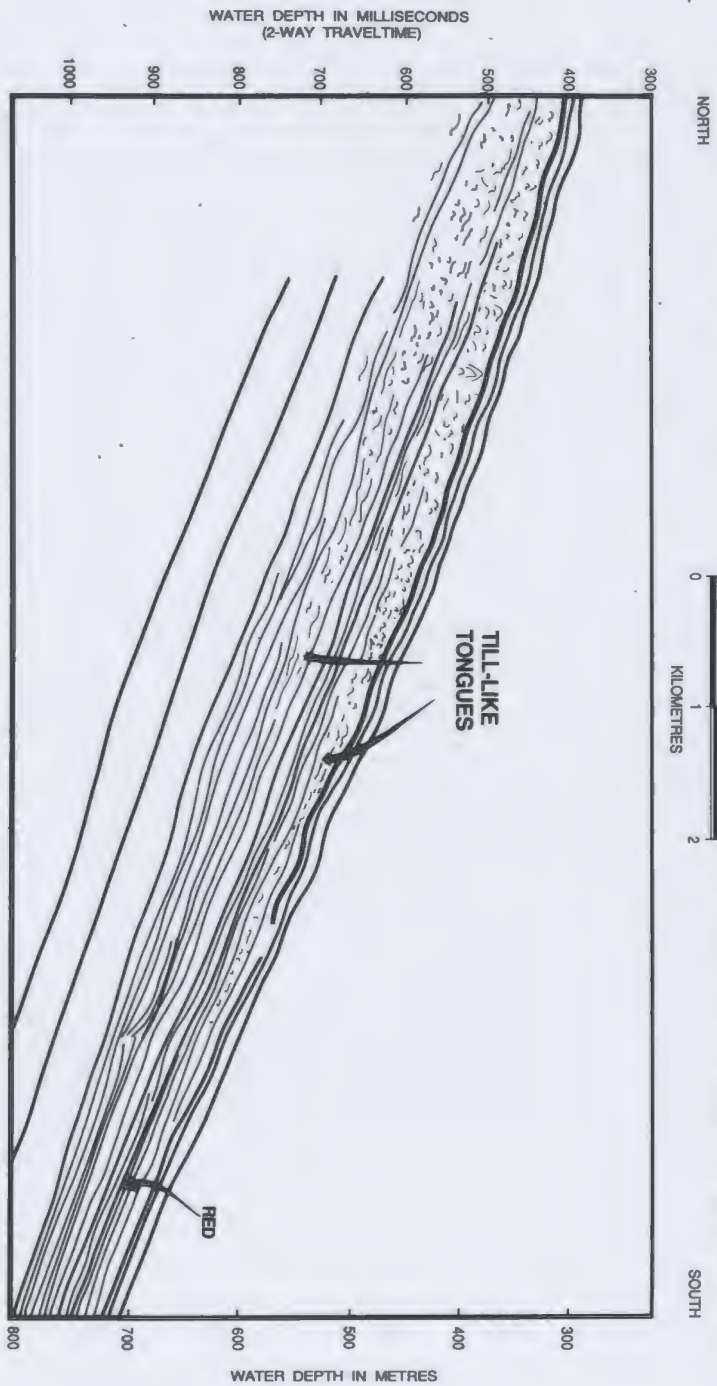
Figure 2.6 SEABED II boomer profile across the outer Scotian Shelf
            and upper slope. Note the two till-like tongues which
            are rooted in outer-shelf tills. Remaining slope
            reflections are parallel, stratified in nature, and
            thin down slope. These horizons appear rooted in the
            outer-shelf tills and till-like tongues. Note the
            interbedded, thin, acoustically incoherent horizons,
            possibly representing debris flow events. Note also
            the stratigraphic depth of traced acoustic horizons
            (Red and Yellow). The large-scale sinuousity of the
            profile was caused by heave in the towed vehicle.
            Small-scale surface irregularities are considered real.

WATER DEPTH IN MILLISECONDS (2-WAY TRAVEL TIME)

WATER DEPTH IN METRES

NORTH

SOUTH

1 KM

ICEBERG SCOUR OR EROSIONAL GULLY

TILL-LIKE TONGUE

OUTER SHELF TILL

YELLOW

RED

TILL-LIKE TONGUE

42
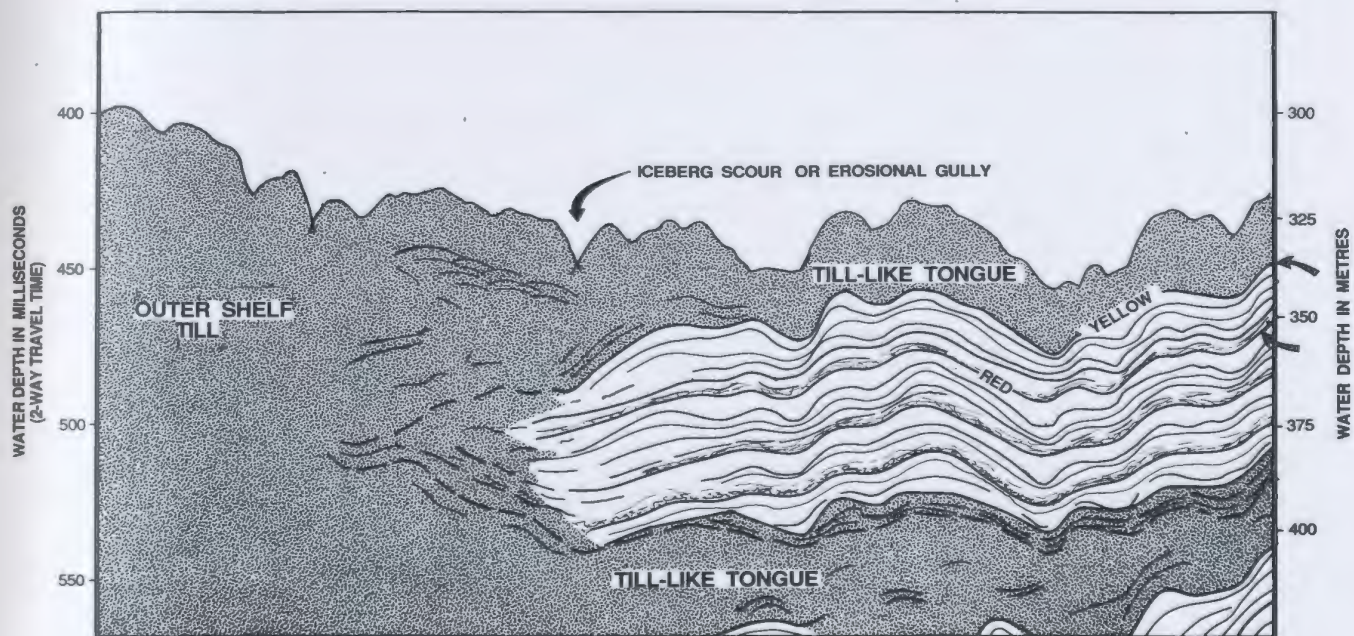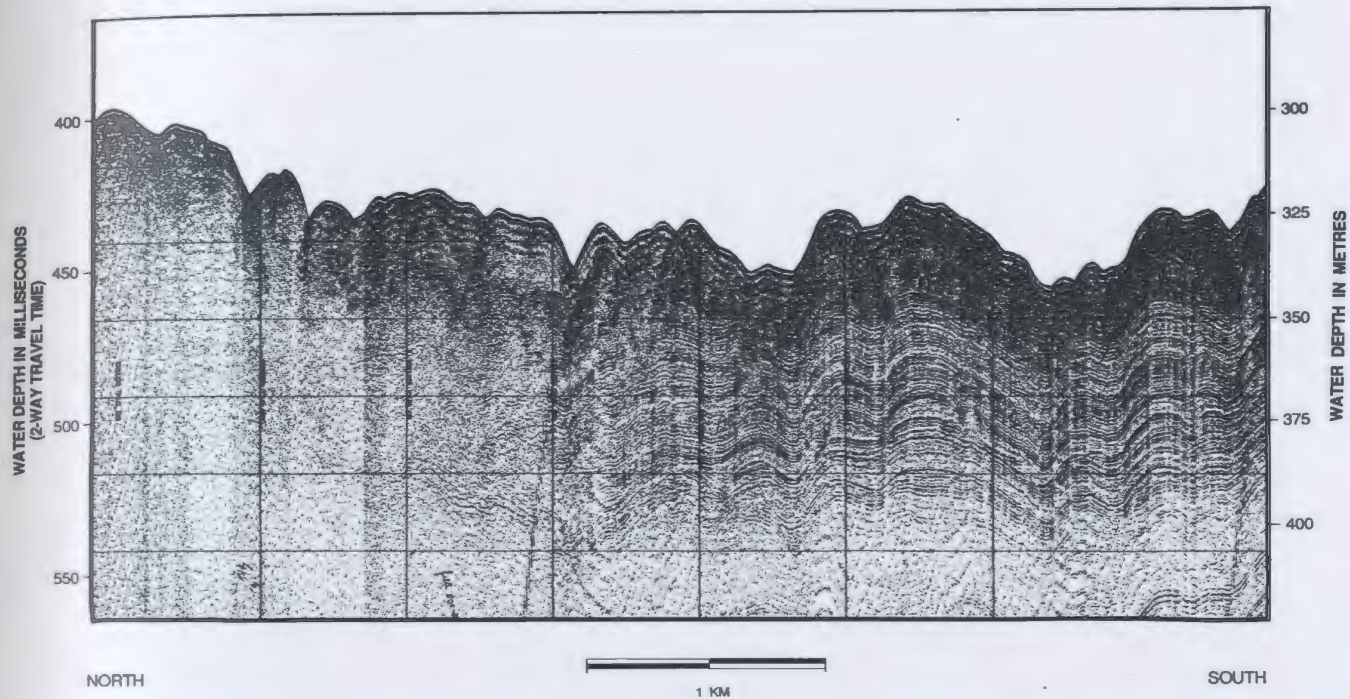
Figure 2.7 SEABED II boomer profile downslope of Figure 2.6. Note that the till-like tongues pinch out, and are stratigraphically equivalent to disturbed zones. The remaining horizons in the figure are evenly stratified, thinning downslope, glacial-marine sediments. Thin, acoustically incoherent, but traceable reflections are interbedded with the stratified sediments. Note the stratigraphic position of the Red and Yellow reflections. Sinuosity of the profile was caused by heave in the towed vehicle.

NORTH

1 KM

SOUTH

TILL-LIKE
TONGUES

EASTERN DISTURBED ZONE

YELLOW

RED

YELLOW

RED

BURIED DISTURBED ZONE

WATER DEPTH IN MILLISECONDS
(2-WAY TRAVEL TIME)

WATER DEPTH IN METRES

WATER DEPTH IN MILLISECONDS
(2-WAY TRAVEL TIME)

WATER DEPTH IN METRES

44
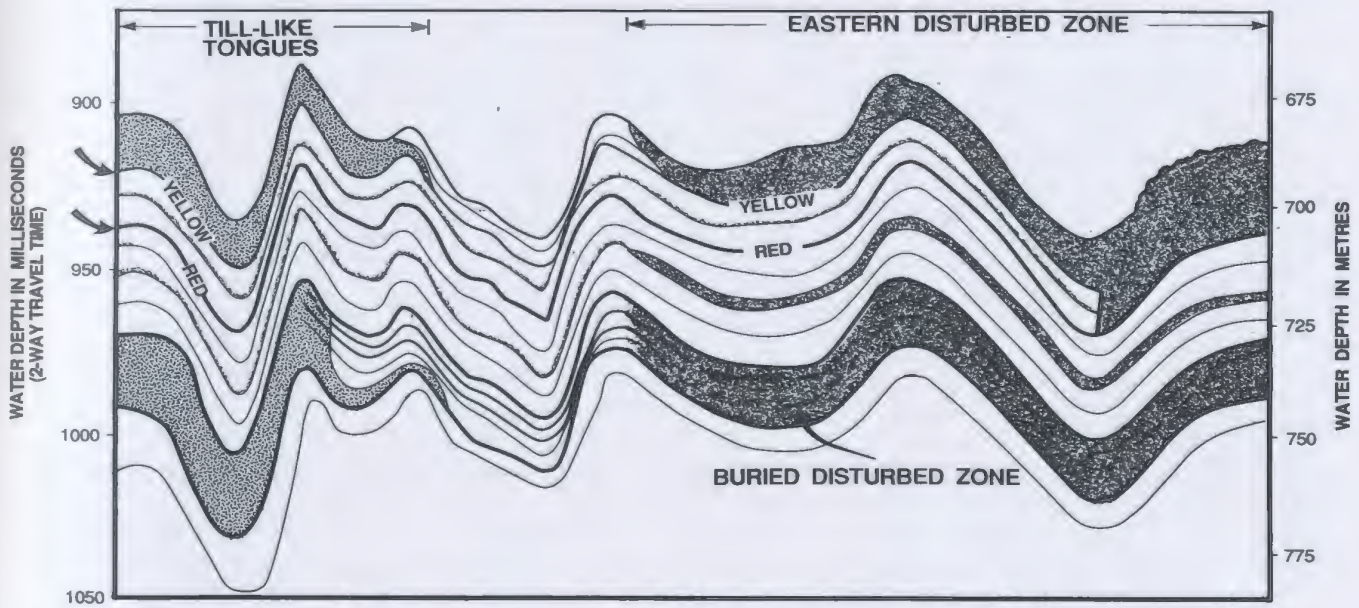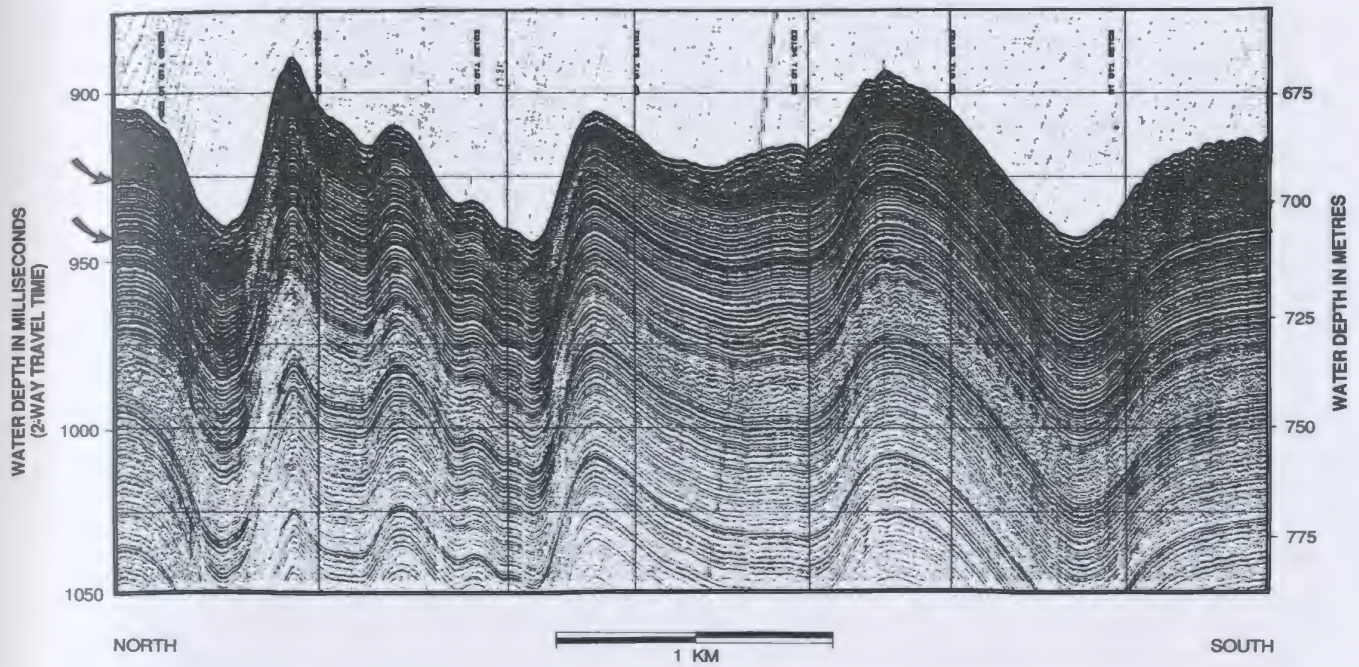
throughout the study area can be traced upslope to terminate in the outer shelf till deposit.

On the upper slope and interbedded with the sequence of parallel reflectors are wedged-shaped beds which pinch out downslope and show incoherent reflections within the bed (Figs. 2.5 and 2.6). They are best observed on Huntec boomer, airgun, or V-fin sparker profiles. It is possible to see these beds at two subbottom horizons. They are referred to as tongues because of their shape. The acoustic characteristic of these tongues resembles that interpreted for till (i.e. the massive, incoherent, amorphous character - cf. King and Fader, 1985), but without sampling they cannot be identified as such. They are therefore referred to as till-like tongues.

The uppermost tongue can be seen on the airgun records of the Hu85001 cruise (Fig. 2.5). This tongue occurs at about 13 ms (ca. 10 m) subbottom on the upper slope. It thins downslope, where at 700 m water depth it is about 35 ms (ca. 25 m) thick and occurs within 6 ms (ca. 4 m) of the seabed surface. The same tongue can be seen further east in the study area on SEABED II profiles from cruise Hu84029 (Fig. 2.6). Here the tongue occurs at 5 ms (ca. 4 m) subbottom and is 35 ms (ca. 25 m) thick at its uppermost slope setting. It continues downslope for about 7 km (660 m water depth) where it has thinned to only 1 ms (ca. 1 m) thick but still occurs at 5 ms (ca. 4 m) subbottom.

A second, underlying tongue is apparent on the Huntec boomer records of the SEABED II system (Fig. 2.6). The surface of this tongue can be seen at 90 ms (68 m) subbottom at its uppermost slope position, where it is about 25 ms (19 m) thick. It gradually thins downslope to about 700 m water depth where it occurs at 52 ms (39 m) subbottom and is 17 ms (13 m) thick. It is stratigraphically equivalent to the horizon which Piper et al. (1985) termed a buried disturbed zone (Fig. 2.7). The second tongue on the Hu85001 airgun record (Fig. 2.5) is at 120 ms (90 m) subbottom and is 40 ms (30 m) thick at 400 m water depth. It thins to 25 ms (19 m) thick and 110 ms (82 m) subbottom by 500 m water depth.

45

It can be argued that these tongues are not till tongues in
their strictest sense (cf. King and Fader, 1986), but rather a
complex deposit of outwashed and slumped glacial sediment released
from a nearby ice margin, probably at the shelf-edge. Without
coring into the units it is impossible to interpret their origin
with any degree of certainty. The important point to note about
these acoustic packages is that they are rooted in possible shelf-
edge till (Figs. 2.5 and 2.6) and hence the material within the
package is likely glacial sediment.

Mid to Lower Slope: Slide Scarps

Between approximately 700 and 2500 m water depth sidescan and
seismic data show widespread occurrence of step-like escarpments
(Fig. 2.8). These features are the scarps left from bedding-plane
slide detachment (Piper et al., 1985), resulting in a terraced
morphology to the seabed and the abrupt termination of reflectors
at each scarp face. The scarps are relatively linear, face
downslope, and are parallel or subparallel to contours. The
escarpments provide evidence that sections of the study area have
had 5-20 m thickness of surface sediment removed (Piper et al.,
1983). Piper et al. (1985) estimate surface sliding has removed
between 4 and 7 X $10^9 m^3$ of sediment.

Mid to Lower Slope: Disturbed Zones

The most notable features within, and comprising almost half
of the studied region are two large areas where the seabed
morphology is highly irregular (Figs. 2.4, 2.9, and 2.10). The
surface of these areas appears hummocky, in many places yielding
hyperbolic acoustic returns on seismic profiles (Figs. 2.9 and
2.10). Pockmarks can be seen on the up-slope end of the surface of
the disturbed zones (Fig. 2.4). Subbottom reflectors are lacking
in the upper 5-15 ms (3-12 m) of sediment in these zones giving the
acoustic records a semi-transparent character (terminology of
Damuth, 1980). The absence of any structure suggests that the zone
lacks any internal organization, or is comprised of tilted blocks

Figure 2.8   Sea MARC I sidescan image and 4.5 kHz profile showing
             scarps resulting from bedding-plane slide detachment,
             and streamlined erosional depressions, interpreted as
             linear scours (Piper et al., 1985). Scarps and scours
             such as these permit coring to deeper stratigraphic
             depths than is otherwise possible by standard piston
             coring techniques (from Piper et al., 1985).

SCARP

SCARP "a"

SCOURS

TOW
VEHICLE
TRACK

61°41'W

61°40'W

42°39'N

42°40'N

SIDESCAN

0   km

SW   SCOURS   NE

SCARP "a"

1700
1800
1900
2000

WATER DEPTH (m)

0   1
km

4.5 kHz SUB-BOTTOM PROFILE
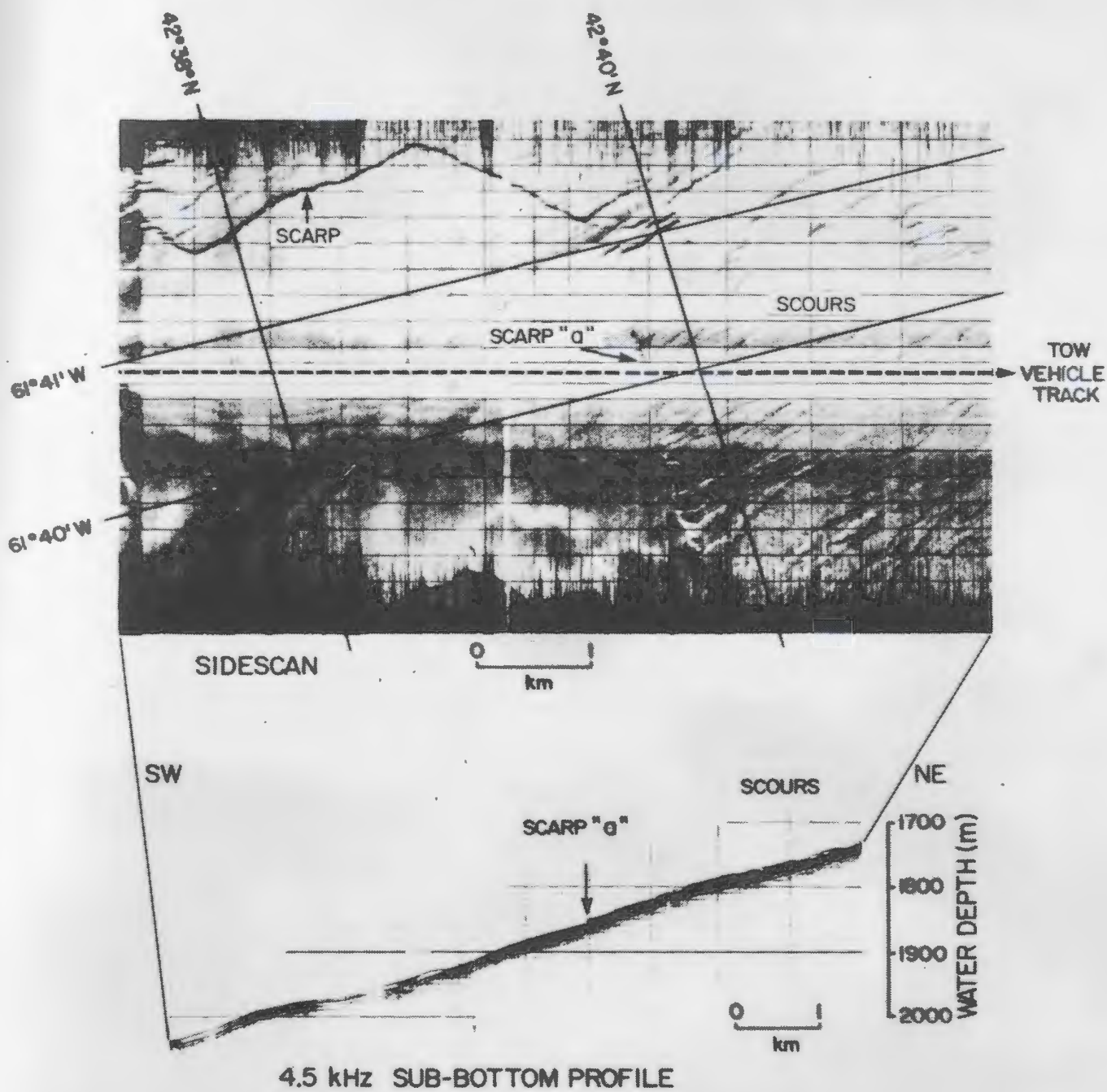
which are small or have dips of more than 15° (Piper et al., 1985). The sediments underlying the disturbed zones are well stratified.

The two anomalous areas are termed the eastern and western disturbed zones by Piper et al. (1985) (Fig. 2.1). The eastern zone is some 5 km wide and extends downslope towards Verrill Canyon. The western disturbed zone is 15 km wide. The two zones are separated by about 5 km of evenly stratified sediment. Further west from the western zone is another area of undisturbed, stratified sediment. The disturbed zones are roughly lobate in plan-view and in profile are thickest at their upslope ends. They appear to originate from the upperslope gullies in about 800 m water depth, and terminate at approximately the 1500 m isobath.

Upslope, the lateral margins of the disturbed zones are fault-bound (Figs. 2.9 and 2.10). Proceeding west on Figure 2.9 the hummocky surface terminates at a scarp, showing the start of an even bottom and parallel reflectors at the near-surface. Deeper in subbottom, however, the profile still shows a semi-transparent zone of no reflectors. The profile is thus still within the disturbed zone. Still further west, continuous internal reflectors are identified at all depths commencing at a recognizable fault. This fault marks the beginning of the undisturbed zone. Downslope, the disturbed zones may either terminate at slide scarps or valleys, or thin on low gradients. Marginal escarpments at the edges of the disturbed zones suggest material has been removed from the surface (Fig. 2.9 and Appendix A - Figs. A12 and A15).

Sets of long, sinuous, subparallel ridges are prominent features on the surface of these disturbed zones. They are typically 6-10 ms (3-5 m) high with a wavelength of 50 m. Generally they are parallel to the contours (transverse to the inferred direction of flow), but tend to swing around at the edges of the disturbed zone to become subparallel to the margin. The most distal parts of the disturbed zones lack these surface ridges.

49

Figure 2.9 V-fin sparker profile showing hummocky morphology and
            semi-transparent internal acoustic character of
            disturbed zones, fault-bound marginal slide block, and
            undisturbed area between the two disturbed zones. Note
            also the key acoustic reflectors.

WATER DEPTH IN METRES

WEST

EAST

WATER DEPTH IN MILLISECONDS
(2-WAY TRAVEL-TIME)

1 KM

WATER DEPTH IN METRES

UNDISTURBED

FAULT

MARGINAL
SLIDE
BLOCK

FAULT

EASTERN
DISTURBED
ZONE

BROWN

GREEN?

RED

YELLOW

RED

PINK

WATER DEPTH IN MILLISECONDS
(2-WAY TRAVEL-TIME)
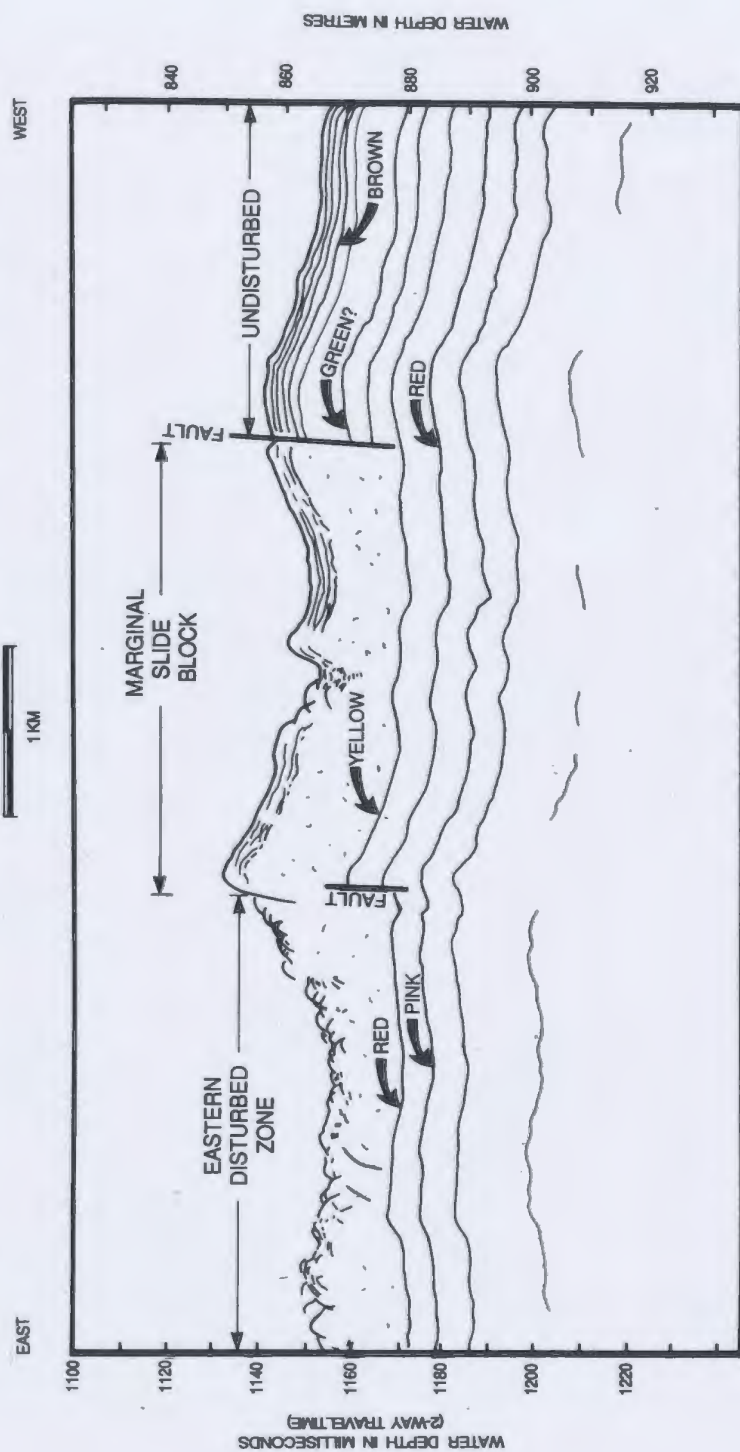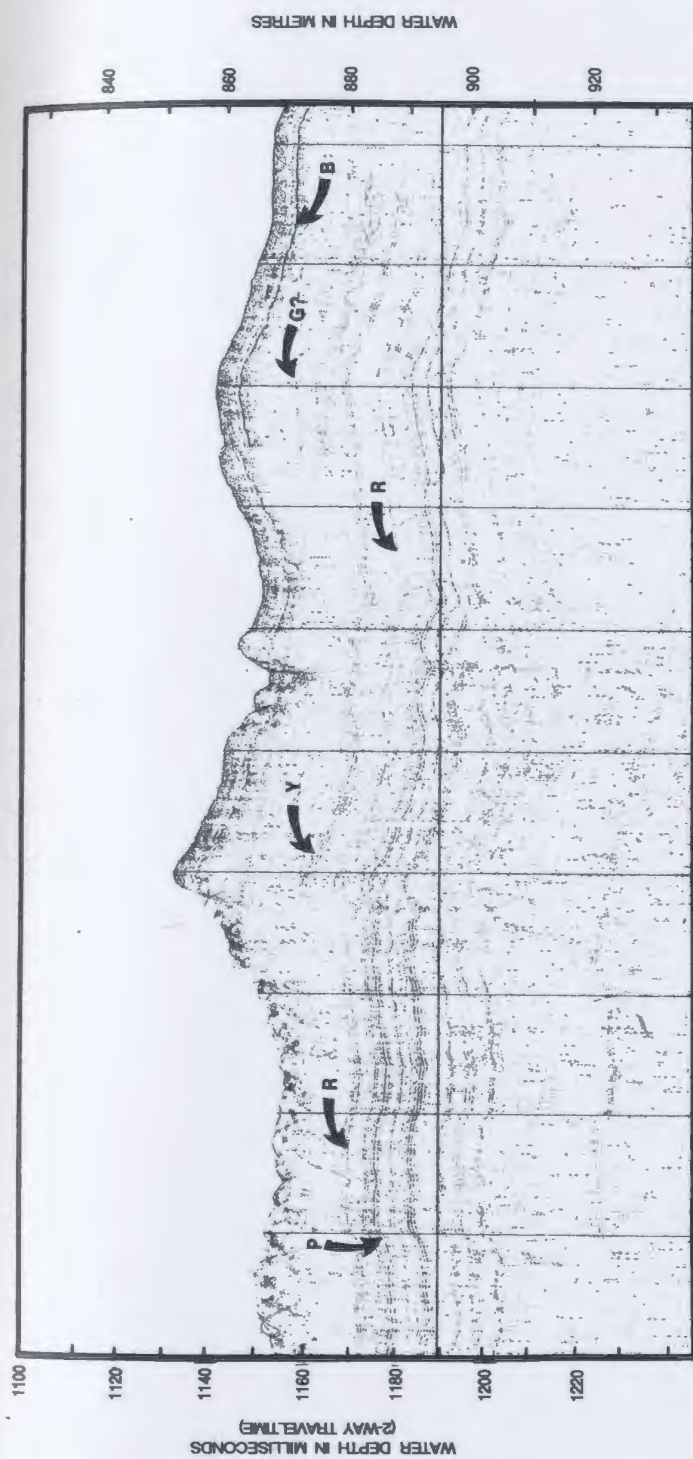
Figure 2.10 V-fin sparker profile over the western disturbed zone
and East Acadia Valley, showing the generally draped
sediment configuration and the distribution of surface
and subsurface disturbed sediment zones (from Piper et
al., 1985).
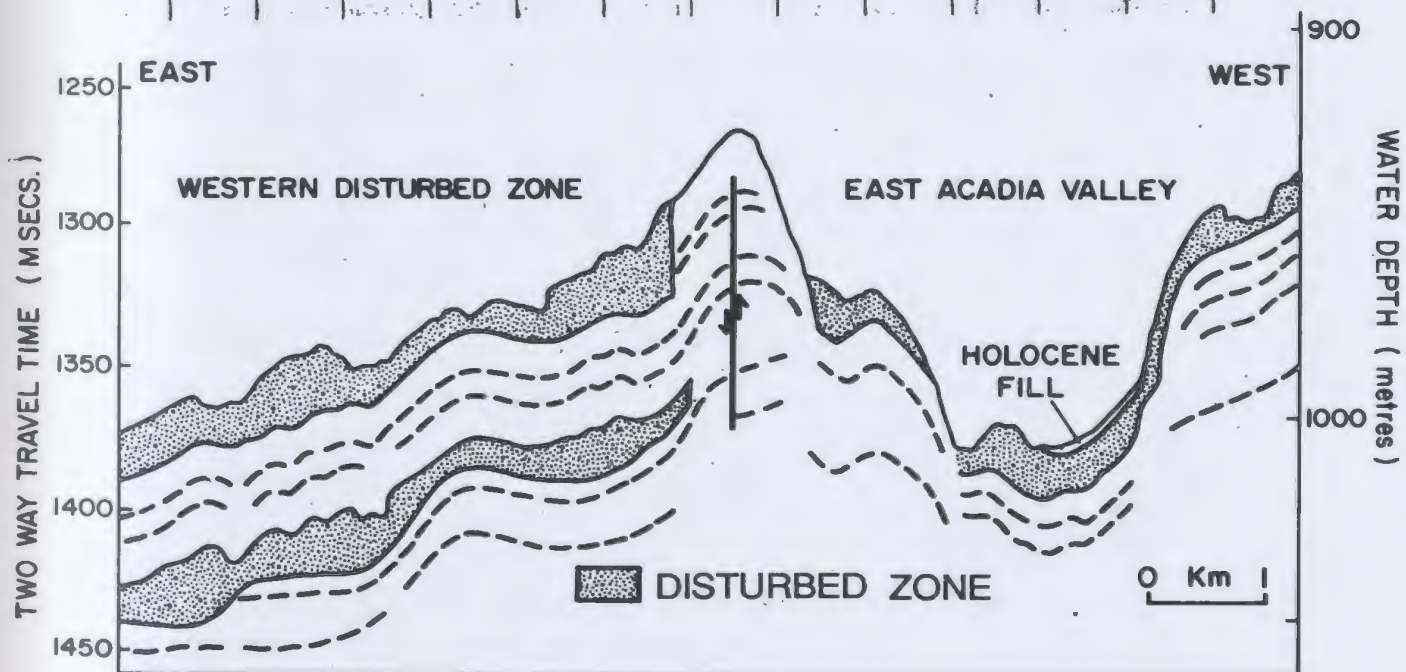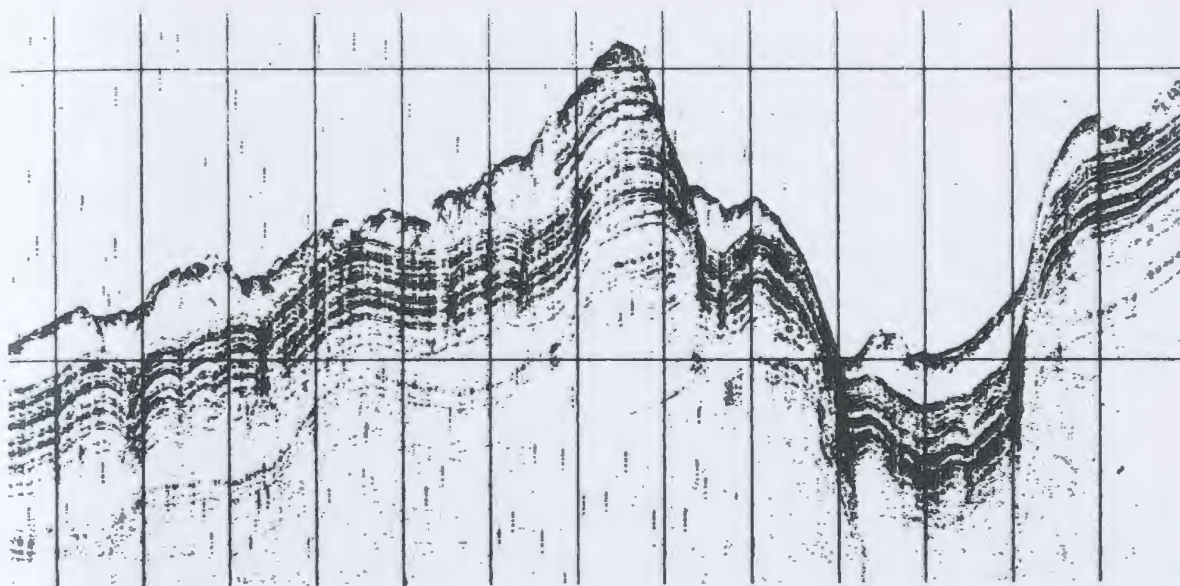
According to Piper et al. (1985) the total volume of disturbed sediment approximates 5×10^9 m^3. This volume consists largely of material derived from sediment slides that have slipped downslope. The surface morphology of the two zones is similar to that seen in retrogressive rotational slumps, both of marine and terrestrial environments (Piper et al., 1983, 1985).

V-fin sparker and Huntec profiles reveal a subsurface horizon with a similar acoustic signature to the disturbed zones at the surface (Figs. 2.7 and 2.10). This buried disturbed zone is approximately 6 ms (ca. 4 m) thick and is characterised by incoherent reflections and a hummocky surface. It is stratigraphically equivalent, and continuous with, the lowermost till-like tongue, but varies slightly in acoustic character from the tongue (Figs. 2.6 and 2.7). It may be interpreted that this zone represents a thick accumulation of debris flows originating from the till tongue. Alternatively it can be interpreted as an older equivalent to the surficial disturbed zones (i.e. zone of surficial sediment failure) (Piper et al., 1985). It can also be interpreted as a zone of internal deformation such as described by O'Leary (1986) on the New England continental slope, or Hill et al. (1982b) in the Canadian Beaufort Sea.

The sediments above and below the disturbed zones consist of coherent, conformable, draping reflections, though the SEABED II profiles of Figures 2.6 and 2.7 show numerous thin horizons between the two tongues, which demonstrate a similar acoustic character to the disturbed zones. These horizons can be traced from the outer-shelf till for many kilometres downslope. They may represent thin, apparently non-erosive, debris flows which travelled downslope from the outer-shelf till. They may also represent thin zones of internal deformation, though it seems unlikely as they can be traced over great distances at the same stratigraphic horizon, no faulting is observed associated with them, and they are rooted in the outer-shelf till.

Mid to Lower Slope: Streamlined Erosional Depressions

Sidescan images downslope from the western disturbed zone show the seafloor is marked by a field of down-slope trending, streamlined, linear depressions that are interpreted as scours (Piper, et al., 1985) (Fig. 2.8). These depressions vary quite considerably in plan-view size (50-2000 m long, and 10-700 m wide) and shape, but everywhere they have flat floors and are only a few meters deep. Their margins, both up and down slope, are generally pointed, though some are subrounded to complexly indented.

The morphology and group association of the depressions suggest they were eroded by downslope travelling currents which selectively scoured easily erodible material (Piper et al., 1985). The currents which created these features were possibly initiated by the slumping event which produced the disturbed zones. These features have been seen by sidescan sonar (Sea MARC) on other continental slopes, yet there origin is still uncertain (W.B.R. Ryan, personal communication, 1986).

Mid to Lower Slope: Valleys and Channels

East and West Acadia Valleys trend south – southeast (Fig. 2.1) and are asymmetric in cross-section with steep walls. These walls can reach as much as 70-200 ms (50-150 m) above the valley floor (Fig. 2.10, Appendix A – Fig. A4). The levees are higher and steeper in the upslope reaches of the valleys. Several small valleys and channels (50-100 m wide and 2-5 ms (1-4 m) deep) lie west of the West Acadia Valley and between the two valleys (Appendix A – Fig. A10). They parallel the main valleys rather than feed into them.

The floor of the West Acadia Valley appears hard from acoustic profiles; possibly representing sandy material (Appendix A – Fig. A4). In contrast the floor of the East Acadia Valley is filled with approximately 10 ms (ca. 7 m) of acoustically transparent sediment: probably debris flow material (Fig. 2.10)

(Piper and Wilson, 1983). These valleys are presently inactive, and are covered by a Holocene drape. They probably acted as conduits for the downslope transport of sediment in the late Pleistocene (Piper et al., 1985).

Mid to Lower Slope: Large Slump Features

Large slump scars are common in the study area, often with marginal escarpments 70–130 ms (50–100 m) high (Fig. 2.11). The majority of slumping appears to be into the Verrill Canyon, or associated with the East or West Acadia Valleys. Many slump scars are, however, noted downslope from the eastern disturbed zone. The slumps into the canyons and valleys may be attributed to failure due to oversteepening. The slumps that have occurred on gentle slope gradients must have been caused by static or cyclic loading, either from earthquake accelerations or from the displaced mass of the disturbed zone.

2.3 Acoustic Stratigraphy

The acoustic stratigraphy of the Verrill Canyon area was first established by Piper and Wilson (1983) and is also reported in Piper et al. (1983). They identified and traced several prominent acoustic reflectors throughout the study area. Table 2.1 summarizes their seismic type section with the addition of one new reflector (Brown) defined in this study. By tracing these reflectors through the seismic records (Fig. 2.12 and Table 2.2) it is possible to determine the acoustic stratigraphy at each core site where a seismic profile passes through or nearly through that site.

Considerable downslope thinning of the strata between reflectors is apparent (Table 2.2, and Table 2.3). For example, at upper slope crossovers (Table 2.2) Brown is a strong reflector at about 6 ms (4.5 m) subbottom and Red is a strong reflector at about 35 ms (26 m) subbottom. At lower slope crossovers Brown is so shallow that it is not distinguishable and Red occurs at about 15 ms (10 m) subbottom.

Figure 2.11 SEABED II boomer profile showing a 70 m mass-movement
scarp. This feature is the result of mass failure, not
faulting, as reflectors underlying the scarp are
continuous and coherent. Note the good depth of
subbottom penetration (100-150 m) with this system.
Note also the jagged appearance of reflectors is not
real but rather is a problem in the computer processing
program.

WATER DEPTH IN MILLISECONDS (2-WAY TRAVELTIME)

WATER DEPTH IN METRES

NORTH

SOUTH

1 KM

MASS-MOVEMENT SCARP
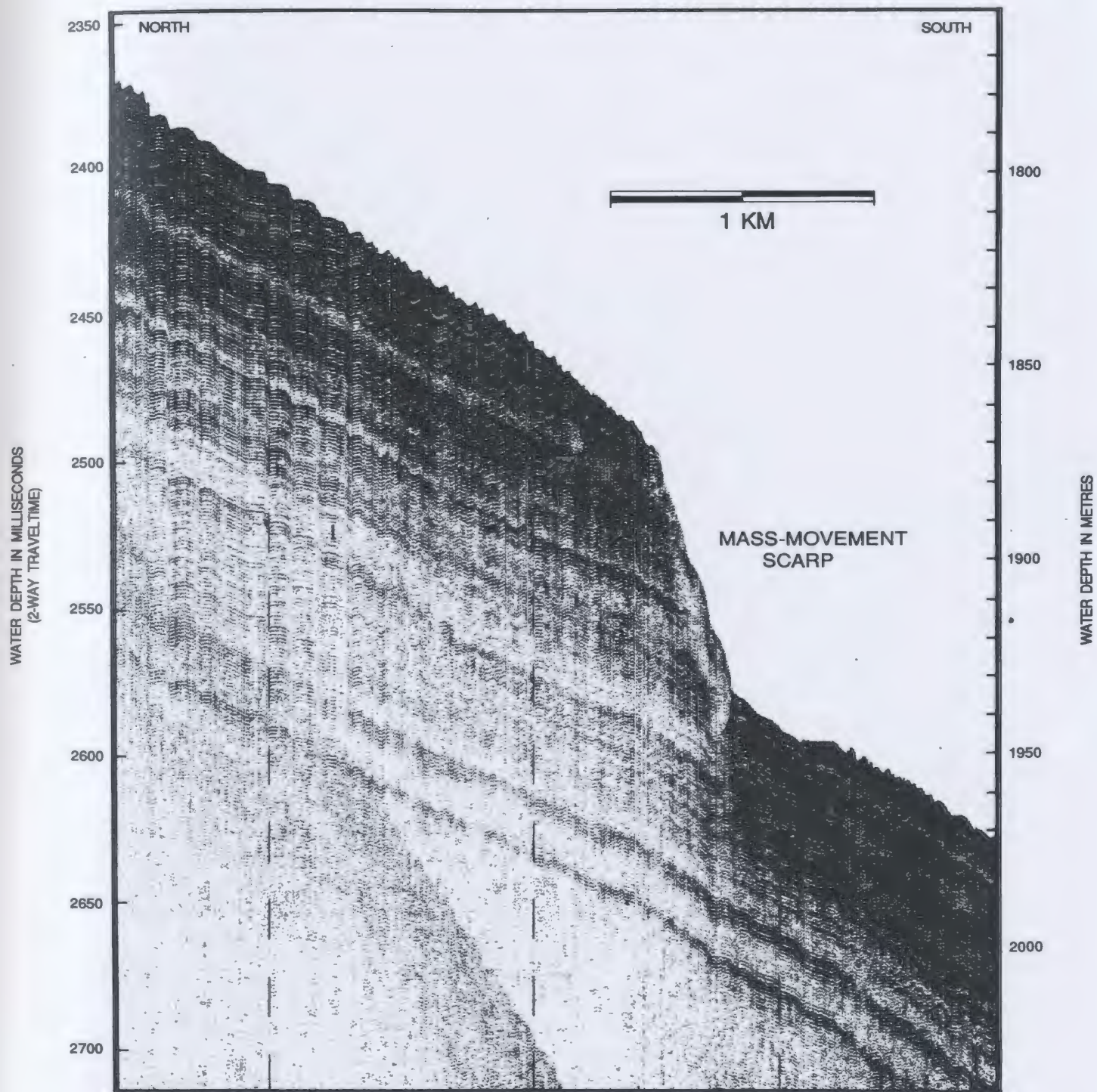
Figure 2.12 Tracks of data used to compile and trace the acoustic
stratigraphy through the core sites (see Tables 2.1,
2.2 and 2.3). C represents cross-overs. Crossovers
provide the chance to check the stratigraphy from one
record type to another and to ascertain that the
various horizons have been traced correctly.

60
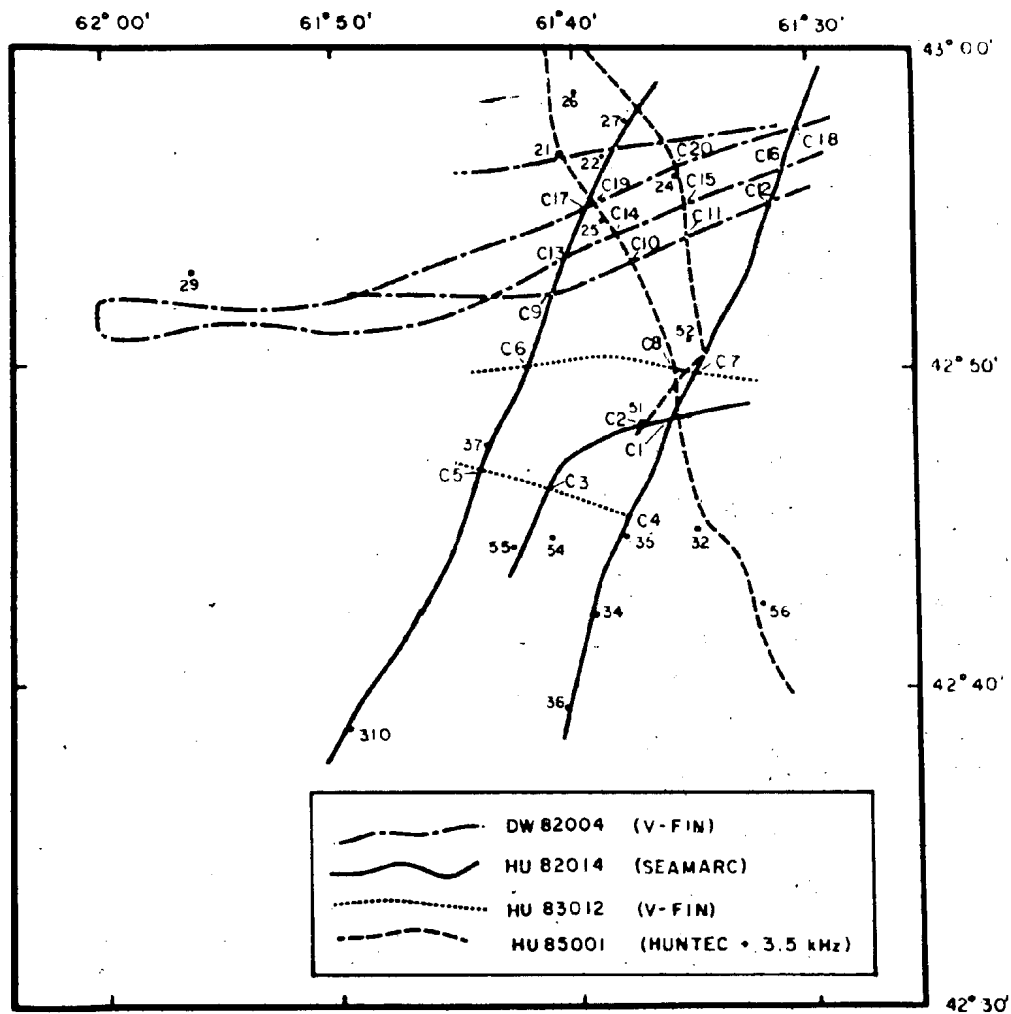
Table 2.1 Subbottom depths of key reflectors (in metres, V=1.5 km/s) (from Piper et al., 1983).

	Location	A	B	C	D
	Day	157	157	157	152
	Time	1530	1845	1950	1950
REFLECTOR					
	Surface	0	0	0	0
*Brown		4.5			
Orange		7			
Green		9		23	
Yellow		12		28	11
Red		18	19	37	18
Pink		25	26	?	25

* the Brown reflector is an addition of this study.

Table 2.2A Acoustic stratigraphy in m and (ms) at line cross-over points (Fig. 2.12).

Crossover	Brown	Orange	Green	Yellow	Red	Pink
C1	4.5 (6)	7 (9)	9 (12)	12 (16)	18 (24)	25 (33)
C2		7 (9)	9 (12)	12 (16)	25 (33)	17 (23)
C3				12 (16)	19 (25)	26 (35)
C4				6 (8)	11 (15)	16 (21)
C5					11 (15)	22 (29)
C6					5 (7)	
C7	5 (7)		9 (12)	12 (16)	19 (25)	28 (37)
C8	5 (7)		10 (13)	14 (19)	19 (25)	24 (32)
C9	4 (5)	?8 (10)	11 (15)	19 (25)	28 (37)	
C10	4.5 (6)	8 (10)		21 (28)	29 (39)	37 (49)
C11					22 (29)	
C12				6 (9)	16 (21)	20 (27)
C13	?4.5 (6)			13 (18)	21 (30)	29 (39)
C14	4.5 (6)	8 (11)	16 (22)	22 (29)	26 (35)	32 (42)
C15					14 (19)	19 (25)
C16				10 (13)	19 (25)	23 (31)
C17	6 (8)		11 (15)	20 (27)	28 (37)	
C18						
C19						
C20	5 (7)	10 (13)	12 (16)	22 (29)		

Table 2.2B Cross-over data collection: system types and ship times

Cross over	Cruise	Time (GMT)	System	Cruise	Time (GMT)	System
C1	82-014	157/15:30	SeaMarc	85-001	80/04:25	Huntec
		153/23:04	SeaMarc			
C2	82-014	153/22:20	SeaMarc	85-001	79/17:00	3.5 kHz
C3	82-014	153/20:10	SeaMarc	83-012	127/11:25	3.5 kHz
C4	82-014	157/13:20	SeaMarc	83-012	126/12:05	3.5 kHz
C5	82-014	152/15:10	SeaMarc	83-012	126/11:30	3.5 kHz
C6	82-014	152/18:20	SeaMarc	83-012	128/20:27	V-Fin
C7	82-014	157/16:00	SeaMarc	83-012	128/19:10	V-Fin
C8	85-001	80/03:55	Huntec	83-012	128/19:20	V-Fin
C9	82-014	152/19:30	SeaMarc	82-004	69/23:30	V-Fin
C10	82-004	70/00:09	V-Fin	85-001	80/02:54	Huntec
C11	82-004	70/00:30	V-Fin	85-001	79/22:36	3.5 kHz
C12	82-014	157/18:30	SeaMarc	82-004	70/01:05	V-Fin
C13	82-014	152/20:00	SeaMarc	82-004	70/03:50	V-Fin
C14	82-004	70/03:21	V-Fin	85-001	80/02:37	Huntec
C15	82-004	70/02:50	V-Fin	85-001	79/22:50	3.5 kHz
C16	82-004	70/02:10	V-Fin	82-014	157/18:50	SeaMarc
C17	82-004	70/11:11	V-Fin	82-014	152/20:30	SeaMarc
C18	82-004	70/11:17	V-fin	85-001	80/02:20	Huntec
C19	82-004	70/11:54	V-Fin	85-001	79/23:05	3.5 kHz
C20	82-014	152/21:10	SeaMarc	85-001	80/02:13	Huntec

Table 2.3   Depth from seafloor to reflector in metres (and ms) at each core site.

Core no.	Surface	Brown	Orange	Green	Yellow	Red	Pink
26	0						
21	0	4.5 (6)	11 (15)	18 (24)	24 (32)		
*22	0			15 (20)	24 (32)		
25	0	5 (7)	9 (12)	19 (25)	22 (30)	28 (37)	
*29	0	5 (7)				26 (35)	
51	0	4.5 (6)	6 (8)	8 (11)	11 (15)	19 (25)	26 (35)
52	0					?20 (27)	
56	0		4.5 (6)		9 (12)	13 (18)	23 (31)
*32	0		4 (5)		9 (12)	15 (20)	23 (31)
34	0				3 (4)	7.5 (10)	14 (19)
310	0			2.5 (3)	6 (8)	14 (19)	20 (27)
36	0						3.5 (5)
*27	0					15 (20)	
24	0					12 (16)	?30 (40)
37	0				?6 (8)	10 (13)	25 (33)
*54	0				12 (16)	16 (21)	24 (32)
55	0				10 (13)	15 (20)	22 (29)
33	0				?5 (7)	10 (13)	

* Acoustic stratigraphy determined by projecting stratigraphy of a profile that passes close to core site, but not over it.

Several factors limit the reliability of acoustic correlation with
core lithostratigraphy: 1) the accuracy of the ship's
navigation system (i.e. ±100 m); 2) the proximity of the seismic
line to the core site; 3) the reliability of the traced acoustic
stratigraphy (i.e. error due to channel crossings where subbottom
horizons are lost, error in crossovers between acoustic systems
with different sound sources (different wave-lengths)); and
4) differences between assumed and actual acoustic velocities in
the sediment (assumed = 1500 m/s).

Figure 2.1 shows the location of the cores with respect to the
morphological features of the area. Table 2.3 shows the depth to
the various reflectors at each core site. Appendix A contains
acoustic profiles through each of the core sites. Cores 21, 22,
and 26 are from the undisturbed area between the two disturbed
zones in the uppermost slope setting. Core site 26 is located
above the slope break in 300 m water depth. No acoustic profiler
lines were run over the core site; however, high-resolution seismic
profiles in proximity to the core site show a sharp bottom return
and a prolonged subbottom echo (terminology of Damuth, 1980) (Fig.
2.2). This characteristic echo-type is typical of many areas on
the Scotian Shelf (King and Fader, 1986; Amos and Knoll, in prep).
A Sea MARC line runs 900 m west of core site 22 (Fig. A1). The
bottom morphology at this position is hummocky and acoustic
resolution is poor but reflectors are discernable. A similar
record type is achieved by the Huntec DTS system over core site 21
(Fig. A2).

High-resolution profiles through upper-slope core sites 25 and
29 display up to 50 ms (ca. 35 m) of subbottom penetration. The
records show a complete, undisturbed sequence of continuous,
parallel reflectors at these sites (Figs. A3 and A4). Core site 29
is located on the eastern levee of the West Acadia Valley. It is
impossible to trace acoustic reflectors identified in the survey
area, across the East Acadia Valley, to the eastern levee of the
West Acadia Valley. Partial stratigraphy, however, is determined

64

based on the similarity in acoustic character and subbottom depth of Brown and Red reflectors on the western side of the valley with Brown and Red reflectors in the main part of the survey area at a similar water depth.

Core sites 51, 52, 32, and 56 progress, in order, downslope from core site 25 and remain in the undisturbed zone. Profiles over core site 52 show that the core was taken from a depression at the base of a scarp face and suggest that the cored material is -- disturbed (Fig. A6). Sequences of parallel, continuous reflectors are apparent at the other core sites (Figs. A5, A7, and A8).

Cores 34, 36, and 310 were taken in the area of erosional steps and linear depressions, outside of the disturbed zones. The erosion of sediment that has taken place at these sites allows coring to greater stratigraphic depths than would otherwise be possible. Core site 34 represents an apparently complete stratigraphic sequence with no sediment having been eroded, but since it is located midslope the reflectors have thinned and are located closer to the seabed surface (Fig. A9). Some surficial sediment erosion has occurred at core site 310 as Green is the first recognizable reflector at 3 ms (ca. 2.5 m) subbottom (Fig. A10). Core site 36 is located at the base of an erosional scarp. The subbottom stratigraphy at this site is still parallel and continuous, but the Pink reflector occurs at 5 ms (ca. 3.5 m) subbottom (Fig. A11).

Several cores were collected within the two disturbed zones. Core site 27 is located at the upslope margin of the eastern disturbed zone in less than 500 m of water depth. The hard seafloor at this depth limits the amount of acoustic penetration and makes acoustic interpretation difficult. A Sea MARC I line passing 1100 m to the east of the core site, however, shows approximately 20 ms (ca. 15 m) of disturbed material overlying the Red horizon (Fig. A1). The thickness of disturbed sediment overlying the Yellow reflector suggests that there has been little removal of material from the area.

Core site 24 is within the upper slope area of the eastern disturbed zone. It lies just to the east of a failure scarp, termed a marginal escarpment, where the undisturbed area begins. The scarp is 20 ms (ca. 15 m) high, thus it appears that this thickness of sediment has been removed from the site. The disturbed zone is 12 ms (ca. 9 m) thick at the core site and overlies the Red reflector (Fig. A12).

Core site 37 is located near the centre of the western disturbed zone. The seabed surface at this location is relatively smooth (Fig. A14). The disturbed zone is 13 ms (10 m) thick at the core site and overlies the Red reflector. The Yellow horizon may lie within the disturbed zone at approximately 5 ms (4 m). Given the thickness of the disturbed zone overlying the Red reflector, and the possible Yellow horizon within the zone, it is conceivable that there has been little net removal of sediment from this site.

Core sites 54 and 55 are located towards the downslope end of, but still well within, the western disturbed zone. The disturbed sediment is 16 ms (ca. 12 m) thick at core site 54 and 13 ms (ca. 10 m) thick at core site 55 (Fig. A15). At both locations these thicknesses of disturbed material overlie the Yellow reflector, indicating very little, if any, net removal of material from the site. Beneath the disturbed zone are parallel, continuous reflectors.

Core 33 was taken near the southeast margin of the western disturbed zone. The surface in this area appears hummocky on a large scale (Fig. A16). The thickness of the disturbed zone near this site is highly variable but approximates 13 ms (ca. 10 m) overlying the Red reflector. A possible Yellow reflector is apparent at 7 ms (ca. 5 m). From these thicknesses it seems probable that some material has been removed from this site, though it may be displaced only a very short distance. The core site is just south of the marginal escarpment marking the edge of the disturbed zone.

2.4 Summary

Due to the perceived significance of the upperslope till-like tongues on sedimentation in the Verrill Canyon area it is important to note where they fit into the defined acoustic stratigraphy. Figure 2.13 is a summary sketch of the significant acoustic features with the stratigraphy labelled and the relative positions of a number of cores indicated. The yellow reflector correlates with the base of the uppermost tongue on the high resolution system of SEABED II (Figs. 2.6 and 2.7). The red reflector correlates with the base of the tongue on the airgun record, but the resolution in this system is not fine enough to differentiate between the yellow and red horizons. The lowermost tongue probably underlies any of the sediment collected in this study.

Figure 2.13 demonstrates core stratigraphic positions based on the interpreted acoustic stratigraphy. From this figure it is apparent that the studied cores can be compiled to produce a composite stratigraphic section. The interpretation of this section will be based on the lithologic/sedimentologic characteristics of the material in the cores combined with the known acoustic characteristics.

Figure 2.13 Summary diagram of a downslope profile through the
study area, demonstrating the acoustic stratigraphy and
stratigraphic relationships of the various features.
Core positions are relative, not real or to scale.

OUTER SCOTIAN SHELF   UPPER SLOPE   MID SLOPE   LOWER SLOPE

400 METRES WATER DEPTH

OUTER SHELF TILL

DISTURBED ZONE

TONGUE

CORE 21
CORE 25
CORE 24
CORE 37
CORE 54
CORE 55

GREEN   ORANGE   BROWN

RED

TONGUE

PINK

YELLOW

2400 METRES WATER DEPTH

CORE 310
CORE 34

SCOURS

BURIED DISTURBED ZONE

CORE 36

69
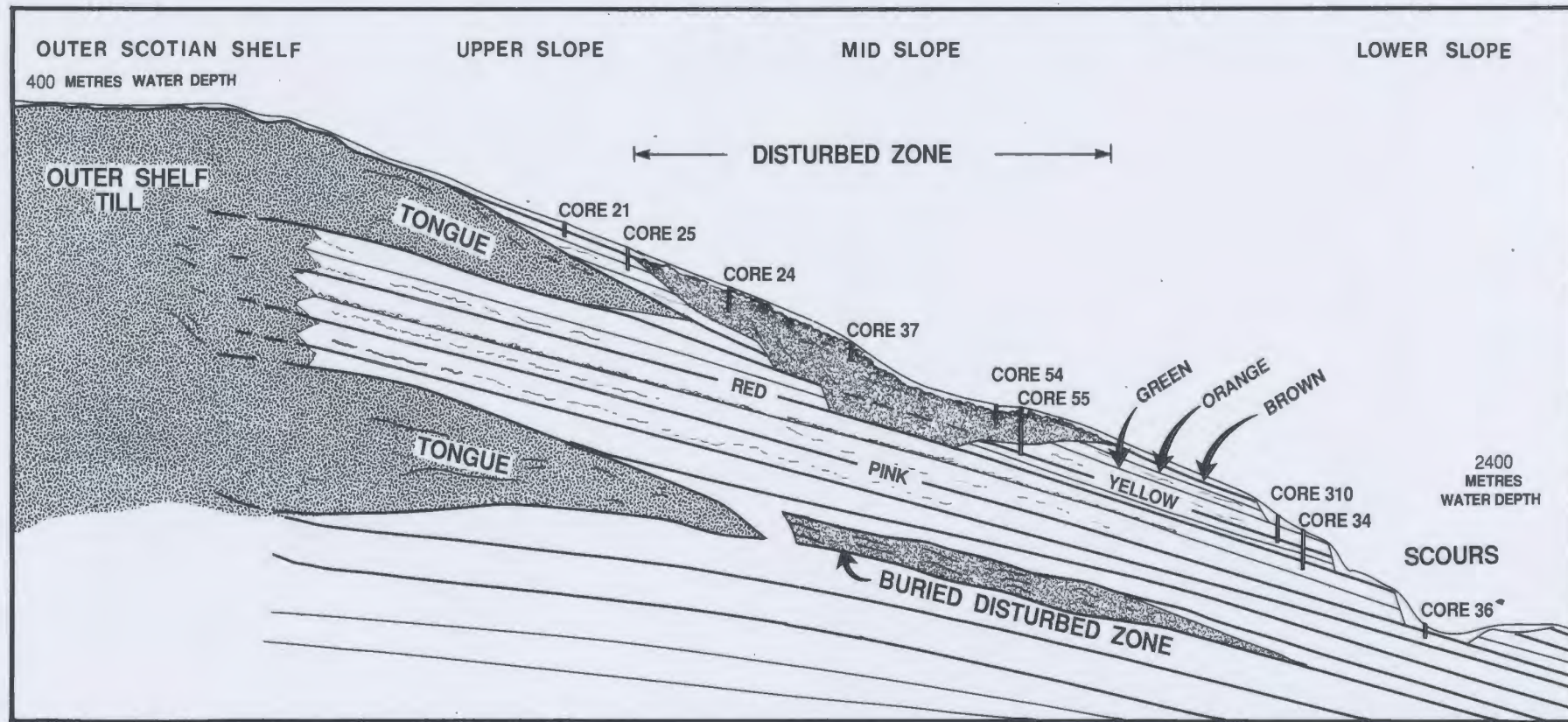
CHAPTER 3
LITHOLOGIES

3.1 Introduction

This chapter presents the findings of detailed lithologic description and grain size analysis of 18 piston cores and corresponding trigger weight cores from the Verrill Canyon area. Based on this research the sediments are categorized into lithologic facies, and facies associations. The sediments are subsequently interpreted as to their mode or modes of deposition.

3.2 Facies Descriptions

The sediments are separated into 5 lithofacies based on sedimentary structures, visual estimates of grain size, the nature of bedding contacts, and colour. These are:

    Facies 1: Bioturbated mottled mud
    Facies 2: Homogeneous mud
    Facies 3: Laminated mud
    Facies 4: Thin-bedded sand
    Facies 5: Poorly sorted mud

Facies 1: Bioturbated mottled mud

This muddy facies is characterized by the presence of bioturbation structures and mottling (Fig. 3.1). Lithologically it varies in texture from clay to sandy-mud and is either olive, olive grey, or dark brown in colour. Planktonic foraminiferal tests are abundant in many parts of this facies. Contacts with most adjacent facies are gradational. Facies 1 comprises the majority of sediment within the top 2 m of most core sequences, and thus is likely being deposited on the Scotian Slope at present. It also occurs at several horizons within the subsurface as thick ($1-5$ m), massive beds. This facies comprises approximately 40-50 % of the total thickness of cored sediment.

Figure 3.1 X-radiograph slab of an example of Facies 1 sediment.
Note *Zoophycos* burrows with backfill structures. Black
mottling can be seen in the cores.

CORE 54   86-111 cm

ZOOPHYCOS ?
BURROWS

FACIES 1

72

In olive coloured sediments bioturbation traces are commonly parallel-sided, subhorizontal burrows, often with crescent-shaped backfill structures (Fig. 3.1). These traces are interpreted to be *Zoophycos* trails (cf. Chamberlain, 1978), and are most easily seen in X-radiographs, but can be seen faintly in the split core face.

Bioturbation in dark brown sediments is typically seen as abundant mottles (black, grey or red), and rare large unfilled burrows. These structures are associated with abundant black authigenic pyrite, the black colour indicating the presence of monosulphide (Thomsen and Vorren, 1984). Thomsen and Vorren (1984) ascribe the pyritization of burrows and traces to the decomposition and decay of organic matter, associated with cold temperatures, and reduced salinity and oxygen content.

Facies 2: Homogeneous mud

Sediments of Facies 2 are dominated by mud but may contain as much as 30 % dispersed fine sand. Foraminiferal tests are commonly abundant. The facies is characterized by either the absence of pronounced sedimentary structures (Figs. 3.2, 3.3, and 3.4) or, locally, the presence of very faint parallel laminations, or "wispy" laminations (cf. Hill, 1981) (Fig. 3.5). These structures are visible in X-radiographs.

Facies 2 occurs as beds between 5 and 20 cm thick, and bedding contacts can be sharp or gradational. These beds are generally olive grey or red brown in colour, but can also be grey brown or brown. This facies comprises approximately 5 % of the total cored sediment.

Facies 3: Laminated mud

Facies 3 is recognized by distinct, generally horizontal, millimetre-thin laminae (Figs. 3.3, and 3.5). The laminae are defined by colour and grain size differences, forming graded sand/silt - mud couplets. Repetition of couplets may produce beds tens to hundreds of centimetres thick. Sand and silt laminae are

Figure 3.2 X-radiograph slab of Facies 2 sediment, showing
structureless nature of this facies. Specks on the
image are likely scattered fine sand. Long, linear,
and predominately vertical structures in the X-
radiograph are algal growths of _Mylenia_, and are post-
depositional.

CORE 54   209-234 cm

FACIES 2

75
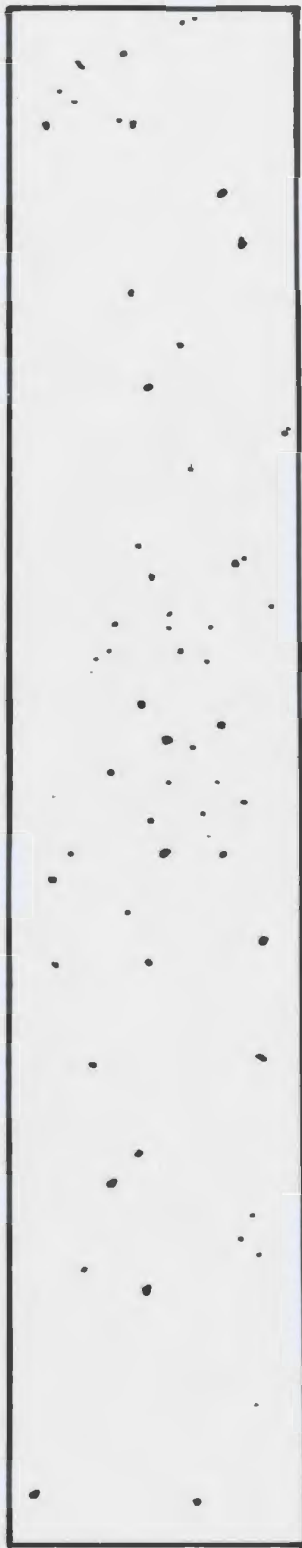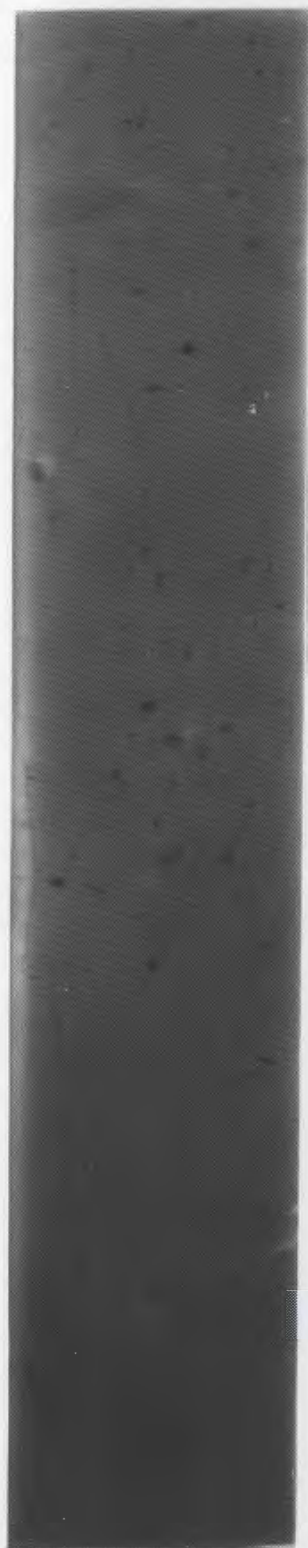
Figure 3.3 X-radiograph slab showing examples of Facies 2, Facies
             3, and Facies 4 sediment. In Facies 2 note the lack of
             sedimentary structures. Fine structures such as wispy
             laminations may be present in Facies 2. In Facies 3
             note the fine scale, yet distinctiveness of
             laminations. Facies 3 passes gradationally upwards
             into Facies 2. Coarse sand and pebbles seen within
             these two facies are believed to be ice rafted debris.
             Facies 4 is seen as a thin bed (1 cm) of fine sand. It
             underlies Facies 3. Facies appearing in this plate are
             grouped into Facies Association B.

CORE 23   109-126 cm
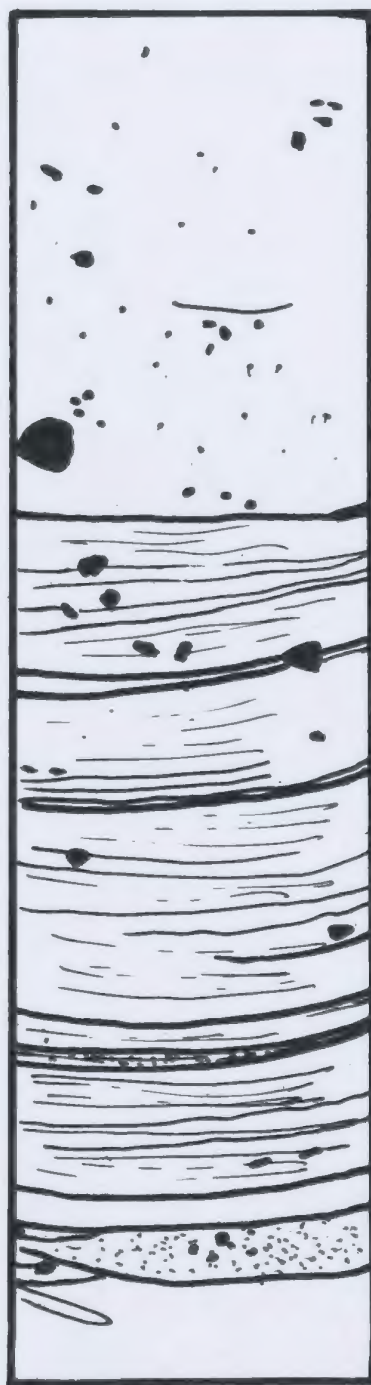
FACIES 2

FACIES 3

FACIES 4

77

typically dark brown in colour and clay laminae are light brown to reddish brown. Individual laminae appear sorted and in some instances cross-laminations are apparent. Clay laminae may be slightly burrowed. Graded bedding occurs locally, evidenced by thinner and less frequent laminae towards the top of the bed (cf. graded laminated bed of Piper (1973)). Lower bedding contacts are sharp, while upper contacts may be sharp or gradational. Larger pebbles or clasts may cut through and downwarp laminae of this facies (Fig. 3.5), or they may be present and yet conform with finer grained laminae. This facies comprises approximately 15 % of total sediment volume of all the cores.

Facies 4: Thin-bedded sand

This facies is easily recognizable in the core as 1-10 cm thick, sorted fine sand - coarse silt beds (Fig. 3.3). These beds occur infrequently throughout the cores, sometimes at the base or within Facies 3 beds, or sometimes within Facies 2 or 5. They are olive-grey in colour at the top of the cores and dark brown in lower parts of the cores. Upper and lower contacts are sharp and horizontal, except where the bed has been post-depositionally deformed. Undisturbed beds may be parallel-sided or lenticular shaped. Rare, faint parallel and cross laminae may be seen in X-radiographs of the Facies. This facies comprises only 1 % of the total cored sediment.

Facies 5: Poorly sorted mud

Relatively structureless muds with varying amounts of sand and gravel are designated as Facies 5. This sediment type thus includes a range of lithologies from muds with occasional scattered sand and gravel (Fig. 3.5) to muds with abundant (30 %) sand and gravel (Fig. 3.4). In some instances the coarser sand and gravel occurs in poorly sorted horizontal laminae. Both normal and inverse grading are developed locally. The facies is dark brown, red brown, or grey brown in colour. Red-brown and grey colour mottling and marbling occurs within some of the dark brown beds.

Figure 3.4   X-radiograph slab of an example of Facies 2 and Facies
5 sediment. Note the sharp contact between the two
facies, the rare occurrence of coarse sediment in
Facies 2, and the abundance of coarse sediment in
Facies 5. There is a hint of structure in Facies 5 in
that pebbles seem to be aligned in a steeply dipping
fashion.

CORE 54   120-145 cm
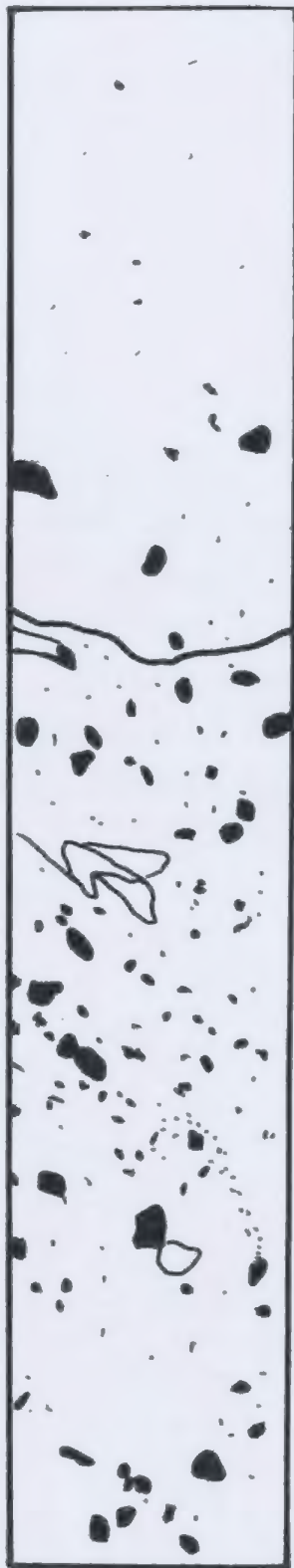
FACIES 2

FACIES 5
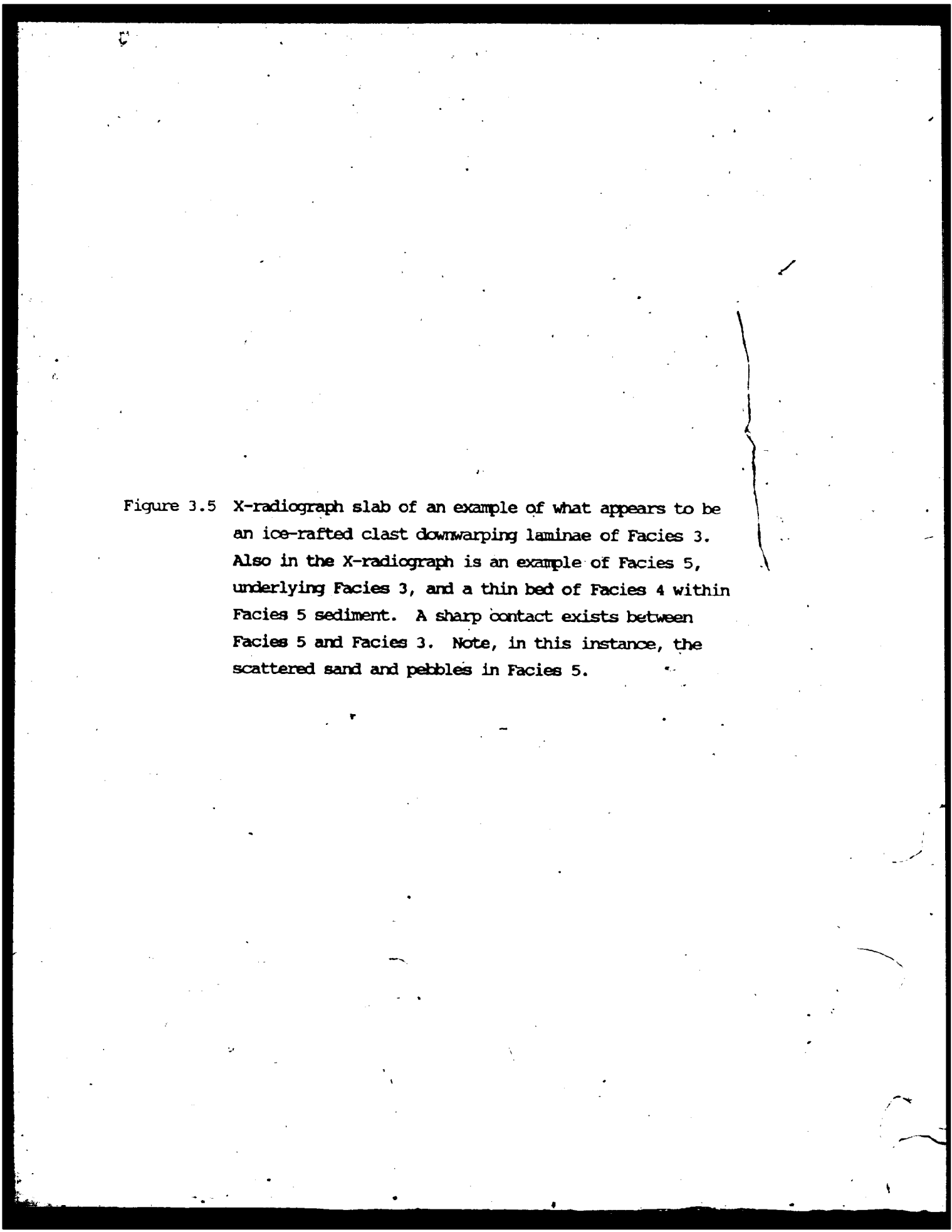
Figure 3.5 X-radiograph slab of an example of what appears to be
            an ice-rafted clast downwarping laminae of Facies 3.
            Also in the X-radiograph is an example of Facies 5,
            underlying Facies 3, and a thin bed of Facies 4 within
            Facies 5 sediment. A sharp contact exists between
            Facies 5 and Facies 3. Note, in this instance, the
            scattered sand and pebbles in Facies 5.

CORE 33   200-221 cm
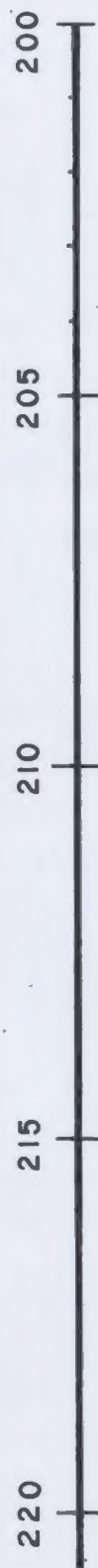
FACIES 2

ICE-RAFTED CLAST

FACIES 3

FACIES 4

FACIES 5

Grain size contrasts between the mottle and the matrix were noted. Bedding contacts are sharp and often irregular. Facies 5 is medium to thick bedded (10 - 100 cm). This facies represents about 40 % of the total of all cored sediment.

3.3 Deformed Beds

Deformed beds are seen only in cores from the acoustically defined disturbed zones (Chapter 2), but not all cores from these zones show deformed bedding. Deformation overprints original depositional features but rarely obliterates facies characteristics such that the original facies cannot be recognized. Sediment from cores of the upslope portions of the disturbed zones is deformed only in several thin (10 cm) horizons (core 37). In cores from the mid-slope area of the disturbed zones (54, 55) deformation is extensive. Deformation features are not observed in cores from the extreme down-slope portions of the disturbed zones.

The types of deformation structures within the cored sediment depend upon the facies and the degree of deformation. Tilted laminae and bedding surfaces, irregular laminae, convoluted laminae, overturned folds, stretched mottles, eyelet (lensoid-shaped) structures, rolled balls, and microfaults are recognized in the sediments and on X-radiographs (Fig. 3.6a-c).

3.4 Grain Size Analysis

Grain size is the basis of classification for clastic sediments and a principal criterion for the interpretation of past and present depositional processes (Kranck and Milligan, 1985). The grain size characteristics of clastic sedimentary deposits depend upon four general factors: (1) grain size distribution at the source; (2) transport history (transport medium, current velocity, distance from source, settling distance); (3) physical changes in size (i.e. flocculation and deflocculation due to mechanical, physicochemical, or biological interactions); and (4) post-depositional processes (bioturbation, current reworking).

Figure 3.6 X-radiograph slabs of deformed sediments (disturbance
recognized by various deformation features): a) tilted
laminae, b) tilted laminae and microfaults,
c) overturned folds and completely homogenized sediment
(i.e. lacking structures).

a

CORE 24   230 - 248 cm

DIPPING LAMINAE

85

b

CORE 55   461 - 486 cm

MICROFAULTS

86
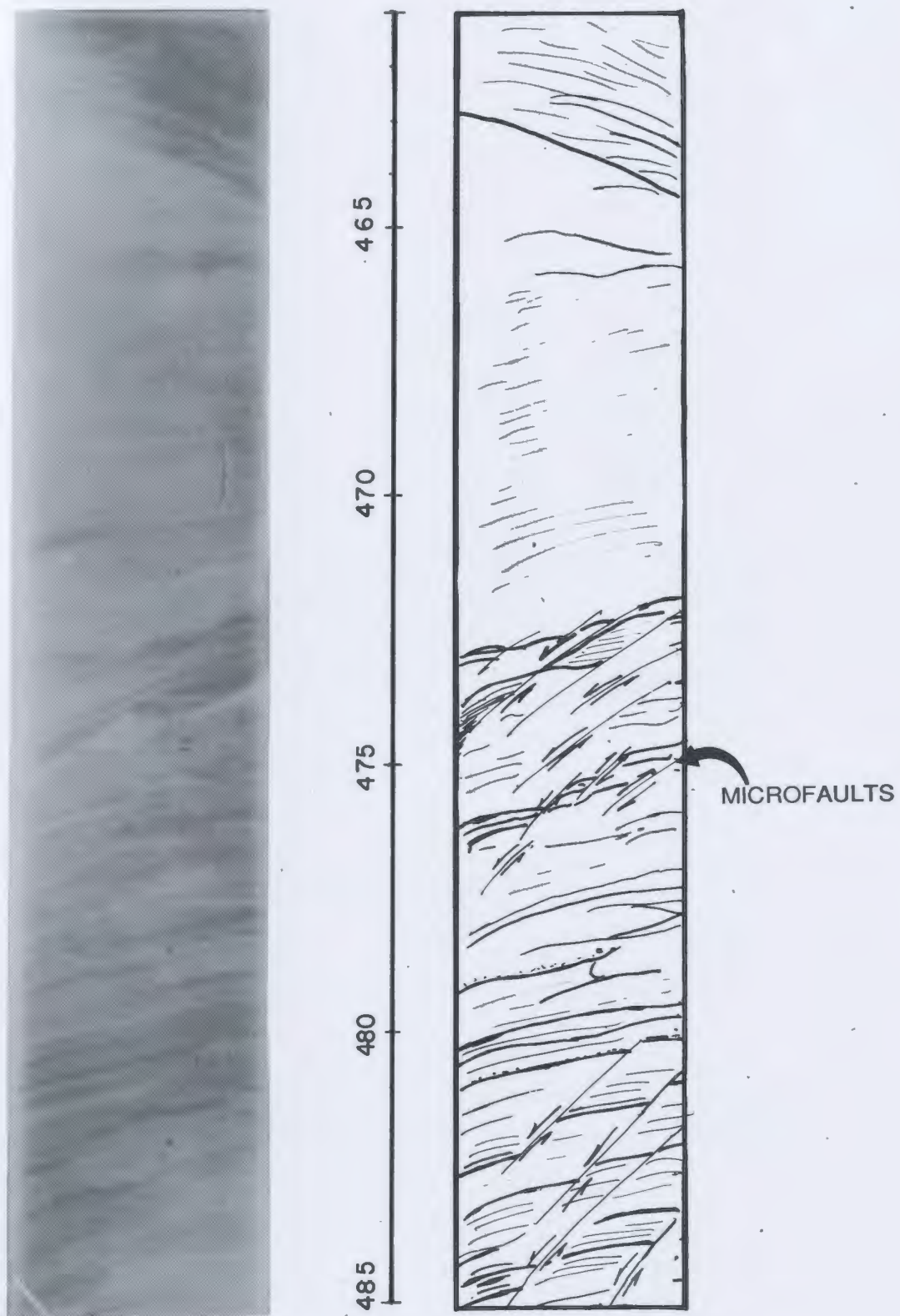
c

CORE 55   191-216 cm
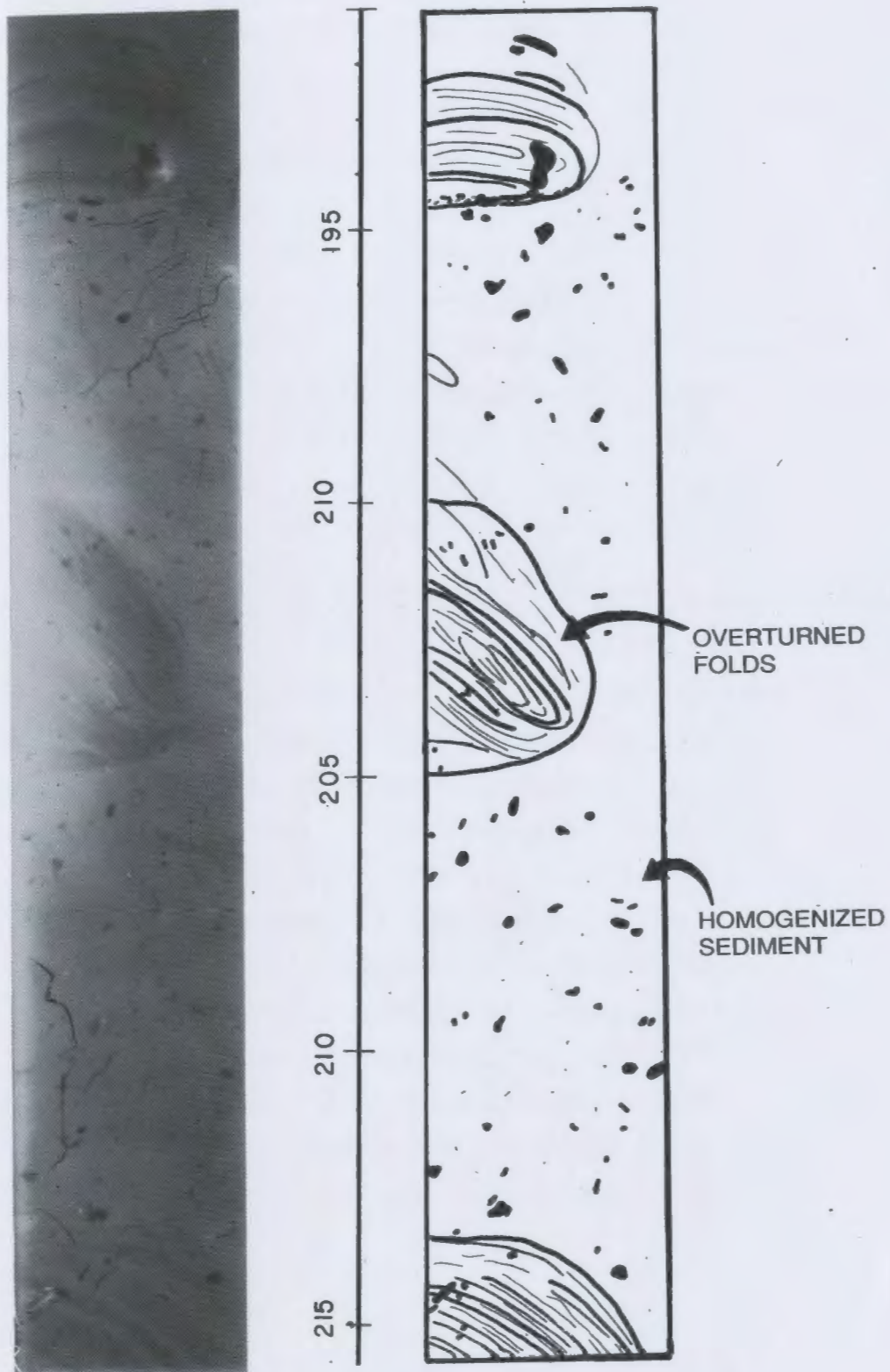
It is difficult, indeed often impossible, to determine the mode of deposition for fine-grained sediments from the grain size distribution (Kranck and Milligan, 1985). Grain size spectra of fine-grained sediments are complicated by their dependence upon both method and duration of sample pretreatment and analysis (Nelsen, 1983; Anderson et al., 1984). It is difficult, therefore, to relate grain size parameters of fine-grained sediments to specific criteria such as paleocurrent velocity (Singer and Anderson, 1984; Anderson and Kurtz, 1985). It is possible, however, to use grain size data to differentiate between sediment types (e.g. facies), to highlight gross trends (e.g. fining downslope), and to recognize anomalies (e.g. ice-rafted debris). Ultimately grain size information can support an interpretation for the mode and environment of deposition of a particular bed or facies, but it cannot be used to determine processes without other supporting evidence.

This study incorporates data from 156 grain size analyses in order to: (1) characterize and classify lithologic facies, (2) compare grain size distributions amongst facies to aid in sedimentological interpretations, and (3) recognize spatial and temporal trends within and between cores. The methods of analysis have been discussed in Chapter 1. Besides gravel/sand/silt/clay ratios, other measures considered important in describing the grain size distribution of a fine-grained sample are the mean, median, mode, and standard deviation. Appendix B includes a table of these measures for each sample. Table 3.1 contains the averages of these measures for each facies and for each analyzed core. A discussion of the gravel, sand, silt, and clay components, and the distribution measures of the various facies and cores follows. Representative grain size distribution curves for each facies are presented in Figures 3.7a-e.

Table 3.1 Average grain size parameters. Percentages of gravel, sand, silt, and clay only were conducted on samples from cores 36, 37, 54 and 55.

Facies	% Gravel	% Sand	% Silt	% Clay	mean phi	median phi	mode phi	Stand. Dev.
1	0.03	8.33	40.19	51.42	8.03	7.95	5.17	2.69
2	0.10	10.39	37.94	51.56	7.80	7.68		2.95
3	0.18	7.22	41.06	51.49	7.56	7.23	4.54	2.72
4	0.10	32.91	36.78	30.20	6.33	5.65	3.71	2.98
5	0.59	14.61	35.22	49.56	7.69	7.71	6.33	3.16

Core no.

Core no.	% Gravel	% Sand	% Silt	% Clay	mean phi	median phi	mode phi	Stand. Dev.
29	0.24	19.20	44.32	36.24	6.98	6.58	4.03	2.96
37	0.26	5.63	37.49	56.55				
54	0.19	8.30	39.80	51.70		NO DATA		
55	0.21	6.03	41.29	52.47				
34	0.36	14.78	35.94	48.90	7.52	7.68	5.68	3.03
36	0.81	12.17	33.82	53.88		NO DATA		
310	0.61	10.28	34.21	54.90	8.15	8.24	7.02	2.98

Figure 3.7 Examples of grain size distribution curves for the five
lithofacies (note the dip in the distribution curve
within silt sizes - about 4 phi - is not real but is a
function of the cut-off used for size analysis between
the settling tower and the sedigraph (53 microns)):
a) Facies 1: note the facies is comprised of a mixture
of sediment sizes from sand to clay, with clay and silt
being predominant. Very little gravel has been
observed in this facies. The bars in the histogram
represent relative frequency percentages at 0.2 phi
intervals, spikes represent logarithmic relative
frequency percentages, the lower curve represents the
cumulative relative frequency percentages, and the
upper curve represents the cumulative probability
frequency percentages.
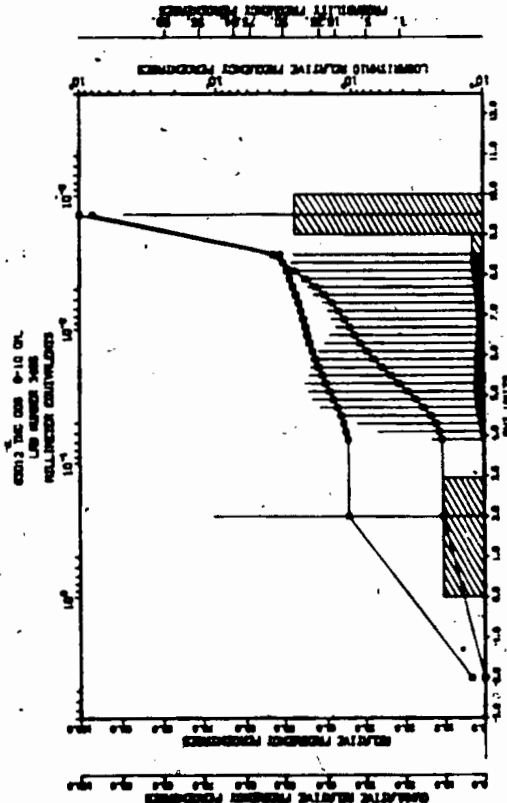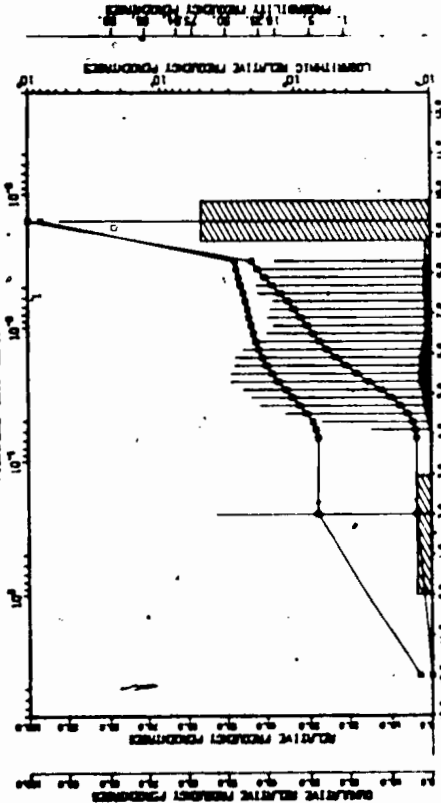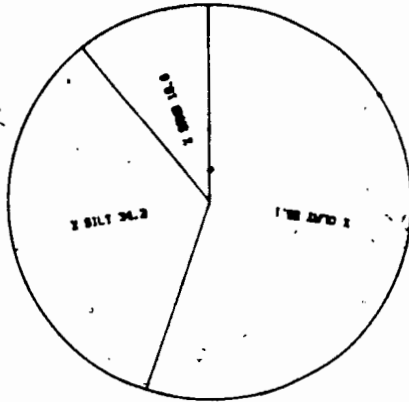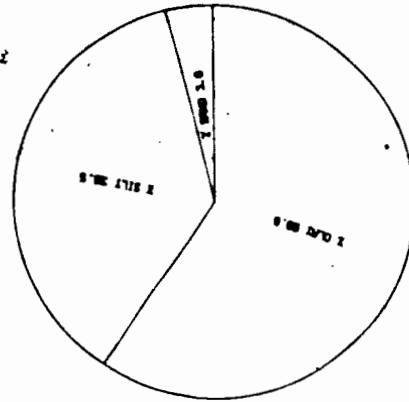
Figure 3.7 b) Facies 2: showing almost equal portions of sand,
silt, and clay in this facies, but the sand portion is
very fine and in fact appears to have a sharp cutt-off
at about 2 phi. Very little gravel has been noted
within this facies. Bars of the histogram represent
logarithmic relative frequency percentages at 0.2 phi
intervals, and the curve represents cumulative
probability frequency percentages.

b

CRUISE 82004 PISTON CORE #9
SAMPLE 2149
MILLIMETER EQUIVALENTS

% SILT 45.0
% SAND 10.2
% CLAY 44.8

CRUISE 82004 PISTON CORE #9
SAMPLE 2152
MILLIMETER EQUIVALENTS

% SILT 40.8
% SAND 24.6
% CLAY 34.6

93
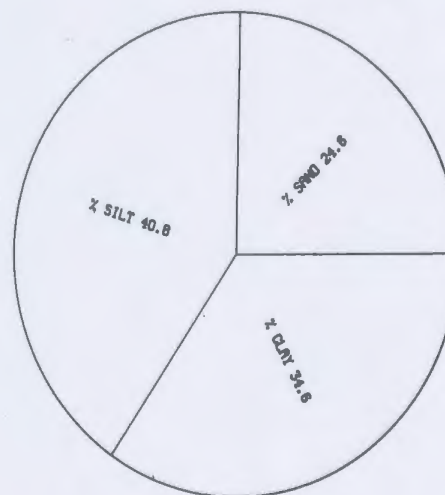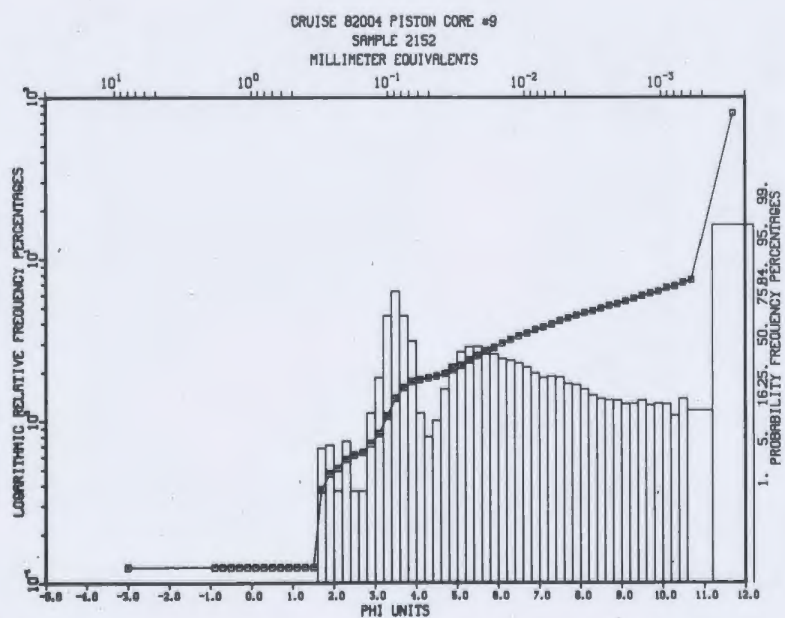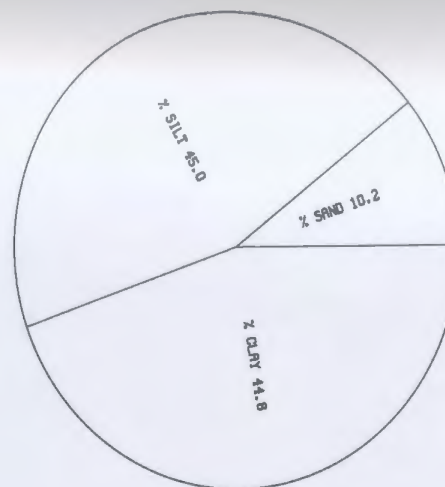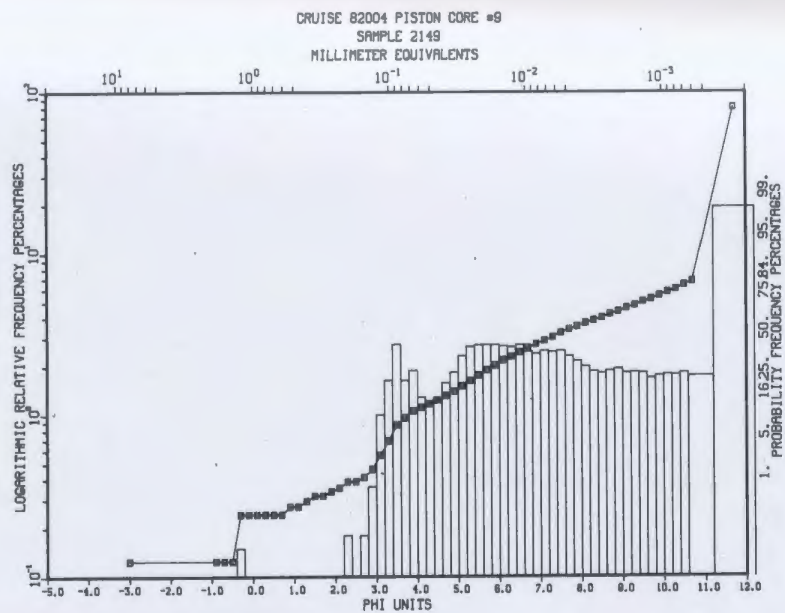
Figure 3.7 c) Facies 3: note the percentages of sand, silt, and
clay are similar to those of Facies 2 but the sand
portion extends into the coarser grain sizes (about 0
phi) and has a more normal distribution (i.e. is
negatively skewed). These analyses are not from
individual lamina but from bulk samples. Distributions
from single lamina are expected to be much better
sorted. Bars of the histogram represent logarithmic
relative frequency percentages at 0.2 phi intervals,
and the curve represents cumulative probability
frequency percentages.
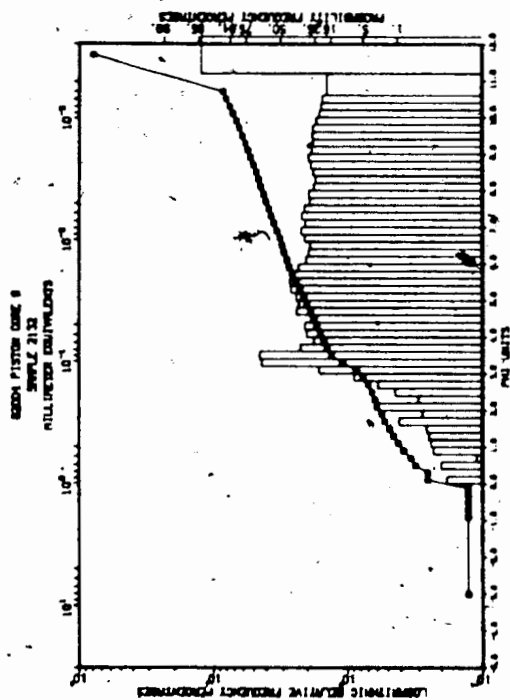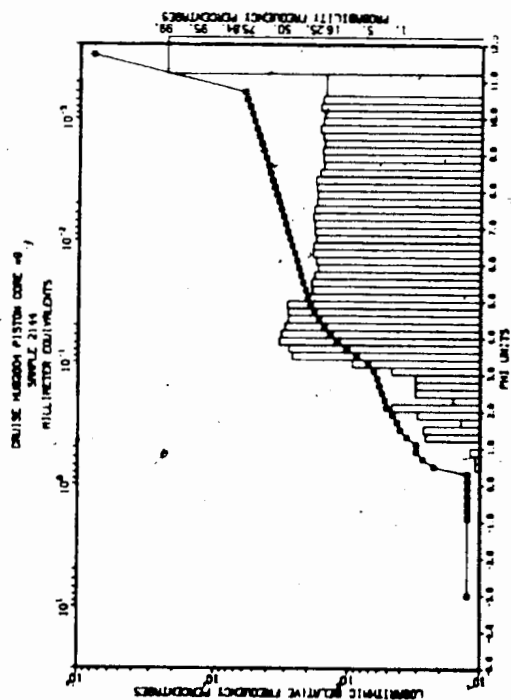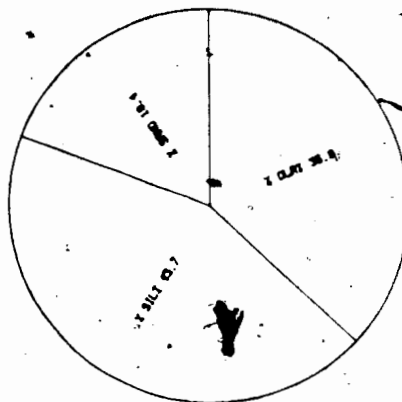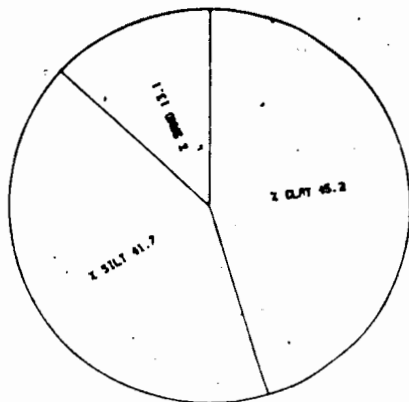
Figure 3.7 d) Facies 4: showing the well sorted nature, and high
fine and very fine sand content (peaking about 3.5 phi)
of the facies. The top diagram is a distribution from
a sample carefully collected within the bed itself,
showing the sorted nature of the facies. The lower
curve is from a bulk sample which includes sediment
surrounding the bed, thus the distribution is more
poorly sorted and positively skewed. The bars in the
histogram represent relative frequency percentages at
0.2 phi intervals, spikes represent logarithmic
relative frequency percentages, one curve represents
the cumulative relative frequency percentages, and the
other curve represents the cumulative probability
frequency percentages.

83-012-4 301-305
SAMPLE 1803
MILLIMETER EQUIVALENTS

65-001-002 / 679   D. PIPER
SAMPLE NUMBER- 3450
MILLIMETER EQUIVALENTS
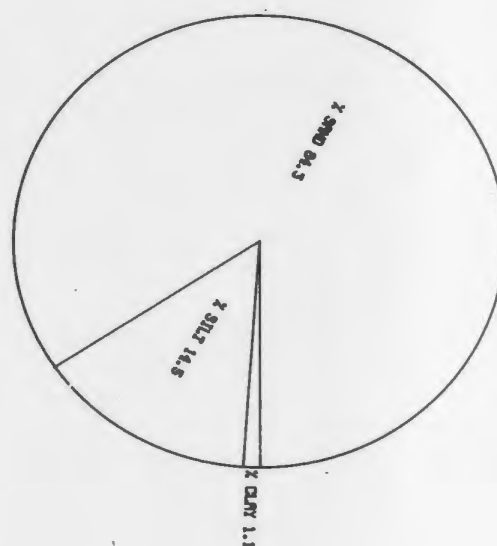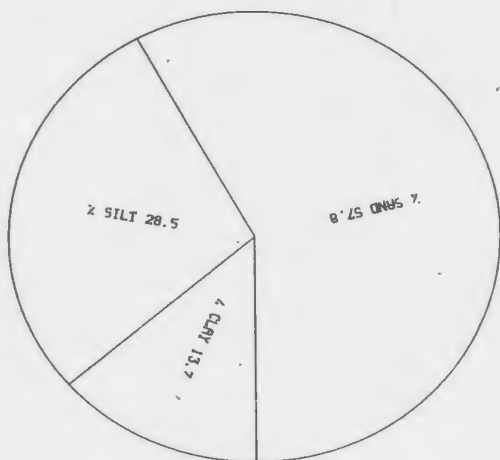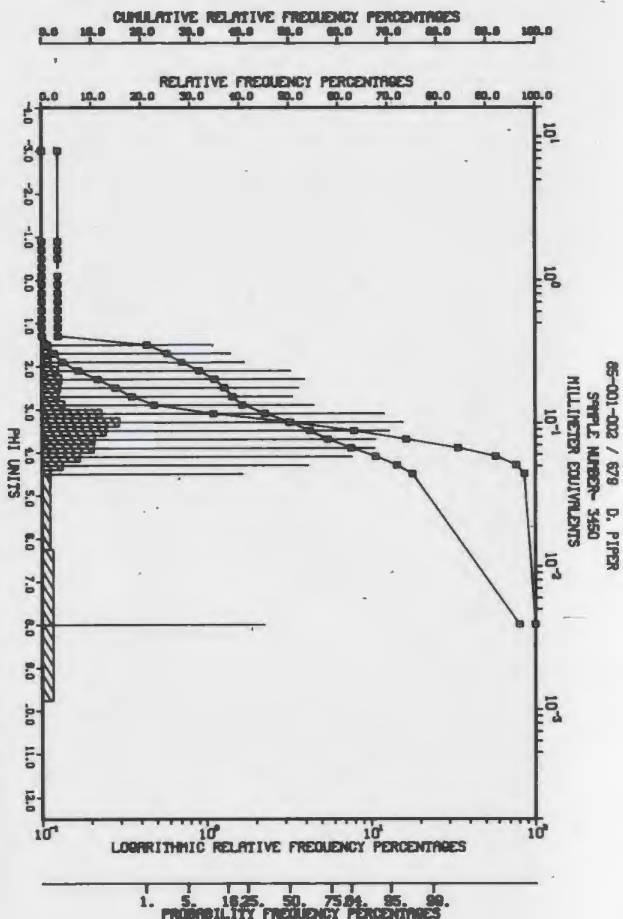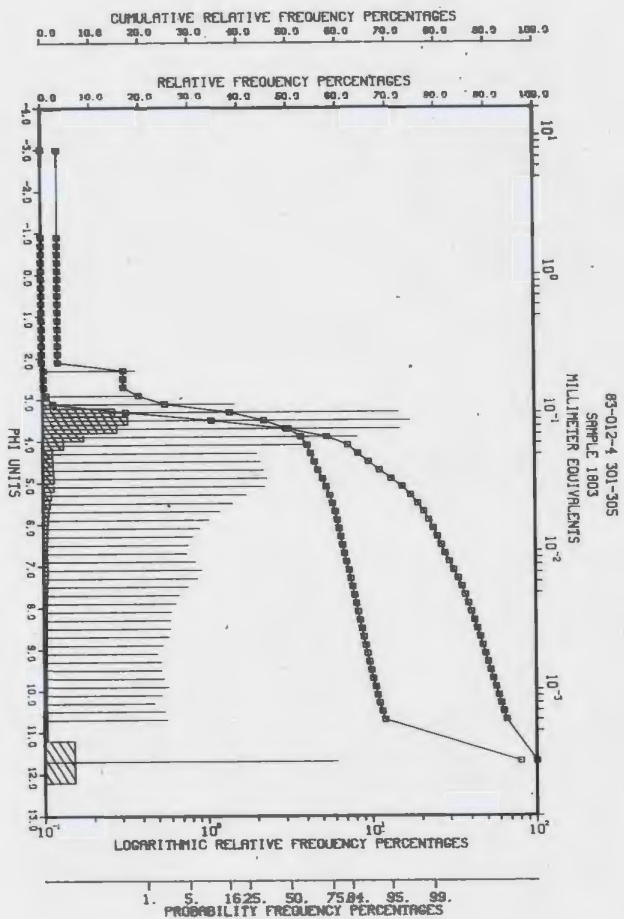
Figure 3.7   e) Facies 5: shows the poorly sorted nature of the
             facies, including a relatively high gravel percentage.
             Bars of the histogram represent logarithmic relative
             frequency percentages at 0.2 phi intervals, and the
             curve represents cumulative probability frequency
             percentages.

CRUISE HU82004 PISTON CORE #9
SAMPLE 2145
MILLIMETER EQUIVALENTS

PROBABILITY FREQUENCY PERCENTAGES
LOGARITHMIC RELATIVE FREQUENCY PERCENTAGES
PHI UNITS

% GRAVEL 0.3
% SAND 11.5
% SILT 36.6
% CLAY 51.6

CRUISE 82004 PISTON CORE #9
SAMPLE 2160
MILLIMETER EQUIVALENTS

PROBABILITY FREQUENCY PERCENTAGES
LOGARITHMIC RELATIVE FREQUENCY PERCENTAGES
PHI UNITS
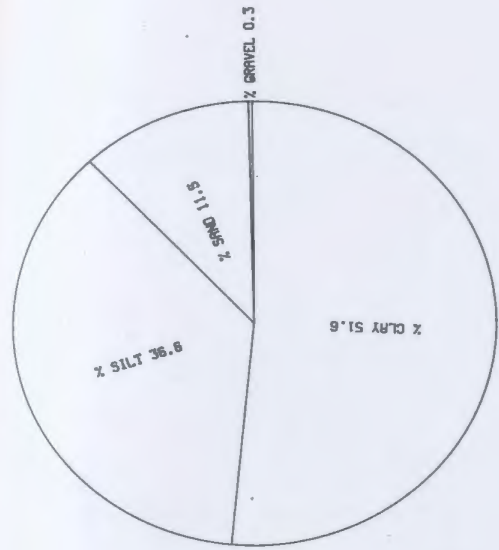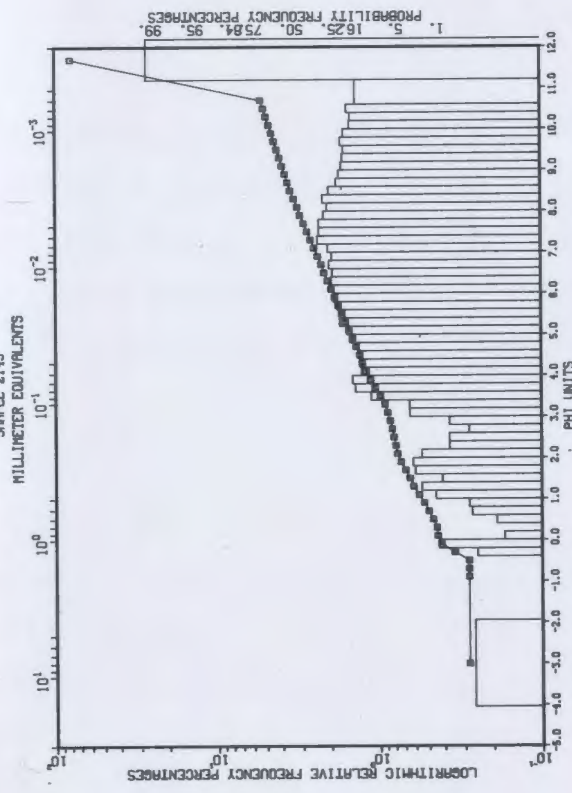
% GRAVEL 3.3
% SAND 17.2
% SILT 43.7
% CLAY 35.8
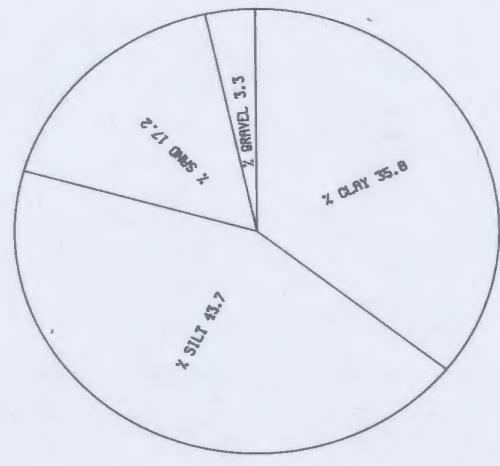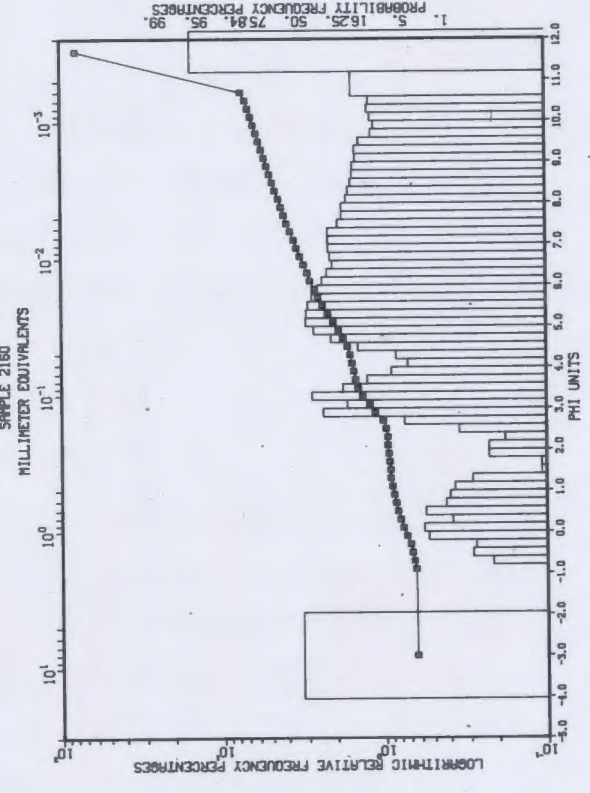
Facies Variations:

It was attempted to classify the defined lithofacies according
to Folk (1954) and Dean et al. (1985), based on sand:silt:clay
ratios (there is not enough gravel present to affect
classification) (Fig. 3.8). Facies 1 and 2 sediments plot
predominately in the mud field, with very little scatter into the
sandy mud range. Facies 3 sediments (Fig. 3.8) plot in the mud and
sandy mud fields. Samples from this facies generally include
several laminae. If individual laminae were sampled it is expected
they would plot into mud, silt, and muddy sand fields because of
the graded couplet nature of the laminae and the high degree of
sorting within each lamina, as described in smear slides. Facies 4
sediments plot in the sandy mud to muddy sand fields (Fig. 3.8).
Sampling intervals generally included mud surrounding the thin
Facies 4 beds. A sample carefully taken within the bed was
composed of 84 % sand and 14 % silt, thus plotting in the silty
sand field. Facies 5 sediments plot in two fields: mud and sandy
mud (Fig. 3.8).

The ternary diagrams of Figure 3.8 show the lithologic
similarity of most of the sediments within the cores. Grain size
differences amongst facies are generally subtle, and are perhaps
better shown by distribution curves and statistical measures (Fig.
3.7, Table 3.1, and Appendix B).

Gravel

Though the gravel fraction of sediment from the Scotian Slope
represents a very small, perhaps insignificant, percentage (0-5 %)
of the total size spectra, its presence is considered significant.
The gravel population is poorly sorted, and consists of numerous
lithologies. Gravel locally downwarps laminae (Fig. 3.5), and can
occur either scattered throughout the cored sediment, or in
concentrated beds or lenses. Gravel is interpreted to be ice-rafted
in origin, though may have been subsequently reworked or ·
resedimented.

100

Figure 3.8 Ternary diagram for classification of sediments
according to their sand, silt, and clay ratio (after
Folk (1954), and Dean et al. (1985), and ternary
diagram plots for each of the facies. Note the
similarity in the grain size classification for most of
the samples.
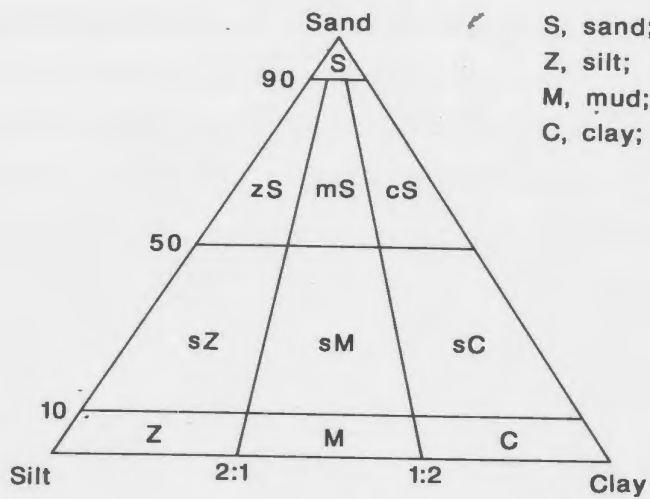
S, sand; s, sandy
Z, silt; z, silty
M, mud; m, muddy
C, clay; c, clayey
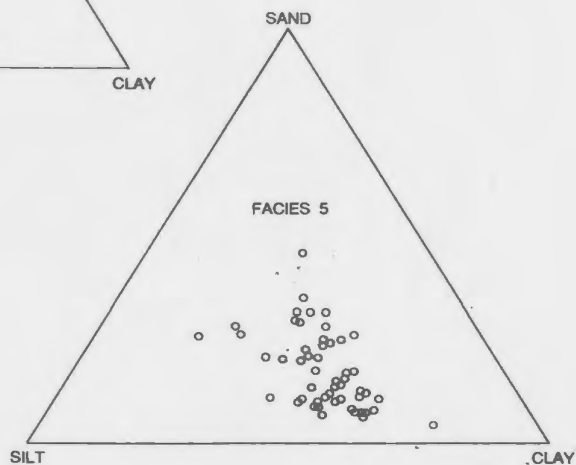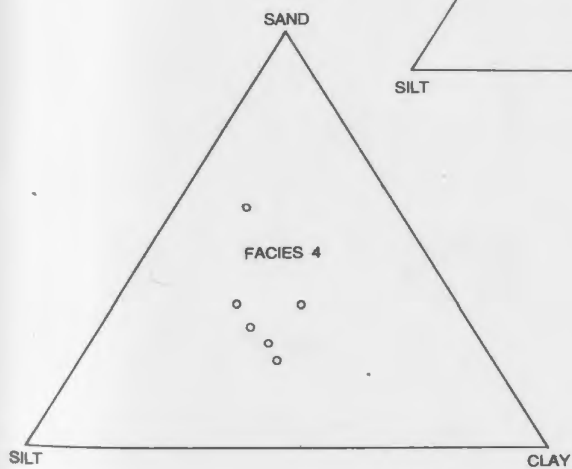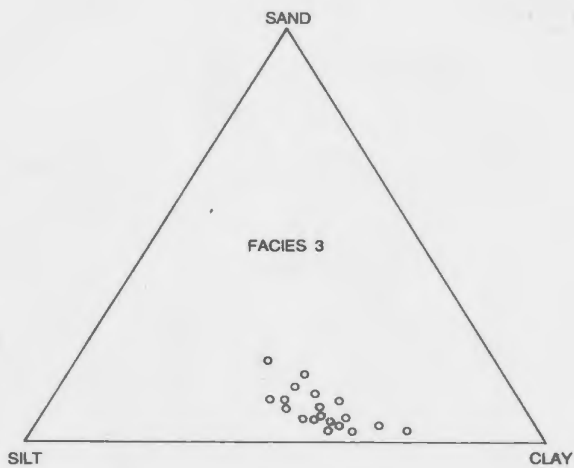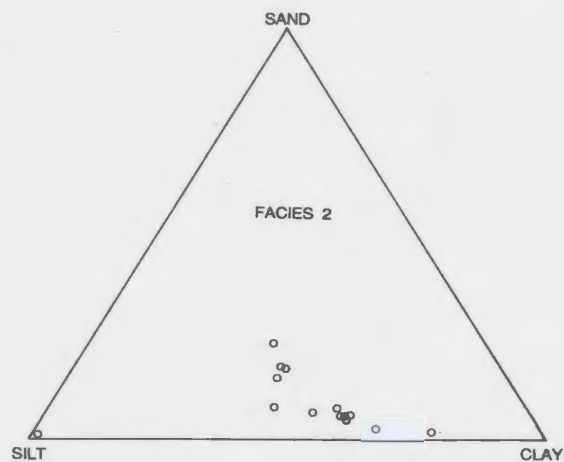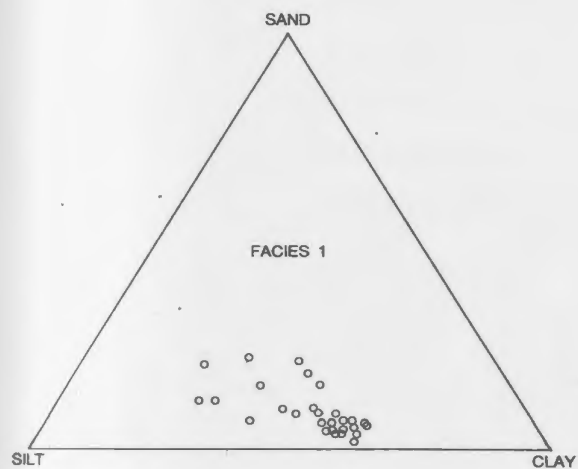
Most samples of Facies 5 contain gravel, sometimes reaching 4.5 % of the sample (Fig. 3.7e). Numerous samples from Facies 3 contain a small percentage of gravel (Appendix B). Only three samples of Facies 1, four of Facies 2, and one of Facies 4 contain any gravel (Appendix B).

Sand

Sand content varies from 0 % to a maximum of 84 % (Table 3.1). If the sand is treated artificially, as a separate population, then this fraction is consistently very well sorted (s.d.= 0.80) and possesses a similar mean size (-3.2 phi) throughout all the facies. The sand fraction is predominantly quartz, some of which is stained red. It is most abundant in Facies 4, and least abundant in Facies 1.

Silt and Clay:

The silt fraction ranges between 20 and 60 %, generally comprising about 30-40 % of the sample. The clay fraction comprises between 13-77 %, but averages between 50-60 % of the sample. Analyses indicate that silts and clays of the studied sediments are typically very poorly sorted. Silt to clay ratios in the cores show a downslope fining trend, ranging from 1.2 in the uppermost slope cores to 0.62 in the lowermost slope cores.

Mean, Median, and Mode:

Only three cores have full grain size analysis available, permitting calculation of statistical measures. Average mean, median, and modal sizes are given in Table 3.1. Statistically (one-way analysis of variance) the means of each facies are not significantly different. Averages from each core show mean, median, and modal sizes decreasing downslope.

Standard Deviation:

Standard deviation (s.d.) or sorting is a measure of variation

103

in the grain size population (Folk, 1980). According to the classification of Folk and Ward (1957) the sediments of the studied cores are all very poorly sorted. Mean standard deviations of the facies indicate that Facies 5 is the most poorly sorted, followed by Facies 4, 2, 3, and 1 in order of increased sorting (decreasing s). Statistical Student's T-tests define only the standard deviations of Facies 5, and 1 as significantly different.

3.5 Facies Interpretations

Deposition of fine-grained sediments in deep ocean environments can occur by a variety of processes, including settling from suspended sediment plumes (nepheloid layers) (Cacchione and Drake, 1986), bottom current reworking (Stow and Lovell, 1979; Chough and Hesse, 1985), Ice rafting (Piper and Slatt, 1977; Hugget and Kidd, 1984), and mass movement (slumps, slides, debris flows, turbidity currents) (Stow and Piper, 1984; Stow, 1985). Figure 3.9 demonstrates the conceptual overlap of these processes.

Distinguishing hemipelagites from contourites from fine-grained turbidites is a most difficult problem (Hesse, 1975; Stow 1979, 1985; Hill, 1984b; Shor et al., 1984). No general set of guidelines exist for such distinction but numerous workers have approached the problem and have established criteria for specific cases (Hesse, 1975; Kurtz and Anderson, 1979; Stow, 1979, 1985; Stow and Lovell, 1979; O'Brien et al., 1980; Stow and Shanmugam, 1980; Hill et al., 1982a; Hill, 1984b; Shor et al., 1984; Stow and Piper, 1984; Chough and Hesse, 1985).

Facies 1: Bioturbated mottled mud

Abundance of bioturbation structures and abundant biogenic material in the form of foraminiferal tests in this facies is suggestive of slow sedimentation rates. Hesse (1975) regards intense bioturbation as one criterion for identification of hemipelagites in ancient slope sequences. Stow (1985), and Chough and Hesses (1985) maintain that bioturbation can be intensive

Figure 3.9 Ternary diagram demonstrating the conceptual overlap
and complexity of sedimentary processes affecting the
continental slope. This process overlap makes it
difficult to recognize the mode of deposition for
certain sediments and demonstrates the short-comings in
classifying sediments according to their mode of
deposition.
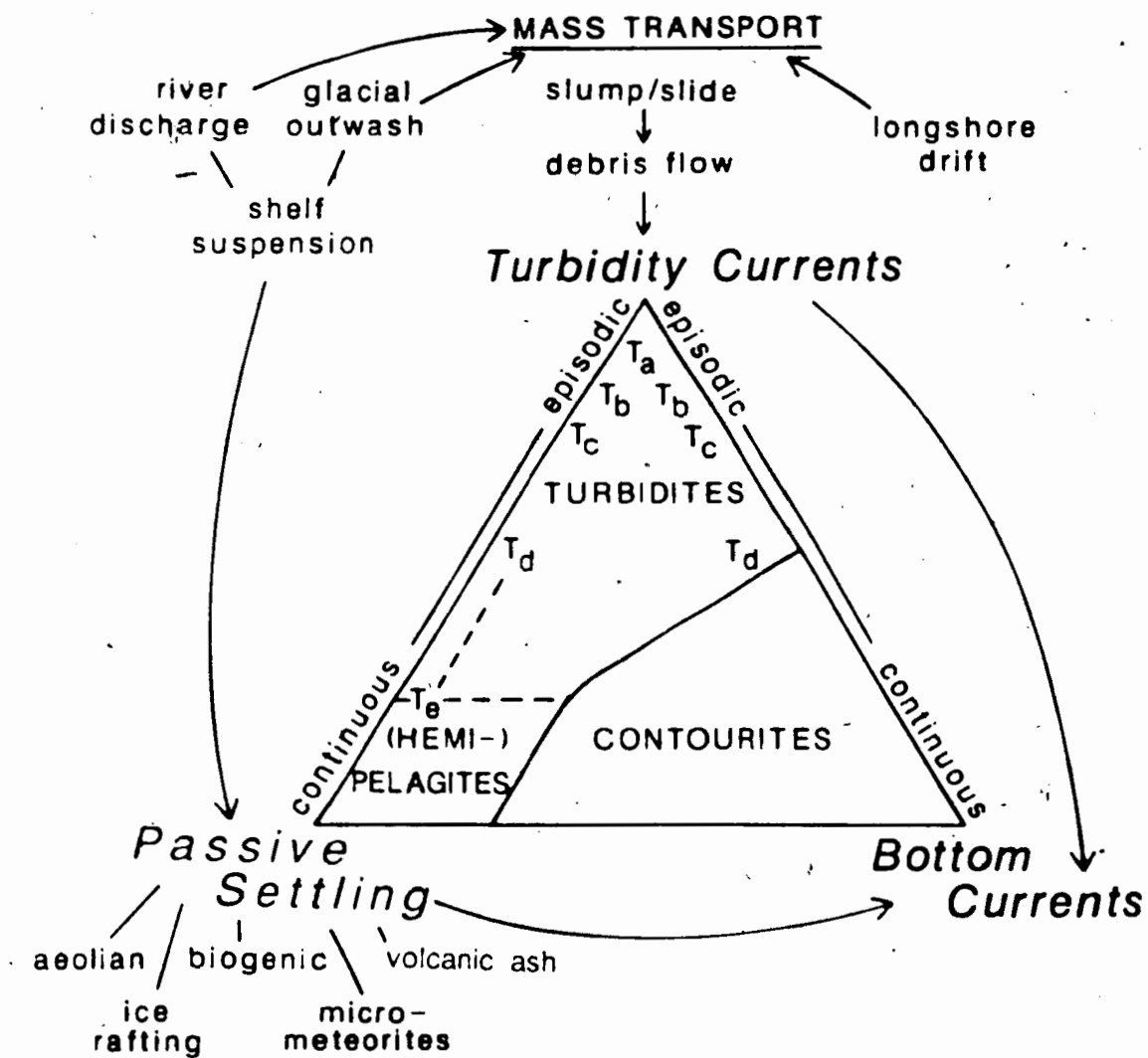
throughout contourites as well as hemipelagites. They also infer
that both deposits may have high biogenic components. Both
processes typically involve low sedimentation rates (<10 cm/1000
yr) (Stow, 1979, 1985).

Contacts between beds of this facies and with other facies are
gradational and often bioturbated beyond recognition. This feature
is ubiquitous in hemipelagites but occurs in contourites as well
(Stow, 1985).

· The lack of coarse sediment within these facies implies that
sediment transport processes were unable to carry coarse sand and
gravel, ice rafting was minimal, and/or there was no source of
coarse material. Facies 1 sediments are presently being deposited
on the continental slope, and hence similar deposits in the
stratigraphic record likely reflect similar oceanographic -
sedimentologic conditions as today. ·

In conclusion, bioturbated, mottled mud may represent either
hemipelagic deposition or deposition from weak, slowly depositing,
bottom currents.

Facies 2: Homogeneous mud

· General lack of primary sedimentary structures in most
occurrences of Facies 2 and grain size distributions of Facies 2
samples (i.e. dominance of fines and cut-off at 2 phi) imply
suspension deposition from a nepheloid layer or from weak currents.
Lack of abundant bioturbation, however, suggests that deposition of
this facies is more rapid than that of Facies 1. Complete
bioturbation may result in thorough mixing, and homogenization of a
sediment, but it is believed that if the homogeneity were due to
bioturbation, some trace of the presence of biota would be
apparent, as it is in Facies 1.

Local wispy laminae within Facies 2 beds may represent cross-
laminations, indicative of traction transport by bottom currents.
These currents may be continuously flowing, such as contour
currents, and hence the deposit is a contourite; they may represent

107

currents generated within a mass flow event and hence the deposit may be part of a turbidite; or they may be the result of a storm event which resuspended sediment, such as a surface storm during reduced sea levels, or a subsurface storm as described by Gardner and Sullivan (1981) and Hollister and McCave (1984) at the HEBBLE site on the Scotian Rise. Wispy beds typically have a higher sand content than other beds of this facies. The preservation of these structures probably reflects a high rate of sediment supply (Hill, 1984a) and rapid burial.

In summary, homogeneous mud was deposited either by hemipelagic processes, or by bottom currents generated by ocean circulation patterns (contour currents), storms, or mass-wasting events. Homogeneous mud may also be generated by thorough mixing of a sedimentary sequence in the shear zone of a slide or slump. In any case deposition is assumed to be rapid enough to avoid significant amounts of post-depositional bioturbation.

Facies 3: Laminated mud

Laminated muds can be generated by a variety of processes (Stow and Bowen, 1978, 1980; Mackiewicz, et al., 1984; Carey and Roy, 1985; Hesse, 1985; Reading, 1986). In the Scotian Slope environment it is possible that beds of this facies were deposited by contour currents (cf. Chough and Hesse, 1985), storms (cf. Gardner and Sullivan, 1981; Hollister and McCave, 1984), or by turbidity currents (cf. Piper, 1978; Stow, 1979; Stow and Shanmugam, 1980; Hesse and Chough, 1980; Mackiewicz et al., 1984).

Very little evidence of bioturbation and a small biogenic component in the sediments of Facies 3 suggest rapid sedimentation. Hemipelagites and contourites are typically deposited slowly (hence, bioturbation is prolific), while turbidites result from relatively rapid deposition (hence, little bioturbation) (Piper, 1978; Stow and Shanmugam, 1980; Stow, 1985; Chough and Hesse, 1985).

Facies 3 seems to occur at all water depths on the Scotian

Slope, including water depths in excess of 1500 m. It is unlikely that it was deposited at these deep-water locations directly by ice-margin melt out (cf. Mackiewicz, et al. 1984), though this process may have had a role in generating a downslope-flowing turbidity current.

Internal structures and sequences (parallel laminations, cross-laminations, grading) and bedding contacts are similar to those of fine-grained turbidites as described in the literature (Heese, 1975; Piper, 1978; Hesse and Chough, 1980; Stow and Shanmugam, 1980; Stow and Piper, 1984).

Fine gravel and coarse sand, presumably ice-rafted in origin, is seen scattered throughout the sediments. There is no evidence that this coarse debris has been winnowed by bottom currents, though in some cases this sediment appears to have been transported and sedimented with surrounding finer sediment.

Furthermore there is abundant acoustic evidence for mass wasting processes in the study area (chapter 2). Turbidity currents are one form of mass-wasting, and are often associated with other types. It is, therefore, highly likely that they occur in the area. Turbidity currents are demonstrably the principal mechanism for transporting sediment to deep continental margins (Hesse, 1975; Piper, 1978), and are expected to have widespread occurrence on the Scotian Slope.

In conclusion, it is believed that Facies 3 results from turbidity currents transporting and depositing fine-grained sediments. The physics of these turbidity currents and their mechanisms of deposition are discussed by Hesse (1975), Piper (1978), Stow and Shanmugam (1980), and Stow and Bowen (1984).

Facies 4: Thin-bedded sand

Sorted sand, the lenticular, ripple shape of some beds, and the rare presence of internal structures such as cross-laminations in Facies 4 suggests that sediment within these beds was deposited by a current, with some of the sediment possibly having been

109

transported as bedload. From the data available it is impossible
to specify whether this current flowed parallel to the contours
(contour current) or downslope (turbidity current). Hill (1984)
considers beds of similar description as turbidites because of
their coarse grain size, water depths they are found in, and bed
thicknesses.

Facies 5: Poorly sorted mud

The pebbly texture of Facies 5 is characteristic of cohesive
debris flows (Pettijohn, 1975; Shanmugam and Benedict, 1978; Hill
et al., 1982a, Visser, 1983), but also of ice-rafted deposits
(Anderson et al., 1979; Kurtz and Anderson, 1979). Hugget and Kidd
(1984) have found ice-rafted debris in sediments at abyssal depth
in the oceans. The coarsest grains observed within Facies 5 are
normally fine gravel. Lowe (1982) notes that many cohesive debris
flow deposits show an upper size limit to the supported particles.
This observation suggests that larger grains, if originally
present, were able to settle through the matrix during flow. If
the gravel in Facies 5 were in situ ice-rafted debris, then a
broader spectrum of sizes would be expected. Grain sizes at outer
shelf and upper slope source areas show a continuous spectrum of
sizes from clay to boulders (King, 1970; Hill et al., 1983).

Bedding contacts are almost always sharp, often irregular, and
sometimes steeply dipping. These features indicate that each bed
is a distinct depositional event and commonly erosional in nature,
thus supporting a mass flow origin. Kurtz and Anderson (1979),
Aksu (1980), and Hill et al. (1982a) use these characteristics as
criteria for distinguishing debris flows from paratills (ice-rafted
debris). A clast that was ice-rafted can be seen in Figure 3.5.
Though the basal contact is sharp it is not erosional, but rather
it downwarps the laminae, possibly from the force of impact when it
fell to the bottom, or possibly from subsequent compaction.

Sediment fabric in Facies 5 is generally isotropic, with the
sand and gravel occurring randomly throughout a mud matrix. This
characteristic can be caused by: 1) the buoyancy effect of the

110

cohesive matrix; 2) lift due to flow turbulence; 3) intergranular dispersive pressure; 4) any combination of the above processes (Lowe, 1979, 1982); and 5) slow accumulation of ice-rafted debris.

Local faint horizontal laminae of coarse grains in Facies 5 can be created by shear sorting, or by laminar flow in a cohesive debris flow (Enos, 1977; Lowe, 1979, Nardin et al., 1979). These laminae can occur at any level within the debris flow. Coarse laminae could also result from winnowing bottom currents, or they may represent lenses of ice-rafted debris.

Poorly developed, normal and inverse grading has been noted locally in Facies 5. These characteristics are often associated with mass flow deposits (Hampton, 1975; Lowe, 1979; 1982; Nardin et al., 1979; Aksu, 1980, 1984). The type of grading that develops depends on the clay mineralogy, grain size distribution, and the nature of the flow (density, water content, rheologic behaviour) (Enos, 1977; Hampton, 1972; Lowe, 1979, 1982; Nardin et al., 1979). Normal grading can be the result of settling of coarser particles into a less-dense underlying matrix. If deposition of the mass flow is rapid (i.e. as in a freezing plug; Enos, 1977; Lowe, 1979, 1982) then the flow itself must be graded. Settling of ice-rafted debris may also produce normal grading. Inverse grading can occur as a result of intergranular dispersive pressure, or through turbulence (Lowe, 1979). Deposition must be rapid for this characteristic to remain in the rock record.

In summary, a wide range of sediment textures and structures characterize Facies 5. It is not always possible to differentiate the mechanism of deposition for these sediments because of the similar characteristics expected for a variety of processes. These types of sediment could result from hemipelagic deposition combined with an ice-rafted component, or they could result from mass movement processes, such as debris flows. It is suspected that the majority of Facies 5 beds were deposited as a result of a combination of these processes, whereby accumulation of ice-rafted and ice-margin meltout debris was followed by instability resulting in numerous thin-bedded debris flows.

111

3.6 Facies Associations: descriptions and distributions

In order to understand the context of the studied lithofacies it is necessary to observe lateral and stratigraphic relationships between facies. To this end facies are grouped into facies associations. Facies associations for this study were created by grouping facies that were observed to occur together and appear to be genetically related.

Facies Association A: Facies 1, 2, and 4

Facies 1 occurs in association with minor amounts of Facies 2, and 4. Facies 1 bedding contacts with Facies 2 are everywhere gradational, while with Facies 4 they are usually sharp but disrupted by bioturbation. This association forms thick (>1 m), correlatable sequences at the tops of all cores and at various stratigraphic horizons within the cores.

Facies Association B: Facies 2, 3, and 4

Facies Association B typically consists of thin individual Facies 4 beds separated by 10-30 cm-thick beds of Facies 3, or 2. Facies 4 may be missing from the sequence, leaving thick sequences of Facies 3 and 2 beds. The association is thickest (>2 m) in mid-slope cores and is correlatable from core to core in this area. Elsewhere the association is seen as thin (<1 m) sequences often interbedded with Facies Association C.

Facies Association C: Facies 5 and 4

Facies Association C generally occurs as thick (1-2 m) sequences of individual Facies 5 beds, occasionally interbedded with thin (cm) beds of Facies 4. Association C occurs within most cores and is commonly either stratigraphically or laterally accompanied by Facies Association B. Together the two associations occur throughout the study area at various correlatable stratigraphic horizons (Figs. 4.2 - 4.5).

3.6 Facies Associations: interpretations

Facies Association A:

As previously discussed it is difficult to distinguish between contourite and hemipelagic sediments. Facies 1 is the dominant facies type in Association A and its characterisitcs meet criteria for hemipelagic and contour current deposition. The fact that, at present, contour currents are not documented on this part of the Scotian Slope implies that the topmost occurrences of Facies 1 were not deposited by contourites; however, it has been suggested by Hill and Bowen (1983) that present-day storms can generate currents which flow parallel to contours. Prolific bioturbation in this facies reflects slow sedimentation.

Facies 2 in Facies Association A resulted from slightly higher sedimentation rates than Facies 1, giving little time for biogenic reworking. The local presence of obscure structures within this facies and the presence of fine sand suggest deposition by weak bottom currents.

The rare occurrence of Facies 4 within this association is believed to result from pulses within these bottom currents that cause temporary increases in current velocity. These pulses increase the competence of the current and its ability to rework bottom sediment.

Sediment colour changes reflect either a change in the sediment source and composition, or a change in depositional environment (e.g. reducing to oxidizing). In this study there is a distinct colour difference between Facies Association A (olive-greys and dark browns) and the other associations (red-browns and browns). This colour difference does not suggest a depositional mechanism, but in this case it can be used as an aid to readily distinguish Facies Association A from other associations. Organic carbon analysis on sediments of different colours show slight differences in percent organic carbon content of Facies 1 from other Facies (Table 3.2), but whether this fact contributes to the

113

colour change is not known. Sediment colour has been used to distinguish hemipelagic sediments from turbidites in both rocks (Hesse, 1975) and recent sediments (Piper, 1973; Stow, 1979, 1981; Hill, 1981). This characteristic, therefore, has potential as an aid for easy recognition and interpretation of sediment types.

Facies Association A is interpreted to reflect sediment deposition and reworking during periods of quiet oceanic conditions and low sedimentation rates. Such criteria may be met during high sea levels (such as at the present), during long periods of ice cover, or during static conditions at the shelf break.

Facies Association B:

The characteristics of Facies Association B compare with data and criteria presented by Hesse (1975), Piper (1978), Stow and Bowen (1978, 1980), Stow (1979), Stow and Shanmugam (1980), O'Brien et al. (1980), Hesse and Chough (1980), and Hill (1981, 1984b) to suggest deposition from a low density, slowly depositing turbidity current.

Facies 4 beds coincide with Stow and Shanmugam's (1980) T_0 and Bouma's (1962) A, B, or C divisions. These are thin to thick beds of sand, often lenticular shaped, with internal cross-laminations. These beds, where they occur, comprise the base of a turbidite unit.

Facies 3 muds are equivalent to Stow and Shanmugam's (1980) T_1, T_2, and T_3 divisions (Piper's (1978) E_1 division). These are laminated muds that form a graded sequence from thin silt laminae to low amplitude climbing ripples (rarely distinguishable in a piston core sample), to thin regular laminae, to thin indistinct laminae. This facies is the most common sediment type in this association. Partial and truncated sequences are the normal mode of occurrence, therefore, evidence of grading is often lacking.

Table 3.2 Organic Carbon Analysis

Core	Depth (cm)	%OC	Facies	Comments
51	324	0.77	3	light brown lamina
	325	0.94	3	dark brown lamina
	363	0.90	3	light brown lamina
	365	0.93	3	dark brown lamina
	580	0.53	5	reddish brown
21	495	0.34	1	olive grey
	550	0.42	1	dark brown
	610	0.33	1	olive grey
	10 TWC	0.72	1	olive green

Facies 2 muds in Facies Association B correspond to Stow and Shanmugam's (1980) T_4, T_5, T_6, and T_7 divisions, and to Piper's (1978) E_2 and E_3 divisions. These are indistinctly laminated, graded, and ungraded, relatively homogeneous muds.

The T_8 division of Stow and Shanmugam (1980) (F of Piper (1978)) is bioturbated mud that caps the turbidite sequence. Bioturbation is seen in thin (5-10 cm) intervals interbedded with sediments of this facies association. It is also noted in the capping mud laminae of some sand/silt - mud couplets.

It is important to note that in the studied cores whole sequences, such as T_0-T_8, or D-F, are never completely preserved. Typically only one or several of these divisions is present in any one turbidite sequence (Hill, 1981; Chough, 1984; Thornton, 1984).

Figure 3.3 is an X-radiograph of a section from one of the studied cores showing Facies Association B. This section is believed to represent one turbidite event, and is the most complete sequence that could be found. At the base of the section is a sand bed less than 1 cm thick (Facies 4) (T_0). Overlying this bed are numerous well defined, silt and clay laminae (Facies 3) (T_3). These laminae become less well defined and thinner up-sequence (T_4). About 10 cm above the basal bed of sand the sequence becomes structureless (Facies 2) (T_6-T_7). The origin of pebbles seen scattered throughout this turbidite sequence is unknown, but it is a common characteristic. They may represent ice-rafted debris dropped into the sediment as the turbidite was being deposited. Some of this gravel, however, seems to conform with the fabric of the beds, suggesting that it was transported and deposited by the turbidity current.

Facies Association C:

An all-encompassing interpretation for this association remains elusive. In some instances Facies 5 sediments fit cited descriptions of debrites (Walker, 1984; Stow, 1986), but in most cases they may represent either sediments with an ice-rafted

116

component, or mass flow deposits at various stages of development.

Facies 4 sediments interbedded with Facies 5, though they are equally interpreted as mass-flow deposits, are believed to have a separate genesis from Facies 5 for several reasons: 1) if they represent bedload deposition it is likely they were deposited from a high density turbidity current. Interpretations do not support the presence of mature, high-density turbidity currents in the formation of Facies Association C; 2) if they resulted from deposition by a turbidity current that evolved from the mass flows which deposited Facies 5 one would expect to see a sequential relationship of sediment textures with Facies 5. No intermediate textures between Facies 5 and Facies 4 have been observed; and 3) they are thinly bedded, which is out of scale with the thicker beds of Facies 5. The conclusion is that Facies 4 beds represent turbidity currents initiated from a different sediment source than Facies 5, and probably generated by different mechanisms than the mass-movement events responsible for Facies 5 beds.

3.7 Deformed Beds: interpretation

Soft sediment deformation features can be generated by a number of mechanisms, including flow shear, loading, compaction, creep, slumping, and sliding. Deformation features from the studied cores are considered to have resulted from large scale sediment slumping and sliding for the following reasons:

1) Effects of deformation cross-cut facies boundaries and bedding contacts and occur throughout thick sequences (>10 m). Features are not facies or bed specific as would likely be the case for convolute intraformational laminations, ball and pillow structures, or load casts and flame structures.

2) The cores containing deformational features are from the acoustically defined disturbed zones. Acoustic data from these zones reveals no evidence of sediment creep (cf. Hill et al., 1982b; Silva and Booth, 1984), but rather that the disturbed zones are similar in morphology and structure to large scale, complex

retrogressive rotational slumps (Piper et al., 1985). Only cores from within these disturbed zones show deformational features.

3) Cores show interbedded blocks or plugs of undisturbed or nearly undisturbed strata within disturbed sequences. If creep were the dominant cause of deformation it is expected that the entire sequence would be disturbed. Likewise structures do not compare to those produced by creep as identified by Bennett et al. (1977).

4) Observed deformational features from the studied cores (Fig. 3.6a-c) compare with features resulting from slumping and sliding (Pettijohn, 1975; Embley and Jacobi, 1977; Hill, 1981, 1983, 1984a; Pickering, 1982, 1984; Jacobi, 1976, 1984; Coniglio, 1986). These features lend support to the Piper et al. (1985) interpretation of the disturbed zones resulting from rotational slumping.

3.8 Summary

Facies relationships and sediment characteristics have led to the following interpretations (Table 3.3 is a synopsis of facies characteristics and interpretations): 1) Facies 1 was deposited by a combination of hemipelagic and contour current processes and might be termed a bioturbated hemipelagite or muddy contourite. 2) Facies 2 was deposited by either: a) combinations of hemipelagic and contour current processes, in which case beds would be termed hemipelagites or muddy contourites, or b) by low-density, slow-moving fine-grained turbidity currents, in which case an individual bed would be termed a fine-grained turbidite. 3) Facies 3 was deposited by low-density, slow-moving turbidity currents, producing laminated fine-grained turbidites. 4) Facies 4 was deposited either as: a) bedload from fast flowing turbidity currents (sandy turbidite), or b) by bottom current pulses (contourite). 5) Facies 5, depending upon the sediment characteristics, was deposited by thin debris flows (fine-grained debrites), or by dense, immature turbidity currents (disorganized turbidites). 6) Deformed beds resulted from large scale sediment failure, such as slumping or

Table 3.3 Synopsis of facies descriptions and interpretations:

Facies	Colour	Description	Interpretation
1	Olive, olive-grey, and dark brown	Thick bedded (1-5 m), bioturbated, mottled clay to sandy mud. Common burrow, trail, and trace structures with associated authigenic pyrite.	Hemipelagic or bottom current deposition
2	Range of colours including olive to red-brown.	Thin to medium bedded (.05-.2 m) mud to sandy mud. Structureless to faint horizontal and wispy laminae.	Hemipelagic or bottom current deposition or tail of fine-grained turbidite. E2 and E3 divisions (Piper, 1978), and T4-T7 divisions (Stow and Shanmugam, 1980).
3	Dark brown, light brown, and red brown	Thin to thick beds (.1-3 m) composed of distinct, thin, parallel laminae and sand/silt - mud couplets.	Deposition from low-density, slow-flowing fine-grained turbidity current. E1 division (Piper, 1978) and T1-T3 divisions (Stow and Shanmugam, 1980).
4	Dark brown or olive grey.	Thin bedded (.01-10 cm), well-sorted, fine sand. Sharp bedding contacts. No obvious internal structures.	Deposition from fast-flowing turbidity current, possibly transported as bedload. T0 division (Stow and Shanmugam, 1980) and CD divisions (Bouma, 1962).
5	Dark brown, red brown, or grey brown.	Medium to thick bedded (.1-1 m) mud with occasional scattered sand and pebble to mud with abundant sand and gravel. Sharp, erosional bedding contacts. Local inverse and normal grading, mottling, and crude sand and pebble laminae.	Deposited by thin, fine-grained debris flows and disorganized turbidites.
deformed beds	N/A	Deformed bedding: features include microfaults, dipping laminae, distorted laminae, overturned folds, convolute laminae, eyelet structures, and homogenized sediment.	Synsedimentary deformation caused by massive sediment failure.

119

sliding, involving downslope displacement and creation synsedimentary deformation features.

Facies Association A is interpreted as sediment deposited and reworked during periods of quiet oceanic conditions and low sedimentation rates (hemipelagites and contourites). Such criteria may be met during high sea levels (such as at the present), during long periods of ice cover, or during static conditions at the shelf break.

The characteristics of Facies Association B suggest deposition from unconfined, low density, slow moving turbidity currents. A single turbidite event may take from weeks to months to fully deposit its load (Piper, 1978; Stow and Shanmugam, 1980). These events were likely initiated by sediment failure in material on the upper slope or shelf break.

Facies Association C was deposited by thin-bedded, fine-grained debris flows (Aksu, 1984; Hill et al., 1982a) and disorganized turbidites, with rare influences of fast flowing turbidity currents depositing beds of Facies 4. Beds comprising Facies Association C were also likely initiated by sediment failure in upper slope or outer shelf glaciogenic deposits.

CHAPTER 4

STRATIGRAPHY

4.1 Introduction

This chapter describes the stratigraphy of the Verrill Canyon
area based on the study of piston cores and acoustic data. Using
lithologic, micropaleontologic, oxygen isotope, chronologic, and
physical property information, combined with the acoustic data of
Chapter 2, correlations between cores are attempted.

4.2 Lithostratigraphy

The sequence of facies associations in each of the cores is
presented in Figures 4.1, 4.2, 4.3, and 4.4. Correlations of
facies associations between cores, based on the acoustic
stratigraphy, have been attempted in Figures 4.2, 4.3, and 4.4. No
correlation lines are drawn in Figure 4.1 because acoustic
resolution is poor at these core sites. Figure 4.2 shows the
downslope correlation of cores from the undisturbed area between
the two disturbed zones. Figure 4.3 demonstrates a cross-slope
correlation of cores, forming an east-west transect of the area.
Figure 4.4 is a compilation of five cores that have been, according
to acoustic information, taken from different stratigraphic
horizons. These five cores in Figure 4.4 produce a composite
stratigraphic sequence about 20 m in measured thickness, but may
represent a thicker sequence if downslope fining trends are taken
into consideration.

4.3 Biostratigraphy

Foraminifera

Foraminiferal types and abundances were studied from 35 cm^3
samples taken from four cores (21, 24, 34, and 310).
Identifications were made by G. Vilks (in Piper and Wilson, 1983,
and personal communication, 1985). Individual abundances of
certain key species can be used to interpret the environment of

121

Figure 4.1 Lithostratigraphy of three cores (27, 24, and 52)
          stratigraphically positioned on depth to the red
          reflector. No correlation is attempted because poor
          acoustic resolution at each of the core sites does not
          permit accurate statigraphic positioning. Note that
          the legend of graphic symbols representing facies
          associations applies to all other figures with core
          representations in them. Also note that a diagonal
          line across a core column represents a missing or void
          section, and a dashed vertical line at the edge of the
          core column designates the separation of a piston core
          from its trigger weight core when no overlap can be
          correlated between the two cores. Core locations are
          plotted on Figures 1.2 and 2.1.

METRES

FACIES ASSOCIATION "A"

FACIES ASSOCIATION "B"

FACIES ASSOCIATION "C"

CORE
52
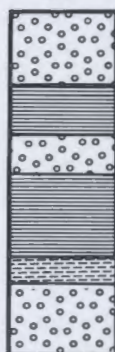
CORE
27

CORE
24

$^{14}C = 15,100 \pm 310$

DEFORMED

12 m
to
RED

8m
to
RED

13 m
to
RED

123
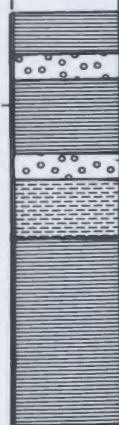
Figure 4.2 Lithostratigraphy and correlation of facies
associations of seven cores (26, 21, 22, 25, 51, 32,
and 56) resulting in a downslope profile (colours
indicate acoustic reflectors established in Chapter 2).
Cores are stratigraphically positioned assuming the
tops of the cores represent the seabed surface. This
positioning emphasises the fact that these cores were
collected from stratigraphically complete (i.e.
unidisturbed) sedimentary sequences. Note downslope
shallowing of acoustic reflectors and thinning of beds.
Core locations are plotted in Figures 1.2 and 2.1.

125
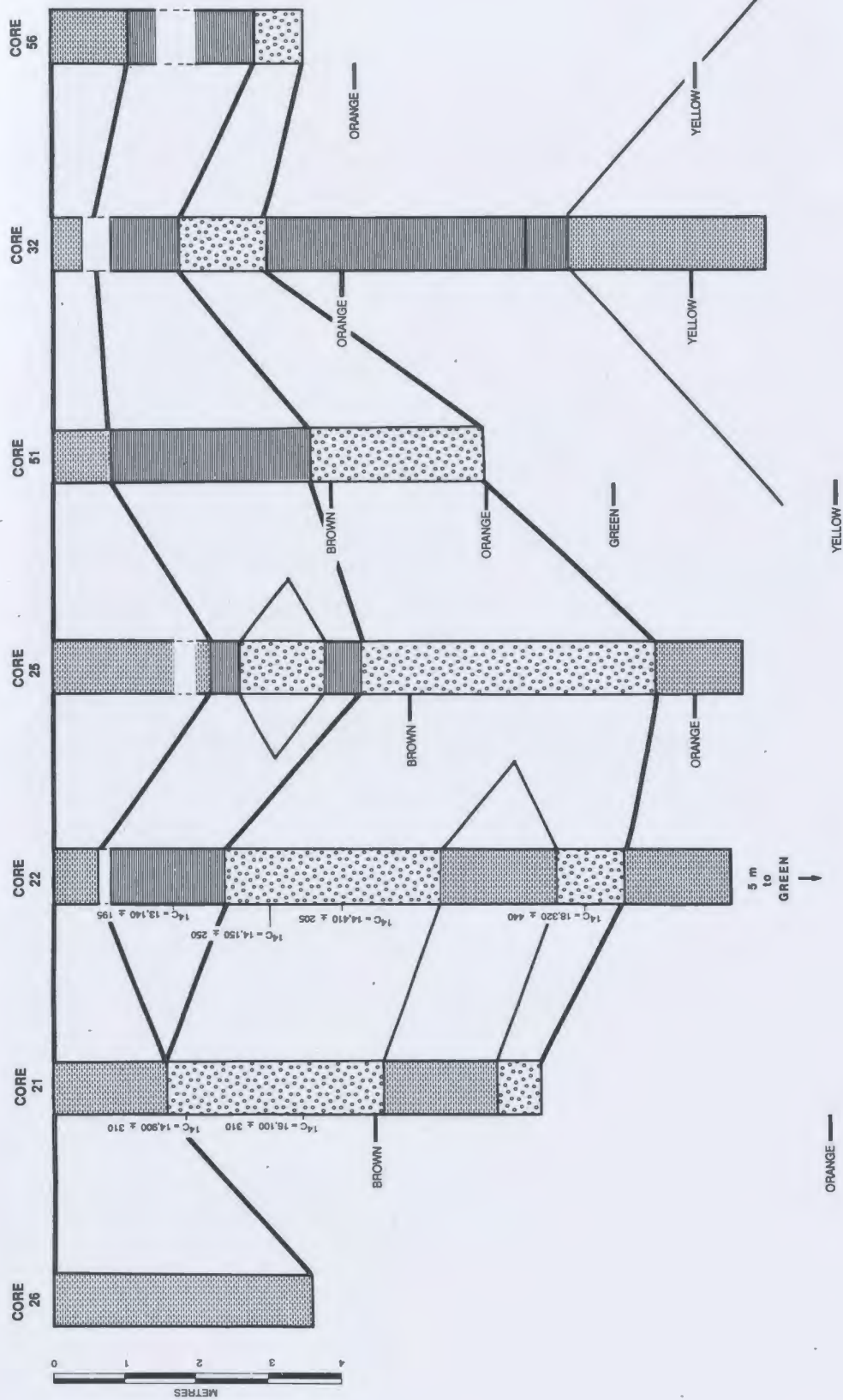
Figure 4.3   Lithostratigraphy and correlation of facies
              associations of six cores (29, 37, 55, 54, 33, and 32)
              resulting in a cross-slope profile (colours indicate
              acoustic reflectors established in Chapter 2.   Cores
              are stratigraphically positioned on the red reflector
              which emphasises that some of the core sites have had
              material removed.   Core locations are plotted on
              Figures 1.2 and 2.1.
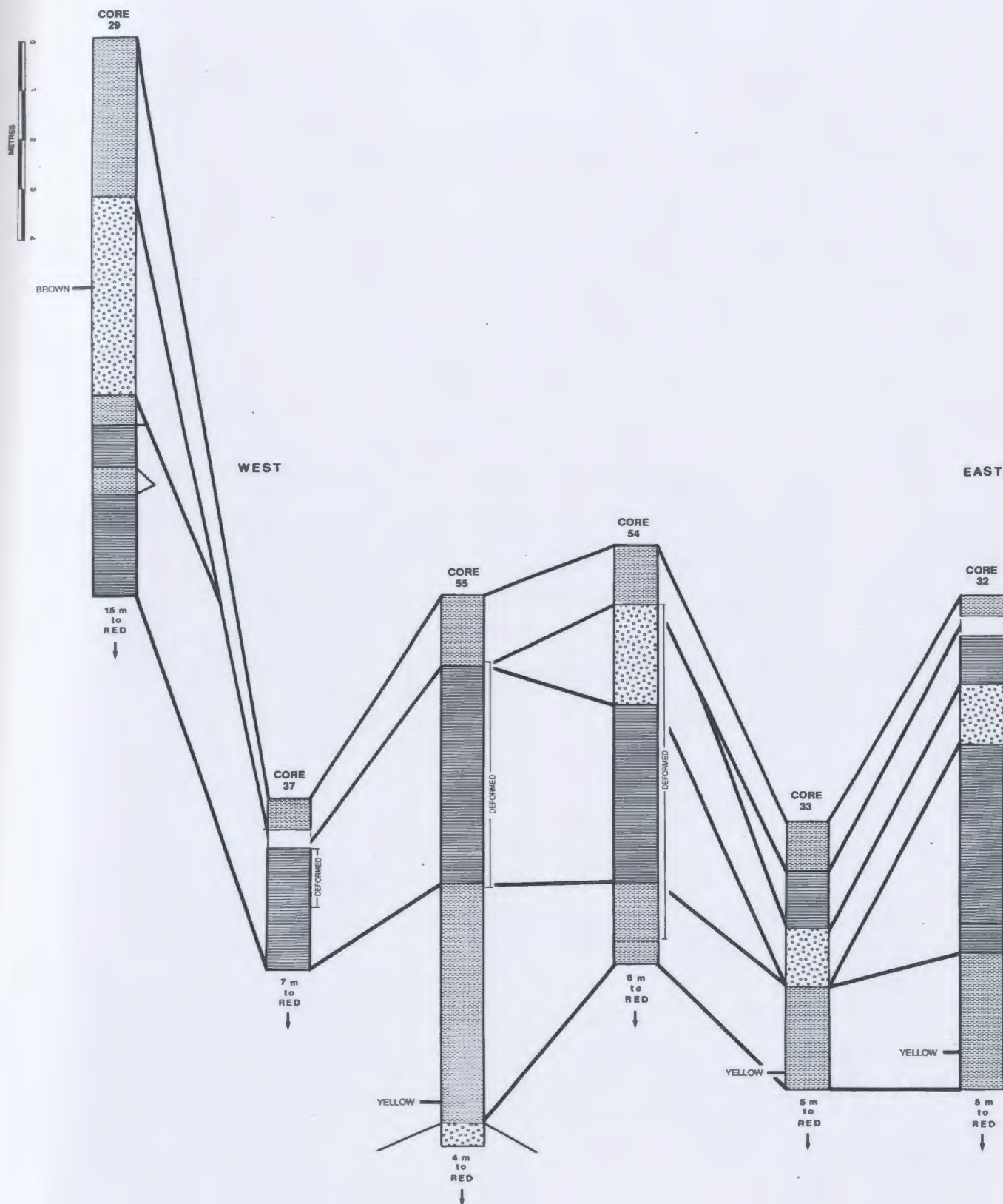
Figure 4.4 Composite lithostratigraphy and facies association
            correlations of cores based on acoustic·data from
            Chapter 2 (colours indicate acoustic reflectors).
            Cores are stratigraphically positioned on the yellow
            reflector, except for core 36 which is aligned on the
            pink reflector. Core locations are plotted on Figures
            1.2 and 2.1.
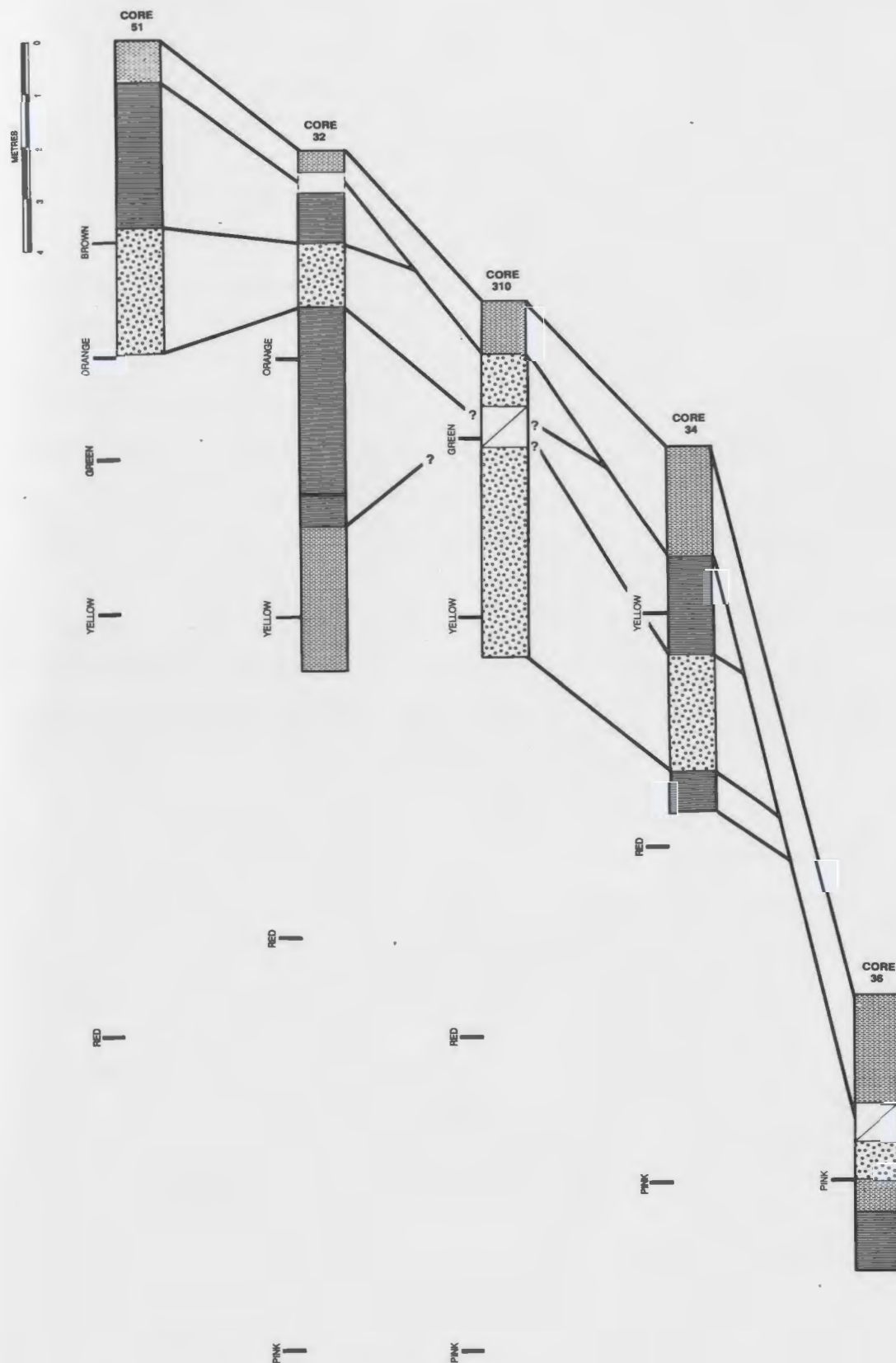
deposition of the sediment in which they are found, assuming they have not been displaced, or have been displaced only minimally (Be et al., 1971; Feyling-Hansen et al., 1971; Lipps et al., 1979; Miller and Lohmann, 1982). Figure 4.5a-d summarizes the data collected in downcore plots of relative abundance curves for certain key foraminifera.

Vilks (personal communication, 1985) has found that the studied cores show three foraminiferal assemblage zones: Zone A contains subarctic planktonic species (Globigerina quinqueloba and G. bulloides making up 15-20 % of the total planktonic foraminifera), low abundances of Neogloboquadrina pachyderma (sinistral) and low benthic percentages. It is interpreted as being post-glacial. Zone B contains high numbers of N. pachyderma (sinistral), high benthic percentages, and the dominance of Cassidulina laevigata in the benthic population. The zone is interpreted as ice distal. In zone C, 65 to 90 % of the N. pachyderma are sinistral, benthic percentages drop off, and C. laevigata remains present but may drop in relative abundance. The zone C assemblage suggests the presence of a proximal ice margin (Mudie, in press).

Vilks (personal communication, 1985) has also determined that the variations in benthic foraminifera are less pronounced than those of the planktonics. The dominant species in zone A are Islandiella helenae, Cassidulina laevigata, Oridorsalis umbonatus, Globobulimina auriculata, and Nonionella labradorica. In zone B Cassidulina laevigata predominates, with some Elphidium excavatum forma clavata, Islandiella helenae, Nonionella labradorica, and N. turgida. In zone C species diversity is lower and C. laevigata and E. excavatum f. clavata are co-dominant with lesser N. labradorica, N. turgida, and I. helenae.

A glacial environment interpreted from foraminiferal assemblages in zones B and C is indicated by the cold water species present and by the ten-fold decrease in total faunas. A decrease in numbers of foraminifera is expected on the continental slope during periods of glaciation because of drastically increased

Figure 4.5   Relative abundances of key foraminifera plotted
             downcore and showing A, B, and C assemblage zones: a)
             core 24, b) core 21, c) core 29, e) core 3₡ f) core
             310. % benthics calculated from total number of
             individuals, % N. pachyderma (sinistral) calculated
             from total number of planktonics, and % C. laevigata
             calculated from total number of benthics. Data is from
             Vilks (in: Piper and Wilson, 1983; and unpubl.).

a

CORE 34

PERCENT

0 20 40 60 80 100

ASSEMBLAGE ZONE A

ASSEMBLAGE ZONE B

ASSEMBLAGE ZONE C

DEPTH DOWN CORE (METRES)

1
2
3
4
5
6

b

CORE 310

PERCENT

0 20 40 60 80 100

ASSEMBLAGE ZONE A

ASSEMBLAGE ZONE B

ASSEMBLAGE ZONE C

DEPTH DOWN CORE (METRES)

1
2
3
4
5
6
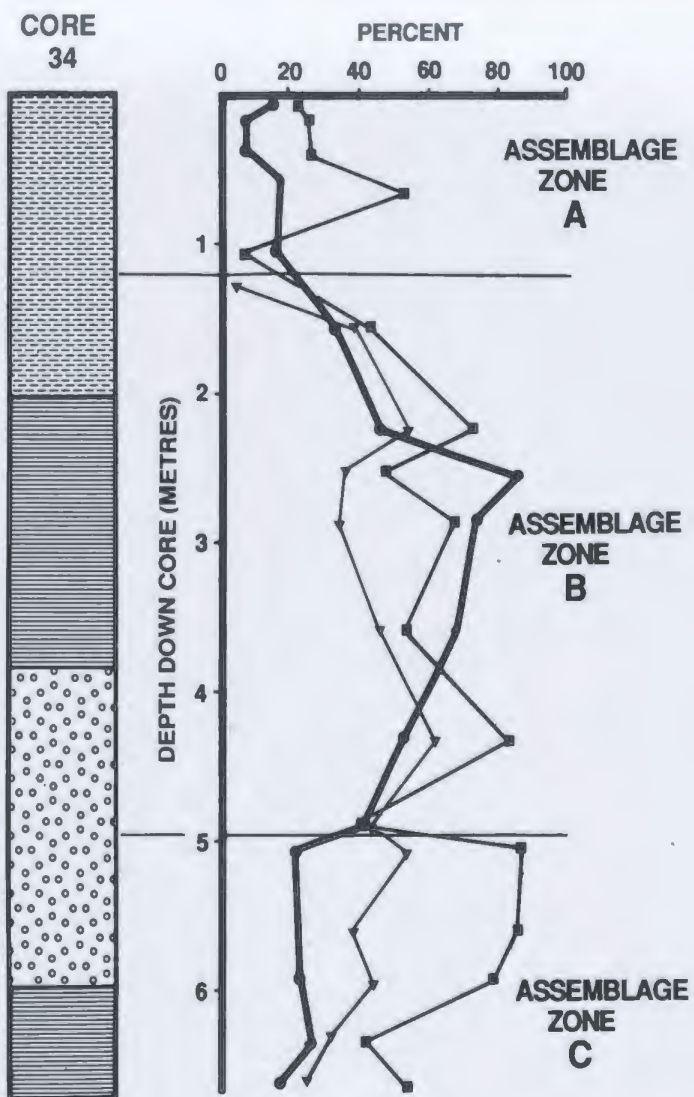
BENTHICS   N. PACHYDERMA (sinistral)   C. LAEVIGATA
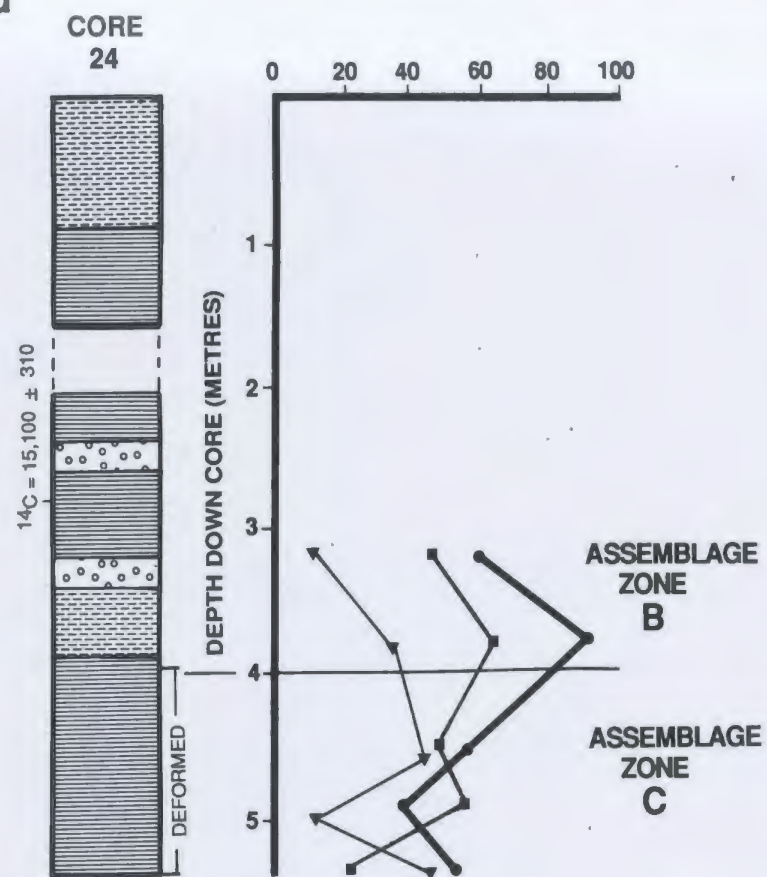
sedimentation rates (see later this chapter).

Mollusca

Several mollusc shells were recovered from the cores, though
for the most part macrofossils are rare. These shells have been
identified (Table 4.1) by F.J. Wagner (in: Piper and Wilson, 1983),
and P. Cole (personal communication, 1985). Except for *Macoma
brevifrons* all species are well within their normal geographic
ranges (the identification of *M. brevifrons* is somewhat doubtful),
but four of the species are not thought to inhabit as great a water
depth as where the samples were taken. These species along with
their cited depth ranges are: *Colus spitzbergensis* (1-548 m),
Macoma brevifrons (9-24 m), *Astarte undata* (9-190 m), and *Macoma
calcarea* (1-360m). The fact that these samples are complete valves
and one sample is a set of both valves together suggests that
reworking, if any, has been minimal. This argument is strengthened
by the fact that radiocarbon dates from these shells show
increasing ages with depth (Table 4.3).

4.4 Oxygen Isotope Stratigraphy

Oxygen isotope analyses were conducted by A.E. Aksu on the
foraminifera collected from cores 32, 310, and 36. Table 4.2
presents the data and Figure 4.6 is a plot of this data against
depth in the cores. Peaks to the right in the curve reflect
interglacial or interstadial periods, or times of major freshwater
discharge. Peaks to the left indicate glacials. The isotope curve
can thus indirectly show fluctuations in climate. The curves show
oxygen isotope stages 1 and 2, and possibly the end of stage 3 (see
Shackleton and Opdyke, 1973, 1976 for isotopic stage definitions).

Table 4.1 Mollusca specimens collected from studied cores
          (Identifications by F.J.E. Wagner).

Core	Depth (cm)	Mollusca	
21	145	Aspodont pelecypod-indet	6 fragments
	188	Bathyarca sp.	1 fragment
	308	Astarte undata (Gould)	2 valves
	395	?Propebela sp. 1 fragment	
	490-495	Aporrhais occidentalis (Bech)	
22	84	Propebela turricula (Montagu)	1 complete specimen
	221	Macoma cf. M. brevifrons (Say)	1 complete shell
	320	Astarte undata (Gould)	1 complete shell
	659	?Colus spitzbergensis	1 fragment
24	67-74	Nautica clausa (Broderys & Sowerby)	1 complete specimen
		Macoma calcarea (Gmelin)	1 single valve
	93	Bathyarca sp.	1 fragment
27	31	Barnacles.	several fragments
		Coral fragments	
29	45	Yoldia Megayoldia thracineformis (Storer)	1 fragment
		Gastropod-indet.	1 fragment

135

Table 4.2 Oxygen Isotope values
(for PDB standard)

Core no.	Sample depth (cm)	^{18}O value (PDB)
32	10-15 TWC	1.07
"	20-25	1.22
"	80-85	3.18
"	122-127	2.36
"	184-190	4.29
"	235-240	3.95
"	345-350	2.93
"	476-481	3.31
"	595-600	3.60
"	677-685	3.94
"	717-725	3.90
310	186-191	3.34
"	289-294	3.74
"	379-384	3.35
"	544-549	3.83
"	605-610	3.85
"	657-663	4.23
36	94-99	3.93
"	225-230	3.96
"	315-320	3.89
"	430-435	2.65

Figure 4.6   Oxygen isotope values plotted for cores 32, 310, and
             36, showing isotopic stages 1, 2, and 3.   Isotopic
             stages are defined by Shackleton and Opdyke, 1973 and
             1976).

138
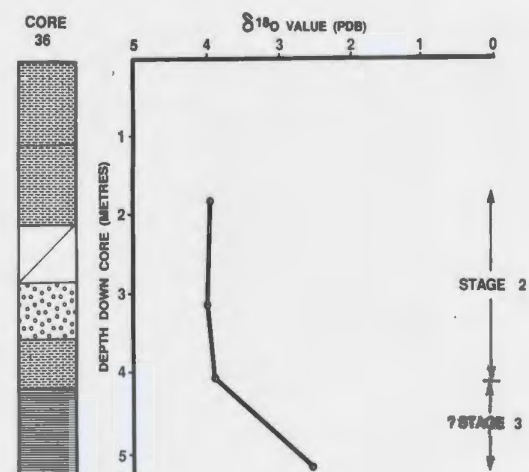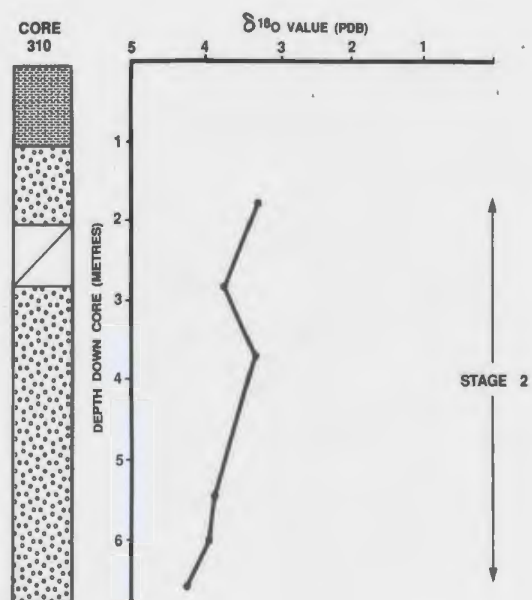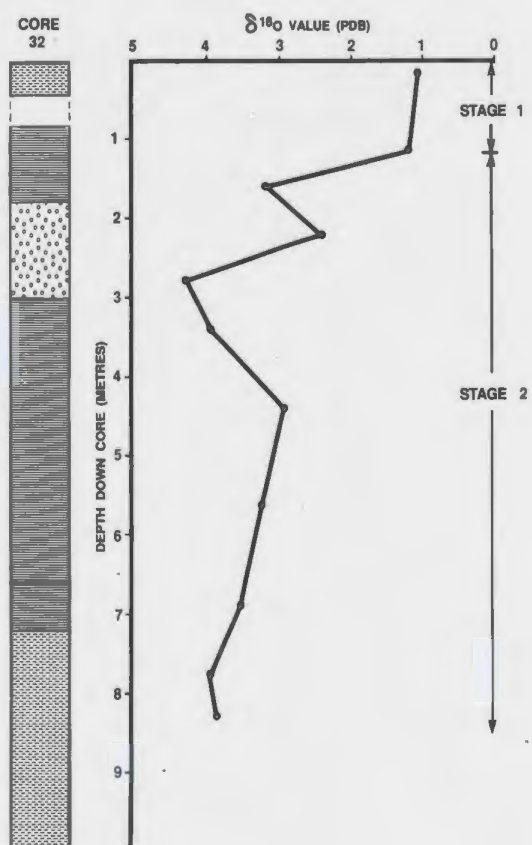
4.5 Carbon-14 Dating

Seven accelerator mass spectrometer (AMS) radiocarbon dates have been determined on samples of mollusc shells (Table 4.3). The fact the dates are stratigraphically consistent within and between cores based on lithologic correlations supports the argument that the shells were either not resedimented, or that downslope displacement was contemporaneous with the shells. In either case the dates represent a legitimate time framework for the stratigraphy represented in the studied cores. These dates range from 18,320 - 13,140 yBP.

4.6 Physical Property Stratigraphy

Physical property measurements, including undrained shear strength, water content, and bulk density were conducted on 10 of the studied cores. These data are illustrated in downcore plots in Figures 4.7a-j, and are presented in tables in Appendix C. Physical properties are dependent upon the depositional environment and subsequent burial history of the sediment, and on characteristics of the sediment itself (e.g. grain size, sediment mineralogy).

At the top of cores (where data exists) the shear strength profile decreases anomalously with depth. This decrease correlates with decreasing water content. Marine sediments generally show increasing shear strengths with depth and decreasing water contents, representing the normal process of consolidation.

Below the anomalous topmost section of the physical property curves, correlation between cores is more difficult. The shape of the various curves seems to be dependent on factors of two orders of importance. The first order control is the grain size of the sediment at the sample level. Good examples of this control can be seen in Figures 4.7e and g where the physical properties have corresponding downcore grain size curves. In these examples changes in grain size can be seen to correlate with changes in physical properties. Bulk density and shear strength properties

Table 4.3 Chronologic data from radiocarbon dates of mollusc shell samples (AMS technique).

Core no.	Depth (cm)	Beta lab no.	^{14}C Age
21	145	Beta-10988	$14,900 \pm 310$
"	308	Beta-10989	$16,100 \pm 310$
22	84	Beta-15242	$13,140 \pm 195$
"	221	Beta-15243	$14,150 \pm 250$
"	320	Beta-15244	$14,410 \pm 205$
"	659	Beta-15245	$18,320 \pm 440$
24	75	Beta-10987	$15,100 \pm 310$

Figure 4.7 Downcore curves of physical property measurements:
a) core 51, b) core 56, c) core 33, d) core 54, e) core
34, f) core 55, g) core 310, h) core 37, i) core 36, j)
core 52. Note the scatter of plotted values, and
decreasing shear strengths at the tops of cores.

a

CORE
51

SHEAR STRENGTH (kPa)

BULK DENSITY (g/cm³)

WATER CONTENT (%)

DEPTH DOWN CORE (METRES)

b

CORE
56

SHEAR STRENGTH (kPa)
0   5   10   15   20

BULK DENSITY (g/cm³)
1.4   1.6   1.8   2.0

WATER CONTENT (%)
30   50   70   90

DEPTH DOWN CORE (METRES)

1

SHEAR STRENGTH (kPa)
0   5   10   15   20

BULK DENSITY (g/cm³)
1.4   1.6   1.8   2.0

WATER CONTENT (%)
30   50   70   90

1

c

CORE
33

SHEAR STRENGTH (kPa)
0   5   10   15   20

WATER CONTENT (%)
30   50   70   90

1

DEPTH DOWN CORE (METRES)

2

3

4

5

143

d

CORE
54

SHEAR STRENGTH (kPa)

BULK DENSITY (G/CM³)

WATER CONTENT (%)

DEPTH DOWN CORE (METRES)

DEFORMED

e

CORE
34

SHEAR STRENGTH (kPa)
0   5   10   15   20

WATER CONTENT (%)
30   50   70   90

GRAIN SIZE (%)
0   25   50   75   100

DEPTH DOWN CORE (METRES)

CLAY

SILT

SAND

GRAVEL

145

f

CORE 55

SHEAR STRENGTH (kPa)

BULK DENSITY (g/cm³)

WATER CONTENT (%)

DEFORMED

DEPTH DOWN CORE (METRES)

g

CORE
310

SHEAR STRENGTH (KPA)
0   5   10   15   20

BULK DENSITY (g/cm^3)
1.4   1.6   1.8   2.0

WATER CONTENT (%)
30   50   70   90

GRAIN SIZE (%)
0   25   50   75   100

DEPTH DOWN CORE (METRES)

1

2

3

4

5

6

SAND

CLAY

SILT   GRAVEL

h

CORE
37

SHEAR STRENGTH (kPa)

WATER CONTENT (%)

i

CORE
36

SHEAR STRENGTH (kPa)

BULK DENSITY (g/cm^3)

WATER CONTENT (%)

CORE 52

WATER CONTENT (%)

BULK DENSITY (g/cm^3)

SHEAR STRENGTH (kPa)

DEPTH DOWN CORE (METRES)

seem to be especially affected. This order of control causes the scatter seen in all of the curves of downcore physical properties.

The second order control on the shape of the physical property curves is sample depth (i.e. burial history). General trends in the curves show increasing shear strengths and decreasing water contents with depth. In some cases, such as in cores 33 and 55 (Figs. 4.7c and f) the profiles are relatively flat. These cores are, however, from the disturbed zones and the sediments in them have been deformed. Physical properties in these cores have, therefore, been altered (i.e. remolded).

Further correlation of the studied cores based on their physical properties may require normalization of the properties with the grain size distribution, as well as with depth of burial. This approach is recommended for further work, but is beyond the scope of this thesis.

4.7 Interpretations

Sequences in the studied cores have been separated into stratigraphic units based on the various stratigraphic data (i.e. lithologic, micropaleontologic, radiocarbon, and oxygen isotope information). These units are correlated from core to core in Figures 4.8 - 4.10. Figure 4.8 is a downslope correlation, Figure 4.9 is a cross-slope correlation, and Figure 4.10 is a stratigraphic compilation. Most obvious is the surface correlation of Facies Association A. It lies above any of the key acoustic horizons, is generally one to two metres thick, and is found at the tops of all cores. This correlatable facies association is termed unit 1.

Unit 1 is roughly the equivalent of foraminiferal assemblage zone A. Carbon-14 studies suggest this unit is younger than 13,000 - 14,000 yBP. The light oxygen isotope values indicate the unit represents isotopic stage 1. It can be concluded from this information that unit 1 was deposited during the warmest episodes of all the sediments studied. It represents latest Wisconsinan and

150

Figure 4.8 Downslope correlation of units. Note the downslope
           shallowing of reflectors and thinning of units.

NORTH ... SOUTH

CORE 26   CORE 21   CORE 22   CORE 25   CORE 51   CORE 32   CORE 56

unit 1   unit 2   unit 3

BROWN   ORANGE   GREEN   YELLOW

14C = 16,100 ± 310
14C = 14,900 ± 310
14C = 18,320 ± 440
14C = 14,150 ± 250
14C = 14,410 ± 205
14C = 13,140 ± 195

5 m to GREEN

METRES
0
1
2
3
4

152
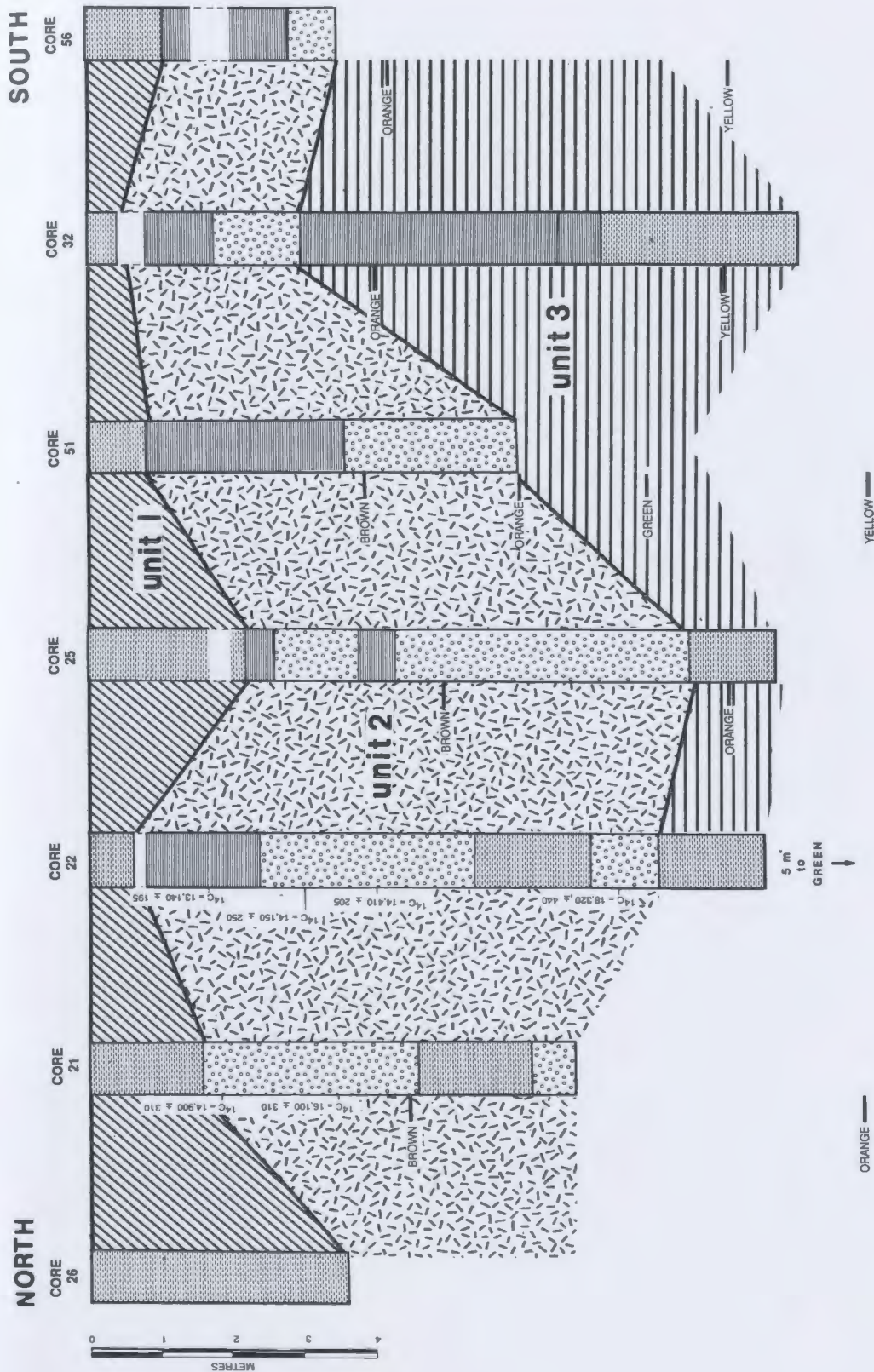
Figure 4.9 Cross-slope correlation of units. Note that cores from
the disturbed zones are missing most of unit 2.
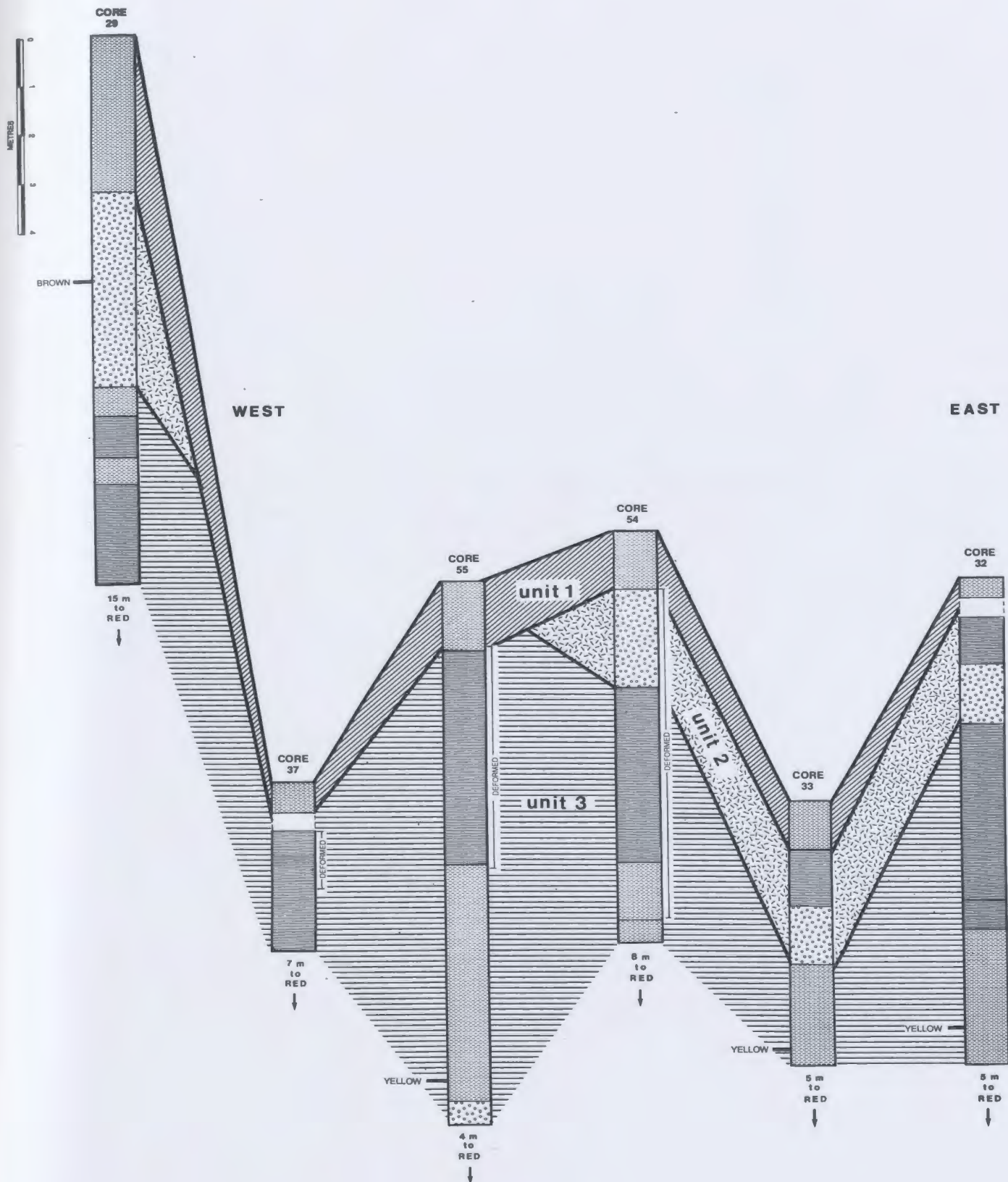
Figure 4.10 Compiled stratigraphic section and correlation of
units.

Holocene deposition up until the present. The unit is, therefore, post-glacial in origin. Sediments forming unit 1 accumulated at an average rate of 5 cm per thousand years. Hill (1981) determined a similar rate for the Holocene surface sediment in his study area further west on the Scotian Slope.

Unit 1 also correlates with the topmost section of the physical property curves, which is best defined by shear strength. The anomalous trend in these curves may be related to increasing grain sizes with depth and possible changing mineralogical composition of the clays with depth.

Immediately underlying unit 1 is a 1-3 m section of Facies Association B followed by a 1-4 m section of Facies Association C. This roughly correlatable sequence is termed unit 2. This unit contains the Orange, Brown, and possibly the Green acoustic reflectors. According to 6 AMS dates in cores 21 and 22 this unit ranges from 18,000 yBP near its base to 13,000 yBP at its top, and thus is entirely Late Wisconsinan in age. These dates indicate high but varied sedimentation rates. The average rate, calculated between the oldest and the youngest dates in the unit, is 111 cm per thousand years.

Foraminiferal assemblage zones B and C occur within unit 2. Oxygen isotope data are consistent with radiocarbon dates suggesting that the unit is within oxygen isotope stage 2. It is concluded from this information, plus radiocarbon data, that unit 2 represents ice-proximal to ice-distal (glacial to late glacial) sedimentation from its base to its top.

There is a 3-5 m-thick section of Facies Association B and a thin occurrence of Facies Association C underlying unit 2. These two associations are separated by a thick (2-3 m) occurrence of Facies Association A in some cores. This sequence is termed unit 3. Unit 3 may be separated from unit 2 by a thin (50 cm) bed of Facies Association A (e.g. core 33). Unit 3 includes Red and Yellow acoustic reflectors.

Unit 3 is similar to unit 2 in sediment types and lithologic

157

sequences. Assuming similar rates of deposition as unit 2, unit 3 dates from about 18,000 yBP back to about 27,000 yBP (assuming that the unit is 10 m thick and has had a rate of deposition of 111 cm per thousand years). The base of the unit may be older as this sedimentation rate does not take into account the slow rates of deposition that occur in the Facies Association A intervals, nor the fact that sedimentation rates probably decrease downslope (i.e. units thin in the downslope direction).

Oxygen isotope results from core 32 and foraminiferal information from cores 34 and 310 are available. The extrapolated dates and the oxygen isotope curve suggest the unit' is within isotopic stage 2. Foraminiferal assemblages in the unit are similar to those in unit 2, but assemblage C dominates, implying predominantly ice-proximal sedimentation.

Only one core (core 36) stratigraphically underlies unit 3. Oxygen isotope data (Table 4.2, p. 136) and physical property information (Fig. 4.7, p. 148) is available on this core. The sedimentary sequence represented in this core is termed unit 4 and is similar in lithologies to units 2 and 3. Extrapolation of a minimum sedimentation rate (36 cm per thousand years, based on depth of oldest carbon-14 date to present) and maximum sedimentation rate (110 cm per thousand years based on the sedimentation rate within unit 2), puts the bottom of the core between 20,000 and 55,000 yBP. The isotope curve suggests the base of core 36 demonstrates the end of isotopic stage 3 (start of stage 2), which occurred about 32,000 yBP (Shackleton and Opdyke, 1973, 1976).

4.8 Summary

The stratigraphic sequence in the studied cores, on the basis of lithologic, oxygen isotope, radiocarbon, paleontologic, and physical property information, is divided into four units, representing about 30,000 years of sedimentation.

The uppermost unit is 1-2 m thick and occurs at the top of all

cores. Deposition of this unit began during the onset of the
Holocene transgression and continues at the present. Deposition
rates were on the order of 5 cm per thousand years for this unit.
Unit 2 dates from about 13,000 yBP to 18,000 yBP. Data suggest it
was deposited during oxygen isotope stage 2. Sedimentation rates
were rapid for the unit, averaging 111 cm per thousand years. No
radiocarbon dates exist for unit 3 but by extrapolating
sedimentation rates it likely commenced more than 27,000 yBP (i.e.
near the beginning of isotopic stage 2). Sediment types are
similar to those found in unit 2. The deepest part of the compiled
stratigraphy is the base of core 36, which demonstrates the end of
isotopic stage 3. It dates at about 32,000 yBP.

On the basis of lithologic, oxygen isotope and foraminiferal
analyses it is evident that sediments of unit 1 reflect post-
glacial deposition. Underlying units are composed of ice-proximal
and ice-distal glacial-marine sediments, deposited during various
stages of the Wisconsinan glaciation.

CHAPTER 5

DISCUSSION and CONCLUSIONS

5.1 Review

The Late Quaternary geology of an area just west of the
Verrill Canyon on the Scotian Slope has been studied through the
examination and analysis of piston cores, and through the use of
high resolution seismic and sidescan data. The study area is a
site of recent hydrocarbon exploration and of known sediment
failure. The region ranges from 500 to 3500 m water depth, with
gently sinuous bathymetric contours, except in the extreme east of
the area where Verrill Canyon crosses the slope.

The Scotian Shelf has been the primary source of sediment for
the Scotian Slope and hence the geology of the study area has been
greatly affected by the geologic history of the adjacent shelf.
King (1970) and King and Fader (1986) suggest that the majority of
Quaternary sediment on the shelf is glacial in origin, hence the
study area must also have been greatly affected by glaciation.
According to King and Fader (1986) a grounded ice sheet extended
across the entire Scotian shelf during the Early Wisconsinan
(between about 70,000 to 50,000 yBP).

The Wisconsinan ice sheet probably entrained, transported, and
deposited abundant glacial debris as it advanced and receded across
terrestrial and marine areas. Periods of minor recessions and
advances probably occurred throughout this period. Oscillations of
the buoyancy line (line of seabed – ice shelf contact) are believed
to be responsible for the development of till tongues on the
continental shelf (King and Fader, 1986). Between about
32,000-16,000 yBP the ice shelf retreated to present land areas. A
surge of grounded ice to parts of the inner and outer shelf may
have occurred during the Late Wisconsinan (King and Fader, 1986;
Amos and Knoll, in press).

Following the last phase of glaciation there was a period of
low relative sea level (-110 to -120 m) and subsequent sea-level

rise until the present (Milliman and Emery, 1968; Scott et al.,
1984; King and Fader, 1986).

On the Scotian Slope, the effects of the last glaciation and
lower sea levels can be seen acoustically from the presence of
tongues of material acoustically resembling till (Fig. 2.5). These
tongues extend into upper slope stratified sediments (Fig. 2.5, 2.6
and 2.7), and the uppermost tongue appears equivalent to unit 3 in
piston cores of this study (Chapter 4). Exposure of till-like
material on the uppermost slope, relict iceberg scours on the upper
slope (Fig. 2.3), and erosional gullies at the shelf break (Fig.
2.2) are also evidence of Wisconsinan glaciation and lower sea
levels.

Mass sediment failure events have occurred in the study area,
indicated by the presence of surficial and buried disturbed zones,
erosional scarps and depressions, and slump scars and deposits
(Fig. 2.1). Piper et al. (1985) estimate surface sliding has
removed between 4 and 7 x $10^9 m^3$ of sediment from the study area.

Acoustic profiles reveal that underneath and outside the
disturbed zones many of the slope sediments are evenly stratified,
yielding continuous, parallel reflectors on acoustic return. Six
key reflectors have been traced throughout much of the study area!
These horizons were used to establish the acoustic stratigraphy at
core sites and thus aid correlation of lithologic units between
cores. Removal of material by erosion and thinning of intervals
between reflectors permitted sampling to deeper acoustic horizons
than would have otherwise been possible.

Examination of sediments in 18 piston cores led to
identification of 5 lithofacies:

    Facies 1: Bioturbated mottled mud
    Facies 2: Homogeneous mud
    Facies 3: Laminated mud
    Facies 4: Thin-bedded sand
    Facies 5: Poorly sorted mud

Bioturbated, mottled mud (Facies 1) is interpreted to represent either hemipelagic deposition or deposition from weak, slowly depositing, bottom currents. Deposition is slow enough to allow for abundant burrowing to occur.

Homogeneous mud (Facies 2) could result from a variety of processes including: deposition by hemipelagic processes; deposition by bottom currents generated by ocean circulation patterns (contour currents), storms, or mass-wasting events; or by thorough mixing of a sedimentary sequence in the shear zone of a slide or slump. In either case deposition is assumed to be rapid enough to avoid significant amounts of post-depositional bioturbation.

On the Scotian Slope, laminated muds (Facies 3) most likely result from turbidity currents transporting and depositing fine-grained sediments by processes discussed by Hesse (1975), Piper (1978), Stow and Shanmugam (1980), and Stow and Bowen (1984).

The thin sand beds (Facies 4) probably result from bedload being transported beneath a current. On evidence within the beds alone it is not possible to specify whether this current flowed parallel to the contours (contour current) or downslope (turbidity current).

Poorly sorted mud (Facies 5) could result from hemipelagic deposition combined with an ice-rafted component, or from mass movement processes, such as debris flows. It is interpreted that Facies 5 beds were deposited by a combination of these processes, whereby accumulation of ice-rafted and ice-margin meltout debris was followed by instability resulting in small-scale, perhaps local, thin-bedded debris flows.

Grain size analyses indicate subtle differences between facies and show a downslope fining trend between cores. The gravel portion is significant, though it represents only a small percentage of the sediment. It is interpreted that gravel comes from a glacial source. This interpretation is supported by the fact that the uppermost post-glacial sediment in the cores contains

162

no gravel.

Synsedimentary deformation features, such as convolute laminae, rolled balls, microfaults, and dipping laminae, were recognized in a few cores from the disturbed zones. These features overprint depositional structures in the facies, and suggest the style of deformation in the disturbed zones was primarily caused by slumping and sliding of blocks of sediment.

Lithofacies were grouped into 3 facies associations:

1) Facies Association A is composed of Facies 1, 2, and 4. .It is interpreted as being deposited by hemipelagic and contour current processes, and subsequently reworked by bioturbation. It is believed that this association predominates during periods of quiet oceanic conditions and low sedimentation rates. Such criteria may be met during high sea levels (such as at the present), during long periods of ice cover, or during static conditions at the s elf break.

2) Facies Association B is composed of Facies 2, 3, and 4. It is interpreted to result by deposition from unconfined, low density, slowly depositing turbidity currents. These turbidity currents were likely initiated by sediment failure in material on the upper slope or shelf break.

3) Facies Association C is composed of Facies 5 and 4. The majority of this association was likely deposited by thin-bedded, fine-grained debris flows (Aksu, 1984; Hill et al., 1982a) and disorganized turbidites. Rare fast flowing turbidity currents deposited beds of Facies 4. Beds comprising Facies Association C were also likely initiated by sediment failure in upper slope or outer shelf glaciogenic deposits.

Downcore variations in lithologic, chronologic, oxygen isotope, foraminiferal, and geotechnical properties were determined in numerous cores. With the aid of the established acoustic stratigraphy it was possible to position piston cores and their studied properties into a correlatable sequence which demonstrates

163

the stratigraphy throughout the study area (Figs. 4.8 - 4.10). This correlation led to the definition of four units.

The uppermost unit (unit 1) is a sequence of sediment that is apparent at the tops of all cores. It is composed of Facies Association A and contains no gravel. A radiocarbon date of 13,000 yBP near its base results in a sedimentation rate for the unit on the order of 5 cm per thousand years. Oxygen isotope data confirm the unit is Holocene in age (isotopic stage 1) and was deposited outside of the influence of glacial ice (post-glacial). An anomalous trend of decreasing shear strengths with depth is consistently seen in this unit.

Units 2, 3, and 4 are composed of Facies Association A, B and C. Unit 2 dates about 18,000 yBP at its base and 13,000 yBP near its top, giving sedimentation rates on the order of 100 cm per thousand years for the unit and 35 cm per thousand years from the base of the unit to the top of the core. Extrapolation of these sedimentation rates to the base of core 36 (deepest part of the stratigraphy sampled) gives ages ranging between 20,000 and 55,000 yBP. This age range is large, but given that calculated sedimentation rates are so variable it is impossible to narrow the range further without actual radiocarbon dates deeper in the stratigraphic sequence.

Oxygen isotope data suggest units 2 and 3 were deposited during isotopic stage 2 (stadial). The base of core 36 (unit 4) shows the end of isotopic stage 3, suggesting the age is about 32,000 yBP for this interval. This date is consistent with the range of dates given above. Foraminiferal analyses indicate these units were deposited under ice-proximal to ice-distal conditions. The presence of gravel in units 2, 3, and 4 is indicative of a glacial origin for these sediments. Shear strengths and bulk densities generally increase, and water contents decrease with depth in these units (i.e. normal consolidation).

164

5.2 Discussion

Geologic History: stratigraphy and sedimentation

From the study of existing literature, and evidence presented in this thesis, it is apparent that, over the past 70,000 years, glacial ice crossed the Scotian Shelf and terminated on the upper slope region of the study area. There is also evidence of major sea-level lowerings over this period. These phenomena had profound affects on sedimentation on the Scotian Slope and account for the majority of Quaternary sediment underlying the study area.

Holocene

Only unit 1, which is Holocene in age, was deposited without the influence of glacial ice. This unit forms a drape over the study area. In fact, sediments of similar type and age have been described forming a drape over the entire eastern Canadian continental slope (Stow, 1981; Hill, 1983, 1984; Swift, 1985). The rate of deposition for the unit is slow. The unit is composed almost exclusively of Facies 1 and 2 sediments, reflecting slow deposition.

It is interpreted that the sediments of unit 1 were deposited primarily by hemipelagic processes. Occurrences of Facies 2 and rare Facies 4 beds near the base of the unit may represent current deposition. These beds indicate the influence of lower relative sea levels at the start of the Holocene. Coastal processes affecting exposed outer shelf material led to shelf spill-over and downslope transport of sediment, resulting in turbidite deposition. Shallower water depths over the upper slope meant that wave-generated and long-shore drift currents played a greater role in resedimenting slope deposits (cf. Stanley et al., 1972a; Inman et al., 1976). Finer sediments and increased bioturbation in the upper part of the unit reflect the rising sea level and drowning of the shelf break during the Holocene transgression.

165

The lack of any gravel in the Holocene sequence suggests that sediment supply from glacial sources is negligible. Hill (1981) maintains that sediments of a similar type to unit 1 in his study area on the Scotian Slope are likely derived from the outer banks of the Scotian Shelf, though their ultimate source could be inshore, shelf, and on land. The recognition of iceberg scours in the north of the study area and on the outer shelf is important to the interpretation of Holocene sedimentation processes on the slope. Based on sea-level curves iceberg scours could not have occurred at these water depths in about 10,000 years. Their still-recognizable presence indicates that supply of sediment to the slope by outer shelf erosion (at least along the shelf directly north of the study area), and off-shelf transport must be minimal or the outer-shelf features would have been removed by erosion and the upper-slope scours would be undetectable due to burial by off-shelf sedimentation. This evidence suggests that most of the sediments comprising unit 1 have been transported within the water column, from a source more distant than the outer shelf. It is accepted theory that sediment can bypass the shelf and upperslope, ultimately to be deposited in deep water environments.

Mid to Late Wisconsinan

The remainder of the sediments studied, including units 2, 3, and 4, comprise the Mid to Late Wisconsinan sequence in the study area. These units, as seen in lithologic correlations and acoustic profiles, thin downslope. In some areas, such as within the disturbed zones, some of the upper portion of this sequence has been removed by mass-wasting processes. This Wisconsinan sequence contains examples of all facies (i.e. Facies 1 to 5).

Gravel and clasts, interpreted to be ice-rafted, are present in small amounts throughout the sequence. This evidence, plus foraminiferal data, and oxygen isotope results from core studies, along with the presence of till-like tongues and iceberg scours on the upper slope, argues that sediments of the Mid to Late Wisconsinan are primarily glacial in origin.

The upper till-like tongue in Figures 2.5, 2.6, and 2.7 could be a true till tongue (cf. King and Fader, 1986), but the formation of such a feature would require a late glacial ice margin which extended into present water depths of 700 m. This required extent is not supported by any other types of evidence. This acoustic feature may also represent an ice-margin delta, deposited on the upper slope by melt-out from nearby glacial ice. This model would require an ice-margin which extended to the outer shelf. This theory fits better with models presented by other workers on east coast glaciation (King and Fader, 1986, Prest, 1984). The tongue may also represent slumped outer-shelf sediments which have spilled over onto the upper slope. Again, however, glacial ice would have been the most likely mechanism for transporting to the outer shelf the large supply of sediment necessary for such a deposit.

In either model, the presence of this upper till-like tongue is possibly indicative of a Late Wisconsinan glacial readvance. Bonifay and Piper (in prep), on the St. Pierre Slope, also show evidence for a Late Wisconsinan glacial readvance. Most of the sediments studied in piston cores of the thesis area (i.e, units 2 and 3) are probably derived from this tongue. The fact that most acoustic reflections on the slope can be traced to, and appear rooted in, outer-shelf/upper-slope till-like bodies is significant evidence supporting the hypothesis that the Wisconsinan sequence is glacial-marine.

The thick deposit of till and till-like material on the outer Scotian Shelf and upper slope (Figs. 2.5, 2.6 and 2.7) could have supplied much Wisconsinan slope sediment through downslope transporting mechanisms. Kurtz and Anderson (1979), Wright and Anderson (1982), and Wright et al. (1983) recognize the importance of sediment gravity flows in modern ice-proximal slope environments of Antarctica and describe sediments similar to those found in units 2, 3, and 4 of this study.

The mechanisms responsible for the deposition of these Late Wisconsinan sediments are likely dependent upon the proximity of the ice margin, and the sea level. Figure 5.1 demonstrates various

167

Figure 5.1 Summary diagram demonstrating history of Wisconsinan
ice margin conditions and related sedimentation
processes for the Verrill Canyon study area.

ca 70,000 yBP

MAJOR ICE ADVANCE → DEPOSITION OF TILL TONGUES,
TURBIDITES, AND DEBRITES

ICE SHEET
TILL
SHELF
S.L.
TILL TONGUE
SLOPE

70,000 - 32,000 yBP

ICE RECESSION → OUTWASH AND OFFSHELF TRANSPORT
S.L.
TURBIDITES, AND DEBRITES
INTERBEDDED WITH HEMIPELAGITES
UNIT 4
ICE
OUTER SHELF TILL
SHELF
PINK
SLOPE

32,000 - 20,000 yBP

ICE ADVANCE / OSCILLATION OF ICE FRONT → ICE PUSH AND OUTWASH
S.L.
ICE-MARGIN DELTA (TILL-LIKE TONGUE)
ASSOCIATED DEBRITES, TURBIDITES,
AND INTERBEDDED HEMIPELAGITES
UNIT 3
ICE
SHELF
SLOPE
YELLOW
RED
PINK

20,000 - 12,000 yBP

ICE RECESSION → LOW SEA LEVEL → COASTAL PROCESSES AND
OFFSHELF TRANSPORT
DEBRITES AND TURBIDITES
UNIT 2
SHELF
SLOPE
PINK
ORANGE
RED
GREEN
YELLOW

12,000 yBP - PRESENT

SEA LEVEL TRANSGRESSION → DROWNING OF SHELF EDGE
S.L.
HEMIPELAGIC DEPOSITION
UNIT 1
SHELF
SLOPE
HEMIPELAGIC
DRAPE

stages of ice margin advance and retreat, and the processes and deposits resultant thereof. As can be seen from this figure, various ice margin positions and sea levels can result in similar deposits, thus it is impossible to tell the proximity of an ice margin based purely on lithologic evidence. Foraminiferal analyses indicate various periods of ice-proximal and ice-distal conditions. These data can be used to support sedimentologic interpretations.

It is believed that Facies Association C sediments in the Wisconsinan sequence reflect sediment input of glacial material onto the slope by thin debris flows of outer shelf and upperslope glacial sediments. Kurtz and Anderson (1979) observe thick sequences of glaciogenic debris flows on the slope of the Weddel Sea in Antarctica. Direct input of ice-rafted debris into beds of this facies association is considered minimal because: 1) the gravel is limited in size to small pebbles (i.e. is crudely sorted); and 2) gravel, in some instances, is crudely laminated and crudely oriented. These features are characteristics of debris flows (Aksu, 1984; Hill et al., 1982a).

The mechanism of generation of debris flows at the Scotian margin is thought to be: 1) rapid sedimentation at an ice front, and subsequent sediment failure, in which case a proximal ice margin is required, or 2) failure of outer shelf/upper slope glacial deposits due to wave loading or other coastal processes, in which case a lowered relative sea level is required.

Facies Association B is composed of resuspended outer shelf/upper slope glacial sediment that was transported downslope within turbidity currents. Anderson et al. (1979) found turbidites on the slope of the western Ross Sea of Antarctica. Ice-rafted debris can be recognized in Facies Association B sediments, though some coarse sand and fine gravel, which seems to occur within an otherwise well-sorted, fine-grained bed, may have been transported within the turbidity current. This idea is suggested because some of this coarser debris does not appear to disrupt or disturb laminae (Fig. 3.3). Transport of fine gravel by a turbidity current would suggest a sediment source within glacial material.

170

Gravel in a fine-grained turbidite also suggests that the competence of fine-grained turbidity currents is much greater than normally considered by workers concerned with slope sedimentation (e.g. Hampton, 1975; Piper et al., 1978; Stow and Shanmugam, 1980, Stow and Bowen, 1980).

Turbidity currents on the Scotian Slope, during the Wisconsinan, may have been generated by a variety of mechanisms, such as: 1) failure of outer shelf/upper slope glacial sediments, (cf. Morgenstern, 1967; Hampton, 1972), 2) Resuspension and downslope transport of glacial material as a result of density currents generated by cold, dense glacial meltwater washing over the shelf-edge (cf. Mackiewicz et al., 1984), or 3) Resuspension and downslope transport of glacial material as a result of coastal processes during a low sea level (cf. Inman et al., 1976; Fukushima et al., 1985).

The mass-sedimentation processes accounting for Facies Associations B and C would result in the greatest amount of material being deposited on the upper slope, with decreasing amounts further downslope as the distance from the source becomes greater. This phenomenon accounts for the thinning of the unit downslope. These processes would also account for the calculated rapid sedimentation rates.

Occurrences of Facies Association A beds in the Wisconsinan sequence imply periods of slow sediment accumulation. During slow deposition abundant bioturbation can take place. Facies Association A can be seen as thin to thick beds within the sequence. Its occurrence is indicative of background sedimentation on the Scotian Slope, but the presence of ice-rafted debris, and oxygen isotope and foraminiferal results indicate it was deposited during glacial (stadial) periods. During relatively stable or static ice-margin periods (i.e. when melting of the ice margin is minimal, thus sediment supply is reduced; and/or when the ice margin does not migrate, hence sediment "push" is minimal), upper slope failures and turbidity currents would not occur and Facies Association A could result.

171

Early to Mid-Wisconsinan

The base of core 36 may penetrate to the Mid-Wisconsinan, based on extrapolated radiocarbon dates. A glacial interstade occurred during this period, marked by glacial recession from the slope and outer shelf areas (Prest, 1984, King and Fader, 1986). Based on oxygen isotope data, the very end of this interstade is sampled in core 36 (unit 4). On acoustic profiles and in core 36, Mid-Wisconsinan sediments do not appear significantly different from Late Wisconsinan material, thus they are interpreted similarly as glacial-marine sediments.

No Early Wisconsinan sediments were sampled in this study, but acoustic profiles penetrate to strata of this age. The Early Wisconsinan is characterised by a major glacial advance known as the Scotian Shelf - Grand Banks advance (Prest, 1984, King and Fader, 1986). It is believed that this advance is represented on the slope by the lowermost till-like tongue of Figures 2.5-2.7. If this tongue is a true till-tongue (King and Fader, 1986) then it implies Early Wisconsinan ice had grounded on the upper slope to present water depths of about 700 m. The tongue may represent an ice-margin delta, as is suggested for the upper till-like tongue, in which case the ice was likely grounded further upslope or on the outer shelf.

This period of major glacial advance is significant to the study area. Advancing ice sheets entrained and transported large volumes of debris, and subsequently deposited it as glacial and periglacial sediment on the outer shelf and upper slope. These deposits are the source of sediment for all subsequent Wisconsinan, and perhaps even Holocene, deposition on the Scotian Slope.

Geologic History: instability

Instability features in the study area have been recognized both on acoustic records and in cores. The acoustic records indicate two large, near-surface zones, about 25 km^2 in size and

172

10-15 m thick, in which sediment failure has apparently occurred
(Fig.2.1). These records provide little evidence for the style of
mass movement. As a result, Piper et al. (1985) avoided using a
name with genetic connotations for these two areas, and termed them
simply 'disturbed zones'. Piper et al. (1985) did note, however,
that the surface characteristics of the disturbed zones are similar
to those of terrestrial retrogressive rotational slumps and
interpreted the zones as submarine rotational slumps. Further
examination of acoustic profiles has provided evidence of slide
blocks occurring at the lateral margins of the disturbed zones
(Fig. 2.9). Other mass-wasting features, such as large slump
scars, scarps, and scours have been identified in the study area
(Chapter 2).

Several cores from the disturbed zones contained no or little
evidence of a massive instability event, but a few, such as cores
54 and 55, contained thick sequences of obviously deformed
sediment. The deformation features occurred throughout about 5 to
7 m of sediment commencing just beneath unit 1. Most of unit 2 has
apparently been removed from the core sites, probably as a result
of the event. The instability phenomenon that resulted in the
creation of the two disturbed zones, therefore, must have occurred
since the deposition of unit 2 and prior to, or during, the early
stages of the deposition of unit 1. This reasoning places a 12,000
to 13,000 yBP date on the event.

Cores from the disturbed zones demonstrated a range of soft-
sediment deformation features, from tilted laminae to overturned
folds and eyelet structures to completely homogenized sediment
(Fig. 3.6a-c). Pickering (1982) classified soft-sediment
deformation into three main types: 1) brittle structures; 2)
viscoplastic structures; and 3) quasiliquid structures. It is
interpreted that dipping laminae and microfaults were caused by
brittle failure in the more competent beds of laminated sediments.
Slight folds, convolute laminae, rolled ball, and eyelet structures
(i.e. flow folds of Jacobi, 1984) were caused by varying degrees of
viscoplastic deformation in ductile sediments. Complete

homogenization of sediment, often surrounding eyelet and ball structures was caused by quasiliquid flow and subsequent mixing in highly ductile sediment.

Deformation structures may be related to both shear stresses acting on the sediments and variations in shear strengths of the sediments. Thus, the degree of deformation varies across the disturbed zone according to the amount of displacement that has occurred, and on the cohesiveness, grain size, water content, pore pressure, and bulk density of the sediment. Brittle-failure structures suggest only minimal shearing of the sediment which will tend to occur in sediments with the highest shear strengths; viscoplastic deformation indicates higher shear stresses or lower sediment shear strengths; and quasiliquid flow likely occurred in high shear zones or sediments with low shear strengths. In the extreme, shear forces combined with low shear strengths have resulted in the displacement of sediment and the complete removal of sedimentary sequences from a site. This scenario is exemplified in core sites 54 and 55 where most of unit 2 is missing. Because deformation occurs in some parts of the disturbed zone and not others, and in some parts of the core and not others - even though sediment types and physical properties are similar (Figs. 4.7a-j) - it is suggested that deformation features within the sediments are primarily related to variations in shear stresses.

The study of deformation features in recently slumped beds of marine sediments is rare, because most recent submarine instability events recorded in the literature have been recognized purely by acoustic means. Jacobi (1976, 1984) provides some examples of sediment deformation features in piston cores. Thorough study of synsedimentary mass failures is easier in outcrop of ancient rocks. Coniglio (1986), for example, studied sedimentary rocks from the Cow Head Group in western Newfoundland. He describes deformation features very similar to those observed in the studied cores and interprets them to represent shear zones within and below massive slide blocks.

Undisturbed or slightly disturbed core sequences can be seen

174

underlain or bounded by sequences of deformation structures in the studied cores. These packages of sediment, similar to those described by Coniglio (1986), are interpreted as slide and slump blocks, bounded on their upper and/or lower surfaces by mobile shear zones. Figure 5.2 summarizes the mechanism proposed for the creation of these deformation features within a slide block.

The disturbed zones of the study area are interpreted to be composed of a complex arrangement of slide blocks, and debris flows, produced as a result of displacement of the sediment during a single, massive failure event. Slide blocks are reflected in the hummocky morphology of the upper slope surface of the disturbed zones. A slide block, showing interstratal deformation, but a coherent surface, is seen in Figure 2.9. Further downslope, the scale of the hummocks on the surfaces of the disturbed zones become smaller, and overall the surfaces appear smoother, suggesting the sediment behaved more viscoplastically. At the most distal margins of the disturbed zones the failed sediment has a smooth surface morphology, it overrides acoustic reflections, seeming to erode very little, and it pinches out in a wedge-shaped fashion. These characteristics typify debris flows as described by Damuth (1978). Downslope from the disturbed zones the seafloor is marked by large-scale erosional scours and depressions. It is suggested that these features were caused by an erosive turbidity current generated as a result of sediment failure in the disturbed zones, and carrying material from the disturbed zones.

From acoustic and core evidence it seems that the disturbed zones of the Verrill Canyon area show a possible example of the transformation in the style of sediment failure from a complex slide in the upslope area, to a cohesive debris flow in the most distal reaches of the disturbed zones, and ultimately to a turbidity current eroding and transporting material further downslope (cf. Morgenstern, 1967; Hampton, 1972).

The cause of this massive slumping event, culminating in the development of the two disturbed zones, can only be speculated upon. Geotechnical measurements on cores from undisturbed areas

175

Figure 5.2 Schematic of slide block demonstrating the theory for
the development of deformation features as observed in
the studied piston cores. The surficial disturbed
zones are composed of a complex arrangement of these
slide blocks (the slide block is on the order of metres
to tens of metres thick).

SEDIMENT DISTURBANCE

increasing shear

parallel laminae

dipping laminae

wavy laminae

microfaults

overturned folds
homogenized sediment
shear plane
parallel laminae

shear plane

UNDISTURBED SLOPE SEQUENCE → FAILURE → SLUMP/SLIDE BLOCK

177
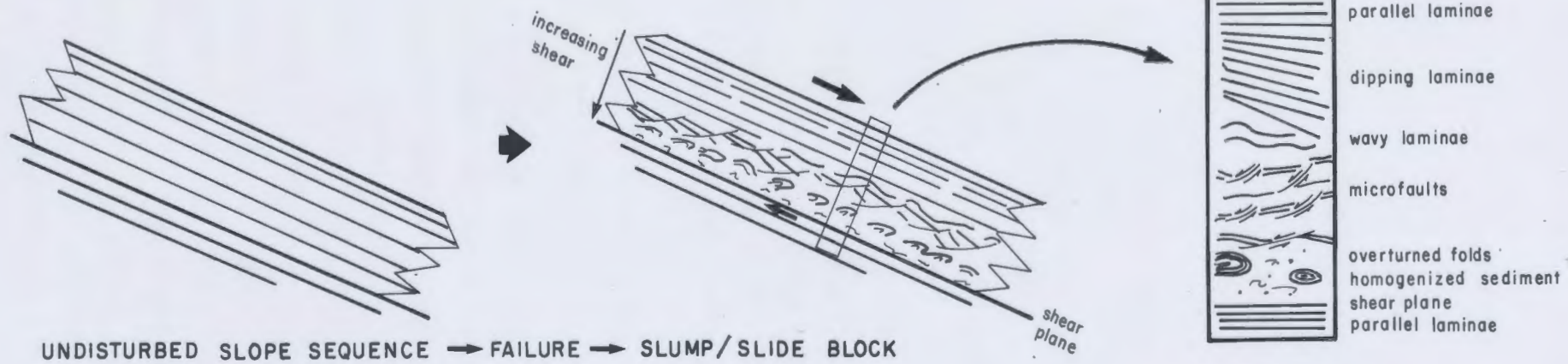
show present normal consolidation to slight apparent
overconsolidation. Moran (personal communication, 1987) suggests
that present physical properties of the sediments would not differ
greatly from their properties at 12,000 yBP (estimated time of mass
failure). From this evidence it appears that sediments in the
study area are, and likely were at 12,000 yBP, statically stable
(i.e. they will not fail under their own weight). This fact leads
to the conclusion that the failure must have been triggered by an
external mechanism.

Ice load could act as an external trigger causing sediment
failure; however, at the estimated time of the event glacial ice
had receded far from the area. Wave loading on the sediments of
the upper slope is a possible cause as well, given that sea levels
were reduced at the time the event occurred. At 12,000 yBP
(approximate timing of failure event) it is estimated that sea
level was between 50 and 75 m lower than at present (Milliman and
Emery, 1968). This places the shallowest parts of the disturbed
zones in 425 - 450 m water depth. This depth is probably too deep
for wave loading to be appreciable enough to effect sediment
stability, especially given that the sediments are believed to be
inherently stable. Moran and Hurlbut (1986) have shown that mass
movements can be generated by wave loading in only limited regions
of the continental slopes off eastern Canada.

The most reasonable explanation for slope instability in the
Verrill Canyon area is horizontal ground accelerations caused by a
seismic event. This explanation has foundation in the fact that
the east coast of Canada is prone to rare, large magnitude
earthquakes (Basham and Adams, 1982; Piper, and Normark, 1982; Keen
et al., in press). In addition, two major earthquakes with
associated sediment failures have been documented on the east coast
of Canada within recent history; namely the 1929 Grand Banks
earthquake (Heezen and Ewing, 1952; Piper and Normark, 1982; Piper
et al., 1984), and a 1933 event off Baffin Island (Keen et al.,
1972; Stein et al., 1979). A second disturbed zone is apparent
between 50 and 75 m subbottom in acoustic profiles from the study

178

area (Fig. 2.7 and 2.10). It appears similar in echocharacter to the surficial disturbed zones and hence it too may have developed as a result of a seismic event (Piper et al., 1985).

The best approach to determine the magnitude of ground accelerations which could cause sediment failure in the study area might be through detailed examination of physical properties of the sediment, with the application of these properties to an infinite-slope nomogram for slope stability analysis (Booth et al., 1985). This approach, however, is beyond the scope of this thesis.

The timing of the sediment failure in the Verrill Canyon area roughly correlates with the last glacial recession. It is also observed that the surficial disturbed zones correlate along the same stratigraphic horizon as the uppermost till-like tongue. Likewise, the buried disturbed zone correlates with the lower till-like tongue (Fig. 2.28). This evidence suggests that sediment failure in the Verrill Canyon area corresponds to episodes of glaciation and deglaciation. Stein et al. (1985) have proposed, for the 1933 event off of Baffin Island, that glaciation ablation, following recession of ice from the area, causes seismicity by reactivating deep basement faults relict from previous tectonic stress regimes. A similar mechanism of seismic activation is proposed for the Scotian Slope. Unfortunately quantitative explanations for recent earthquakes off eastern Canada are still lacking (Keen et al., in press).

5.3 Conclusions

The stratigraphy and sedimentology of the Verrill Canyon study area has been determined using the study of sediment in piston cores combined with acoustic controls. Figure 5.1 shows the development of the acoustic stratigraphy of the area. It demonstrates the complex interrelationships of the shelf and its geologic history, with sedimentation on the Scotian Slope, and the dominant effect that glaciation has had on sedimentation of the slope.

A major glacial advance during Early Wisconsinan time led to the deposition of thick sequences of glacial and proglacial sediments at the outer shelf and upper slope. These sediments were reworked and deposited downslope through the remainder of the Early and Middle Wisconsinan. The uppermost part of this sequence has been sampled and has been classified as units 4 and 3. They are composed of debris flows (Facies Association C), turbidites (Facies Association B), and bioturbated sediments (Facies Association A). Bioturbated beds reflect background slope sedimentation and represent periods of slow deposition.

A Late Wisconsinan glacial readvance again led to deposition of glacial material on the upper slope and outer shelf. Mass-movement processes such as debris flows (Facies Association C) and turbidity currents (Facies Association B) transported these sediments further downslope. These sediments form unit 2.

Holocene deposition on the Scotian Slope has been dominated by processes with slow sedimentation rates such as hemipelagic deposition. The results are fine sediment sizes and prolific bioturbation. Sediment source areas no longer appear to be the glacial and proglacial deposits on the outer shelf and upper slope, but rather the provenance and transportation history of the sediment appears to be more complex. The Holocene sequence forms a readily recognizable sediment drape overlying all of the study area.

5.4 Implications for Offshore Development

Offshore industrial and scientific activities involve the construction of structures on the seafloor. The geological and geotechnical questions raised by these activities are of two kinds: will natural processes cause slumping and other sediment failures which in turn put the security of the structure at risk; and 2) will the presence of the structure impose or induce loads and forces on the seabed that will cause instability in the sediment, again putting the security of the structure at risk?

Brown (in press) provides a list of 14 geological features and processes known to affect seabed stability of the eastern Canadian continental margin. Seven of these items apply to the Verrill Canyon study area and should be considered as possible constraints to development:

1) Lithology - the majority of Wisconsinan sediments on the uppermost slope are interpreted to have been deposited by processes related to glaciation (ice rafting, till tongues, glacial melt-out). Coarse detritus, such as boulders, resulting from these processes (especially on the upper slope) can interfere with well drilling and foundation support structures (McMillan, in press). Hill et al. (1983) observed boulders on the upper Scotian Slope during a submersible dive. In deeper water on the Scotian Slope Wisconsinan sediments are interpreted to have been largely deposited by mass-movement processes. These processes are thought to be inactive at the present, and beds deposited by them are generally thin.

2) Stratigraphy - the sediments examined for this thesis are apparently geotechnically stable, but for the occurrence of intervals of low shear strengths, such as at the base of unit 1, and within the disturbed zones where much of the sediment has been remolded. The observation of interstratal deformation, as observed in the slide block on Figure 2.9, does suggest, however, that there have been subsurface horizons that were geotechnically weaker.

3) Seismicity - large seismic events have occurred on the eastern Canadian margin with a frequency of an estimated 10,000 to 100,000 years (Piper and Normark, 1982), and have possibly affected the study area. Smaller seismic events are considered to be much more frequent (Adams, 1986).

4) Slumps - the area shows several massive slump deposits (disturbed zones), along with numerous slump scars and erosional surfaces. The study area thus has a history of instability.

5) Buried channels - Piper et al. (1985) have identified numerous buried channels in the area, and several apparently relict channels

at the surface. These channels may contain coarse sediment which can interfere with well drilling and pile driving.

6) Ice scours - relict iceberg scours are apparent on the upper slope. Though icebergs pose no modern threat in this area, the effects of scouring on the geotechnical properties of the bottom sediment is not known (Lewis et al., 1986). The presence of scours can, therefore, be considered a possible constraint to development.

7) Pockmarks - these structures are apparent on the upper slope and penetrate the disturbed zones, thus are possibly still active. As yet not much is known of pockmarks, the processes which cause them, nor the sediment properties associated with them. They are thought to be indicative of gas seepage (Josenhans et al., 1978), and to date it has been the general consensus of industry to avoid working near them.

The Verrill Canyon area, therefore, demonstrates examples of geologic constraints to industrial development in a passive margin continental slope setting. This environment in the past has been considered relatively risk-free. What this study establishes is that no general geologic model for passive margin slopes is universal. Rather each area of interest needs to be surveyed for its own suite of constraints to development. Only then can the risk to the project and to the environment be minimized.

REFERENCES

Adams, J.A. (1986) Changing assessment of seismic hazard along the
    southeastern Canadian margin. Third Canadian Conference on
    Marine Geotechnical Engineering, St. John's, Newfoundland,
    v.1, p. 42-53.

Aksu, A.E. (1980) Late Quaternary Stratigraphy,
    Paleoenvironmentology and Sediment History of Baffin Bay and
    Davis Strait. Unpubl. Ph.D. Thesis, Dalhousie University,
    Halifax, Nova Scotia. 771 pp.

Aksu, A.E. (1984) Subaqueous debris flow deposits in Baffin Bay.
    Geo-Marine Letters, v.4, p. 83-90.

Aksu, A.E. (1985) Planktonic foraminifera and oxygen isotope
    stratigraphy of CESAR cores 102 and 103: preliminary results.
    IN: Jackson, H.R.; Mudie, P.J.; and Blasco, S.M. (eds.),
    Initial Geological Report on CESAR - The Canadian Expedition
    to Study the Alpha Ridge, Arctic Ocean, Geological Survey of
    Canada Paper 84-22, p. 115-124.

Amos, C.L., and Knoll, R. (in press) The Quaternary sediments of
    Banquereau, Scotian Shelf. Geological Society of America
    Bulletin.

Anderson, J.B. and Kurtz, D. (1985) The use of silt grain size
    parameters as a paleovelocity gauge: A critical review and
    case study. Geo-Marine Letters, v.5, p. 55-59.

Anderson, J.B., Kurtz, D.D., and Weaver, F.M. (1979) Sedimentation
    on the Antarctic continental slope. IN: Doyle, L.J. and
    Pilkey, O.H.(eds.), Geology of the Continental Slopes.
    Society of Economic Paleontologists and Mineralogists Special

183

Publication no. 27, p.265-283.

Anderson, J.B., Singer, J.K., Taylor, R.S., and Ledbetter, M.T.
(1984) A comparison of electronic grain size analysis
methods. Society of Economic Paleontologists and
Mineralogists Research Conference, San Jose, California.
p. 5-7.

ASTM (1981) Annual Book of ASTM Standards. Part 19, Test D424-59
and D423-66. American Society for Testing of
Materials, p. 124-129.

Basham, P.W., and Adams, J. (1982) Earthquake hazards to offshore
development on the Eastern Canadian continental shelves. IN:
Proceedings of the Second Canadian Conference on Marine
Geotechnical Engineering, (separate).

Be, A.W.H., Vilks, G., and Lott, L. (1971) Winter distribution of
planktonic foraminifera between the Grand Banks and the
Caribbean. Micropaleontology, v.17, no.1, p. 31-42.

Bennett, R.H., Lambert, D.N., and Hulbert, M.H. (1977)
Geotechnical properties of a submarine slide area on the
U.S. continental slope northeast of Wilmington Canyon. Marine
Geotechnology, v.2, p. 245-261.

Bidgood, D.E.T. (1974) A deep-towed sea bottom profiling system.
IN: Proceedings OCEANS 74, I.E.E.E. conference (Institute of
Electrical and Electronic Engineers), Halifax, N.S., v.2,
p. 96-107,.

Blatt, H., Middleton, G., and Murray, R. (1980) Origin of
Sedimentary Rocks. Prentice-Hall, New Jersey. 782 pp.

Bonifay, D., and Piper, D.J.W. (in prep.) Late Wisconsinan ice
margin sedimentation on the upper continental slope off St.

184

Pierre Bank, eastern Canada. Canadian Journal of Earth Sciences.

Booth, J.S., Sangrey, D.A., and Fugate, J.K. (1985) A nomogram for interpreting slope stability of fine-grained deposits in modern and ancient marine environments. Journal of Sedimentary Petrology, v.55, p. 29-36.

Bouma, A.H. (1962) Sedimentology of some Flysch Deposits. Elsevier, Amsterdam. 168 pp.

Bouma, A.H. (1979) Continental slopes IN: Doyle, L.J. and Pilkey, O.H. (eds.), Geology of Continental Slopes. Society of Economic Paleontologists and Mineralogists Special Publication no. 27, p. 1-15.

Bouma, A.H., Moore, G.T., and Coleman, J.M. (eds.) (1976) Beyond the shelf break. American Association of Petroleum Geologists short course, v.2, New Orleans, La. 163 pp.

Bowles, J.E. (1970) Engineering Properties of Soils and Their Measurements. McGraw-Hill, New York. 187 pp.

Brown, J.D. (in press) Seafloor stability under loads. IN: Chapter 14 of Geology of the Continental Margin off Eastern Canada, M.J.Keen and G.L.Williams (eds.); Geological Survey of Canada, Geology of Canada, no. 2. [also Geological Society of America, The Geology of North America, v.I-1].

Burke, C.A., and Drake, C.L. (eds.) (1974) The Geology of Continental Margins. Springer-Verlag, New York. 1009 pp.

Cacchione, D.A. and Drake, D.E. (1986) Nepheloid layers and internal waves over continental shelves and slopes. Geo-Marine Letters, v.6, p. 147-152.

185

Carey, D.L., and Roy, D.C. (1985) Deposition of laminated shale: A field and experimental study. Geo-Marine Letters, v.5, p. 3-9.

Chamberlain, C.K. (1978) Recognition of trace fossils in cores. IN: Basan, P.B. (ed.), Trace Fossil Concepts. Society of Economic Paleontologists and Mineralogists short course No. 5, Oklahoma City.

Chough, S.K. (1984) Mud turbidites and associated hemipelagic muds in the Ulleung (Tsushima) Basin. Society of Economic Paleontologists and Mineralogists Research Conference contributed abstracts, San Jose, California. p. 28-29.

Chough, S.K., and Hesse, R. (1985) Contourites from Eirik Ridge, south of Greenland. Sedimentary Geology, v.41, p. 185-199.

Coniglio, M. (1986) Synsedimentary submarine slope failure and tectonic deformation in deep-water carbonates, Cow Head Group, western Newfoundland. Canadian Journal of Earth Sciences, v.23, p. 476-490.

Cook, H.E., Field, M.E., and Gardner, J.V. (1981) Characteristics of sediments on modern and ancient continental slopes IN: Scholle, P. and Shearing, D. (eds.), Sandstone Depositional Environments. American Association of Petroleum Geologists memoir 31, p. 329-364.

Damuth, J.E. (1978) Echocharacter of the Norwegian - Greenland Sea: Relationship to Quaternary sedimentation. Marine Geology, v.28, p. 1-36.

Damuth, J.E. (1980) Use of high frequency (3.5-12 kHz) echograms in the study of near bottom sedimentation processes in the deep-sea: a review. Marine Geology, v.38, p. 51-75.

Dean, W.E., Leinen, M., and Stow, D.A.V. (1985) Classification of
deep-sea fine-grained sediments. Journal of Sedimentary
Petrology, v.55, p. 250-256.

Doyle, L.J. and Pilkey, O.H. (eds.) (1979) _Geology of the_
Continental Slopes. Society of Economic Paleontologists and
Mineralogists Special Publication no. 27, 374 pp.

Doyle, L.J., Pilkey, O.H., and Woo, C.C. (1979) Sedimentation on
the eastern United States continental slope. IN: Doyle,
L.J. and Pilkey, O.H. (eds.), _Geology of the Continental_
Slopes, Society of Economic Paleontologists and
Mineralogists Special Publication no. 27, p. 119-130.

Egloff, J., and Johnson, G.L. (1975) Morphology and structure of
the southern Labrador Sea. Canadian Journal of Earth
Sciences, v.12, p. 2111-2133.

Embley, R.W., and Jacobi, R.D. (1977) Distribution and morphology
of large submarine sediment slides and slumps on the Atlantic
continental margins. Marine Geotechnology, v.2, p. 205-228.

Embley, R.W. (1980) The role of mass transport in the distribution
and character of deep ocean sediments with special reference
to the North Atlantic. Marine Geology, v.38, p. 23-50.

Emery, K.O. (1968) Relict sediments on the continental shelves of
the World. American Association of Petroleum Geologists
Bulletin, v.52, p. 445-464.

Enos, P. (1977) Flow regimes in debris flows. Sedimentology,
v.24, p. 133-142.

Feyling-Hanssen, R.W., Jorgensen, J.A., Knudsen, K.L., and
Andersen, A.L. (1971) Late Quarternary Foraminifera from
Vendsyssel, Denmark, and Sandes, Norway. Bulletin of the

Geological Society of Denmark, v.21, part 2-3, Copenhagen, 317 pp.

Flint, R.F. (1971) _Glacial and Quaternary Geology_. John Wiley, New York, 892 pp.

Flood, R.D. (1980) Deep-sea sedimentary morphology: modelling and interpretation of echo-sounding profiles. Marine Geology, v.38, p. 77-92.

Folk, R.L. (1954) The distinction between grain size and mineral composition in sedimentary rock nomenclature. Journal of Geology, v.62, p. 344-359.

Folk, R.L. (1980) _Petrology of Sedimentary Rocks_. Hemphill publishing Co., Austin, Texas. 184 pp.

Folk, R.L., and Ward, W.C. (1957) Brazos River Bar, a study in the significance of grain size parameters. Journal of Sedimentary Petrology, v.27, p. 3-27.

Fukushima, Y., Parker, G., and Pantin, H.M. (1985) Prediction of ignitive turbidity currents in Scripps Submarine Canyon. Marine Geology, v.67, p. 55-81.

Fulton, R.J. (ed.) (1984) Quaternary Stratigraphy of Canada - A Canadian contribution to IGCP Project 24. Geological Survey of Canada Paper 84-10, 210 pp.

Gardner, W.D., and Sullivan, L.G. (1981) Benthic storms: temporal variability in a deep-ocean nepheloid layer. Science, v.213, p. 329-331.

Gibbs, R.J., Mathews, M.D., and Link, D.A. (1971) The relationship between sphere size and settling velocity. Journal of Sedimentary Petrology, v.41, p. 7-18.

Grant, D.R. and King, L.H. (1984) A stratigraphic framework for
    the Quaternary history of the Atlantic Provinces, Canada. IN:
    Fulton, R.J. (ed.), Quaternary Stratigraphy of Canada - A
    Canadian contribution to IGCP Project 24. Geological Survey
    of Canada Paper 84-10, p. 173-191.

Hackett, D.W., Syvitski, J.P.M., Prime, W., Sherin, A.G. (1986)
    Sediment size analysis system users guide. Geological Survey
    of Canada Open File Report No. 1240, 25 pp.

Hampton, M.A. (1972) The role of subaqueous debris flows in
    generating turbidity currents. Journal of Sedimentary
    Petrology, v.42, p. 775-793.

Hampton, M.A. (1975) Competence of fine-grained debris flows.
    Journal of Sedimentary Petrology, v.45, p. 834-844.

Heezen, B.C. (1974) Atlantic type continental margins.
    IN: Burke, C.A., and Drake, C.L. (eds.), The Geology of
    Continental Margins. Springer-Verlag, New York, p. 13-24.

Heezen, B.C., and Ewing, M. (1952) Turbidity currents and
    submarine slumps, and the 1929 Grand Banks earthquake.
    American Journal of Science, v.250, p. 849-873.

Heezen, B.C., Tharp, M., and Ewing, M. (1959) The floors of the
    ocean: I. The North Atlantic. Geological Society
    of America Special Paper no. 65, 122 pp.

Hesse, R. (1975) Turbiditic and non-turbiditic mudstones of the
    Cretaceous flysch sections of the East Alps and other basins.
    Sedimentology, v.22, p. 387-416.

Hesse, R. (1985) Sedimentology of siltstone and mudstone.
    Sedimentary Geology, v.41, Special Issue, p. 113-301.

Hesse, R. and Chough, S.K. (1980) The Northwest Atlantic Mid-
    Ocean Channel of the Labrador Sea: II. deposition of parallel
    laminated levee-muds from the viscous sublayer of low density
    turbidity currents. Sedimentology, v.27, p. 697-711.

Hill, P.R. (1981) Detailed Morphology and late Quaternary
    Sedimentation of the Nova Scotia Slope, South of
    Halifax. Unpublished Ph.D. thesis, Dalhousie
    University. 331 pp.

Hill, P.R. (1983) Detailed morphology of a small area on the Nova
    Scotian continental slope. Marine Geology, v.53, p. 55-76.

Hill, P.R. (1984a) Sedimentary facies of the Nova Scotian upper
    and middle continental slope, offshore eastern Canada.
    Sedimentology, v.31, p. 293-309.

Hill, P.R. (1984b) Facies and sequence analysis of Nova Scotia
    Slope muds: Turbidite vs. 'Hemipelagite' deposition. IN:
    Stow, D.A.V., and Piper, D.J.W. (eds.) Fine-Grained
    Sediments: Processes and Products. Blackwell Publishing,
    London, p. 311-318.

Hill, P.R., Aksu, A.E., and Piper, D.J.W. (1982a) The deposition
    of thin-bedded subaqueous debris flow deposits, IN: Saxov,
    S. and Nieuwenhuis, J.K. (eds.), Marine Slides and other Mass
    Movements. Plenum Press, New York, p. 273-287.

Hill, P.R., and Bowen, A.J. (1983) Modern sediment dynamics on the
    shelf-slope boundary off Nova Scotia. IN: Stanley, D.J., and
    Moore, G.T. (eds.) The Shelf Break: critical interface on
    continental margins. Society of Economic Paleontologists and
    Mineralogists Special Publication no. 33, p. 265-276.

Hill, P.R., Moran, K.M., and Blasco, S. (1982b) Creep deformation

of slope sediments in the Canadian Beaufort Sea.
Geo-Marine Letters, v.2, p. 163-170.

Hill, P.R., Piper, D.J.W., and Normark, W.R. (1983) PISCES IV
submersible dives on the Scotian Slope at 63°W;
Current Research, part A, Geological Survey of
Canada Paper 83-1A, p. 65-69.

Hollister, C.D.; and McCave, I.N. (1984) Sedimentation under deep-
sea storms. Nature, v.309, p. 220-225.

Holtz, R.D., and Kovacs, W.D. (1981) An Introduction to
Geotechnical Engineering. Prentice-Hall, New Jersey. 733 pp.

Hugget, Q.J., and Kidd, R.B. (1984) Identification of ice-
rafted and other exotic material in deep-sea dredge hauls.
Geomarine Letters, v.3, p. 23-29.

Hutchins, R.W., Dodds, J., And Fader, G. (1985) Seabed II:
High-resolution acoustic seabed surveys of the deep ocean.
IN: Advances in underwater technology and offshore
engineering, V 3: Offshore Site Investigation. Proceedings of
an International Conference, London. Graham and Trotman Ltd.,
p. 69-84.

Hutchins, R.W., McKeown, D.L., and King, L.H. (1976) A deep-tow
high resolution seismic system for continental shelf mapping.
Geoscience Canada, v.3. p. 95-100.

Inman, D.L. (1952) Measures for describing the size distribution
of sediments. Journal of Sedimentary Petrology, v.22,
p. 125-145.

Inman, D.L., Nordstrom, C.E., Flick, R.E. (1976) Currents in
submarine canyons: an air-sea-land interaction. Annual Review
of Fluid Mechanics, v.8, p. 275-310.

Ives, J.D. (1978) The maximum extent of the Laurentide ice Sheet along the east coast of North America during the last glaciation. Arctic, v.31, p. 24-53.

Jacobi, R.B. (1976) Sediment slides on the northwestern continental margin of Africa. Marine Geology, v.22, p. 67-173.

Jacobi, R.B. (1984) Modern submarine sediment slides and their implications for melange and the Dunnage Formation in north-central Newfoundland. Geological Society of America Special Paper 198, p. 81-102.

Jansa, L.F. and Wade, J.A. (1975) Geology of the Continental margin off Nova Scotia and Newfoundland. IN: van der Linden, W.J.M. and Wade J.A. (eds.), Offshore Geology of Eastern Canada, v.2, Geological Survey of Canada paper 74-30, p. 51-105.

Josenhans, H.W., King, L.H., and Fader, G.B. (1978) A sidescan sonar mosaic of pockmarks on the Scotian Shelf. Canadian Journal of Earth Sciences, v.15, p. 831-840.

Keen, M.J., Adams, J., Moran, K., Piper, D.J.W., and Reid, I. (in press) IN: M.J.Keen and G.L.Williams (eds.), Chapter 14 of Geology of the Continental Margin off Eastern Canada; Geological Survey of Canada, Geology of Canada, no. 2. [also Geological Society of America, The Geology of North America, v.I-1].

Keen, M.J., Johnson, J. and Park, I. (1972) Geophysical and geological studies in eastern and northern Baffin Bay and Lancaster sound. Canadian Journal of Earth Science, v.9, p. 689-609.

bottom imaging and charting. OCEANS 83 (IEEE conference proceedings of the third working symposium on Oceanographic data systems), v.2, p. 649-653.

Kranck, K. and Milligan, T.G. (1985) Origin of grain size spectra of suspension deposited sediment. Geo-Marine Letters, v.5, p. 61-66.

Krumbein, W.C. (1934) Size frequency distribution of sediments. Journal of Sedimentary Petrology, v.4, p. 65-77.

Krumbein, W.C. (1936) Application of logarithmic moments to size frequency distribution of sediments. Journal of Sedimentary Petrology, v.6, p. 35-47.

Krumbein, W.C. and Pettijohn, F.J. (1938) Manual of Sedimentary Petrology. D. Appleton-Century Co., Inc. 549 pp.

Kurtz, D.D., and Anderson, J.B. (1979) Recognition and sedimentologic description of recent debris flow deposits from the Ross and Weddell Seas, Antarctica. Journal of Sedimentary Petrology, v.49, p. 1159-1170.

Leeder, M.R. (1982) Sedimentology: Process and Product. George Allen and Unwin, Boston. 344 pp.

Lewis, C.F.M., Parrott, D.R., Simpkin, P.G., and Buckley, J.T. (eds.) (1986) Ice Scour and Seabed Engineering. Environmental Studies Revolving Funds Report No. 049, Ottawa. 322 pp.

Lipps, J.H., Berger, W.H., Buzas, M.A., Douglas, R.G., Ross, C.A. (eds.) (1979) Foraminiferal Ecology and Paleoecology. Society of Economic Paleontologists and Mineralogists Short Course No.6, Houston, 198 pp.

Keller, G.H., Lambert, D.N., and Bennet, R.H. (1979) Geotechnical
     properties of continental slope deposits: Cape Hatteras to
     Hydrographers Canyon. IN: Doyle, L.J. and Pilkey,
     O.H. (eds,), Geology of the Continental Slopes. Society of
     Economic Paleontologists and Mineralogists Special Publication
     no.27, p. 131-152.

King, L.H., (1970) Surficial geology of the Halifax-Sable Island
     map area. Marine Science Paper 1, Dept. Energy Mines and
     Resources, Canada. 16 pp.

King, L.H. (1980) Aspects of regional surficial geology related to
     site investigation requirements - Eastern Canadian Shelf. IN:
     Ardus,D.A. (ed.), Offshore Site Investigation. Graham and
     Trottman, London, p. 37-59.

King, L.H., and Fader, G.B. (1986) Wisconsinan Glaciatian on the
     continental shelf - southeast Atlantic Canada. Geological
     Survey of Canada Bulletin 363, 72 pp.

King, L.H., and MacLean,B. (1970) Pockmarks on the Scotian Shelf.
     Geological Society of América Bulletin, v.81, p 3141-3148.

King, L.H., and MacLean, B. (1976) Geology of the Scotian Shelf.
     Geological Survey of Canada paper 74-31.

King, L.H., and Young, J.F. (1977) Paleocontinental slopes of East
     Coast geosyncline (Canadian Atlantic Margin). Canadian
     Journal of Earth Sciences, v.14, p. 2553-2564.

Knott, S.T., and Hersey, J.B. (1956) Interpretation of high-
     resolution echo-sounding techniques and their use in
     bathymetry, marine geophysics, and geology. Deep-Sea
     Research, v.14, p. 36-44.

Kosalos, J.G., and Chayes, D. (1983) A portable system for ocean

Lowe, D.R. (1979) Sediment gravity flows: their classification and
some problems of application to natural flows and deposits.
IN: Doyle, L.J. and Pilkey, O.H. (eds,), Geology of the
Continental Slopes. Society of Economic Paleontologists and
Mineralogists Special Publication no.27, p. 75-82.

Lowe, D.R. (1982) Sediment gravity flows II: Depositional models
with special reference to the deposits of high-density
turbidity currents. Journal of Sedimentary Petrology, v.52,
p. 279-297.

Mackiewicz, N.E., Powell, R.D., Carlson, P.R., Molnia, B.F..
(1984) Interlaminated ice proximal glaciomarine sediments in
Muir inlet, Alaska. Marine Geology, v.57, p. 113-147.

Mayewski, P.A., Denton, G.H., and Hughes, T.J. (1978) Late
Wisconsinan ice sheets in North America. IN: Denton, G.H. and
Hughes, T.J. (eds.), The Last Great Ice Sheets. Wiley
Interscience, N.Y., p. 67-170.

McIver, N.L. (1972) Cenozoic and Mesozoic stratigraphy of the Nova
Scotia Shelf. Canadian Journal of Earth Sciences, v.9, p.
54-70.

McMillan, N.J. (in press) Boulder beds: impediments to drilling on
the shelves. IN: Chapter 14 of Geology of the Continental
Margin off Eastern Canada, M.J.Keen and G.L.Williams (eds.);
Geological Survey of Canada, Geology of Canada, no. 2. [also
Geological Society of America, The Geology of North America,
v.I-1].

Middleton, G.V. (1978) Facies. IN: Fairbridge, R.W., and
Bourgeois, J. (eds.), Encyclopedia of Sedimentology. Dowden,
Huthinson, and Ross, Stroudsberg, Pa., p. 323-325.

Miller, K.G., and Lohmann, G.P. (1982) Environmental distribution

of recent benthic foraminifera on the Northeastern United
States continental slope. Geological Society of America
Bulletin, v.93, p. 200-206.

Milliman, J.D., and Emery, K.O. (1968) Sea levels during the past
35,000 years. Science, v.162, p. 1121-1123.

Moran, K., and Hurlbut, S.E. (1986) Analysis of potential slope
instability due to wave loading on the Scotian Shelf.
Proceedings of the Third Canadian Conference on Marine
Geotechnical Engineering, St. John's Newfoundland, v.2,
p. 503-504.

Morgenstern, N.R. (1967) Submarine slumping and the initiation of
turbidity currents. IN: Richards, A.F. (ed.), Marine
Geotechnique. University of Illinois Press, Chicago,
p. 189-220.

Mosher, D.C. and Asprey, K.W., 1986. A technique for slabbing
fine-grained sediment in piston cores. Journal of Sedimentary
Petrology, v.56, p. 565-567.

Mudie, P.J. (in press) Paleoenvironmental intepretation of
Quaternary depositional environments: microfosssil
assemblages. IN: Keen, M.J., and Williams, G.L. (eds.),
Chapter 11 of Geology of the Continental Margin off Eastern
Canada. Geological Survey of Canada, no.2, [also Geological
Society of America, The Geology of North America, v.I-1].

Nardin, T.R., Hein, F.J., Gorsline, D.S., and Edwards, B.D. (1979)
A review of mass movement processes, sediment and acoustic
characteristics and contrasts in the slope and base-of-slope
systems versus canyon-fan-basin floor systems. IN: Doyle,
L.J. and Pilkey, O.H. (eds.), Geology of the Continental
Slopes. Society of Economic Paleontologists and
Mineralogists Special Publication no.27, p. 61-73.

Nelsen, T.A. (1983) Time- and method-dependent size distributions of fine-grained sediments. Sedimentology, v.30, p. 249-259.

O'Brien, N.R., Nakazawa, K., and Shuichi, T. (1980) Use of clay fabric to distinguish turbiditic and hemipelagic siltstones and silts. Sedimentology, v.27, p. 47-61.

O'Leary, D. (1986) Seismic structure and stratigraphy of the New England Continental Slope and the evidence for slope instability. United States Department of the Interior Geological Survey Open File Report 86-118, 182 pp.

Palmer, H.D. (1979) Man's activities on the continental slope. IN: Doyle, L.J. and Pilkey, O.H. (eds.), Geology of the Continental Slopes. Society of Economic Paleontologists and Mineralogists Special Publication no.27, p. 17-24.

Pereira, C.P.G. (1979) Studies of continental slopes assist East Coast exploration. Offshore Resources, v.2, p. 34.

Pettijohn, F.J. (1975) Sedimentary Rocks (3rd ed.). Harper and Row Publishers, New York. 628 pp.

Pickering, K.T. (1982) A Precambrian upper basin-slope and prodelta in Northeast Finnmark, North Norway - a possible ancient continental slope. Journal of Sedimentary Petrology, v.52, p. 171-186.

Pickering, K.T. (1984) Deep-water fine-grained sedimentation and tectonics in small fault-controlled basins in a post-subduction strike-slip continental margin: upper Ordovician Point Leamington Formation, New Bay area, North-central Newfoundland. Society of Economic Paleontologists and Mineralogists Research Conference contributed abstracts, San Jose, California. p. 143-146.

197

Piper, D.J.W. (1973) The sedimentology of silt turbidites from the
Gulf of Alaska. IN: Initial reports of the deep-sea drilling
project, v.18, U.S. Government Printing Office, Washington,
p. 847-867.

Piper, D.J.W. (1978) Turbidite muds and silts on deepsea fans and
abyssal plains. IN: Stanley, D.J., and Kelling, G. (eds.),
Sedimentation in Submarine Canyons, Fans, and Trenches.
Dowden, Hutchinson, and Ross, Stroudsberg, Pa., p. 163-176.

Piper, D.J.W. (1980) Manual of Sedimentary Techniques.
Unpubl. report for Department Of Geology, Dalhousie
University, Halifax, Nova Scotia.

Piper, D.J.W., Farre, J.A., and Shor, A. (1985) Late Quaternary
slumps and debris flows on the Scotian slope.
Geological Society of America Bulletin, v.96, p. 1508-1517.

Piper, D.J.W., and Normark, W.R. (1982) Effects of the 1929 Grand
Banks earthquake on the continental slope of eastern Canada.
Current Research, Part B, Geological Survey of Canada paper
82-1B, p. 147-151.

Piper, D.J.W., Normark, W.R., and Sparkes, R. (1987) Late Cenozoic
stratigraphy of the central Scotian Slope, Eastern Canada.
Bulletin of Canadian Petroleum Geology, v.35, p. 1-11.

Piper, D.J.W., and Slatt, R.M. (1977) Late Quaternary clay mineral
distribution on the eastern continental margins of Canada.
Geological Society of America Bulletin, v.88, p. 267-272.

Piper, D.J.W., Sparkes, R., Farre, J.A., and Shor, A. (1983)
Mid-range sidescan and 4.5 kHz Sub-bottom profiler
survey of mass-movement features, Scotian Slope at
61° 40'W. Geological Survey of Canada Open File 938.

Piper, D.J.W., Sparkes, R., Mosher, D.C., Shor, A.N., and Farre, J.A. (1984) Seabed instability near the epicentre of the 1929 Grand Banks earthquake, Geological Survey of Canada Open File 1131.

Piper, D.J.W. and Wilson, E. (1983) Surficial geology of the upper Scotian Slope west of Verrill Canyon. Geological Survey of Canada Open File 939.

Prest, V.K. (1984) The late Wisconsinan glacier complex. IN: Fulton, R.J.(ed.), Quaternary Stratigraphy of Canada - A Canadian contribution to IGCP Project 24. Geological Survey of Canada Paper 84-10, p. 21-36.

Prior, D.B., and Coleman, J.M. (1984) Submarine slope instability. IN: Brunsden, D, and Prior, D.B. (eds.), Slope Instability. John Wiley and Sons Ltd., p. 419-455.

Quinlan, G., and Beaumont, C. (1981) A comparison of observed and theoretical postglacial relative sea level in Atlantic Canada. Canadian Journal of Earth Sciences, v.18, p. 1146-1163.

Reading, H.G. (ed.) (1986) Sedimentary Environments and Facies (2nd edition). Blackwell Scientific Publications, London. 615 pp.

Ryan, W.B.F., (1982) Imaging of submarine landslides with wide-swath sonar. IN: Saxov, S, and Nieuwenhuis, J.K. (eds.), Marine Slides and other Mass Movements. Plenum Press, New York. p. 175-188.

Saxov, S. (1982) Marine slides - some introductory remarks. IN: Saxov, S, and Nieuwenhuis, J.K. (eds.), Marine Slides and other Mass Movements. Plenum Press, New York, p. 1-8.

Saxov, S, and Nieuwenhuis, J.K. (eds.) (1982) <u>Marine Slides and</u>
<u>other Mass Movements</u>. Plenum Press, New York. 353 pp.

Scott, D.B., Medioli, F.S., and Duffet, T.E. (1984) Holocene rise
of relative sea level at Sable Island, Nova Scotia, Canada.
Geology, v.12, p. 173-176.

Shackleton, N.J. and Opdyke, N.D. (1973) Oxygen isotope and
paleomagnetic stratigraphy of Equatorial Pacific core
V28-238: oxygen isotope, temperatures, ice volumes on a 10^5
and 10^6 year scale. Quaternary Research, v.3, p. 39-55.

Shackleton, N.J., and Opdyke, N.D. (1976) Oxygen isotope and
paleomagnetic stratigraphy of Pacific core V28-239, Late
Pliocene to Latest Pleistocene. Geological Society of America
Memoir 145, p. 449-464.

Shepard, F.P. (1973) <u>Submarine Geology</u> (3rd ed.). Harper and Row,
New York. 517 pp.

Shor, A.N., Kent, D.V., and Flood, R.D. (1984) Contourite or
turbidite?: magnetic fabric of fine-grained Quaternary
sediments, Nova Scotia continental rise. IN: Stow, D.A.V.,
and Piper, D.J.W. (eds.), <u>Fine-Grained Sediments: Processes</u>
<u>and Products</u>. Blackwell Publishing, London, p. 257-274.

Silva, A.J., and Booth, J.S. (1984) Creep behavior in submarine
slope sediments. Society of Economic Paleontologists and
Mineralogists Research Conference contributed abstracts, San
Jose, California, p. 170-175.

Simm, R.W., and Kidd, R.B. (1983) Submarine debris flow detected
by long-range side-scan sonar 1,000-kilometers from source.
Geo-Marine Letters, v.3, p. 13-16.

Singer, J.K., and Anderson, J.B. (1984) Use of total grain size distributions to define bed erosion and transport for poorly sorted sediment undergoing simulated bioturbation. Marine Geology, v.57, p. 335-359.

Spencer, D.W. (1963) The interpretation of grain size distribution curves of clastic sediments. Journal of Sedimentary Petrology, v.33, p. 180-190.

Stanley, D.J. (ed.) (1969) The New Concepts of Continental Margin Sedimentation. Short course lecture notes, American Geological Institute, Washington, D.C. 289 pp.

Stanley, D.J., Fenner, P., and Kelling, G. (1972a) Currents and sediment transport at the Wilmington Canyon shelf break as observed by underwater television. IN: Swift, D.J., Duane, D.B., and Pilkey, O.H., (eds.), Shelf Sediment Transport: Process and Pattern. Stroudsburg, Dowden, Hutchinson, and Ross Inc., London. p. 621-644.

Stanley, D.J., Swift, D.J.P., Silverberg, N., James, N.P., and Sutton, R.G. (1972b) Late Quaternary progradation and sand "spillover" on the outer continental margin off Nova Scotia, southeast Canada. Smithsonian Contributions to Earth Science, No.8, 88 pp.

Stein, S., Sleep, N.H., Geller, R.J., Wang, S-C, and Kroeger, G.C. (1979) Earthquakes along the passive margin of eastern Canada. Geophysical Research Letters, v.6, p. 537-540.

Stow, D.A.V. (1977) Late Quaternary stratigraphy and sedimentation of the Nova Scotia outer continental margin. Unpublished Ph.D. thesis, Dalhousie University.

Stow, D.A.V. (1979) Distinguishing between fine-grained turbidites

and contourites on the Nova Scotia deep water margin. Sedimentology, v.26, p. 371-387.

Stow, D.A.V. (1981) Laurentian Fan: morphology, sediments, processes, and growth pattern. American Association of Petroleum Geologists Bulletin, v.65, p. 375-393.

Stow, D.A.V. (1985) Fine-grained sediments in deep water: an overview of processes and facies models. Geo-Marine Letters, v.5, p. 17-23.

Stow, D.A.V. (1986) Deep Sea Clastics. Chapter 12. IN: Reading, H.G. (ed.) Sedimentary Environments and Facies (2nd edition). Blackwell Scientific Publications, London. p. 399-444.

Stow, D.A.V., and Bowen, A.J. (1978) Origin of lamination in deep-sea fine-grained sediments. Nature, v.274, p. 324-328.

Stow, D.A.V., and Bowen, A.J. (1980) Physical model for the transport and sorting of fine-grained sediments in turbidity currents. Sedimentology, v.27, p. 31-46.

Stow, D.A.V., and Lovell, J.P.B. (1979) Contourites: their recognition in modern and ancient sediments. Earth Science Review, v.14, p. 251-291.

Stow, D.A.V., and Piper, D.J.W. (eds.) (1984) Fine-Grained Sediments: Processes and Products. Blackwell Publishing, London. 659 pp.

Stow, D.A.V., and Shanmugam, G. (1980) Sequence of structures in fine-grained turbidites: comparison of recent deep-sea and ancient flysch sediments. Sedimentary Geology v.25, p. 23-42.

Swift, S.A. (1985) Late Pleistocene sedimentation on the continental slope aand rise off western Nova

Scotia. Geological Society of America Bulletin, v.96, p. 832-841.

Thomsen, E., and Vorren, T.O. (1984) Pyritization of tubes and burrows from Late Pleistocene continental shelf sediments off Norway. Sedimentology, v.31, p. 481-492.

Thornton, S.E. (1984) Origin of sedimentary structures in hemipelagic basin sediments: Santa Barbara Basin, California Borderland. Society of Economic Paleontologists and Mineralogists Research Conference contributed abstracts, San Jose, California, p. 192-197.

Visser, J.N.J. (1983) Submarine debris flows from the upper Carboniferous Dwyka tillite formation in the Kalahari basin, South Africa. Sedimentology, v.30, p. 511-523.

Walker, R.G. (1984) Facies Models (2nd ed). Geoscience Canada, Reprint series 1, Toronto, Ontario. 317 pp.

Wentworth, C.K. (1922) A scale of grade and class terms for clastic sediments. Journal of Geology, v.30, p. 337-392.

Wright, R., Anderson, J.B., and Fisco, P.P. (1983) Distribution and association of sediment gravity flow deposits and glacial/glacial-marine sediments around the continental margin of Antarctica. IN: Molnia, B.F. (ed.), Glacial-Marine Sedimentation. Plenum Press, New York, p. 265-300.

Wright, R., and Anderson, J.B. (1982) The importance of sediment gravity flow to sediment transport and sorting in a glacial marine environment: eastern Weddell Sea, Antarctica. Geological Society of America Bulletin, v.93, p.951-963.

203

APPENDIX A

(Acoustic Profiles Through Core Sites)

Figure A1   Sea MARC I 4.5 kHz profile over core sites 22 and 27.
             Acoustic resolution is poor at these sites but several
             acoustic horizons have been defined.
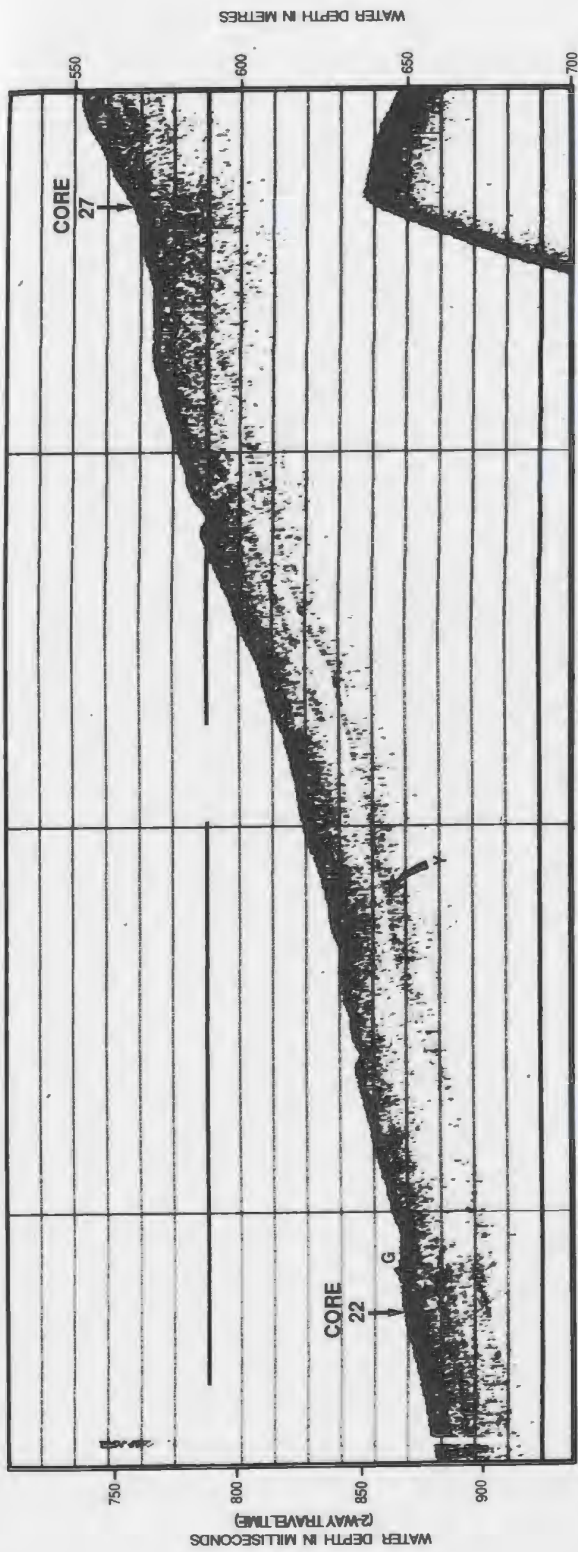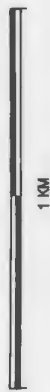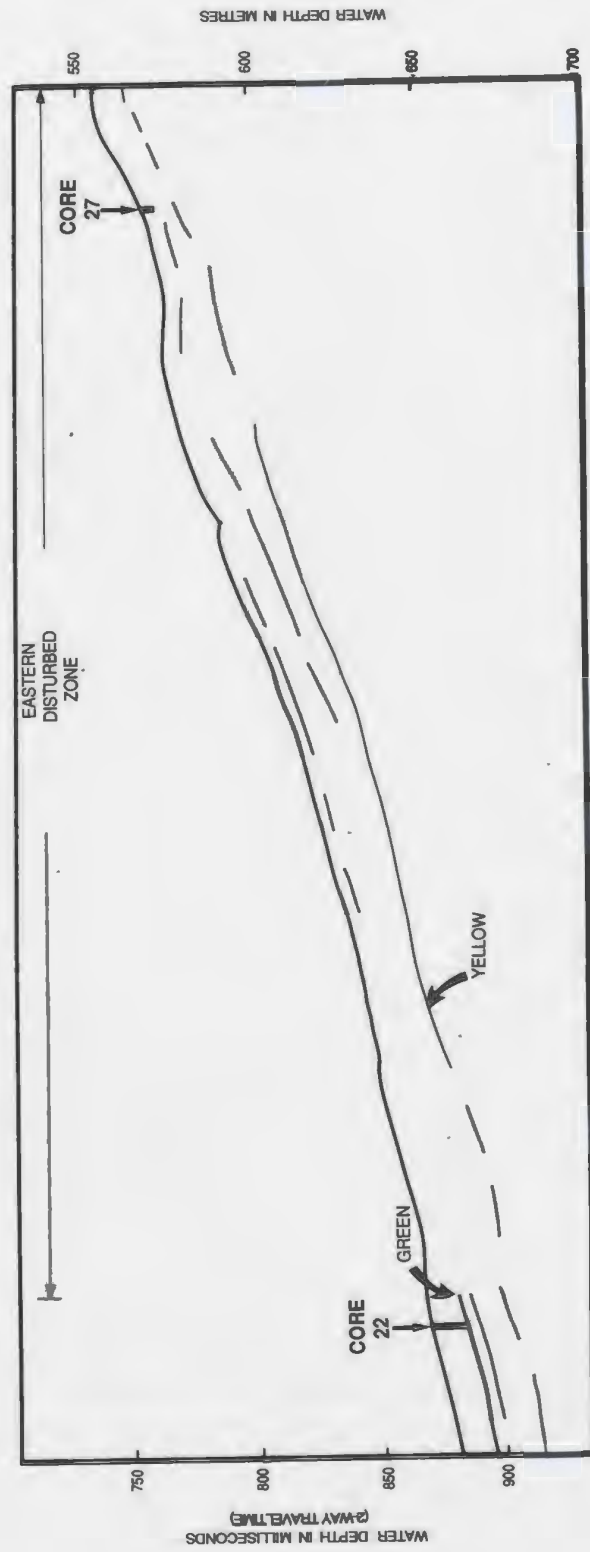
Figure A2   Huntec DTS boomer profile over core site 21 showing
             acoustic reflectors apparent at core site. Note the
             hummocky, erosional characteristic of the seafloor.

WATER DEPTH IN METRES

WATER DEPTH IN MILLISECONDS
(2-WAY TRAVELTIME)

WATER DEPTH IN METRES

WATER DEPTH IN MILLISECONDS
(2-WAY TRAVELTIME)

Figure A3   Huntec DTS boomer profile over core site 25 showing key
acoustic horizons at this site. Note the abundance of
continuous, parallel reflectors in the subbottom at
this site.

Figure A4   V-fin sparker profile over core site 29 and West Acadia Valley. Key reflectors at this site were determined by picking reflectors of similar acoustic character and subbottom depth to those of similar water depths in the main part of the survey area.

WEST

1 KM

EAST

WEST ACADIA VALLEY

CORE 29

WATER DEPTH IN MILLISECONDS (2-WAY TRAVELTIME)

WATER DEPTH IN METRES

BROWN

RED

212
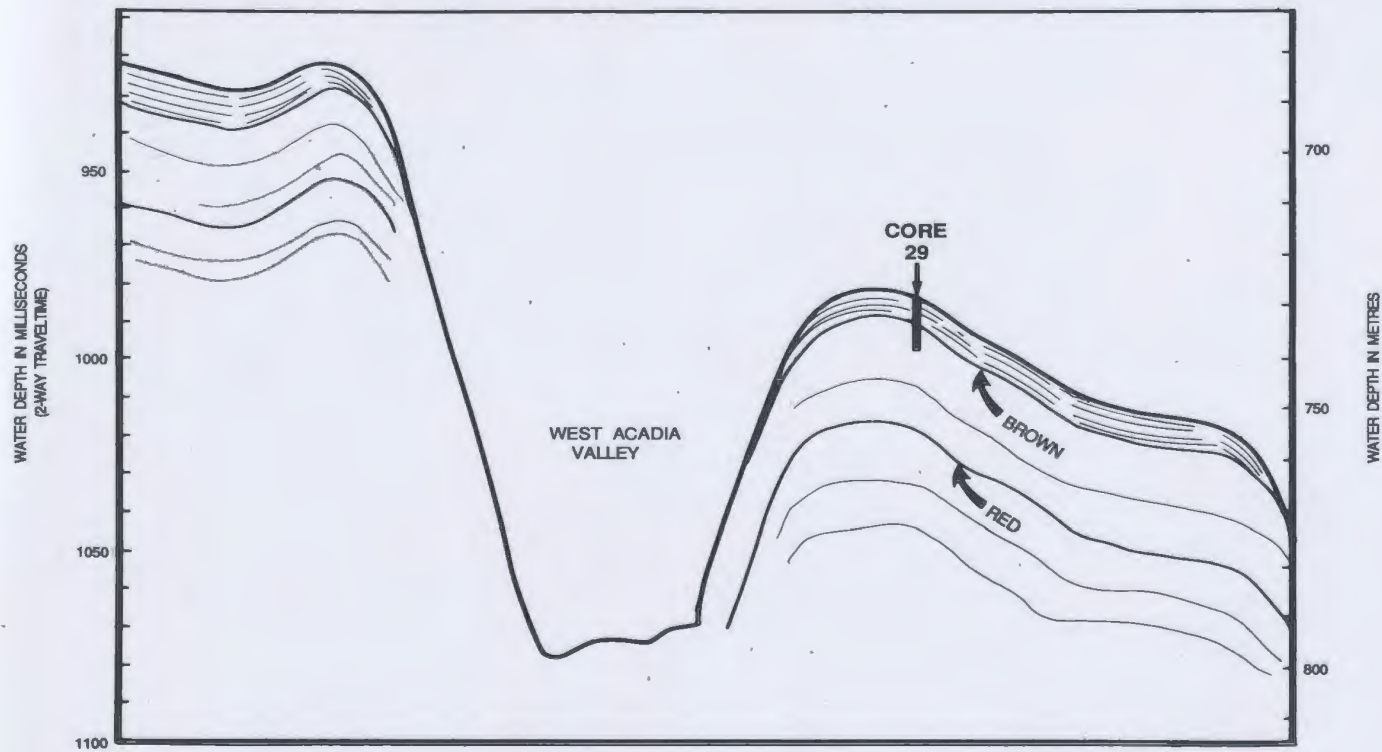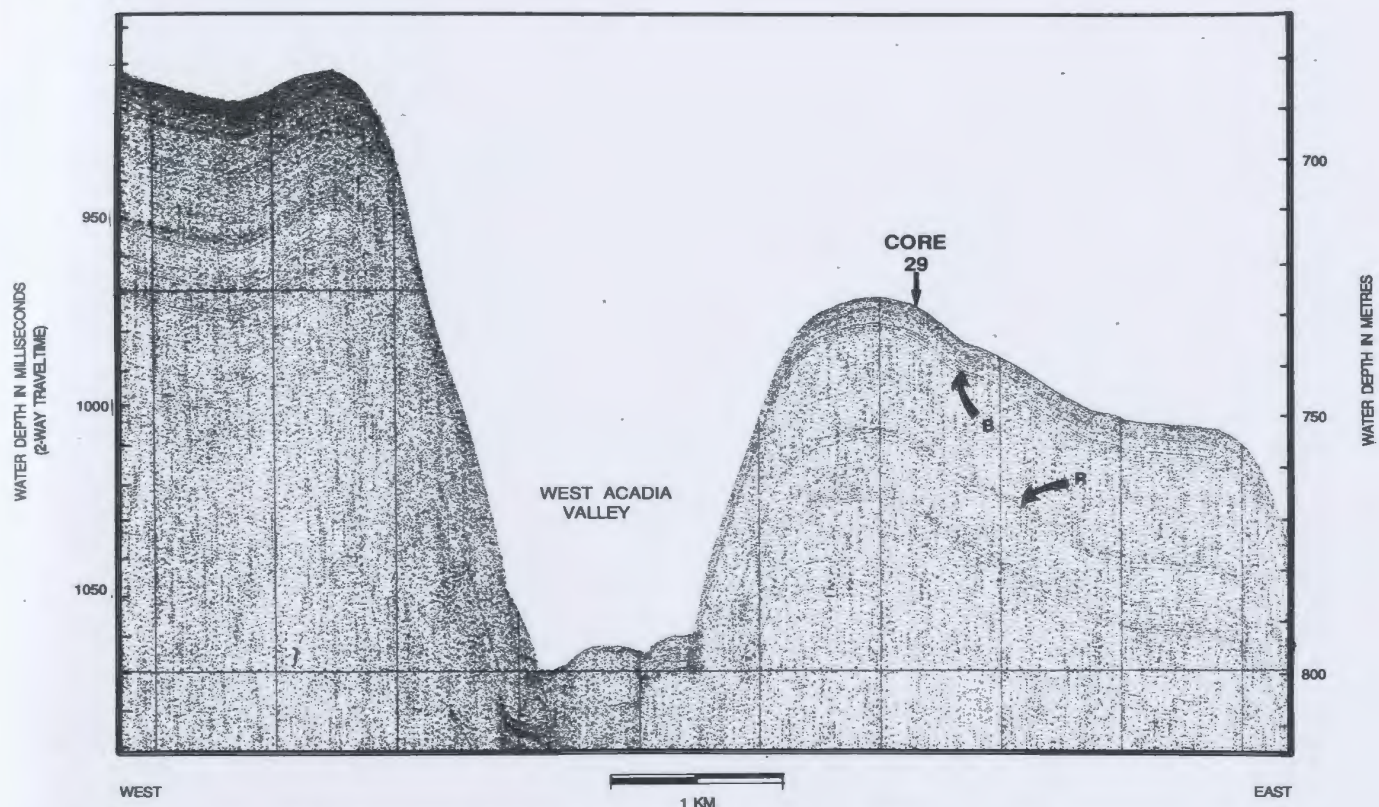
Figure A5   Sea MARC I 4.5 kHz profile over core site 51 showing
             complete undisturbed sequence of key acoustic
             reflectors. Note the easily distinguished
             echocharacter of the western disturbed zone in the
             western portion of the profile.

WATER DEPTH IN METRES

WATER DEPTH IN METRES

EAST

WEST

1 KM

CORE 51

G

O

B

P

R

Y

WATER DEPTH IN MILLISECONDS
(2-WAY TRAVELTIME)

CORE 51

BROWN ORANGE GREEN

YELLOW RED

PINK

WESTERN DISTURBED ZONE

WATER DEPTH IN MILLISECONDS
(2-WAY TRAVELTIME)

214

Figure A6   Sea MARC I 4.5 kHz profile over core site 52. Note the
            core was taken in what appears to be a slump deposit,
            where the acoustic stratigraphy cannot be defined.

SOUTH   NORTH

1 KM

216
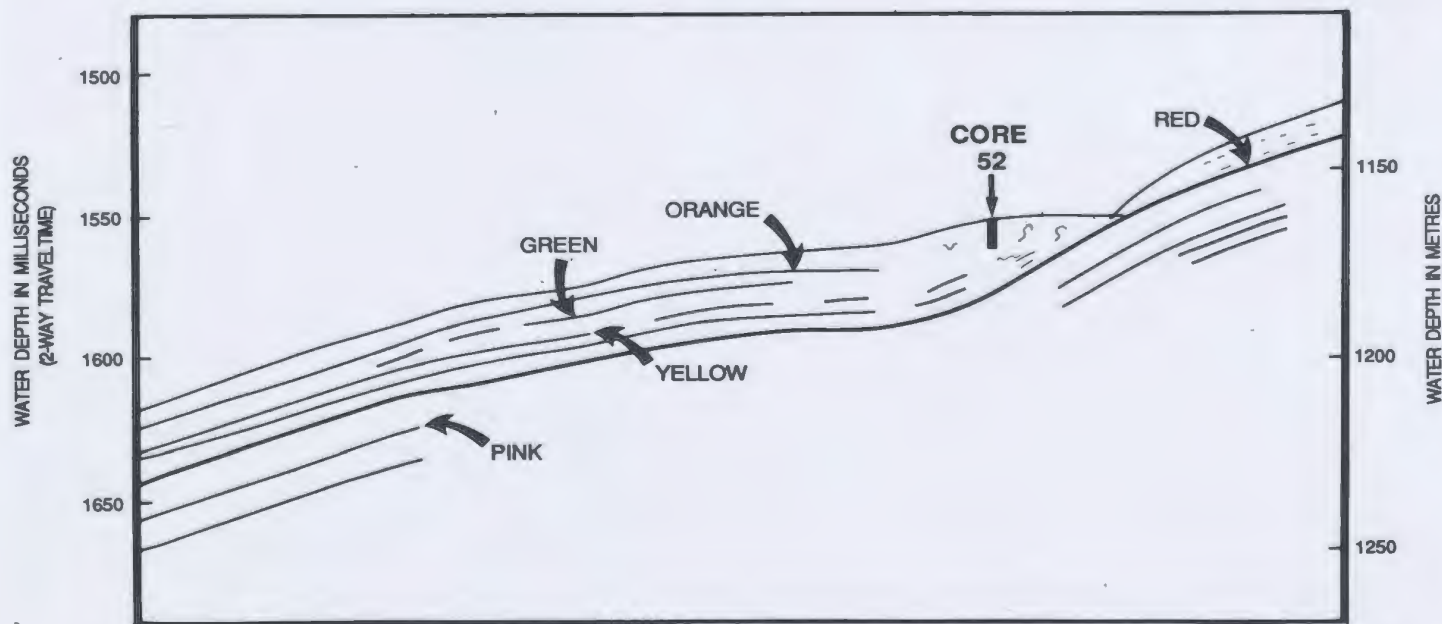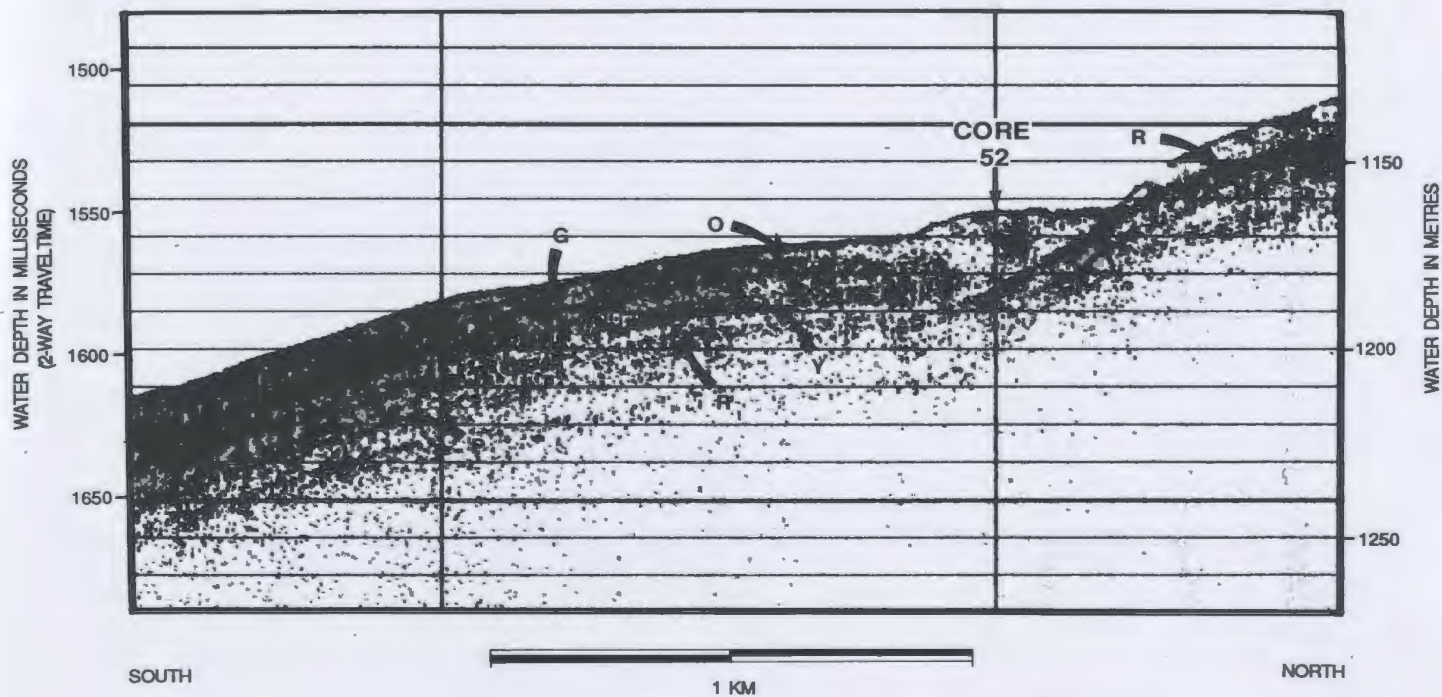
Figure A7   Huntec DTS boomer profile over core site 32 showing the
key acoustic horizons recognized at the site.

218
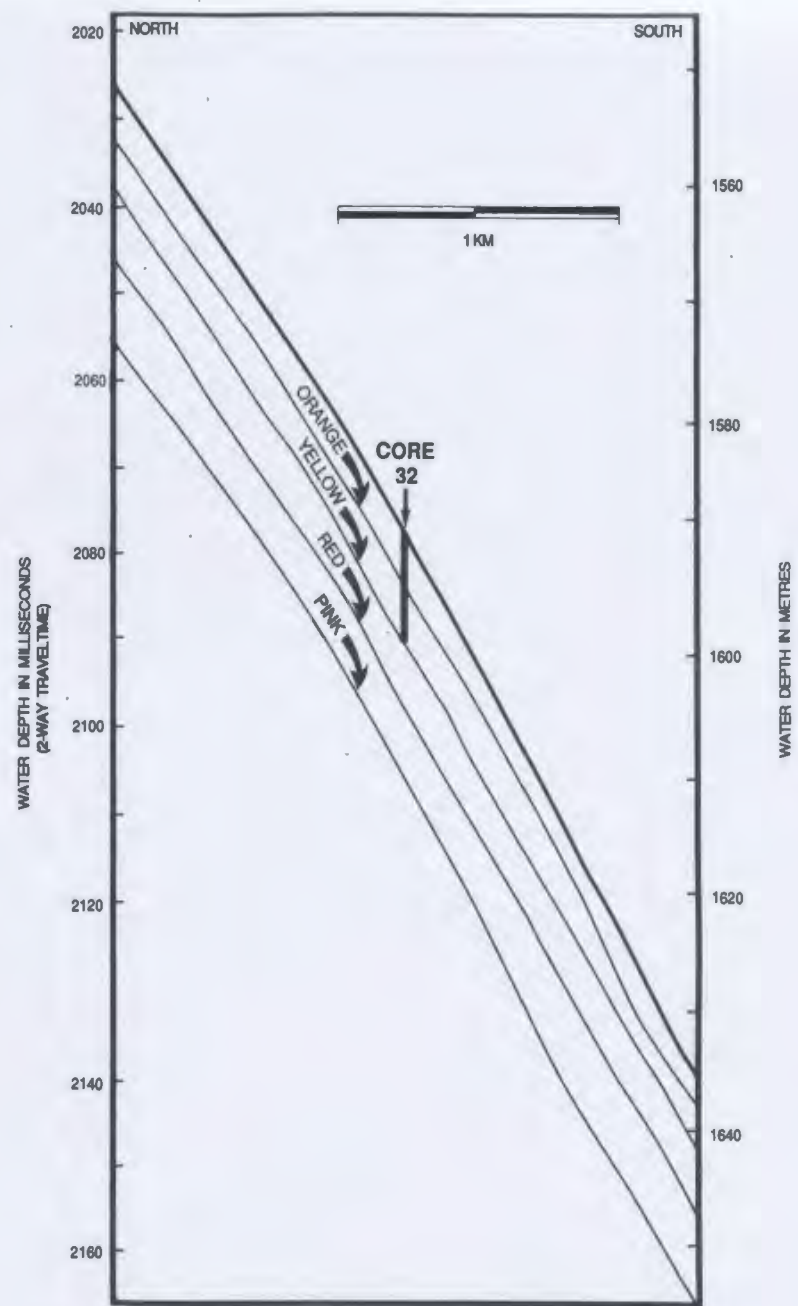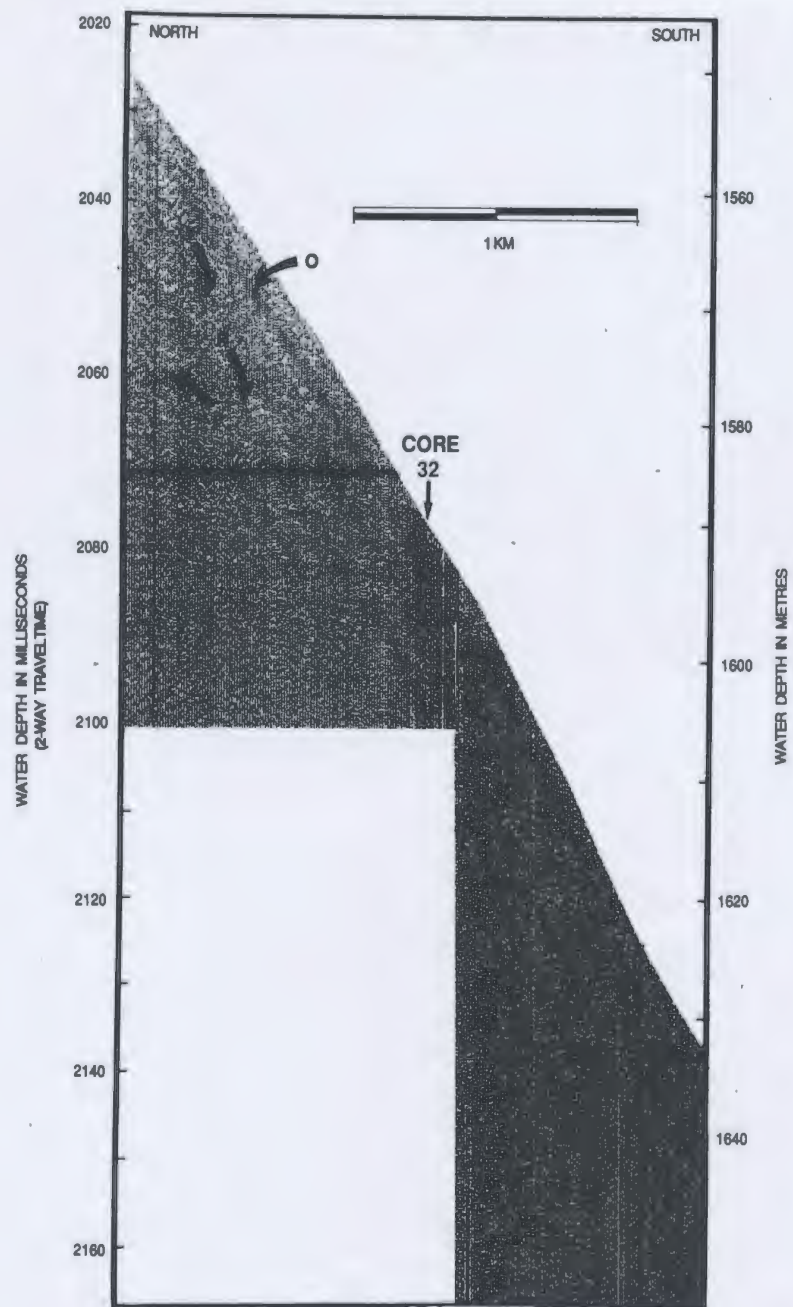
Figure A8   3.5 kHz profile over core site 56 showing key acoustic
            reflectors at this site. Note the continous, coherent,
            parallel nature of the reflectors. This echotype is
            characteristic of undisturbed areas on the slope.

Upper panel labels: CORE 56, Y, O, R, P
Vertical axis (left): WATER DEPTH IN MILLISECONDS (2-WAY TRAVELTIME); 2450, 2500, 2550, 2600, 2650, 2700
Vertical axis (right): WATER DEPTH IN METRES; 1850, 1900, 1950, 2000
SOUTH — 1 KM — NORTH

Lower panel labels: CORE 56, YELLOW, ORANGE, RED, PINK
Vertical axis (left): WATER DEPTH IN MILLISECONDS (2-WAY TRAVELTIME); 2450, 2500, 2550, 2600, 2650, 2700
Vertical axis (right): WATER DEPTH IN METRES; 1850, 1900, 1950, 2000

Figure A9   Sea MARC I 4.5 kHz profile over core site 34, showing
            that key acoustic horizons have thinned downslope and
            are closer to the surface.
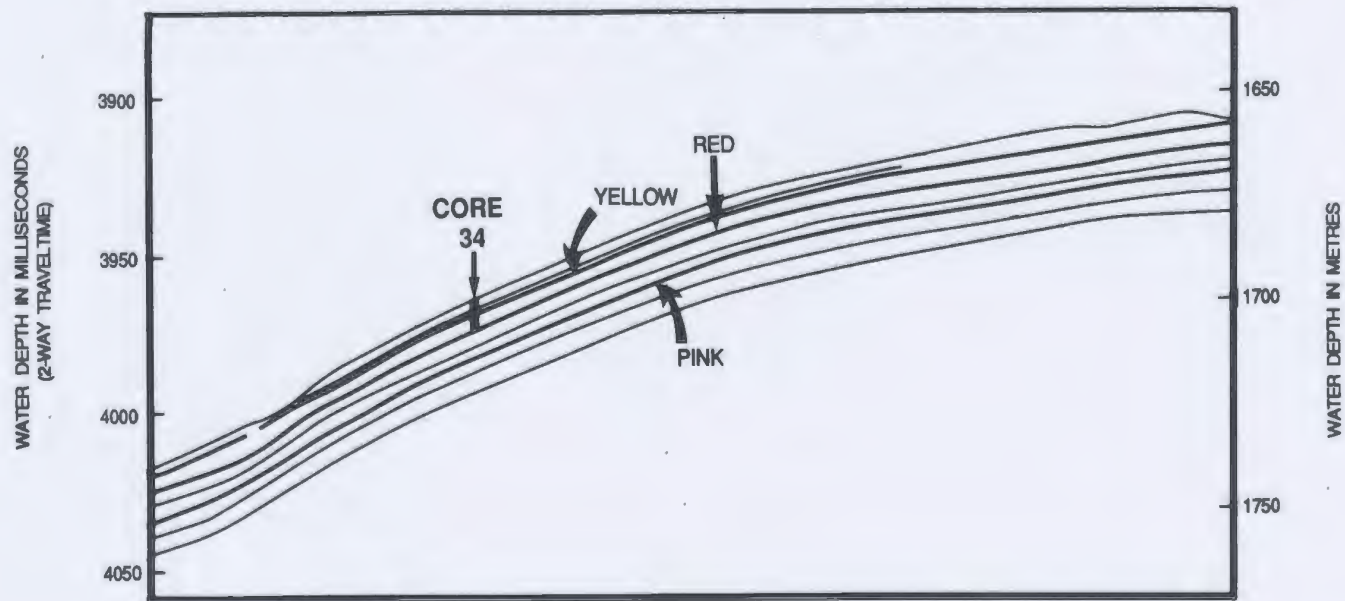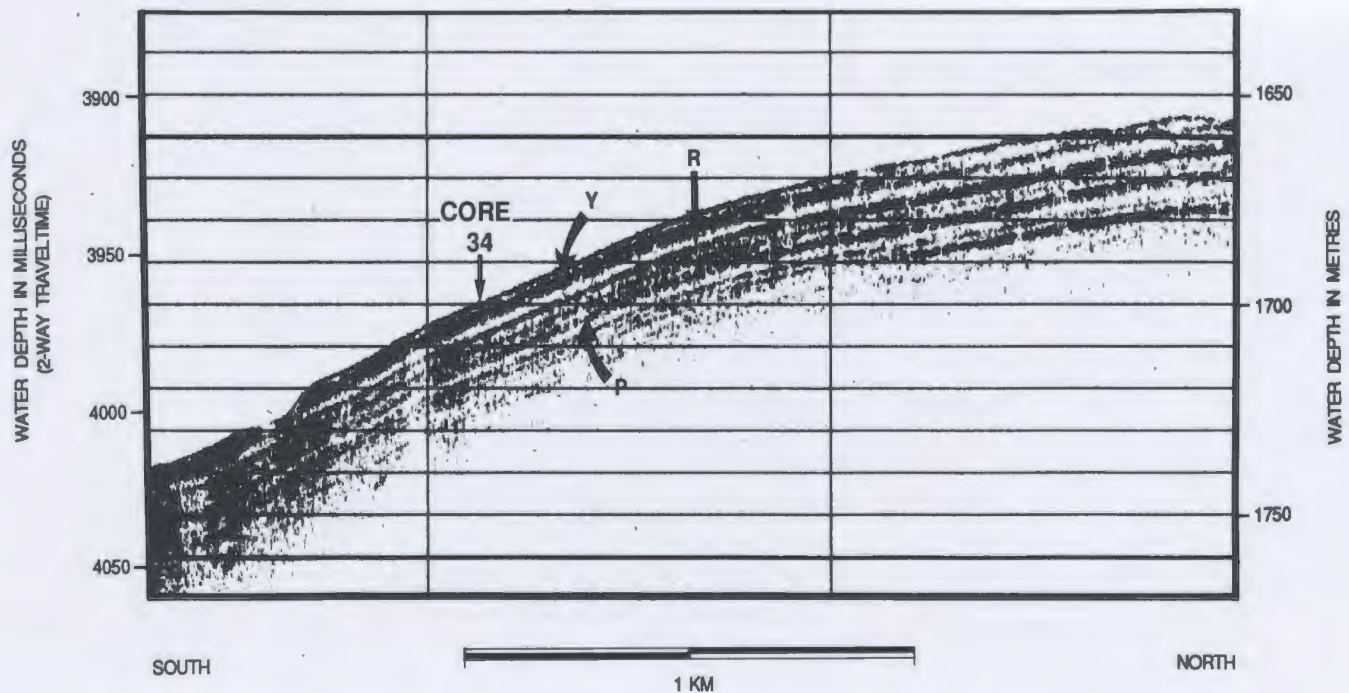
Figure A10 Sea MARC I 4.5 kHz profile over core site 310 and small
erosional valley between West and East Acadia Valleys.
Note the shallowest key reflector is Green, suggesting
that sediment has been removed from the site.

Top panel axis labels:

WATER DEPTH IN MILLISECONDS (2-WAY TRAVELTIME)

2350
2400
2450

WATER DEPTH IN METRES

1750
1800
1850

CORE 310
G
Y
R
P
Y
R
P

SOUTH

1 KM

NORTH

Bottom panel axis labels:

WATER DEPTH IN MILLISECONDS (2-WAY TRAVELTIME)

2350
2400
2450

WATER DEPTH IN METRES

1750
1800
1850

CORE 310
GREEN
YELLOW
RED
PINK
SMALL EROSIONAL VALLEY
YELLOW
RED
PINK
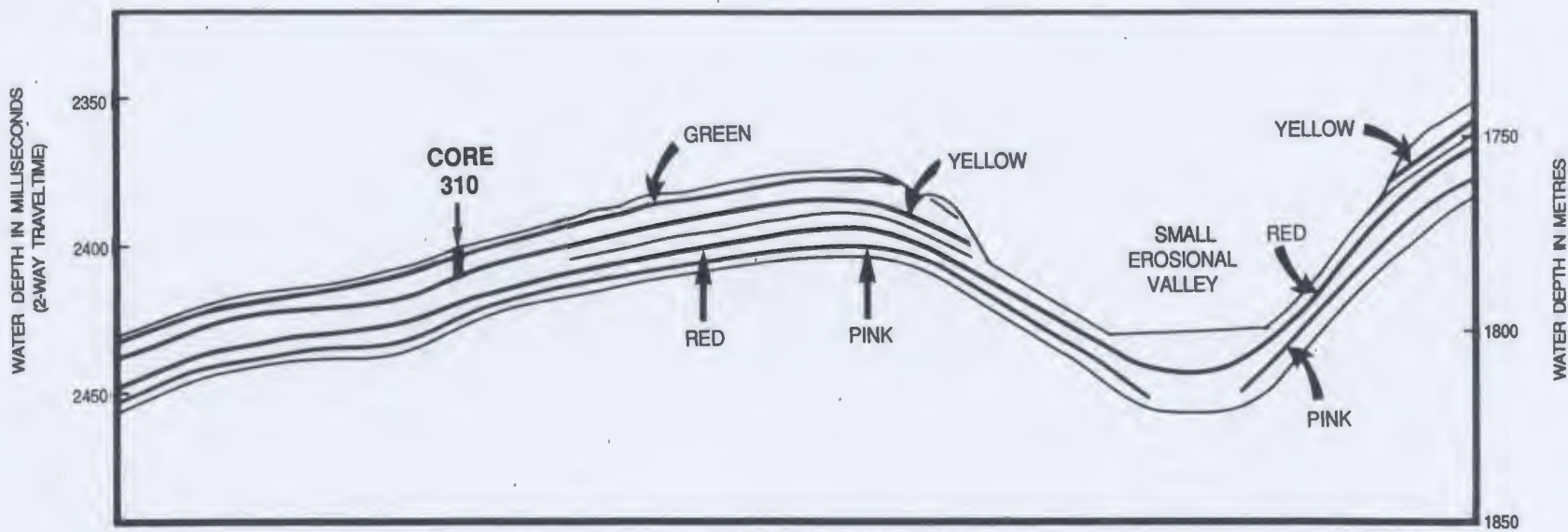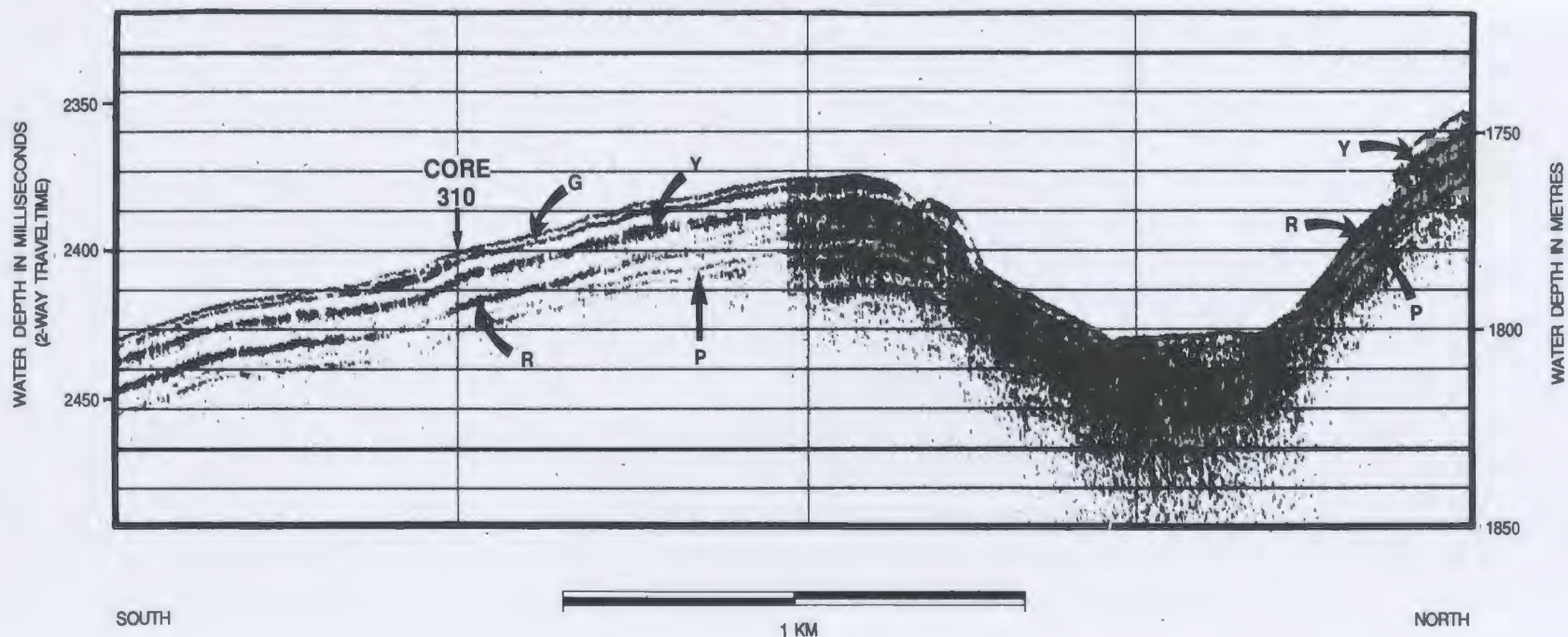
Figure A11   Sea MARC I 4.5 kHz profile over core site 36 showing
Pink as the shallowest key reflector. Note the scarps,
resulting from bedding-plane slide detachment; and
scours which are the profiles of the linear erosional
depressions as seen on sidescan images. Note also the
termination of the Red reflector at the scarp face.
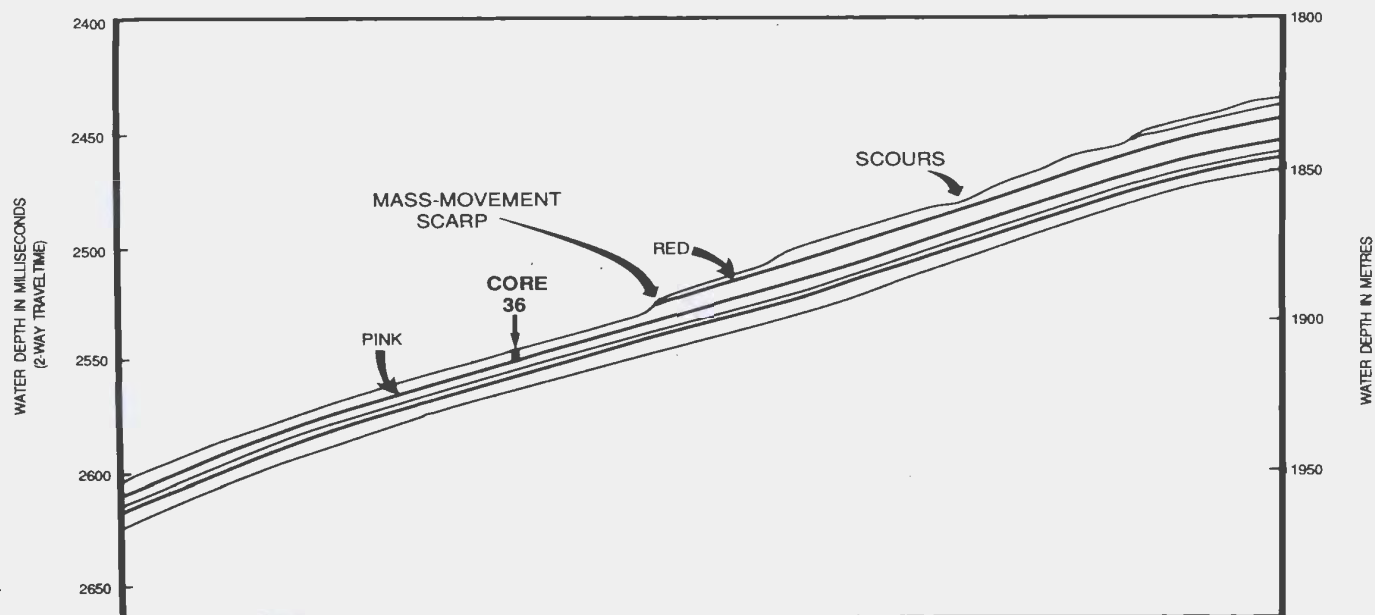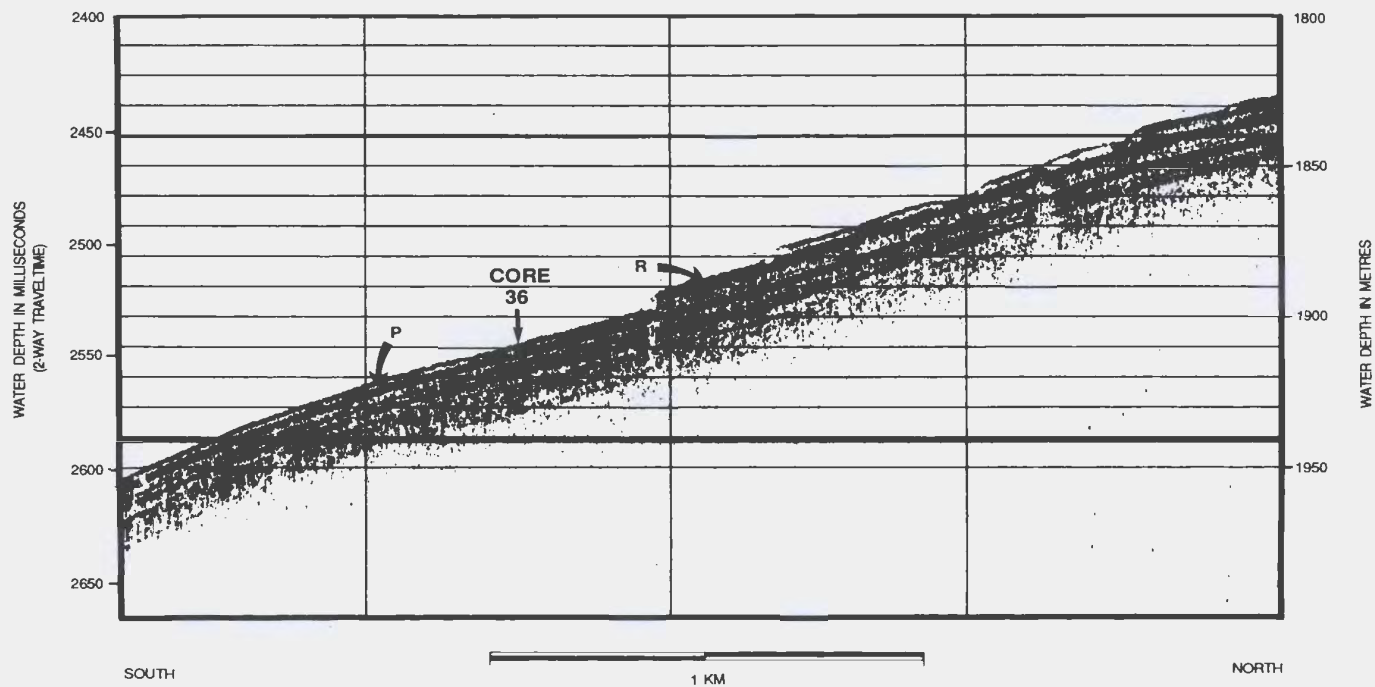
Figure A12 V-fin sparker profile over the eastern disturbed zone
and core site 24, showing key acoustic horizons. Note
the termination of reflectors and the relief at the
marginal escarpment where the disturbed zone begins,
suggesting sediment has been removed from the area.
Note also the characteristic hummocky morphology and
transparent nature of the acoustic profile over the
disturbed zone.
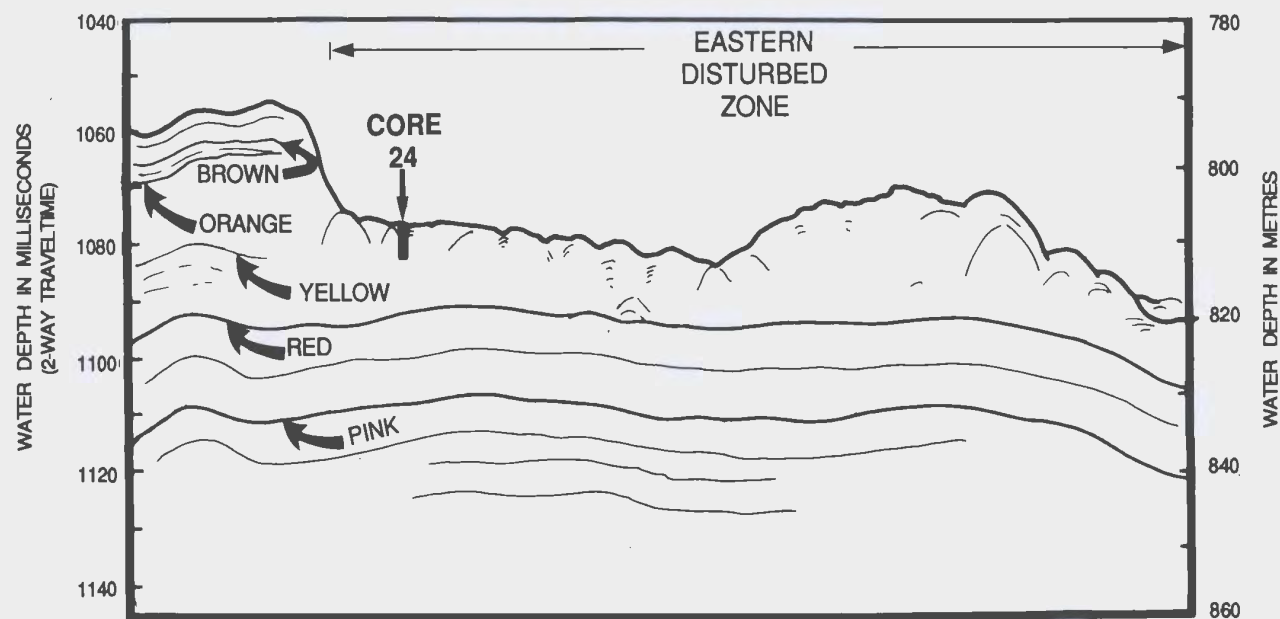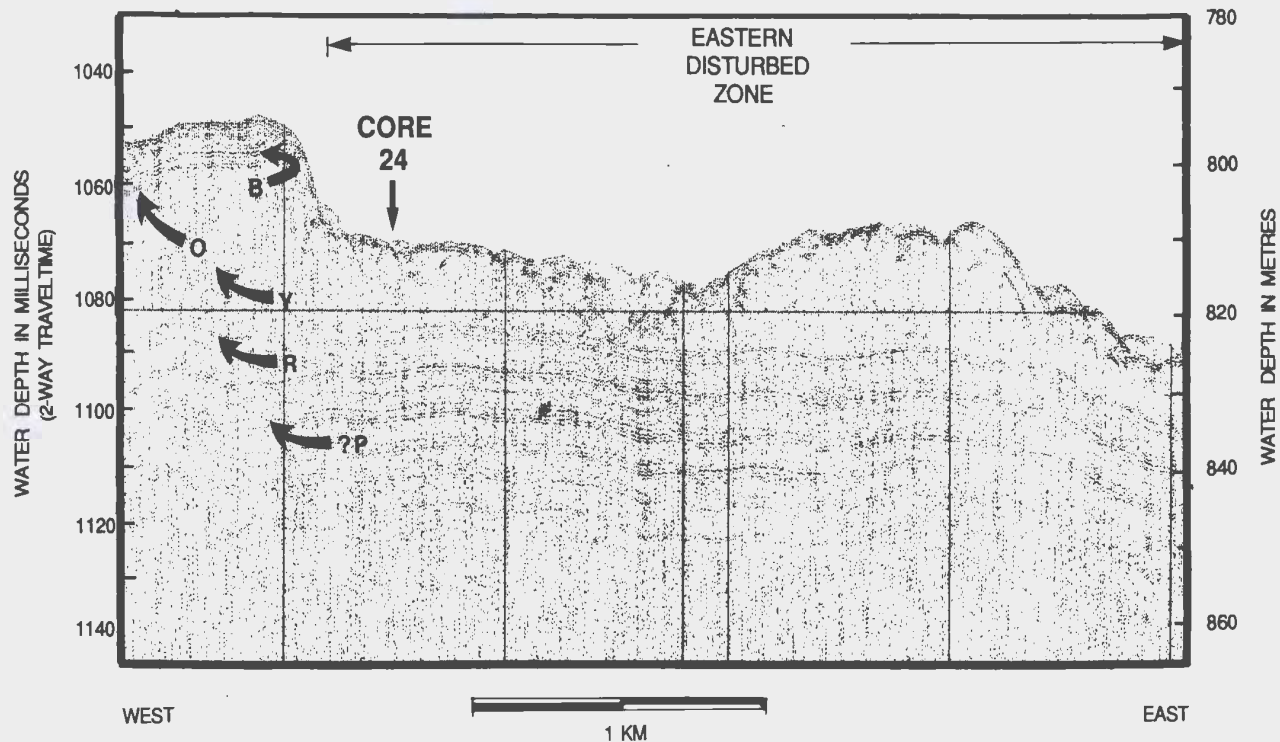
Figure A13   Sea MARC I 4.5 kHz profile over core site 37 within the western disturbed zone, showing the key acoustic horizons at the site.   Note that Red is the first recognizable reflector.
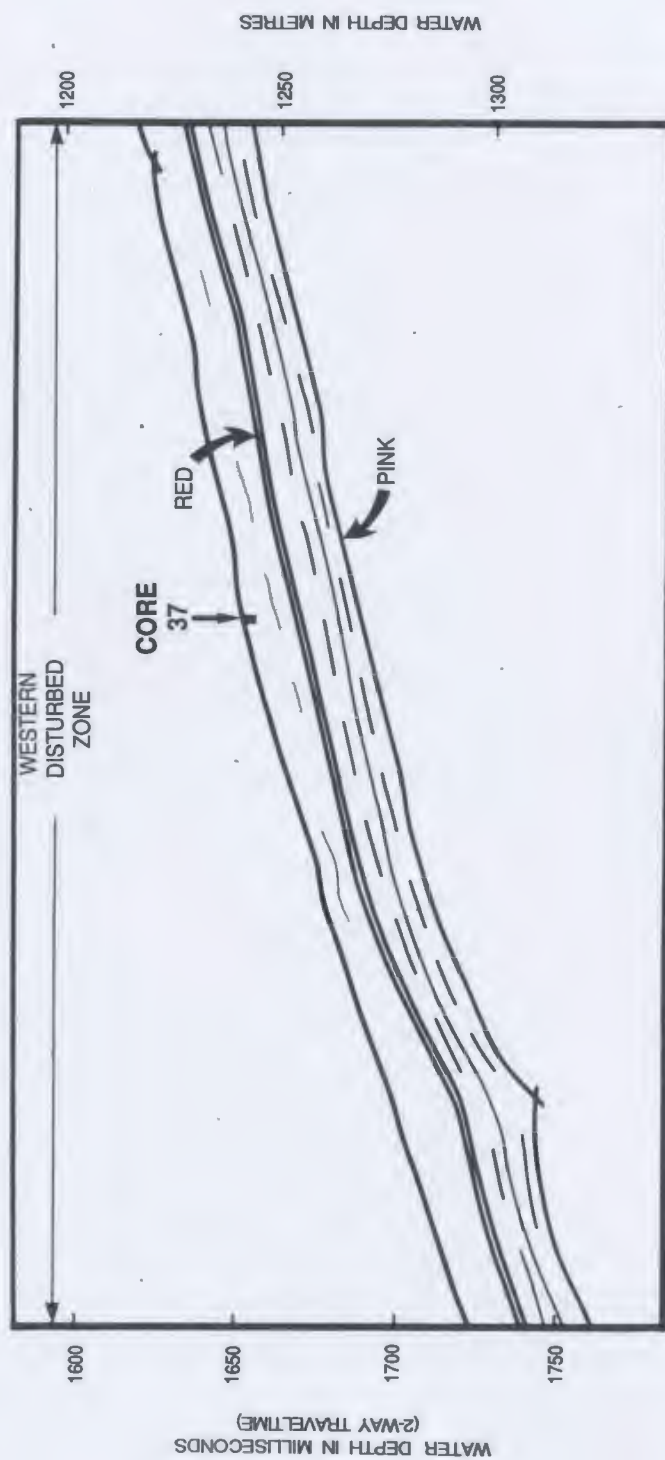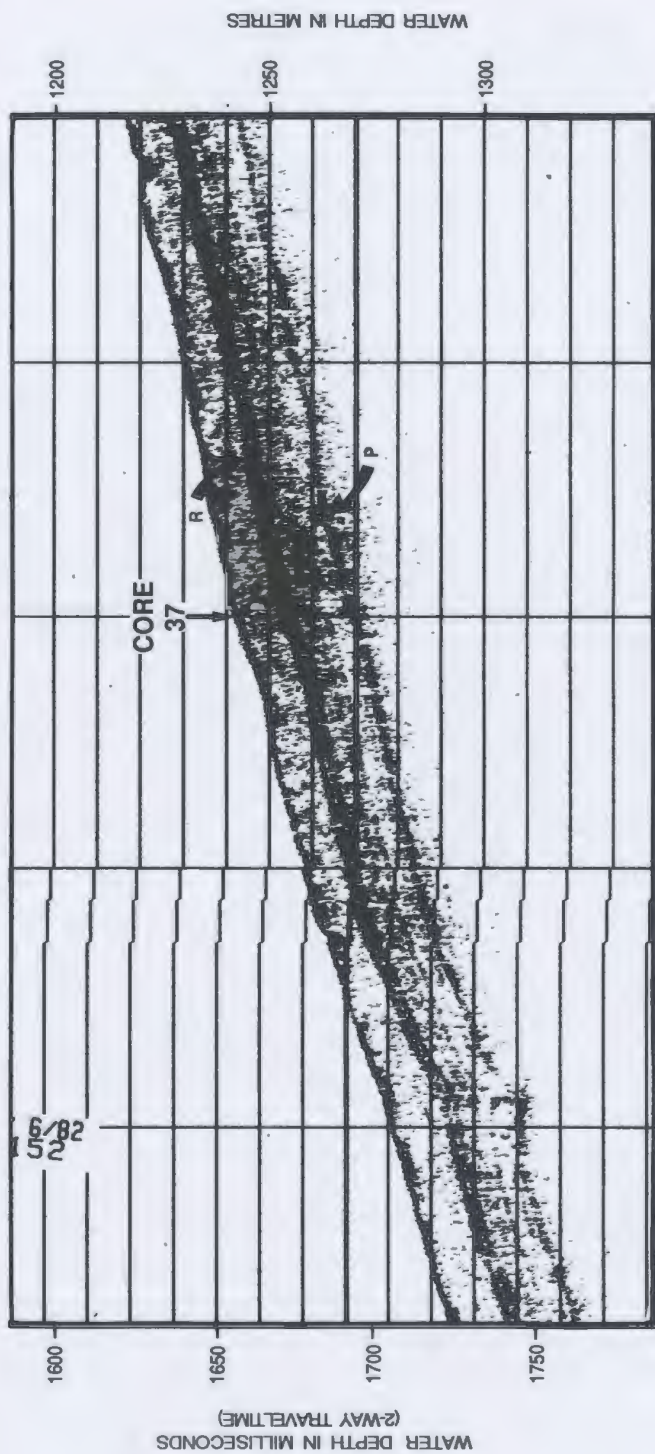
Figure A14 Sea MARC I 4.5 kHz profile over core sites 54 and 55,
and within the western disturbed zone, showing key
acoustic reflectors at the sites. Note that Yellow is
the shallowest horizon recognized.

WATER DEPTH IN METRES

1400

1450

1500

5/82
53

CORE
54

CORE
55

1850

1900

1950

2000

2050

WATER DEPTH IN MILLISECONDS
(2-WAY TRAVELTIME)

NORTH

1 KM

SOUTH

WATER DEPTH IN METRES

1400

1450

1500

WESTERN
DISTURBED
ZONE

CORE
54

PINK

CORE
55

RED

YELLOW

1850

1900

1950

2000

2050

WATER DEPTH IN MILLISECONDS
(2-WAY TRAVELTIME)

Figure A15 Sea-MARC I 4.5 kHz profile over core site 33 and over
the western disturbed zone, showing key acoustic
reflectors at the site. Note the termination of
horizons at the marginal escarpment.
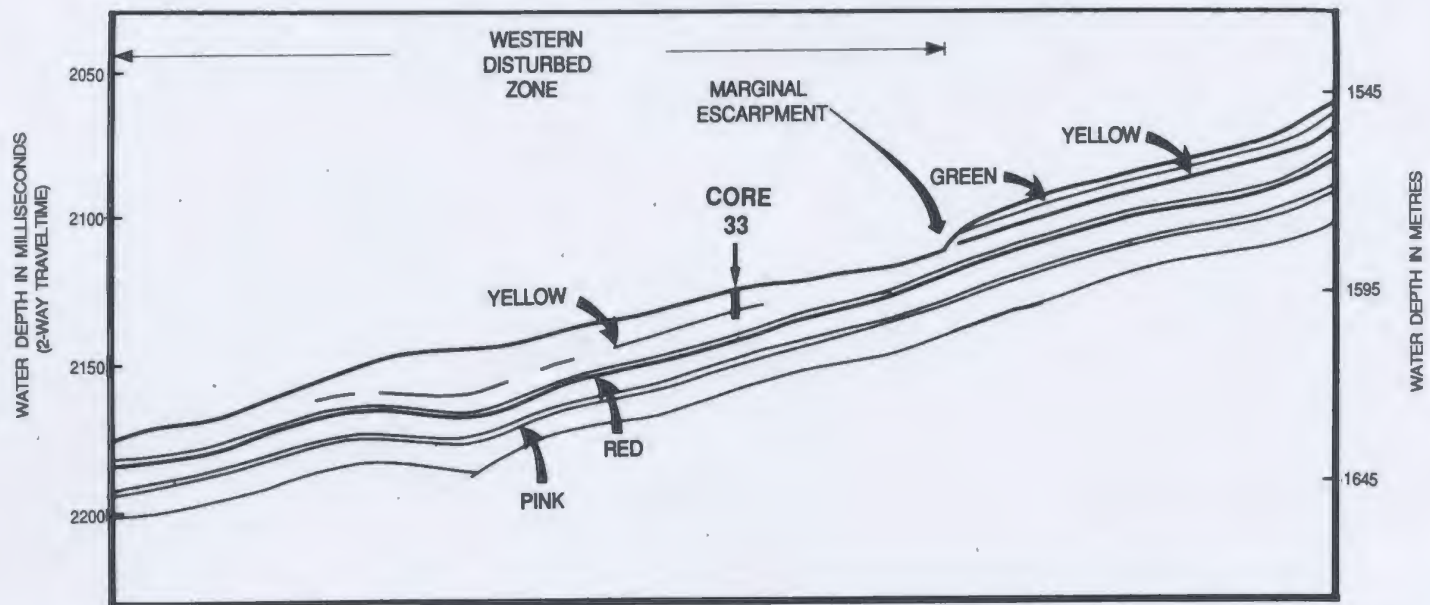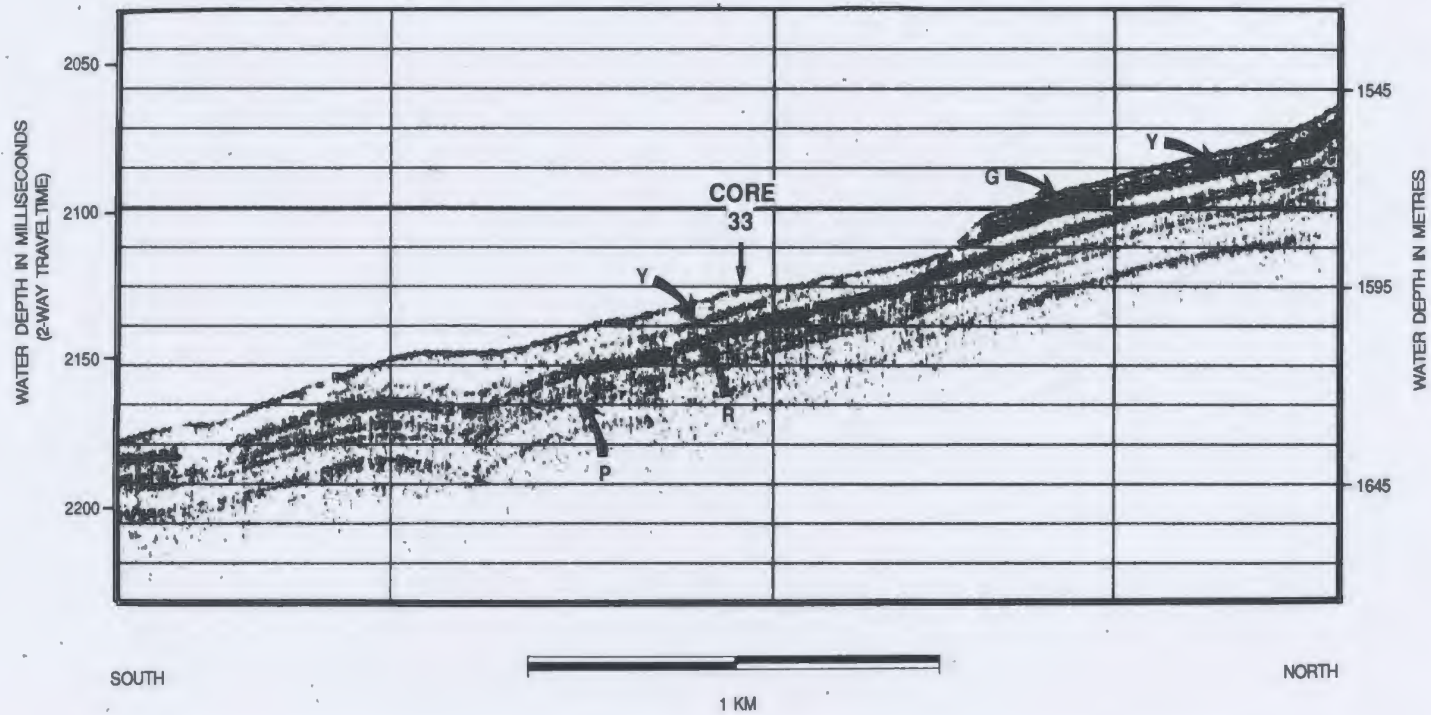
APPENDIX B

(GRAIN SIZE DATA)

List of Abbreviations

```
%GR   . . . . . . percent gravel
%SA   . . . . . . percent sand
%SILT . . . . . percent silt
%CLAY . . . . . percent clay
MED   . . . . . median
S.D.  . . . . . standard deviation
KURT  . . . . . kurtosis
SKEW  . . . . . skewness
CRST% . . . . . coarsest percentile
```

CORE NO.	DEPTH (cm)	FACIES	%GR	%SA	%SILT	%CLAY	MEAN (phi)	MED. (phi)	MODE (phi)	S.D.	KURT.	SKEW.	CRST% (phi)
34	154	5	.3	9.5	39.44	50.76	8.04	7.9	7.5	3.04	2.57	-.45	3.3
34	335	5	0	6.71	39.66	53.63	8.31	8.3	7.5	2.77	2.36	-.39	3.9
34	391	5	.48	12.94	38.69	47.89	7.74	7.7	7.3	3.16	2.59	-.47	3.1
34	415	5	.02	10.61	41.64	47.73	7.67	7.7	5.7	2.97	2.23	-.28	3.9
34	432	5	.6	16.97	35.79	46.64	·7.47	7.5	5.3	3.33	2.43	-.43	1.7
34	446	5	.01	7.44	32.04	60.52	8.58	8.7	8.1	2.75	2.89	-.68	5.1
34	462	5	.2	11.82	35.54	52.44	7.97	8.1	8.7	3.07	2.6	-.53	4.7
34	477	5	0	6.18	32.11	61.71	8.69	8.8	8.9	2.67	2.96	-.69	5.1
34	492	5	.3	10.24	34.47	54.99	8.18	8.3	7.9	3	2.77	-.6	3.1
34	507	5	0	7.46	33.23	59.31	8.5	8.6	7.9	2.77	2.6	-.59	3.1
34	522	5	.2	10.8	37.18	51.82	7.99	8.1	7.5	3	2.64	-.51	3.1
34	535	5	1.2	13.43	33.3	52.08	7.84	8.1	7.9	3.33	3.1	-.72	2.9
34	555	5	.3	11.62	28.83	59.24	8.33	8.7	8.7	3.16	3.1	-.84	2.9
34	571	5	2.8	20.8	31.26	45.14	7.01	7.5	7.5	3.87	2.57	-.58	.7
34	599	5	.55	16.44	30.2	52.84	7.84	8.1	8.1	3.39	2.55	-.62	2.5
34	614	5	0	15.64	30.86	53.5	7.98	8.2	2.9	3.21	2.29	-.54	2.7
34	586	5	2.2	43.23	24.28	30.29	5.55	4.9	2.7	3.91	1.99	.16	4.5
34	631	5	.54	24.24	27.17	48.04	7.32	7.7	3.1	3.67	2.02	-.39	1.3
34	644	5	1.1	22.86	29.51	46.52	7.28	7.5	3.1	3.55	2.28	-.4	1.5
34	660	5	.1	31.33	26.7	41.86	6.81	7.1	3.1	3.66	1.73	-.12	1.1
34	674	5	2.04	29.36	29.69	38.91	6.53	6.7	3.1	3.79	2.14	-.23	1.1
34	690	5	.03	13.84	32.81	53.32	8.02	8.2	7.7	3.11	2.39	-.54	2.9
34	114	2	0	7.26	36.55	56.19	8.41	8.5	7.7	2.75	2.21	-.41	3.1
34	169	2	.12	6.22	41.81	51.85	8.24	8.1	5.5	2.76	2.21	-.26	3.5
34	182	2	0	7.72	48.76	43.52	7.7	7.3	5.1	2.8	1.78	.11	3.5
34	13	2	0	6.02	35.93	58.05	8.41	8.5	9.3	2.57	2.23	-.38	3.7
34	215	3	0	10.27	48.09	41.64	7.58	7.1	3.9	2.82	1.82	.14	3.5
34	229	3	.6	3.18	37.64	58.58	8.67	8.7	3.9	2.64	3.99	-.73	3.9
34	241	3	.34	15.98	38.36	45.33	7.57	7.5	3.5	3.12	2.1	-.2	3.1
34	320	3	0	7.79	45.83	46.38	7.89	7.5	3.7	2.8	1.98	-.08	3.5
34	364	3	.5	4.88	41.58	53.04	8.33	8.1	3.9	2.74	3.18	-.49	3.9
34	197	4	0	21.13	40.98	37.9	7.11	6.5	3.5	3.02	1.69	.29	3.2
34	258	4	0	29.25	42.04	28.71	6.41	5.3	3.5	2.92	2.07	.6	3.2
34	301	4	0	57.77	28.5	13.73	5.01	3.7	3.5	2.43	4.58	1.66	3.2
34	21	1	0	6.4	38.4	55.2	8.17	8.3	9	2.53	2.07	-.26	3.5
34	53	1	0	21.06	37.23	41.71	7.1	7	5.4	3.14	1.92	-.08	1.7
34	36	1	0	4.64	36.85	58.51	8.41	8.5	4.2	2.49	2.16	-.32	3.7
34	44	1	0	15.39	36.06	48.55	7.67	7.8	0	3.05	1.97	-.25	1.9
34	74	1	0	8.63	39.72	51.63	8.02	8.1	4.2	2.82	2.16	-.3	3.3
34	380	1	0	4.59	39.01	56.4	8.51	8.2	7.4	2.62	2.41	-.4	3.9
310	197	5	.22	20.49	33.65	45.63	7.3	7.5	7.7	3.47	2.11	-.38	.7
310	300	5	.77	7.44	33.51	58.28	8.4	8.5	7.9	2.98	3.81	-.9	5.1
310	344	5	3.9	7.24	30.42	58.44	8.17	8.5	8.3	3.52	4.9	-1.34	5.1
310	385	5	0	14.99	33.1	51.91	7.86	8.1	7.3	3.19	2.35	-.53	2.5
310	400	5	.6	6.48	31.32	61.6	8.61	8.9	8.5	2.85	4	-.95	5.1
310	410	5	.02	9.69	35.72	54.57	8.22	8.3	7.5	2.9	2.28	-.45	3.1
310	449	5	.62	10.48	30.31	58.59	8.32	8.7	7.5	3.14	3.43	-.91	5.5
310	434	5	.57	7.24	29.34	62.84	8.65	9	8.7	2.96	4.05	-1.06	5.5
310	479	5	.6	16.57	28.61	54.25	7.9	8.3	7.9	3.33	2.59	-.65	2.7
310	495	5	.4	11.94	29.69	57.97	8.29	8.5	7.9	3.1	2.96	-.76	2.7
310	510	5	1.02	21.35	35.02	42.61	7.63	7.3	7.3	3.45	2.48	-.46	1.1
310	535	5	.67	34.01	29.52	35.8	6.33	6.1	2.9	3.66	1.84	.05	1.1
310	549	5	3.83	21.05	30.62	44.51	6.95	7.3	7.9	3.92	2.7	-.62	2.5
310	464	2	0	2.4	31.34	66.26	9.12	9.1	7.9	3.32	3.03	-.64	2.0
310	285	2	0	4.89	31.39	63.72	8.87	8.9	7.7	2.56	3.06	-.72	5.7
310	G12	1	0	5.81	35.67	58.52	8.42	8.5	4	2.49	2.25	-.36	3.3
310	12	1	0	18.15	36.95	44.9	7.38	7.3	3.2	3.02	1.94	-.15	2.9
310	24	1	0	6.86	34.05	59.09	8.4	8.5	4	2.56	2.39	-.45	3.3
310	39	1	0	4.99	34.67	60.34	8.52	8.7	9.8	2.48	2.4	-.44	3.5
310	75	1	0	5.99	36.52	57.49	8.4	8.5	7	2.6	2.64	-.5	4.9
310	179	1	0	8.42	36.4	55.18	8.28	8.3	7.8	2.83	2.59	-.52	3.9
310	164	1	4.4	5.4	40.02	50.19	7.79	7.9	7.6	3.47	4.86	-1.21	.9
310	150	1	0	4.2	40.33	55.47	8.45	8.3	5.8	2.62	2.16	-.29	3.9
310	135	1	0	1.81	36.31	61.88	8.85	8.9	7.4	2.38	2.46	-.43	5.1
310	105	1	0	15.11	47.57	37.32	7.19	6.6	3.4	2.83	1.85	-.28	3.3
310	90	1	0	6.97	35.63	57.3	8.41	8.5	7.4	2.65	2.38	-.44	3.5
310	314	1	.01	6.28	32.15	61.56	8.67	8.8	7.9	2.69	2.83	-.67	3.9
310	329	1	0	5.57	31.98	62.45	8.75	8.9	8.3	2.63	2.94	-.69	5.1

CORE NO.	DEPTH (cm)	FACIES	%GR	%SA	%SILT	%CLAY	MEAN (phi)	MED. (phi)	MODE (phi)	S.D.	KURT.	SKEW.	CRST% (phi)
310	121	1	0	6.3	40.27	53.43	8.26	8.3	7.1	2.72	2.19	-.31	3.3
29	560	5	0	31.78	32.3	35.92	6.52	6.1	3.3	3.41	1.84	.152	2.9
29	696	5	0	26.44	45.58	27.99	6.3	5.5	3.4	2.94	2.18	.49	2.9
29	670	5	0	10.84	47.72	41.44	7.58	7.1	5.3	2.91	1.81	.12	3.1
29	841	5	0	13.62	33.98	52.4	8.06	8.1	3.5	2.99	1.91	-.3	3.1
29	540	5	.26	11.5	36.63	51.61	8	8.1	7.3	3.16	2.53	-.51	3.5
29	480	5	0	29.56	33.52	36.92	6.82	6.3	3.3	3.21	1.66	.26	2.7
29	710	5	3.29	7.14	43.68	35.84	6.68	6.5	3.3	3.55	3.15	-.52	2.8
29	290	5	.19	25.51	54.22	20.08	5.92	5.1	3.3	2.64	2.96	.86	2.9
29	421	5	0	28.35	45.69	25.96	6.2	5.3	3.3	2.8	2.26	.62	2.9
29	626	2	0	17.64	42.41	39.95	7.27	6.9	3.7	3.04	1.8	.06	3.1
29	856	2	.3	16.92	41.69	41.09	7.3	7	3.3	3.08	2.07	.06	3.1
29	270	2	0	15.21	44.27	40.52	7.38	8.5	3.5	2.99	1.71	.19	3.1
29	30	2	0	24.64	40.78	34.58	6.9	6.3	3.5	2.99	1.85	.3	2.9
29	626	2	0	17.64	42.41	39.95	7.27	6.9	3.7	3.04	1.8	.06	3.1
29	856	2	.3	16.92	41.69	41.09	7.3	7	3.3	3.08	2.07	.06	3.1
29	526	4	0	34.35	29.94	35.71	6.55	6.1	3.3	3.42	1.7	.19	1.5
29	520	4	.63	33.92	42	23.45	5.84	5.3	3.1	2.97	2.68	.35	2.7
29	155	1	0	6.7	53.5	39.7	7.54	7.1	5.8	2.58	2	.23	3.5
29	114	1	0	11.7	58.1	30.3	6.88	6.1	5.4	2.65	2.26	.47	3.5
29	959	1	.2	11.1	61.1	27.6	6.67	5.9	5.6	2.38	2.62	.57	3.1
29	975	1	0	20.1	55.9	24	6.32	5.7	3.6	2.62	2.61	.55	1.9
29	100	1	0	9.4	46.2	44.4	7.81	7.3	6	2.9	2.08	-.08	3.5
29	205	1	.5	7.85	43.99	47.65	7.93	7.7	3.4	2.83	2.92	-.36	3.1
29	990	1	.05	21.91	46.44	31.6	6.6	6.1	3.5	2.8	2.15	.28	3.1
37	74	5	.26	8.26	39.63	51.76							
37	154	5	1.39	7.6	39.96	51.05							
37	65	3	.18	4.71	38.86	56.25							
37	74	3	.18	8.12	38.97	51.9							
37	106	3	.11	5.46	35.54	58.89							
37	117	3	0	6.29	40.11	53.6							
37	134	3	0	5.28	41.73	52.99							
37	167	3	.52	10.93	38.56	49.99							
37	172	3	1.34	8.45	34.69	55.52							
37	184	3	.24	3.61	29.97	66.18							
37	202	3	0	2.54	25.52	71.94							
37	225	3	0	5.31	44.08	50.61							
37	238	3	0	2.68	40.32	56.99							
37	G11	1	0	3.78	39.06	57.17							
37	G23	1	0	3.58	37.88	58.54							
37	G33	1	0	3.55	34.96	61.49							
36	245	5	0	9.92	42.93	47.15							
36	384	5	0	4.5	19.68	75.82							
36	445	5	.28	20.65	35.37	43.7							
36	273	5	0	20.15	40.72	39.13							
36	354	5	0	19.63	37.35	42.57							
36	413	5	.53	28.67	32.74	38.06							
310	303	4	0	5.76	35.00	59.24							
36	325	4	0	1.66	21.34	77.02							
36	G6	4	0	5.41	36.19	58.4							
36	G39	4	0	5.37	36.84	57.74							
56	G45	1	0.00	8.51	36.04	56.44							
56	G100	1	0.00	3.16	36.39	60.44							
56	85	5	0.18	6.02	30.61	63.19							
55	208	5	0.00	7.39	40.00	52.61							
58	288	5	0.00	5.30	43.42	51.28							
55	351	5	0.00	2.25	38.39	59.35							
55	481	5	0.00	4.63	43.75	51.62							
55	541	2	0.88	10.71	34.55	53.86							
55	621	1	0.23	3.97	43.11	52.69							
55	1021	1	0.00	2.93	47.93	49.14							
55	1055	5	0.54	11.03	39.16	49.26							
54	86	1	0.00	18.27	43.90	37.83							
54	151	5	0.20	8.51	41.30	49.99							
54	289	5	0.00	7.63	49.42	42.95							
54	403	5	0.07	8.56	37.70	53.66							
54	462	3	0.63	3.25	43.64	52.48							
54	490	5	0.14	8.24	25.30	66.33							
54	562	5	0.68	12.51	36.58	50.22							

CORE NO.	DEPTH (cm)	FACIES	%GR	%SA	%SILT	%CLAY	MEAN (phi)	MED. (phi)	MODE (phi)	S.D.	KURT.	SKEW.	CRST% (phi)
54	651	3	0.00	3.14	44.11	52.75							
54	809	3	0.00	4.57	36.28	59.15							

APPENDIX C

(PHYSICAL PROPERTY DATA)

<u>List of Abbreviations</u>

```
SS . . . . . . shear strength (undrained)
WC . . . . . . water content
BD . . . . . . bulk density
Rmld SS . . remolded shear strength
```

Core 85-001-01

Depth (m)	SS (kPa)	WC (%)
0.39		48
0.7		71.85
0.95	13.1191	
1.16	11.2511	
1.41	11.3788	
1.66	10.0341	
1.92	9.9063	
2.17	11.5127	
2.52	14.5917	
2.69	13.1252	
2.91	11.9143	
3.25	10.5756	
3.5	13.1191	
4.0	13.393	
4.36	13.6546	
4.6	15.9365	
5.1	11.9143	
5.3	10.4479	
5.45	15.9365	
5.48		50.7424
5.7	17.409	
5.95	17.6768	

Core Hu85-001-02

Depth (m)	SS (kPa)
3.85	11.7865
4.1	11.7805
4.35	12.3159
4.65	13.3869
4.9	14.0562
5.15	15.6626
5.4	16.3381
5.65	14.4639
5.9	13.1191
6.2	11.1111
6.33	11.1172
6.45	8.166
6.64	8.1599

240

Core 85-001-04

Depth (m)	SS (kPa)	BD (g/cm3)	WC (%)
0.08			99.99
0.13	6.2918		
0.26	7.3628		
0.28	14.9933		
0.29			85.98
0.33			80.79
0.41	8.9753		
0.48	14.5917		
0.49			80.25
0.57	7.8983		
0.6			72.49
0.63	4.1499		
0.65		1.498	99.99
0.66			71.11
0.74		1.483	87.63
0.76	6.8334		
0.78	18.0784		
0.82	14.1962		
0.86		1.729	37.23
0.9			52.03
0.94			63.22
0.97	7.3567		
1.17			66.79
1.18	16.472		
1.2			72.63
1.23	2.9451		
1.36			61.09
1.38	6.8273		
1.51		1.667	61.95
1.53	3.8822		
1.82	4.156		
1.85			60.6
2.05	5.3487		
2.36	7.2289		
2.38		1.752	46.45
2.4		1.705	52.69
2.55		1.738	54.22
2.6	9.6446		
2.89		1.734	54.72
2.92	6.2918		
3.14			53.81
3.29	6.8273		
3.53		1.747	52.27
3.59	6.9673		
3.82		1.765	50.9
3.88	7.3628		
3.92		1.784	49.1
4.02	13.253		
4.03		1.819	45.15
4.12	12.8575		
4.25	16.8736		
4.27	13.253		
4.29			46.18
4.58	16.6058		
4.62		1.787	48.49
4.68	14.5917		
4.88			44.3167
4.91			35.4813
4.93		1.723	57.16
5.12		1.784	48.86
5.18	14.7317		
5.38	14.5978		
5.45		1.788	42.81
5.62		1.698	35.73
5.65	16.8675		

Core 85-001-04 (cont'd)

Depth (m)	SS (kPa)	BD (g/cm3)	WC (%)
5.95	18.2122		
5.99			44.41
6.23	18.8816		
6.48	17.8045		
6.51			42.06
6.7	17.9445		
6.88		1.827	43.97
6.92	18.6139		
6.96		1.816	45.95
7.11	18.7416		
7.17		1.838	42.34
7.4	15.401		
7.43		1.815	45.77
7.67	18.34		
7.69		1.831	42.71
7.85			34.2765
7.88	17.1413		
7.93	14.324		
7.95		1.846	41.52
8.04	19.2832		
8.09		1.758	52.38
8.22	12.4498		
8.44		1.711	

Core number 85001-05

Depth (m)	SS (kPa)	WC (%)	BD (g/cm3)
0.4	14.19		
0.45		68.01	1.65
0.62	10.04		
0.65		97.51	
0.75	11.52		
0.8		65.22	1.66
0.9	10.04		
1		47.55	1.79
1.05	8.7		
1.15		64.5	1.65
1.25	8.16		
1.35	1.21		
1.4		60.1	
1.48		64.35	1.64
1.5	5.63		
1.68	7.23		
1.82	5.23		
1.87		62.09	
2.06	6.02		
2.08		63.57	1.67
2.28	6.15		
2.56	10.18		
2.86	9.1		
2.88		49.39	1.77
3.19	7.63		
3.22		61.3	1.69
3.37		49.09	1.72
3.45	9.9		
3.51		54.62	1.75
3.69	8.03		
3.95	8.31		
4.01		46.18	1.8
4.2	9.37		
4.42		54.02	1.74

Core number 85001-05 (cont'd)

Depth (m)	SS (kPa)	WC (%)	BD (g/cm3)
4.45	4.45		
4.81		47.76	1.79
4.84	12.98		
4.91		43.65	1.63
5.09		46.69	1.8
5.15	12.19		
5.4	12.44		
5.41		41.66	1.75
5.6	8.83		
5.8		72.19	1.64
5.83	10.98		
6.09	10.31		
6.21		60.67	1.69
6.37	8.57		
6.41		59.03	1.65
6.57	10.58		
6.59		59.15	1.63
6.88	8.43		
7.01		57.93	1.71
7.17	.6.69		
7.44		55.25	
7.46	11.78		
7.76		60.83	1.69
7.78	9.38		
7.94		50.79	1.7
8.08	9.63		
8.1		55.27	1.73
8.4	8.71		
8.49		59.87	1.61
8.55		57.87	1.71
8.69	11.65		
8.75	9.1		
9	8.17		
9.02		63.68	1.68
9.25	9.37		
9.33		60.38	1.702
9.51	4.82		
9.59	8.57		
9.61		62.78	1.68
9.87		53.55	1.74
9.89	11.24		
10.18	9.78		
10.21		54.42	1.74
10.45	8.7		
10.55		55.18	1.73
10.7	8.84		
10.87		62.19	
10.93	6.83		
10.99		61.26	1.64

243

Core Hu85-001-06

Depth (m)	SS (kPa)	BD (g/cm3)	WC (%)
0.35	13.2591		
0.65	12.4498		
0.8	6.8334		
0.95	10.9772		
1.1	6.0241		
1.25	6.0302		
1.35	5.6225		
0.26	21.32		
0.42		1.637	70.82
0.45			64.51
0.55		1.636	60.32
0.6			64.08
0.7			61.36
0.85			79.54
1		1.594	80.27
1.15			
1.3		1.471	99.99

CORE 83012-03

Depth (m)	SS (kPa)	WC (%)	Rmld SS (kPa)
0.1	13.534	68.285	5.358
0.25	8.042	69.207	
0.4	11.337	66.279	
0.55	8.042	44.946	5.715
0.7	8.042	55.325	
0.85	3.658	55.263	
1	4.021	45.058	1.429
1.15	6.58	51.452	
1.3	9.14	45.069	3.929
1.45	10.239	51.345	
1.6	8.042	48.342	
1.75	10.974	46.665	6.429
1.9	8.414	8.867	
2.05	6.58	42.655	
2.2	7.316	77.147	3.215
2.45	13.171	36.546	
2.6	7.316	44.226	
2.75	10.974	44.284	
2.9	7.316	41.296	
3.45	0.736	44.858	
3.6	6.914	49.761	
3.9	12.072	48.081	
4.05	6.58	39.274	1.429
4.35	9.876	38.758	
4.65	13.534	41.4	
4.95	7.316	43.44	5.715
5.1	11.337	41.686	

Core 83012-04

Depth (m)	SS (kPa)	WC (%)
0.1	15.357	65.243
0.15		
0.4	12.435	55.743
0.6		
0.7	10.238	57.001
0.75		
1.1	3.658	66.944
1.14		
1.5	4.02	62.363
1.55		
1.65	4.02	60.194
1.8	5.482	50.181
1.95	3.295	48.504
2.1	6.217	49.018
2.25	5.482	62.655
2.3		
2.4	7.316	49.602
2.55	8.014	37.191
2.7	8.041	57.478
2.85	7.316	60.192
3	4.756	31.292
3.15	8.777	48.856
3.3	10.611	53.809
3.35		
3.45	9.14	60.942
3.6	7.316	58.342
3.75	6.943	58.691
3.9	7.678	48.492
4.11	4.393	46.324
4.26	8.414	43.391
4.41	8.041	61.041
4.49		
4.56	5.119	49.576
4.71	8.041	54.837
4.86	9.14	50.647
5.01	6.58	54.566
5.09		
5.16	2.922	47.238
5.3	4.02	47.084
5.5	12.072	49.29
5.65	8.414	38.844
5.8	2.196	27.959
5.95	11.699	41.327
6.1	12.072	44.834
6.25	10.238	39.894
6.4	12.798	40.282
6.55	16.456	33.72
6.7	6.217	33.527

Core number 83012-06

Depth (m)	BD (g/cm3)	SS (kPa)	rmld SS (kPa)	WC (%)
2.35		3.678		
2.47				45.326
2.5		8.777	7.85	
2.62	1.778			38.810
2.65		22.674		
2.75	1.53			39.199
2.8		14.269	6.072	
2.9	1.473			47.909
2.95		21.575		
3.05	1.477			48.811
3.1		10.974		
3.2	1.501	14.632	7.85	47.750
3.27	1.348			51.400
3.35		11.337		
3.42	1.499			41.923
3.5		14.995		
3.56				31.785
3.65		20.85	9.64	
3.7	1.456			48.472
3.8		10.239		
3.86	1.423			55.532
3.95		11.337		
4.03	1.531			34.755
4.1		8.777	8.57	
4.15				31.729
4.25		11.337		
4.32	1.549			33.514
4.4		8.777		
4.47				38.690

Core 83-012-08

Depth (m)	SS (kPa)	WC (%)	BD (g/cm3)	Rmld SS (kPa)
0.05	3.658			1.67
0.1		61.812		
0.2	6.953			
0.35	1.461	50.419		
0.67	1.098			
0.72		54.522		
1.95	7.679			5.25
2		54.601	1.39	
2.7	9.876			2.45
2.77		41.569	1.575	
2.85	8.777			
2.93		56.539	1.363	
3	6.953			
3.07		42.753		
3.15	8.042			1.37
3.25		41.598	1.504	
3.3	10.239			
3.4		64.25	1.342	
3.45	6.58			2.57
3.52		51.342	1.4	
3.7	10.239	47.13		1.64
3.85	9.876	53.683		
4	5.855	50.897		
4.15	14.995	63.11		1.95
4.3	8.042	47.229		
4.45	12.798	46.445		
4.6	9.14	43.018		12.5
4.75	6.953	43.285		
4.9	7.679	51.784		
5.05	6.58	41.141		2.57
5.2	9.876			1.69
5.35	10.611			
5.5	7.679			
5.8	7.679			5.25
6.1	5.855			
6.22		39.48	1.365	
6.4	6.58			
6.47		39.96	1.328	

83012-10

Depth (m)	SS (kPa)	WC (%)	BD (g/cm3)	Rmld SS (kPa)
0.05	14.632			4.??5
0.12		52.892	1.359	
0.15				48.9
0.2	10.611			
0.26		61.089	1.379	
0.35	10.238			
0.41		70.399	1.35	33
0.5	14.994			8.929
0.7	8.777			3.572
0.77		67.814		
0.85	10.611			
0.93		65.581	1.262	
1	2.559			
1.08		45.548	1.447	
1.15	5.482			
1.24		60.208	1.307	2.5
1.3	5.482			
1.37		65.894	1.314	
1.45	6.217			
1.52		58.517	1.431	32
1.6	2.922			1.072
1.67		59.206	1.335	
1.75	5.482			
1.81		60.538	1.411	
1.9	6.953			
1.99		46.235	1.52	
2.8	7.678			2.5
2.87		55.113	1.303	
2.95	10.97			
3.02		54.429	1.345	
3.1	8.777			
3.16		57.876	1.372	27.6
3.25	9.512			1.786
3.31		55.728	1.427	
3.4	11.699			
3.46		52.555	1.442	
3.55	14.269			
3.8	11.699			3.929
3.87		42.045	1.379	
3.95	8.777			
4.01		58.069	1.35	24.4
4.1	10.974			
4.21		52.696	1.394	
4.25	8.777			2.143
4.36		56.13	1.434	
4.4	10.611			
4.51		51.255	1.39	
4.6				23.7
4.65	7.678			
4.66		50.603	1.435	
4.8	10.974			19.1
4.81		47.333	1.521	
4.95	5.482			
4.97		50.897	1.496	
5.1	11.336			
5.12		31.807	1.592	
5.3	13.896			5.358
5.35				16.1
5.37		31.988	1.5	
5.52		36.013	1.508	
5.6	6.953			
5.66		39.487	1.512	
5.75	7.316			2.5
5.8			1.562	
5.81		35.938		
5.9	8.777			

83012-10 (cont'd)

Depth (m)	SS (kPa)	WC (%)	BD (g/cm3)	Rmld SS (kPa)
5.95		45.856	1.449	21.4
6.1	10.974			
6.11		43.449	1.398	
6.25	6.58			
6.26		50.431	1.398	
6.4	9.512			20.7
6.42		46.768	1.374	
6.55	11.336			
6.56			1.235	
6.58		24.753		